THE UNIVERSITY OF QUEENSLAND

AUSTRALIA

Automatic Control of Dual LVADs as a BiVAD

Michael Charles Stevens

Bachelor of Engineering (Medical)

A thesis submitted for the degree of Doctor of Philosophy at

The University of Queensland in 2014

School of Information Technology and Electrical Engineering

Abstract

In this thesis, we investigate automated methods for the control of rotary blood pumps in the treatment of heart failure. Heart failure is a common end-point for many forms of cardiovascular disease resulting in significant morbidity and mortality. Ventricular assist devices (VADs) are blood pumps designed to assist a failing heart and are used both to support patients whilst they are awaiting a heart transplant, or as an alternative to transplantation. Small rotary VADs can provide long-term support of the left ventricle (LVAD), right ventricle (RVAD) or both ventricles of the heart simultaneously. Unfortunately, the lack of a commercially available rotary RVAD has led to the implantation of two rotary LVADs as an *ad hoc* biventricular assist device (BiVAD). Clinicians currently operate such dual LVADs at a constant speed, which ensures balanced left and right pump flows for inactive patients. However, changes in levels of patient activity will lead to altered cardiac output requirements, which may disturb this balance. In turn, this can lead to undesirable events such as pulmonary venous congestion or ventricular suction. A control system that automatically adjusts pump speed with changes in the required cardiac output could alleviate such events and so offer significant benefits. However, while such physiological control systems have been investigated for single LVADs, limited work has been completed on dual LVAD control. In addition, there is no generally accepted framework for the evaluation of these systems that encompasses a broad range of patient scenarios, activity levels and heart conditions. Therefore, the primary aim of this thesis was to develop and evaluate a number of physiological control systems suitable for dual rotary LVADs.

The first objective was to characterise the methods that are currently used to operate dual LVADs in the clinic. Using both in-vitro and in-vivo methods, it was shown that balanced left and right flow rates could be obtained by operating the RVAD slower than the LVAD, albeit at speeds below the manufacturer's recommendations (1400 – 1800 RPM), which, according to other investigators, may adversely affect impeller washout. Operating both at the same design speed is only possible in patients with high pulmonary vascular resistance (PVR), high left ventricular contractility or high RVAD outflow cannula resistance. This thesis demonstrates that if the RVAD outflow cannula is restricted to a diameter between 6.5 and 8.1 mm, suitable steady-state haemodynamics (systemic flow rate 5 $L.min^{-1}$, MAP 90mmHg and LAP less than 25mmHg) can be achieved while maintaining impeller stability and optimal device washout. It was also established that changes in pump speed or outflow graft diameter were required to overcome elevations in pulmonary vascular resistance, thereby justifying the necessity of a physiological control system for dual LVADs.

The second objective was to develop an in vitro evaluation protocol for control system testing utilising a mock circulation loop (MCL). The testing protocol consisted of simulating three patient scenarios (postural change, valsalva manoeuvre and exercise) consecutively. Four performance metrics were also devised, in order to quantify controller performance with respect to haemodynamic stability, congestion

avoidance, suction avoidance and exercise. We showed that the scenarios were useful for evaluation of control systems because they subjected the systems to preload and afterload changes similar to those observed in-vivo. However, the lack of a simulated baroreflex caused discrepancies in haemodynamics between the MCL and those reported in literature. The scenarios were replicated with a high degree of repeatability, and we showed that the performance metrics can be used for accurate and efficient comparisons of control system performance.

The third objective was to experimentally compare a number of LVAD physiological control systems from the literature using our proposed evaluation protocol in order to determine the most suitable candidate for dual LVAD control. The key finding from this comparison was that a control system based on the native Frank-Starling response was the best performing system with respect to all aspects/metrics evaluated. In particular, it produced zero suction events (compared to 0.12 events per second caused by constant speed control), kept left atrial pressure below 15mmHg for nearly the entirety of the simulation, and increased pump flow in exercise by 3.1 $L.min^{-1}$ (compared to 1.62 $L.min^{-1}$ with constant speed control). This is the first time a Frank-Starling control system has been evaluated with respect to three different patient scenarios and the results highlight the advantages of this system over other previously proposed control systems.

The final objective was to adapt the Starling-like control system into a dual LVAD control system. A master/slave control strategy was designed and a number of configurations compared using our evaluation protocol. Based on this evaluation, we demonstrated that the left/right master/slave physiological control system using a preload-matching slave controller produced fewer suction events than constant speed control (0.01 vs. 0.15 s^{-1}), had a lower risk of pulmonary congestion than the other control systems, and had an effective flow increase in exercise higher than constant speed control (4.33 vs. 2.09 $L.min^{-1}$). In this way, we demonstrated the efficacy of physiological control of dual LVADs via a master/slave approach based on the Frank-Starling law of the heart. Potential future work could involve extending the evaluation framework by the inclusion of a simulation of the baroreflex, investigating the use of other control strategies in both single and dual LVAD Starling-like control systems and in-vivo and clinical validation of the dual LVAD physiological control system.

Declaration by author

This thesis is composed of my original work, and contains no material previously published or written by another person except where due reference has been made in the text. I have clearly stated the contribution by others to jointly-authored works that I have included in my thesis.

I have clearly stated the contribution of others to my thesis as a whole, including statistical assistance, survey design, data analysis, significant technical procedures, professional editorial advice, and any other original research work used or reported in my thesis. The content of my thesis is the result of work I have carried out since the commencement of my research higher degree candidature and does not include a substantial part of work that has been submitted to qualify for the award of any other degree or diploma in any university or other tertiary institution. I have clearly stated which parts of my thesis, if any, have been submitted to qualify for another award.

I acknowledge that an electronic copy of my thesis must be lodged with the University Library and, subject to the General Award Rules of The University of Queensland, immediately made available for research and study in accordance with the *Copyright Act 1968*.

I acknowledge that copyright of all material contained in my thesis resides with the copyright holder(s) of that material. Where appropriate I have obtained copyright permission from the copyright holder to reproduce material in this thesis.

Publications during candidature

Publications Arising From Thesis

Peer-reviewed Papers

Stevens MC, Wilson SJ, Bradley AP, Fraser JF, Timms DL. Physiological control of dual rotary pumps as a biventricular assist device using a master/slave approach. Artif. Organs. 2014; Published Online Ahead of Print (21 April 2014).

Stevens MC, Mason DG, Bradley AP, Wilson SJ, Fraser JF, Timms DL. Comparison of Linear and Non-Linear control of Flow and Pressure in a Rotary Left Ventricular Assist Device. Medical and Biological Computing and Engineering. 2014; Accepted with Major Revisions (19 April 2014).

Stevens MC, Gregory SD, Nestler F, Thomson B, Choudhary J, Garlick B, et al. In-vitro and in-vivo characterisation of three different modes of pump operation when using an LVAD as an RVAD. Artif Organs. 2014; Published Online Ahead of Print (24 March 2014).

Stevens, M.C., Bradley, A.P., Wilson, S.J., Mason, D.G. (2013). Evaluation of a Morphological Filter in Mean Cardiac Output Determination: Application to Left Ventricular Assist Devices. Medical and Biological Engineering and Computing, 51 (8): 891 – 899.

Conference Abstracts

Stevens MC, Wilson SJ, Bradley AP, Timms DL. Physiological Control of Dual Rotary Left Ventricular Assist Devices using a Master/Slave Approach. 21st Congr. Int. Soc. Rotary Blood Pumps. Yokohama; 2013.

Stevens MC, Gaddum NR, Pearcy M, Salamonsen RF, Timms DL, Mason DG, et al. Frank-starling control of a left ventricular assist device. Annual International Conference of the IEEE Engineering in Medicine and Biology Society. Boston, MA: IEEE; 2011. p. 1335–8.

Stevens MC, Mason DG, Bradley A, Wilson S, Gregory SD, Timms DL. Do patients need a "smart" controller? An In-Vitro Investigation into the Effect of Patient Variance on Physiological Control. 20th Congress of the International Society for Rotary Blood Pumps. Istanbul; 2012.

Stevens MC, Timms DL, Salamonsen RF, Lovell NH, Hayward C. The effects of both increased RBP speed and RVAD support on maximal LVAD flow during exercise. 20th Congress of the International Society for Rotary Blood Pumps. Istanbul; 2012.

Timms D, **Stevens M**, Gregory S, Thomson B, Choudhary J, Pauls J., et al. Investigating the Operating Characteristics of Dual Rotary LVADs as a BiVAS. 20th Congress of the International Society for Rotary Blood Pumps. Istanbul, Turkey.; 2012.

Stevens MC, Timms DL, Nestler F, Mason DG. Automatic Control of a Dual Rotary Biventricular Assist Device. Australian Biomedical Engineering Conference. Brisbane; 2012.

Stevens MC, Timms DL, Gregory SD, Mason DG, Fox J, Fraser JF. Replicating Daily Activities with a VAD. A repeatable in-vitro test bed for the evaluation of RBP physiological control systems. 19th Congress of the International Society for Rotary Blood Pumps. Louisville, KY; 2011.

Stevens MC, Mason DG, Timms DL, Pearcy MJ, Fraser JF. Which RBP Physiological Controller Is Most Physiologic? Comparing Control Systems in Repeatable Autoregulatory Testing Scenarios. 19th Congress of the International Society for Rotary Blood Pumps. Louisville, KY; 2011.

Publications Related To Thesis

Peer-reviewed Papers

AlOmari AH, Savkin A V, **Stevens M**, Mason DG, Timms D, Salamonsen R, et al. Developments in control systems for rotary left ventricular assist devices for heart failure patients: a review. Physiol Meas. 2013;34(1):R1–27.

Gaddum NR, **Stevens MC**, Lim E, Fraser JF, Lovell NH, Mason DG, et al. Starling-like Flow Control of a Left Ventricular Assist Device; In Vitro Validation. Artif. Organs 38 (3): E46-56.

Gaddum NR, Timms DL, **Stevens M**, Mason D, Lovell N, Fraser JF. Comparison of Preload-Sensitive Pressure and Flow Controller Strategies for a Dual Device Biventricular Support System. Artif Organs. 2012; 36(3):256–65.

Gregory SD, **Stevens M.C.**, Wu E, Fraser JF, Timms D. (2013). In Vitro Evaluation of Aortic Insufficiency with a Rotary Left Ventricular Assist Device. Artif. Organs 37 (9): 802-809.

Salamonsen RF, Lim E, Gaddum N, Alomari A-HH, Gregory SD, **Stevens M**, et al. Theoretical Foundations of a Starling-Like Controller for Rotary Blood Pumps. Artif Organs. 2012; 36(9):787–96.

Conference Abstracts

Pauls JP, Gregory SD, **Stevens MC**, Tansley GD. Evaluation of Controller Response to Exercise Simulations Compared to Physiological Data. 21st Congr. Int. Soc. Rotary Blood Pumps. Yokohama; 2013.

Gregory SD, **Stevens M**, Timms D, Pearcy M. Replication of the Frank-Starling response in a mock circulation loop. Annual International Conference of the IEEE Engineering in Medicine and Biology Society. Boston, MA: IEEE; 2011. p. 6825–8.

Timms DL, Gregory SD, **Stevens MC**, Fraser JF. Haemodynamic modelling of the cardiovascular system using mock circulation loops to test cardiovascular devices. Conf Proc Annu Int Conf IEEE Eng Med Biol Soc. IEEE; 2011; 2011:4301–4.

Publications included in this thesis

Stevens MC, Gregory SD, Nestler F, Thomson B, Choudhary J, Garlick B, et al. In-vitro and in-vivo characterisation of three different modes of pump operation when using an LVAD as an RVAD. Artif Organs. 2013; Published Online Ahead of Print (24 March 2014). – incorporated as Chapter 2

Contributor	*Statement of contribution*
Michael Stevens (Candidate)	*Wrote Ethics Application (100%)* *Designed and performed in-vitro experiments (60%)* *Assisted with in-vivo experiments (5%)* *Data Analysis (100%)* *Wrote and edited the paper (70%)*
Dr. Shaun Gregory	*Designed and performed in-vitro experiments (20%)* *Assisted with in-vivo experiments (5%)* *Wrote and edited the paper (10%)*
Frank Nestler	*Designed and performed in-vitro experiments (10%)* *Assisted with in-vivo experiments (5%)* *Wrote and edited the paper (5%)*
Dr. Bruce Thomson	*Assisted with in-vivo experiments (50%)*
Dr. Jivesh Choudhary	*Assisted with in-vivo experiments (20%)*
Dr. Bruce Garlick	*Assisted with in-vivo experiments (10%)*
Jo Philipp Pauls	*Designed and performed in-vitro experiments (10%)*

Dr. John Fraser	*Assisted with in-vivo experiments (5%)* *Wrote and edited the paper (5%)*
Dr. Daniel Timms	*Wrote and edited the paper (10%)*

Stevens MC, Wilson SJ, Bradley AP, Fraser JF, Timms DL. Physiological control of dual rotary pumps as a biventricular assist device using a master/slave approach. Artif. Organs. 2013; Published Online Ahead of Print (April 21 2014). - Incorporated as Chapter 5.

Contributor	*Statement of contribution*
Michael Stevens (Candidate)	*Designed and performed in-vitro experiments (100%)* *Data Analysis (80%)* *Wrote and edited the paper (60%)*
Stephen Wilson	*Wrote and edited the paper (10%)* *Data Analysis (10%)*
Andrew Bradley	*Wrote and edited the paper (10%)* *Data Analysis (10%)*
John Fraser	*Wrote and edited the paper (10%)*
Daniel Timms	*Wrote and edited the paper (10%)* *Initial design concept (100%)*

Stevens, M.C., Bradley, A.P., Wilson, S.J., Mason, D.G. (2013). Evaluation of a Morphological Filter in Mean Cardiac Output Determination: Application to Left Ventricular Assist Devices. Medical and Biological Engineering and Computing, 51 (8), 891 - 899. - included as Appendix

Contributor	*Statement of contribution*

Michael Stevens (Candidate)	*Designed and performed in-silico experiments (100%)* *Data Analysis (100%)* *Wrote and edited the paper (70%)*
Andrew Bradley	*Wrote and edited the paper (10%)*
Stephen Wilson	*Wrote and edited the paper (10%)*
David Mason	*Wrote and edited the paper (10%)*

Contributions by others to the thesis

Significant contributions were made by the following people.

Prof Robert Salamonsen: Initial concept design of the Starling-like control system evaluated as part of Chapter 4.

Dr Nicholas Gaddum: Initial development and evaluation of the Starling-like control system evaluated as part of Chapter 4.

Dr David Mason: Initial concept for the evaluation protocol described in Chapter 3.

Dr Shaun Gregory and Dr Daniel Timms: Assisted with mock circulation loop modifications and design described in Chapter 3.

Professors Stephen Wilson and Andrew Bradley: Proof read and provided critical feedback on the thesis in order to clarify the aims, objectives and conclusions of this thesis.

Statement of parts of the thesis submitted to qualify for the award of another degree

None.

Acknowledgements

I firstly would like to acknowledge my supervisors at the ICET laboratory, Dr Daniel Timms and Dr Shaun Gregory. Daniel, thank you for giving me the opportunity to complete both my honours project and my PhD in a new and exciting field. It was amazing to watch you take the lab from a small number of people in an unused office into a fully-functional and world-renowned engineering laboratory. Thank you as well for giving me the opportunity to work with you in Houston, it was a great experience. Shaun, it has been an absolute pleasure working alongside you and getting to know you over the last four years. Thank you for all of the times that you have assisted me, not only with mock circulation loop modifications but also with all of my silly questions throughout my time at the lab. Thanks for all of your advice during my candidature, particularly during the stressful times.

Secondly, I would like to thank my UQ supervisory team, Professors Stephen Wilson and Andrew Bradley. You both have provided me with useful advice countless times throughout my project. It was great to get an alternative perspective on my project. I am so grateful that I had two relaxed, knowledgeable and sometimes funny supervisors at UQ. I would also like to acknowledge the advice and support that Dr David Mason provided in the early stages of my PhD.

Thirdly, I would like to thank Professor John Fraser at The Prince Charles Hospital. Thank you for always finding time in your busy schedule to meet for lunch to discuss my progress. The best part was that even if you could not directly help me, you always put me in touch with someone who could. Thank you for welcoming me into your team at the CCRG and I look forward to collaborating in the future.

I would like to acknowledge the financial support provided by The Prince Charles Hospital Foundation. I was involved in three grants (lead investigator on Novice Researcher and Small Equipment grants and a co-investigator on an Experienced Researcher grant) which totalled over $80 000 of funding. Without the financial support offered by the Foundation, I would not have been able to complete my project to the standard it is today. I would also like to acknowledge the financial support provided by the University of Queensland, which enabled me to travel to numerous conferences around the world.

I'd also like to thank all of the other researchers I have worked with at the ICET lab. Dr Nick Greatrex and Frank Nestler, you have provided me with an ear to vent to as well as countless pieces of advice. Dr Nick Gaddum, I always enjoyed collaborating with you, whether via email or in person, and you are a huge inspiration to me.

I would really like to thank my parents, Tony and Linda, for their love, encouragement, lunches, coffees, living space and general assistance. I really appreciate everything you both did for me, especially when I injured my back and was confined to my bed for a couple of months. I love you both so much. My sisters Claire and Rachel also deserve thanks for always believing in me and never doubting me once. Thanks to you both.

I would like to thank the support of my best friend Thu Mon. Words can't express my gratitude properly, but I'll try. You've been a fantastic source of encouragement and support, especially in the last 12 months of my candidature. You made the difficulties in this journey not only bearable, but also enjoyable. You get 10^{10} friendship points!

I'd also like to thank Nick Wiggins, one of my best friends over the last 10 years. You've consistently been a good friend that can make me laugh, inspire me musically, share tough times and provide a good distraction. Thanks mate.

Finally, I'd like to thank all of my other colleagues and students at the ICET lab and in Houston that I have worked with over the last 4 years, although your names are too numerous to mention here. I learnt something from each and every one of you.

Keywords

Heart failure, rotary blood pump, biventricular assist device, physiological control, ventricular assist device.

Australian and New Zealand Standard Research Classifications (ANZSRC)

ANZSRC code: 090304 Medical Devices -40%

ANZSRC code: 110201 Cardiology (incl. Cardiovascular Diseases)-30%

ANZSRC code: 091302 Automation and Control Engineering -30%

Fields of Research (FoR) Classification

FoR code: *0903 Biomedical Engineering - 40%*

FoR code: *1102 Cardiorespiratory Medicine and Haematology - 30%*

FoR code: *0913 Mechanical engineering – 30%*

Table of Contents

List of Figures

List of Tables

Nomenclature

Abbreviation/ Parameter	Meaning	Unit
a	Pressure offset for Starling-like and Master controllers	mmHg
ACT	activated clotting time	s
AoP	aortic pressure	mmHg
AoP_{set}	setpoint of AoP for pulsatile TAH automatic control	mmHg
ARX	autoregressive exogenous	N/A
a_{slave}	gain of slave control for pulsatile TAH automatic control	N/A
B	structuring element of morphological filter	N/A
BiVAD	biventricular assist device	N/A
b_{slave}	offset of slave control for pulsatile TAH automatic control	mmHg
BW	body weight of animal	kg
C	Compliance	$mL.mmHg^{-1}$
c	offset for the slave control system	mmHg
C_{EDV}	End-diastolic volume offset for starling function of MCL ventricles, used to shift PV loops left or right	mL
CO	cardiac output	$L.min^{-1}$
CP	animal-specific constant for pulsatile TAH automatic control	$L.min^{-1}.mmHg^{-1}$
C_{SD}	Vertical offset for systolic/diastolic ratio as a function of HR	N/A
C_{sm1}	Vertical offset for starling function of the MCL ventricles	N/A

CVD	cardiovascular disease	N/A
CVP	central venous pressure	mmHg
ECMO	extracorporeal membranous oxygenation	N/A
EDPVR	end diastolic pressure volume relationship	$mmHg.mL^{-1}$
EDV	End diastolic ventricular volume	mL
ESC	extremum seeking control	N/A
ESPVR	end systolic pressure volume relationship	$mmHg.mL^{-1}$
FA	full assist	N/A
FL	fuzzy logic	N/A
FLC	fuzzy logic control	N/A
FOM_{CONG}	Measure of the percentage of time that left and right atrial pressures are kept below levels that would cause venous congestion\	%
FOM_{EX}	Measure of the VAD contribution to increase in flow rate during exercise	L
FOM_{REST}	Measure of the percentage of time that key haemodynamic signals remain in a safe region	%
FOM_{SUC}	Number of suction events per second	s^{-1}
H	pump pressure head	mmHg
HF	Heart Failure	N/A
HP	high pass	N/A
HR	Heart rate	N/A

HSI	Harmonic suction index	N/A
HVAD	HeartWare ventricular assist device	N/A
IABPS	intra-aortic balloon pump	N/A
ICA	index of current amplitude	A
K_{HR}	Adjusts MCL ventricular contractility based on HR	min
K_{s1}	Sensitivity of the suction resistance to ventricular volume	N/A
K_{s2}	Sensitivity of the suction resistance to ventricular volume	mL^{-1}
K_{sc}	Sensitivity of the Starling-like control system	$L.min^{-1}.mmHg^{-1}$
K_{sc1}	Sensitivity constant for Master control system	N/A
K_{sc2}	Sensitivity constant for Master control system	$L.min^{-1}.mmHg^{-1}$
K_{SD}	Gain for systolic/diastolic ratio as a function of HR	Min
K_{slave}	Sensitivty for the slave control system	N/A
K_{sm1}	Starling sensitivity constant in the MCL, surrogate for ESPVR	N/A
K_{sm2}	Starling sensitivity constant in the MCL, surrogate for ESPVR	mL^{-1}
$K_{starling}$	Gain for electropneumatic regulators that varies with preload	N/A
K_{ven}	Gain for electropneumatic regulators that varies for left and right ventricles	N/A
L	inertance	$Pa\ m^{-3}\ s^{-2}$
LA	left atrium	N/A

LAP	left atrial pressure	mmHg
LP	low pass	N/A
LV	left ventricle	N/A
LVAD	left ventricular assist device	N/A
LVADQ	left ventricular assist device flow rate	$L.min^{-1}$
LVEDP	left ventricular end diastolic pressure	mmHg
LVF	left ventricular failure	N/A
MAP	mean aortic pressure	mmHg
MCFP	mean circulatory filling pressure	mmHg
MCL	mock circulation loop	N/A
MCP	mean circulatory pressure	mmHg
MF	morphological filter	N/A
MLHF	mild left heart failure	N/A
MOC	multi-objective control	N/A
MPAP	mean pulmonary arterial pressure	mmHg
MPQ	Mean pulmonary flow rate	$L.min^{-1}$
MS	master/slave	N/A
MSQ	mean systemic flow rate	$L.min^{-1}$
N	number of suction events during a simulation	N/A
NC	normally closed	N/A

NM	numerical model	N/A
PA	pulmonary artery	N/A
PAC	pulmonary arterial compliance	$mL.mmHg^{-1}$
PAP	pulmonary arterial pressure	mmHg
PD	proportional and derivative	N/A
P_{EDM}	end diastolic pressure of the master pump	mmHg
P_{EDS}	end diastolic pressure ventricular pressure of the slave pump	mmHg
P_{EDS_target}	target slave inlet pressure	mmHg
PI	proportional and integral	N/A
P_{in}	Pump inlet pressure	mmHg
PID	proportional, integral and derivative	N/A
Pi_{ratio}	ratio between differential pressure pulsatility and flow pulsatility	$mmHg.min.L^{-1}$
Pi_x	Pulsatility	N/A
PRD	systolic/diastolic ratio	N/A
PVC	pulmonary venous compliance	$mL.mmHg^{-1}$
PVR	pulmonary vascular resistance	$Dynes.s.cm^{-5}$
PWM	pulse width modulation	N/A
$Q_{exercise}$	total flow rate during exercise	L
Q_{LVAD}	measured flow rate through the LVAD	$L.min^{-1}$

$Q_{LVADmin}$	minimum left pump flow rate each cardiac cycle	$L.min^{-1}$
Q_{meas}	Measured flow rate used in calculation of target flow for Starling-like control system	$L.min^{-1}$
Q_{rest}	total flow rate during rest	L
Q_{RVAD}	measured flow rate through the RVAD	$L.min^{-1}$
Q_{TRACL}	Target flow rate for Starling-like control system, determined using the radial about the control line method.	$L.min^{-1}$
Q_{TRAXI}	Target flow rate for Starling-like control system, determined using the radial about the x-intercept method.	$L.min^{-1}$
$Q_{VADexercise}$	flow rate throught the VAD during exercise	L
Q_{VADM}	master pump flow rate	$L.min^{-1}$
Q_{VADM_target}	target flow rate for the master control system	$L.min^{-1}$
$Q_{VADStarget}$	target slave flow rate	$L.min^{-1}$
Q_{VFT}	Target flow rate for Starling-like control system, determined using the vertical flow target method	$L.min^{-1}$
R	resistance	$Dynes.s.cm^{-5}$
RA	right atrium	mmHg
RACL	Radial about the control line	N/A
RAP_{set}	setpoint of RAP for pulsatile TAH automatic control	mmHg
RAXI	Radial about the x-intercept	N/A
RBP	rotary blood pump	N/A
RPM	revolutions per minute	N/A

R_{suc}	Value of fluid resistance between ventricle and pump inlet, used to simulate ventricular suction	$mmHg.s.mL^{-1}$
RV	right ventricle	N/A
RVAD	right ventricular assist device	N/A
RVADQ	right ventricular assist device flow rate	$L.min^{-1}$
RVEDP	right ventricular end diastolic pressure	mmHg
RVF	right ventricular failure	N/A
SNR	signal to noise ratio	N/A
SSC	slope seeking control	N/A
SV	stroke volume	mL
SVC	systemic venous compliance	$mL.mmHg^{-1}$
SVO_2	mixed venous oxygen saturation	%
SVR	systemic vascular resistance	$Dynes.s.cm^{-5}$
T	Total length of simulation	s
TAH	total artificial heart	N/A
T_{good}	Time that left or right atrial pressure spends within a predefined safe range for avoiding pulmonary congestion	s
T_{isafe}	Time that a haemodynamic signal spends in a predefined safe region (used for FOM_REST)	s
$T_{iunsafe}$	Time that a haemodynamic signal spends in a predefined unsafe region (used for FOM_REST)	s
T_{poor}	Time that left or right atrial pressure spends within a predefined safe range for producing pulmonary congestion	N/A

T_{sys}	Systolic time each cardiac cycle	s
VAD	Ventricular assist device	N/A
V_{lv}	ventricular volume	mL
V_p	time varying voltage waveform, surrogate for time varying elastance, used to produce cyclic ventricular pressure in the MCL	Volts
V_{reg}	Voltage sent to the electropneumatic regulators to control contractility in the MCL	Volts
VRI	Venous return index	L.
V_{th}	threshold volume for suction resistance, suction activates when ventricular volume falls below this value	mL
w	weighting factor for morphological filter	N/A
x	signal before being subject to morphological filter	N/A
y	signal after being subject to morphological filter	N/A
α	gain for the flow-matching slave control system	N/A
ΔP	differential pressure	mmHg
ΔP_{aopv}	differential pressure between aorta and pulmonary vein	mmHg
Δt_i	length of the ith suction event	S
η	average speed penetration into suction	%
ρ	percentage of total time spent in suction	%
ω	pump rotational speed	RPM

1 Introduction

Cardiovascular disease (CVD) is one of the biggest killers in Australia, responsible for 31.7% of deaths in 2010 [1]. Cardiovascular disease is also one of the most expensive disease groups in Australia. In 2004-05, its cost was $5.9 billion, 11% of all health expenditure [2]. The situation in Australia is similar to that of the developed world [3], [4]. Therefore, there is both a moral and practical obligation to treat CVD in an effective manner.

Heart failure (HF) is one of the most severe forms of CVD, and describes any condition in which the ability of the heart to pump blood is diminished. The ideal treatment for a patient with HF is a heart transplant. However, the demand for donor hearts greatly outweighs supply. In 2011, there were approximately 260 000 patients with HF in Australia, yet only 65 transplants were performed [5]. Therefore alternative approaches (either surgical, pharmacological or mechanical treatments) are used.

Surgical techniques, such as coronary artery bypass grafting, are only suitable for patients with blocked coronary arteries, which is a subset of heart failure patients. Surgical approaches are also associated with a high risk of mortality. Pharmacological methods are also associated with high mortality, with 12-month survival rates less than 25% [6], [7]. Mechanical therapy involves implantation of a device into the patient to pump blood around the body, and offers improved survival rates over pharmacological treatment [6]. The two main types of mechanical devices are ventricular assist devices (VADs) and total artificial hearts (TAHs).

Total artificial hearts are devices designed to completely replace the two failed ventricles. First generation TAHs (CardioWest and Abiocor) are pulsatile pumps whose percutaneous pneumatic drivelines (CardioWest) and large size (Abiocor) limit their use to date [8]. On the other hand, VADs are designed to be implanted without removing the native ventricle, making them smaller than TAHs. Ventricular assist devices assist a failing ventricle pump blood around the body, and have been shown to improve patient outcomes over pharmacological methods [6].These pumps can assist the left ventricle (LVAD), right ventricle (RVAD) or both ventricles simultaneously (BiVAD).The use of rotary blood pumps as opposed to pulsatile blood pumps has resulted in longer support durations and improved patient outcomes due to their smaller size, higher efficiency and smaller power consumption [9].

The majority of VAD patients receive only an LVAD, however there are a number of patients who develop right ventricular failure post-operatively and therefore require biventricular support. It is difficult to determine an exact proportion, with the range reported in literature between 5 and 50% [10]–[15]. The lack of a commercially available rotary RVAD has led to clinicians implanting two rotary LVAD as an ad hoc biventricular assist device [16]–[19]. Despite some reported success, clinicians report difficulties in setting appropriate pump speeds in this configuration in order to achieve balance

between systemic and pulmonary flows [16], [18]. Without careful flow balancing, there is a higher risk of complications, such as pulmonary congestion or ventricular collapse.

Flow balancing can be achieved by manual variation of pump speed under the guidance of echocardiography. However, frequent adjustments must be made. Saito et al. (2011) reported daily adjustments of speed in the immediate postoperative period [18]. Furthermore, as the patient's condition improves and they become more active, corresponding changes in the patient's circulatory system may disturb the flow balance previously established by the clinician in the acute care setting. This may limit their capacity to perform everyday tasks. As the current approach to setting pump speeds is one of "set and forget", an automatic control system for pump speed could improve the quality of life of patients by ensuring balanced flow. This control system should adjust pump flows in a physiological manner similar to the native heart, because that is what the human body expects.

Development of a physiological control system for dual LVADs requires knowledge of the limitations of current operating modes for these devices, in order to identify how much control action is necessary to restore balance between flows. Clinicians have proposed a number of different operating modes, which need to be compared using the same testing protocol in order to establish their advantages and disadvantages. Particularly, the ability of these operating modes to handle transient changes in vascular resistance should be assessed.

The control system for dual LVADs will be complex due to the use of multiple input and output control variables. Logically, development could be aided by the development of a physiological control system for a single LVAD. Provided that the single LVAD control system has been evaluated thoroughly, it could possibly be adapted for dual LVAD use.

Development and assessment of physiological control systems for rotary LVADs initially occurs in the low-cost in-silico and in-vitro environments before moving onto the more expensive in-vivo and clinical environments. To reduce the quantity (and therefore expense) of in-vivo trials, and to ensure maximum safety of participants in clinical studies, in-silico and in-vitro evaluation must be thorough. Therefore, a robust and comprehensive evaluation protocol must be developed.

1.1 Aim and Objectives

The aim of this thesis is to design and evaluate a physiological control system for a dual rotary LVAD system operating as a BiVAD. In order to meet this aim, the following objectives were devised.

1. Investigate the different operating modes of dual rotary LVADs as a BiVAD that have previously been presented in literature.
2. Develop an evaluation framework for in-vitro assessment of physiological control systems.

3. Develop a physiological control system for a rotary LVAD control system and evaluate using the evaluation framework.
4. Modify the rotary LVAD physiological control system into a BiVAD physiological control system and assess using the evaluation framework.

1.2 Background

Development of a suitable rotary BiVAD control system requires knowledge of the cardiovascular system. The following section provides the reader with background knowledge required for understanding of the topic. It encompasses descriptions of the anatomy and physiology of the human heart and circulatory system, heart failure and its prevalence, and treatment of heart failure using VADs. The information that follows is an overview, and more detail can be found in references [20]–[22].

1.2.1 The Human Heart and Circulatory System

The human heart consists of left and right sides. The left side of the heart pumps oxygenated blood to the various tissues throughout the body via the systemic circulation, while the right side of the heart delivers deoxygenated blood to the lungs via the pulmonary circulation. Each side of the heart consists of two chambers, an atrium and a ventricle, connected with one-way atrioventricular valves. The ventricles produce the majority of force required to propel blood through the circulatory system, while the atria act as primer pumps to assist with ventricular filling. Figure 1.1 shows the anatomy of the human heart in detail.

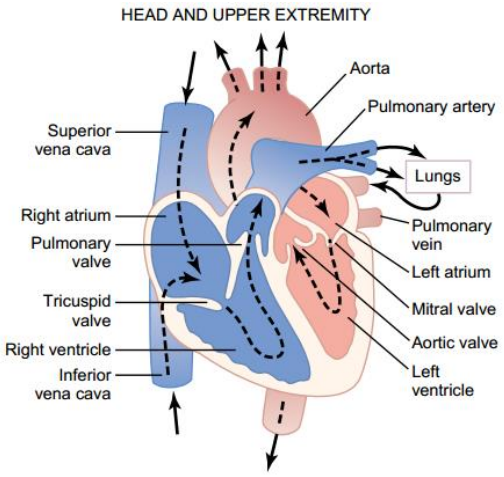

Figure 1.1: Anatomy of the human heart [20].

Figure 1.2 shows the pathway of blood through the heart and circulatory system. Deoxygenated blood flows from the systemic venous circulation into the right atrium (RA) via the superior and inferior vena cava. This blood moves into the ventricle via the tricuspid valve when the ventricular muscle is relaxed. When the ventricular muscle contracts, the deoxygenated blood is ejected from the right ventricle (RV) into the pulmonary artery (PA) via the pulmonary valve. The blood is oxygenated as it passes through the pulmonary circulation before returning to the left atrium (LA). Blood then passes through the mitral valve into the left ventricle (LV), before being ejected into the aorta via the aortic valve. Blood then passes throughout the systemic circulation, delivering oxygen to muscles and organs, before returning to the RA via the vena cavae to begin the cycle again.

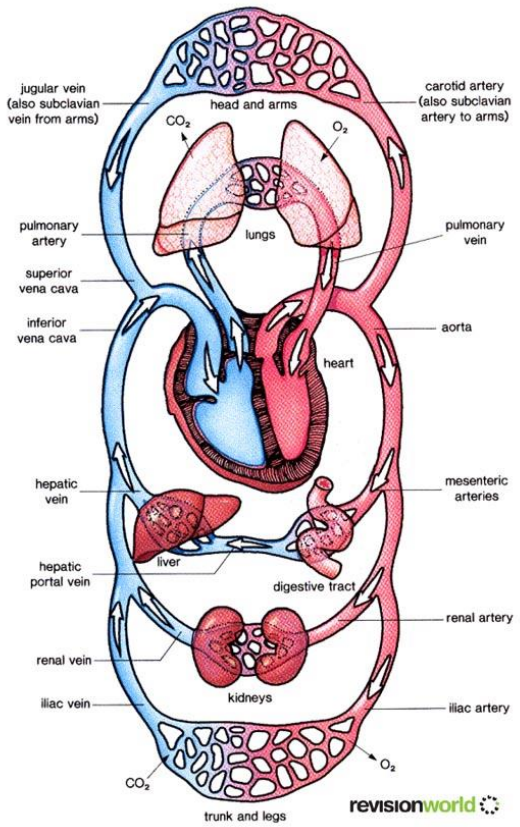

Figure 1.2: Human Circulatory System [23]

1.2.2 The Cardiac Cycle

Cardiac muscles undergo a period of contraction (systole) and relaxation (diastole) each heartbeat. During diastole, the ventricles fill with blood, while in systole blood is ejected. The period encompassed by one contraction and one relaxation is referred to as the cardiac cycle. Figure 1.3 shows typical LV, LA and systemic arterial pressures during the different phases of the cardiac cycle.

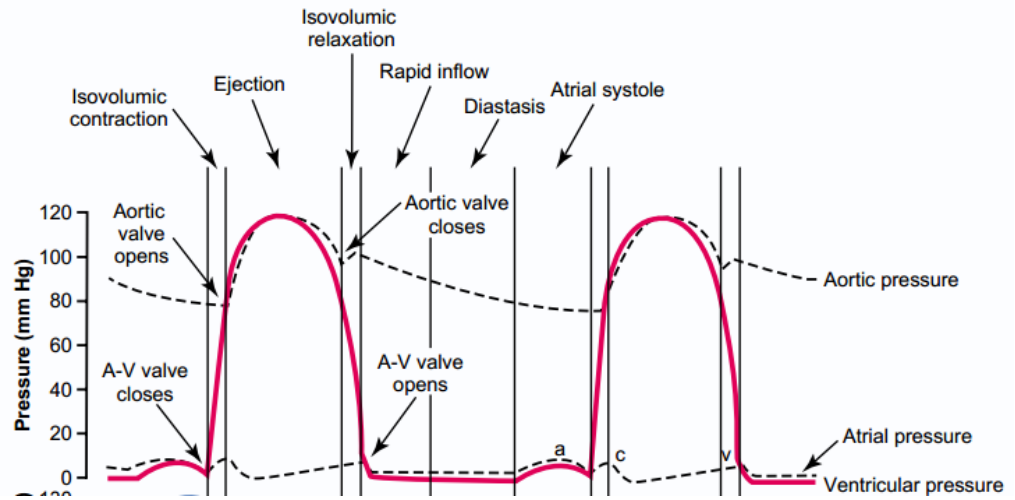

Figure 1.3: Aortic, left atrial and left ventricular pressure waveforms during the cardiac cycle [20].

The cardiac cycle can be further divided into four distinct phases. In Phase I, ventricular filling, venous blood moves from the atria into the ventricles via the atrioventricular valves, until the intraventricular pressure equals the atrial pressure. There are three distinct stages of filling. In the first stage of filling, the ventricles rapidly fill with blood, due to the pressure difference between the atrium and the ventricle at the end of systole. During the next stage (diastasis), venous blood still returning from the veins flows directly into the ventricle. Towards the end of ventricular diastole, contraction of the atria forces even more blood into the ventricle. During Phase 1 the ventricular muscle is relaxed, resulting in an increase in ventricular volume but only a small increase in intraventricular pressure. The relationship between intraventricular volume and pressure during this phase is known as the end-diastolic pressure-volume relationship (EDPVR). An example of an EDPVR is the lower blue line in Figure 1.4.

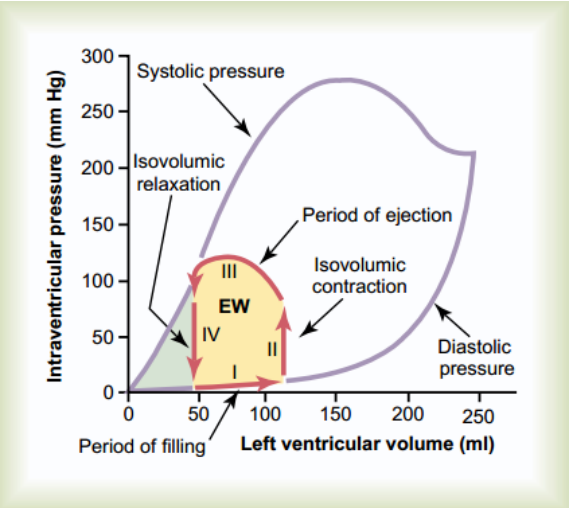

Figure 1.4: Left ventricular pressure and volume during the four phases of the cardiac cycle (red line). The blue lines show examples of end-systolic pressure-volume and end-diastolic pressure volume relationships [20]**.**

Phase II, isovolumic contraction, is the beginning of systole. In this phase the ventricular muscle contracts, causing a rapid increase in intraventricular pressure. However, the ventricular volume remains unchanged. This is because the one-way atrioventricular valves are closed, preventing backflow into the atria, while the aortic and pulmonary valves (also referred to as the semilunar valves), remain closed because the intraventricular pressure remains below the arterial pressure. This phase is quite short, as it only takes about 0.02-0.03 seconds for the ventricles to build up enough pressure to open the semilunar valves.

Phase III, ejection, begins when the intraventricular pressure rises above arterial pressure (above 80mmHg for the aorta and 8mmHg for the pulmonary artery), which enables blood to be ejected from the LV into the aorta and from the RV into the PA. Initially the intraventricular pressure continues to rise after the semilunar valves open because the ventricle is still contracting. Eventually the

intraventricular pressure peaks and begins to fall as blood is ejected from the ventricle. The end of this phase occurs when the intraventricular pressure falls below the arterial pressure. The relationship between intraventricular pressure and volume at the end of this phase is referred to as the end-systole pressure-volume relationship (ESPVR). An example of an ESPVR is shown by the upper blue line in Figure 4.

Finally, in Phase 4, isovolumic relaxation, the ventricular cardiac muscle relaxes, resulting in a rapid drop in intraventricular pressure. The elevated arterial pressure forces blood back towards the ventricles, which snaps the semilunar valves shut. The volume remains constant in this phase because the intraventricular pressure is greater than the atrial pressure, preventing the atrioventricular valves from opening. At the end of this short phase (0.03 to 0.06 seconds) the intraventricular pressures return to their low diastolic levels and the cardiac cycle begins again.

1.2.3 The Frank-Starling Law of the Heart

The strength of ventricular muscle contraction during systole is proportional to the volume of blood that fills the ventricle during diastole. This phenomenon is known as the Frank-Starling mechanism, and ensures that the ejected volume is proportional to the venous return[24]. The explanation for this phenomenon is that when the end-diastolic volume increases due to increased venous return, the cardiac muscle fibres are stretched further than normal. Like all striated muscle, higher pre-tensioning moves the myosin and actin filaments of the cardiac muscle closer to the optimal position for force generation. The result is that the muscle contracts with increased strength during the following period of systole.

Essentially, the Frank-Starling mechanism ensures that the heart pumps all the blood that is returned to it from the veins (within physiological limits) [20]. This means that cardiac output (CO) becomes dependent on the intraventricular end-diastolic pressure, or preload, as shown by the CO curves in Figure 1.5. This relationship is also referred to as preload sensitivity.

High preload sensitivity is essential because preload changes with venous return, which in turn varies with patient activity. For example, standing up from a supine position causes increased pooling of blood in the systemic venous circulation, which reduces preload to the right ventricle [25], [26].The reduced preload results in reduced RV stroke volume, ensuring that ventricular outflow matches inflow and therefore preventing the ventricle from emptying completely. Conversely, during exercise muscles contract around the veins, squeezing blood back to the right atrium and thereby increasing preload [20]. Healthy ventricles respond to this by increasing the strength of their contractions, forcing more blood out of the ventricle and therefore matching the increased venous return, preventing damming of venous blood in the atria.

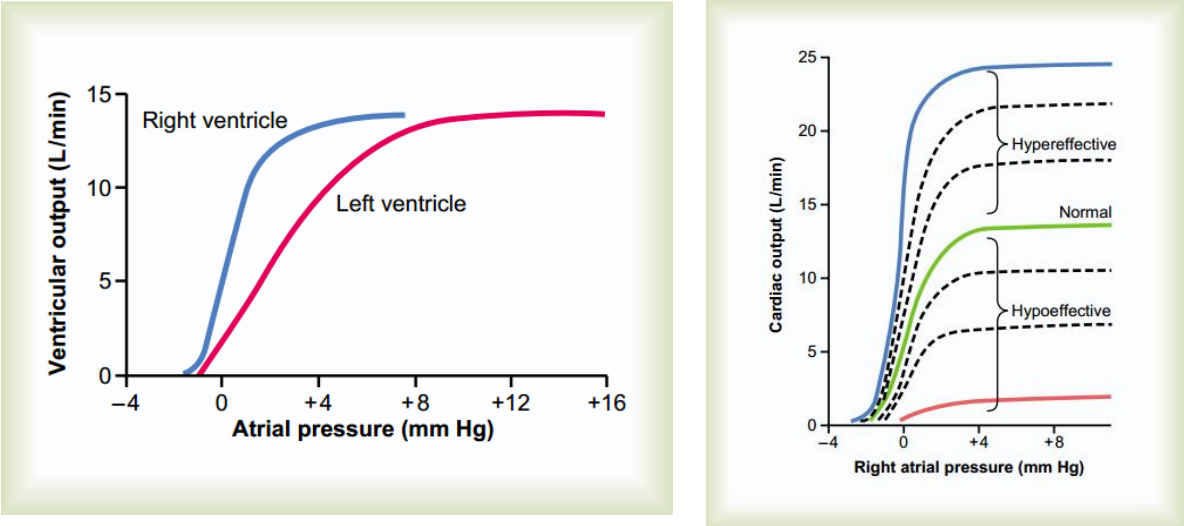

Figure 1.5: Cardiac output curves, which show the relationship between left and right ventricular output and preload as a result of the Frank-Starling mechanism (left). The sensitivity of cardiac output to preload and the maximum cardiac output increase with sympathetic nervous stimulation of the heart, and decrease with heart failure (right)[20].

It is important to note that no single curve describes the relationship between CO and preload. Instead, a family of curves is used. The slope and maximum flow rate of the curves shown in Figure 1.5 (left) varies with changes in contractility, caused by sympathetic and parasympathetic stimulation (Figure 1.5, right). The slope and maximum cardiac output are also diminished in heart failure.

1.2.4 Heart Failure

Heart failure describes any condition that prevents the heart from pumping adequate blood flow to peripheral organs and tissues, preventing them from receiving sufficient oxygen[20]. Some common causes of HF include myocardial infarction, coronary artery disease, chronic hypertension, valve disease and idiopathic cardiomyopathy [21]. Regardless of the cause, the effect of heart failure is that the pumping ability of the heart is severely depressed. This results in a reduced preload sensitivity, leading to damming of venous blood in the right atrium, and a reduced maximum cardiac output.

Reduced cardiac output means that oxygen supply to vital organs such as the kidneys, brain and liver is also reduced. In order to restore CO to 5 L/min, compensatory mechanisms are activated by the body. These mechanisms, activated by sympathetic nervous stimulation, include increased heart rate and contractility (where possible) to directly increase CO, and increased venous tone to increase preload and indirectly increase CO via the (albeit damped) Frank-Starling mechanism[20].

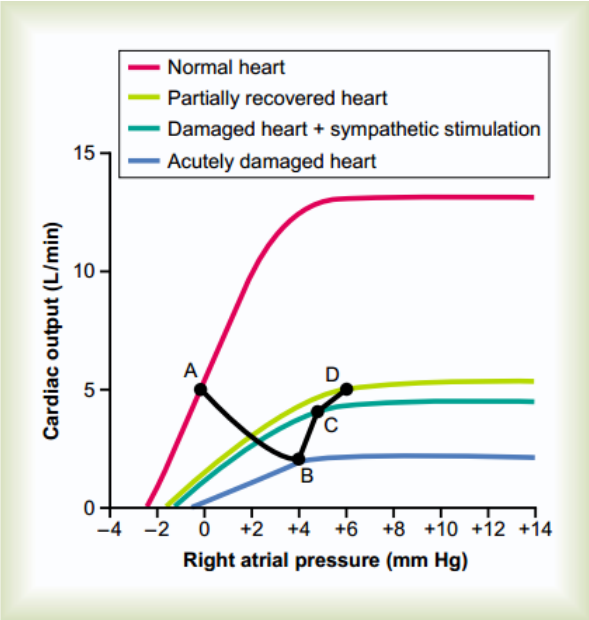

Figure 1.6: Variation of the cardiac output curves during various stages of heart failure.

The compensatory sympathetic stimulation of heart rate and contractility cannot be maintained for extended periods of time. The failure of the pumping function of the heart results in an increase in preload and therefore an increase in stroke volume. Consequently, there is partial restoration of CO at the expense of increased LAP/RAP. This highlighted in Figure 1.6, which shows the changes in CO curves before HF (red), during initial onset of HF (blue), after sympathetic nervous stimulation (dark green) and after further recovery (light green). The black points show the steady-state condition of the patient's CO and right atrial pressure. Even with compensatory mechanisms activated the slope and maximum value of the CO curve are both severely diminished. In order to restore CO to 5 L/min, the right RA pressure has to increase dramatically. The result is that when at rest, the patient may not exhibit signs of heart failure other than an elevated RA pressure. However, the depressed maximum cardiac output caused by heart failure means that the exercise capacity of these patients is limited. These patients therefore have a lower quality of life than their healthy counterparts. Appropriate treatment is necessary to increase the duration and quality of life of HF patients.

HF can be treated surgically, pharmacologically or mechanically. Over the last thirty years mechanical therapy has become a viable HF treatment worldwide due to advances in blood pump technology.

1.2.5 Treatment of Heart Failure using Mechanical Therapy

Treatment of heart failure using mechanical therapy can be achieved using three types of devices: intra-aortic balloon pumps (IABPs), ventricular assist devices (VADs) or total artificial hearts (TAHs). Intra-aortic balloon pumps are one of the most commonly used cardiac assist devices in the world [27]. These devices unload the LV, increase cardiac output and improve coronary flow in patients with acute HF. However, these devices are not suitable for patients with chronic end-stage HF [28]. Furthermore, these devices are associated with an average complication rate of 20-30%, making them suitable for short term use only[29]. TAHs are devices designed to completely replace a failing heart, and are therefore only targeted towards patients with severe HF. Commercially available TAHs are large and difficult to implant in small patients, further limiting their application [30]. VADs are pumps designed to mechanically assist a failing ventricle of the heart pump blood around the human body, and can support the left ventricle (LVAD), right ventricle (RVAD), or both ventricles simultaneously (Figure 1.7).

Mechanically unloading the ventricles using VADs was proven by Rose et al. (2001) to have better 12 month survival rates than optimal medical management alone (52% vs. 25%) [6]. Ventricular assist devices can be used to treat a wide variety of patients due to their small size, and have mechanical life spans ranging from 12 months to over 6 years. For these reasons, VADs are now an established method of treating HF patients, and have been used as a bridge-to-transplant, bridge-to-destination (for patients ineligible for a transplant) and, in some rare cases, as a bridge-to-recovery.

1.2.6 Generations of Ventricular Assist Devices

VADs are classified as first, second and third generation devices according to their mode of operation [32]. Examples of the three different generations are shown in Figure 1.8.

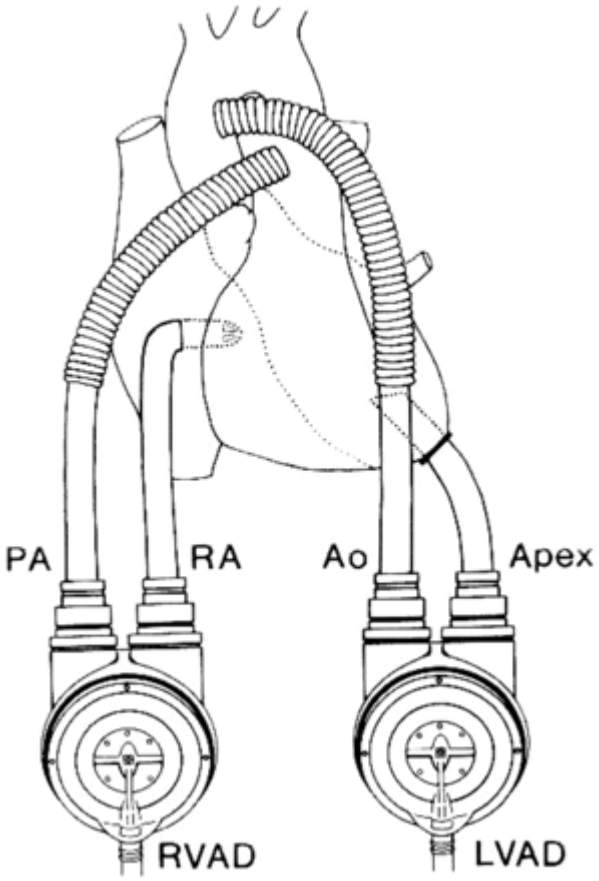

Figure 1.7: Left ventricular assist device (LVAD) connected between the left ventricle and the aorta, and a right ventricular assist device (RVAD) connecting the right atrium and the pulmonary artery[31].

Figure 1.8: Examples of first, second and third generation ventricular assist devices. Left: PVAD (Thoratec Corporation, Pleasanton, CA, USA). Middle: HeartMate II (Thoratec Corporation, Pleasanton, CA, USA). Right: HVAD (HeartWare Inc., Massachusetts, USA).

First generation VADs are volume displacement pumps (commonly referred to as pulsatile pumps in the literature), whose pumping mechanism is similar to that of the native ventricle. These devices were designed with the intention of delivering a pulse to the circulatory system in order to replicate normal physiological flow. To meet this requirement, these devices incorporated electrically or pneumatically actuated diaphragms or pusher plates[22]. Most of these pumps were paracorporeal due to their large size, and thus utilised percutaneous cannulae and drivelines which placed limitations on the quality of life of the recipient. Another major complication is that their multiple moving parts result in a short mechanical lifespan, with expected device failure rate between 35 and 64% after 24 months[6], [33], [34]. Other reported complications with first generation devices include abdominal complications and infections caused by percutaneous driveline and/or cannulae [35], [36]. Despite the improvement in survival rates over medical management, the disadvantages of first generation VADs limit support duration as well as patient quality of life.

Second generation VADs are rotary pumps, which have improved upon the aforementioned shortcomings of first generation VADs. Unlike pulsatile VADs, rotary VADs deliver a continuous flow of blood to the circulatory system. These VADs are either axial or centrifugal rotary blood pumps (RBPs), consisting of a rotating impeller providing forward flow of blood with few moving parts. In second generation VADs, the impeller is suspended using a mechanical bearing, such as a pivot bearing. These devices significantly improve patient haemodynamics and quality of life when compared to first generation VADs [9], [37]–[39]. However, the use of mechanical bearings and seals is associated with increased thrombogenicity and acquired platelet dysfunction[40].

Third generation VADs are rotary pumps whose impeller is suspended using non-contact bearings, which eliminates some of the issues associated with second generation devices. These bearings can be hydrodynamic, magnetic or combinations of both[41].

The benefits of both second and third generation VADs have resulted in a steady increase in their usage over the last eight years, with the number of rotary LVAD implantations performed per year in the USA surpassing the number of heart transplants for the first time in 2009 [42]. Support duration has also increased, with some patients supported for over six years [43].

Most HF patients present with LV failure only, so implantation of a rotary LVAD is sufficient. However, patients with concomitant right heart failure do not benefit from only an LVAD and require biventricular support. Furthermore, the need for additional RV mechanical assistance post LVAD implantation is reportedly between 5 and 50% [10]–[15]. These patients could also benefit from biventricular support. Therefore, there is a need for mechanical biventricular assistance.

1.2.7 Dual Rotary Left Ventricular Assist Devices as Biventricular Assist Devices

The aforementioned advantages of rotary VADs have encouraged their use as LVADs over the last decade. However, biventricular support with rotary VADs is difficult because there are no commercially available rotary RVADs. There are some rotary BiVAD systems under development [44], [45], however it may be a long time before these devices are ready for clinical implantation. For this reason, clinicians have implanted two rotary LVADs as a BiVAD [16], [17], [46]–[48]. An example of this is shown in Figure 1.9. The small size of rotary LVADs enabled total implantation of both pumps, whilst their long durability has enabled long support durations and in some cases enabled rotary BiVAD patients to be discharged from the acute care environment [16].

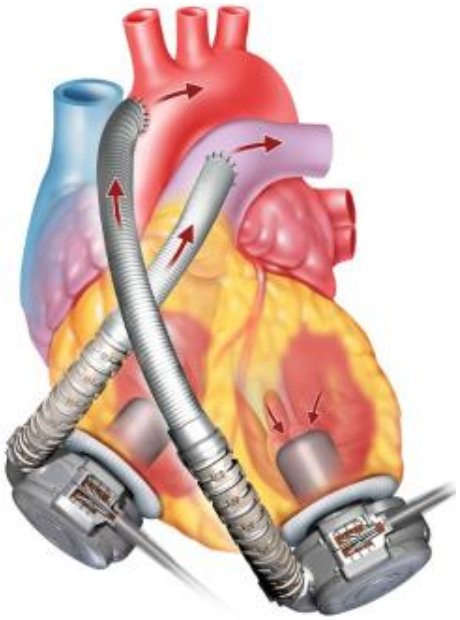

Figure 1.9: Two HeartWare HVADs (HeartWare Inc., Massachusetts, USA) implanted as a biventricular assist device [49]

Despite the aforementioned success of dual rotary LVAD systems, setting appropriate pump speeds in order to achieve balance between systemic and pulmonary flow is difficult[16], [18]. Without careful management of pump speeds and therefore flow rates, there is a higher risk of causing systemic or pulmonary oedema (flooding of the circulations). Flow management is performed by adjusting pump speeds under the guidance of echocardiography [50]. However, frequent adjustments must be made – Saito et al. (2011) report daily adjustments of speed in the immediate postoperative period [18]. Furthermore, as the patient's condition improves and they become more active, corresponding changes in the patient's circulatory system may disturb the flow balance previously established by the clinician in the acute care setting. This may limit their capacity to perform common daily tasks.

The main reason for the problem of balancing flows in a dual rotary LVAD system is that, unlike the native heart, rotary blood pumps do not have a Frank-Starling mechanism. In other words, the flow rate of blood is not as sensitive to preload as the native ventricle.

1.2.8 Preload Sensitivity of Rotary Ventricular Assist Devices

The sensitivity of a native healthy ventricles to changes in preload (the Frank-Starling law) was discussed in Section 1.2.3. It is the primary autoregulatory method of the ventricles and ensures that the volume of blood ejected each heartbeat (and consequently total flow rate) depends on the volume of blood that fills the ventricle. In contrast, when operated at a constant speed, the flow rate produced by a rotary VAD depends not on the pump preload (inlet pressure) but the difference between outlet and inlet pressure (effectively the differential between afterload and preload). Studies by Salamonsen et al.

[51] and Fukamachi et al. [52] have both shown that this difference in dynamics means that rotary pumps are less sensitive to isolated changes in preload than the native ventricle, and even pulsatile pumps, when operated at a constant speed (Figure 1.10). Supporting a failing ventricle, which already has a diminished preload sensitivity, with a device that has low preload sensitivity may result in the under- or over-pumping of blood from the ventricle. Under-pumping means that increased venous return caused by increased patient activity will not be compensated for by sufficient increase in VAD flow. This may result in excess venous blood damming up the atria, placing limitations on the patient's exercise capacity, and may lead to pulmonary or systemic venous congestions. On the other hand, over-pumping occurs when VAD flow exceeds venous return. This results in a reduction in ventricular volume. Excessive over-pumping can result in complete drainage of the ventricle, which causes collapse of the ventricle wall over the inlet cannula of the VAD in a phenomenon known as ventricular suction[53]. Suction may result in reduced forward flow of blood, haemolysis, ventricular arrhythmias and tissue damage at the VAD inlet cannula site [50], [53]–[56].In order to change pump flow rate more dramatically during significant preload changes, speed changes are required.

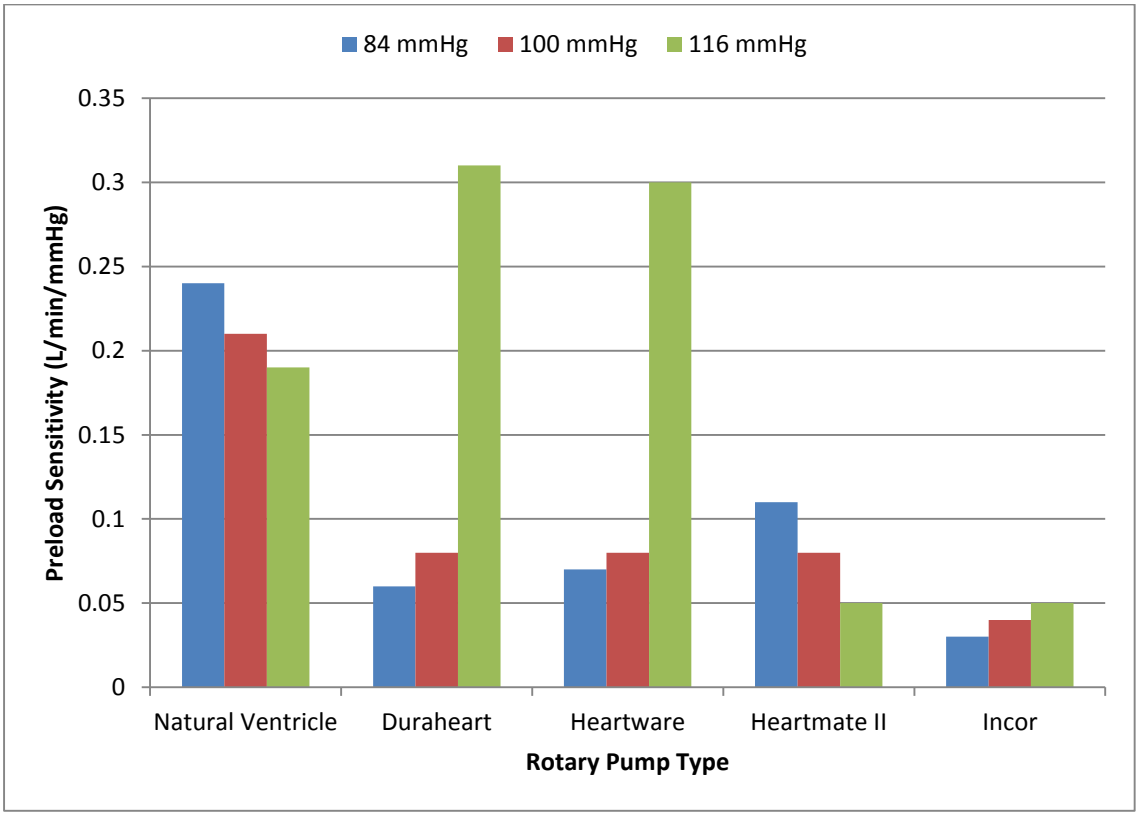

Figure 1.10: Preload sensitivity of the native left ventricle and some commercially available rotary VADs at three different afterloads. Data obtained from Salamonsen, Ayre and Mason (2011) [51].

Whilst the patient is in the acute care setting, speed changes can be performed under the guidance of echocardiography to minimise the risk of over- or under-pumping. However, VAD patients are commonly discharged home when their condition improves[57], [58].This means that the rotational

speed of their pumps remains fixed for longer periods of time. Discharged patients are also more active than their acute care counterparts, resulting in more variations in venous return as they undergo common patient scenarios. These two factors mean that discharged rotary BiVAD patients are more predisposed to ventricular suction and flow imbalance. There is clearly a need for a control system that can automatically vary the speed of both pumps to meet these criteria.

1.2.9 Physiological Control of VADs

Physiological control systems for rotary LVADs are designed to automatically adjust LVAD output in order to prevent ventricular suction and to match LVAD flow to meet cardiac demand. Significant research has been conducted in the field of rotary LVAD control, however little of this research has been extended into the control of dual LVADs. Literature reviews of LVAD and BiVAD control systems are presented in Chapters 4 and 5 respectively.

Boston, Antaki and Simaan (2003) highlighted three design criteria that should be fulfilled by an LVAD physiological control system[59], based on discussions with clinicians in their institute. These criteria are

- Cardiac output should be above the minimum value (usually between 3-6 $L.min^{-1}$) required to support the activity level of the patient
- Left atrial pressure (LAP) should be maintained below 10-15 mmHg to avoid pulmonary oedema and above 0mmHg to avoid suction.
- Systolic arterial pressure should be maintained between patient specific limits to limit sensitivity to afterload.

Given that arterial pressure is predominately modified pharmacologically, a physiological control system for an LVAD should adjust pump speed primarily to maintain preload within a reasonable range whilst ensuring suitable cardiac output. BiVAD control systems should also meet these criteria as well as the equivalent criteria for pulmonary circulation. Therefore, right atrial pressure (RAP) should be subject to the same criteria as left LAP, whilst pulmonary arterial pressure (PAP) should be maintained between patient limits like aortic pressure (AoP).

A physiological control system that can automatically adjust the speed of both pumps to maintain balanced flows would improve the survivability, quality of life and exercise tolerance of dual rotary LVAD patients who are discharged home. Design and testing of such a system requires an appropriate evaluation environment.

1.2.10 Evaluation of Control Systems for Ventricular Assist Devices

Prior to their approval for clinical use, control systems for VADs require thorough performance evaluation in order to prove their efficacy. This section briefly summarises the testing apparatus used

for evaluation of rotary LVADs and their control systems. A literature review of the tests used to quantify control system performance is given in Chapter 3.

1.2.10.1 In-silico evaluation

Preliminary control system design and evaluation is performed in-silico, using a numerical model (NM) of the circulatory system. Numerical models used for control system evaluation commonly represent the circulatory system using lumped parameter models (Figure 1.11). Sections of the circulation are lumped together and given a single value for vessel resistance (R), compliance (C) and inertance (L). These values are represented using the electrical analogues of resistance, capacitance and inductance respectively. Flow and fluid pressure are represented as electrical current and voltage respectively. Each lumped element is effectively a second-order RLC circuit.

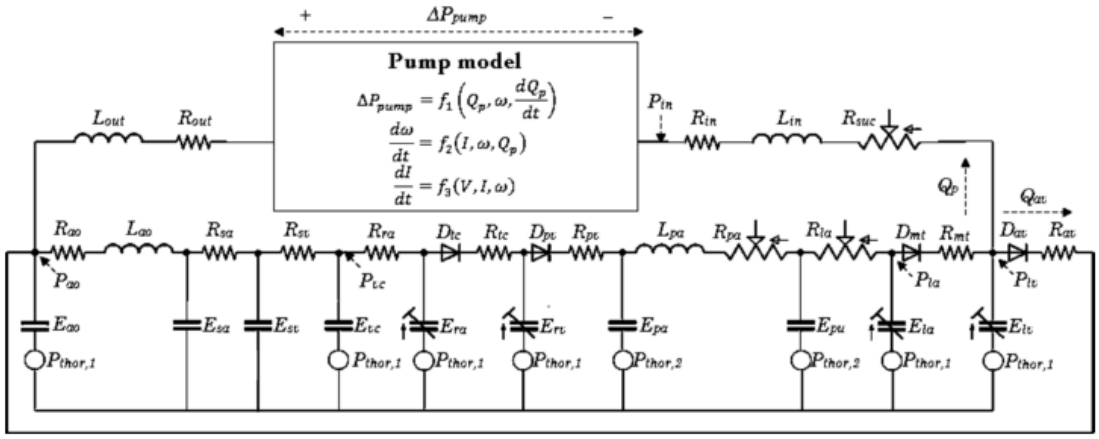

Figure 1.11: Example of a lumped parameter model of an LVAD and the cardiovascular system [60]**.**

The heart chambers are modelled in a slightly more complex manner. Each chamber is modelled with its own RLC circuit. The compliance is variable, with time-varying elastance theory used to represent changes in ventricular and atrial wall stiffness during the cardiac cycle. Briefly, the pressure-volume relationship within each heart chamber is modelled using Equation (1.1).

$$P(t) = e(t)P_{es} + \big(1 - e(t)\big)P_{ed} \tag{1.1}$$

where P(t) represents the intraventricular pressure, P_{es} the end-systolic pressure, P_{ed} the end diastolic pressure and e(t) the time varying elastance function. This function enables transitions from end-diastolic pressure to end-systolic pressure in a manner similar to the native heart and is independent of preload and afterload [61], [62] (Figure 1.12).

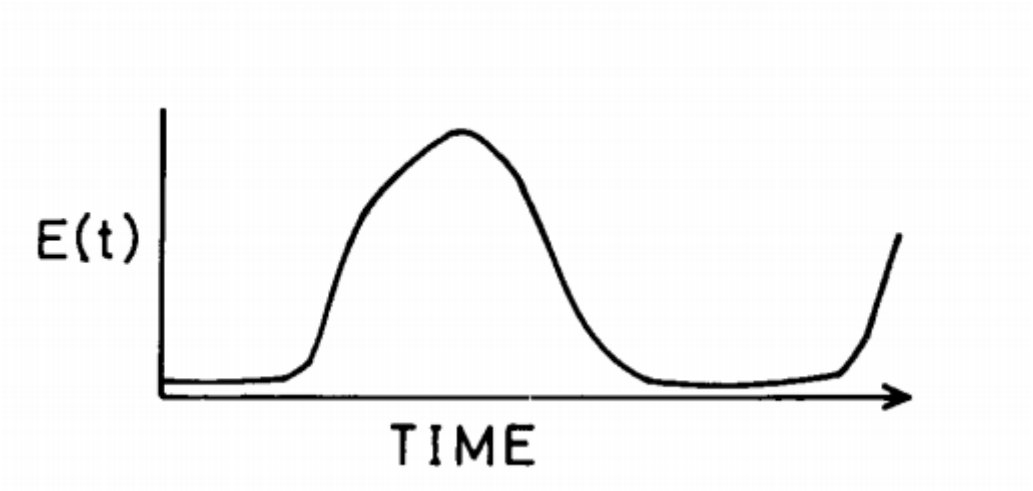

Figure 1.12: Example of a time-varying elastance function [63]

Both P_{es} and P_{ed} are calculated as functions of ventricular volume, known as end-systolic (ESPVR) and end-diastolic (EDPVR) pressure volume relationships respectively. Figure 1.13 shows an example of ESPVR and EDPVR curves. The ESPVR is usually linear, with the slope dictating the inotropic state of the heart. Changes to ESPVR are used to change the inotropic state of the heart independently of preload, therefore enabling simulations of heart failure (reduced ESPVR) or exercise (higher ESPVR). Diodes are placed between atrial and ventricular circuits and between ventricular and arterial circuits to simulate the function of the heart valves to complete the simulation of the native heart.

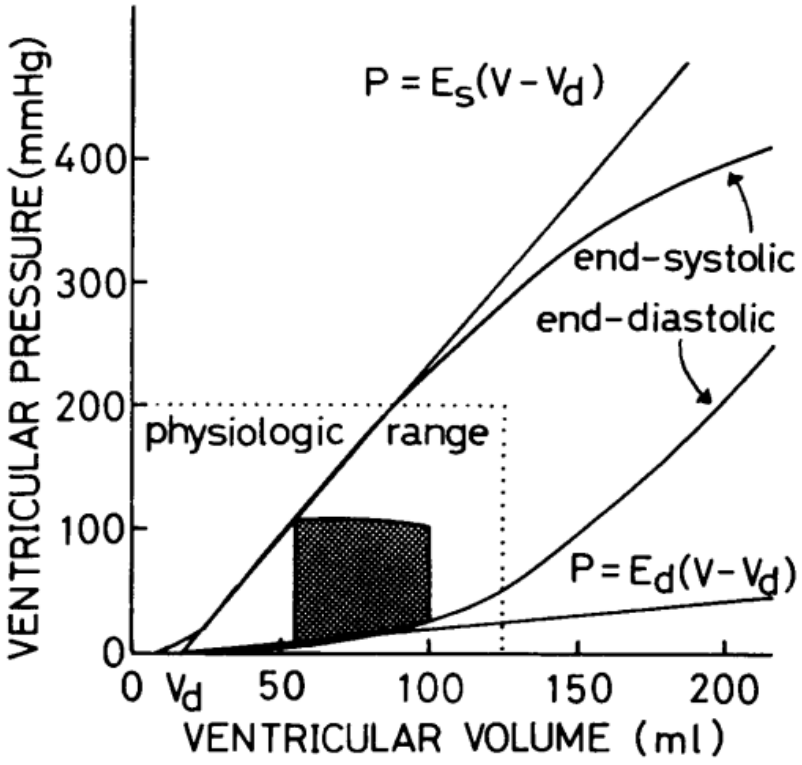

Figure 1.13: Example of end-systolic (E_s) and end-diastolic (E_d) pressure-volume relationshitionships used in in-silico modelling of heart chambers [63]**.**

Since the numerical model is a combination of lumped elements, the model order is governed by the total number of lumped elements. Thus model complexity can be scaled by increasing or reducing the number of lumped elements. The higher the complexity, the higher the model accuracy but the longer the time it takes to solve and the more difficult the control design. Conversely, over-simplification decreases simulation time but results in less accuracy and can result in poor control system design.

One advantage of using numerical models for control system evaluation is that all individual circulatory parameters can be varied precisely. This enables detailed and quantitative understanding of low-level control system behaviour for a variety of circulatory conditions. This environment is therefore ideal for evaluating typical control system characteristics, such as rise and settling times, overshoot and steady state error. Additionally, numerical models provide a safe environment for control system design and development. Failure modes and design flaws can be identified and corrected quickly before moving to in-vitro or in-vivo evaluation, where the consequences of failure can be costly. One key limitation of numerical models is the difficulty of modelling rotary pump dynamics in-silico. The dynamic effects of the pump must be isolated from those of the circulatory system and pump cannulae. Only then can these components be independently varied in order to reflect the inter-patient differences in circulation dynamics, cannula length, and inflow/outflow cannula placements. Finally, another limitation of most models is that inclusion of more complex phenomena such as non-linear vessel wall compliance increases model complexity and therefore computation time.

1.2.10.2 Mock Circulation Loops

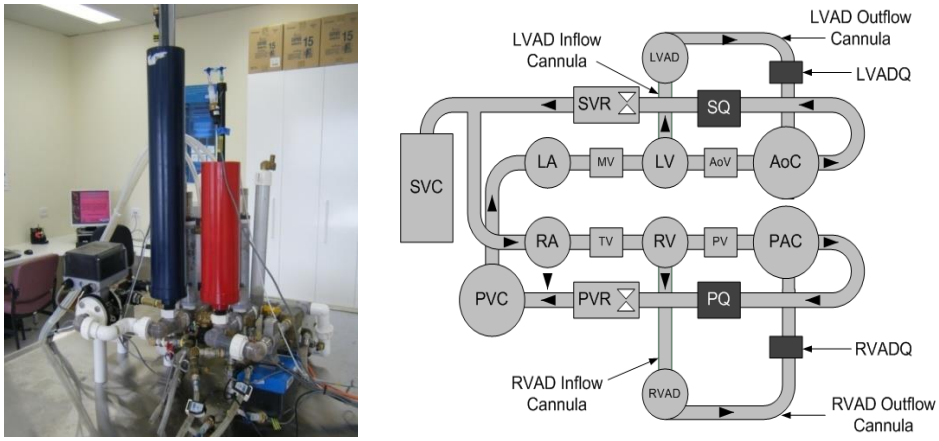

Figure 1.14: Mock circulation loop (left) and schematic (right), located at The Prince Charles Hospital [64].

After control system evaluation in the NM, the system is usually next simulated in a bench top environment using a mock circulation loop (MCL). Like numerical models, MCLs are lumped parameter models. However, MCLs are mechanical rather than mathematical representations of the heart and circulatory system. An example of a MCL is shown in Figure 1.14.

Mock circulation loops incorporate time-varying elastance theory to simulate the changes in ventricular wall stress. Early MCLs did not actively replicate the Frank-Starling mechanism of the heart, so the preload sensitivity of these models were very low. More recently, preload-sensitive ventricluar contraction has been incorporated, ensuring that the pressure-volume relationships were similar to those modelled numerically.

One advantage of MCLs include the ability to test control systems using real pumps, which means that the effect of practical issues such as actuator limits and non-linearities on the control system can be evaluated. Additionally, as pump dynamics are difficult to model in-silico, in-vitro evaluation is required to gain a true understanding of system behaviour. The use of a bench top testing rig allows realistic analysis of pump control systems without the difficulties and risks associated with animal or human studies. Like numerical models, repeatability is high and some parameters can be easily controllable. However, one disadvantage is that it is generally difficult to vary the compliance in the loop, limiting the number of scenarios that can be simulated. Additionally, the cost and difficulty of adding more lumped elements to the system is greater in the MCL than in NM due to the mechanical nature of the system.

1.2.10.3 In-vivo Models

Unlike in-silico and in-vitro evaluation, in-vivo evaluation involves testing a VAD control system using an animal model. Sheep, goats and cows are the most commonly used. The main advantage of in-vivo evaluation is that the controller's effect on real, not simulated, haemodynamics can be assessed. This is an essential step before a controller can be clinically accepted. However, in-vivo studies are expensive. Long term recovery studies are more expensive than short-term acute studies because of the staff and equipment requirements. In-vivo experiments are also highly variable, due to the natural differences between animals. This is more reflective of the variable nature of clinical evaluation, however it makes it difficult to consistently characterise control system performance. Another disadvantage of in-vivo studies is that models of heart failure are difficult to obtain in a stable and reproducible manner, and extreme conditions cannot be tested without loss of the animal. Therefore, in-vivo evaluation should primarily be used to confirm control system performance already established in-silico and in-vivo, and to assess effects of systems on haemolysis, thrombosis and survivability.

1.2.10.4 Clinical Trials

Clinical trials are necessary in order for physiological control systems to gain regulatory approval and therefore be incorporated into medical devices. These trials are useful for established long term efficacy and benefits of physiological control systems. However, these trials are expensive and are inherently high-risk due to the use of human subjects.

1.3 Thesis Outline

The structure of this thesis closely follows the aims outlined in Section 1.1.

Chapter 2 describes the evaluation of current methods of dual LVAD operation. It highlights that while all current methods of dual LVAD operation can produce stable steady-state haemodynamics, speed changes are required to maintain pulmonary and systemic flow during changes in vascular resistance. This chapter sets the scene for the remainder of the thesis. This chapter is based on the publication "In-vitro and in-vivo characterisation of three different modes of pump operation when using an LVAD as an RVAD" in the scientific journal Artificial Organs.

A physiological control system may be able to automatically adjust the speed of both pumps to accommodate changes in the circulatory system. Before development of such as system can commence a suitable evaluation framework must be established. **Chapter 3** describes the methodology that was used to assess both LVAD and BiVAD control systems developed throughout the thesis. It summarises previous methods of control system evaluation and justifies the case for more thorough, quantitative comparison.

There has been significant work in the field of physiological control of rotary LVADs, and it may be possible to adapt one of the better performing single-LVAD control systems for use in a dual LVAD. However, inconsistent evaluation techniques between investigators means that direct comparison of controllers from literature is not possible. **Chapter 4** describes the comparison of a number of control systems from literature using the evaluation framework established in Chapter 3. The result of this chapter is an experimental justification of the LVAD control system adapted for use in Chapter 5.

The best control system determined from the experiments in Chapter 4 was modified to become a physiological control system for dual LVAD operation. The design and evaluation of this controller is discussed in **Chapter 5.**

Chapter 6 brings together the final conclusions from all chapters, highlights some of the limitations of this thesis and makes recommendations for future work.

2 Current Operating Modes of Dual Left Ventricular Assist Devices

The success of implantable rotary LVAD support, in conjunction with a lack of a clinically available long-term rotary implantable RVAD, has led to clinicians using dual implantable rotary LVADs in order to achieve long term biventricular support. Three methods of adapting an LVAD for right ventricular support have been proposed in literature. These are operating the right pump at a lower speed than the left pump, operating both devices at their design speeds while relying on the cardiovascular system to adapt, and operating both pumps at their design speeds while restricting the diameter of the RVAD outflow graft. These three methods have been used clinically, however their effects on haemodynamics have yet to be compared experimentally.

The purpose of this chapter is to investigate how clinicians have previously managed dual LVAD operation in the clinical arena. The chapter begins with a review of the literature surrounding this field, which identifies three different operating modes. These three modes are then compared using a mock circulation loop and an acute non-recovery animal model in order to determine their effects on aortic pressure, left atrial pressure and cardiac output.

The significance of this chapter is that it presents a thorough comparison of the three modes of operation of dual rotary LVADs for the first time. Clinicians can use the findings from this experiment to aid in identifying which approach is best for their patient. Another significant finding in this chapter is that it establishes that there is a need for physiological control systems for dual rotary blood pumps.

The work completed in this chapter has been published as a manuscript entitled "In-vitro and in-vivo characterisation of three different modes of pump operation when using an LVAD as an RVAD" in the scientific journal Artificial Organs (published online March 26 2014). The methods and results of this chapter were taken directly from that publication. The introduction was extended to provide the reader with more background information, and the conclusion extended to provide context for this thesis.

2.1 Aim

The aim of this chapter was to assess the ability of current modes of operation of dual LVADs with respect to restoring resting patient haemodynamics and responding to transient changes in pulmonary vascular resistance (PVR) and preload. To meet this aim, a number of objectives were devised.

- Review the literature regarding clinical and experimental use of dual LVADs as a BiVAD
- Compare current operating modes in-vitro.
- Compare current operating modes in-vivo.
- Make recommendations for each mode, and highlight areas where physiological control may improve functionality.

2.2 Literature Review

The first reported use of dual rotary LVADs as a BiVAD was by Frazier et al. (2004) who implanted two Jarvik 2000 LVADs (Jarvik Heart Inc., New York, NY, USA) [40]. The right pump was implanted because RV function worsened after LVAD-only support. The patient only lived for 12 days post-implant, but the authors suggest that earlier RVAD implantation may have benefitted the patient. Device speeds were not mentioned in this paper. Since then, dual rotary LVADs have been used numerous times to provide biventricular assistance.

In many of these cases, the functionality of both ventricles can be severely reduced, or sometimes non-existent. Consequently, the flow balancing ability of the ventricles is reduced because of their diminished Frank-Starling response. Therefore, management of left and right pump speeds is important to prevent ventricular suction or venous congestion. Three different management strategies have emerged.

2.2.1 Mode 1: RVAD speed lower than LVAD design speed.

Adaptation of an LVAD for RV support may require reduction of the output power relative to the left pump. The simplest way that this can be achieved is by operating the RVAD at a speed lower than the design speed. This results in a lower flow rate for a given differential pressure. This section summarises all clinical and experimental reports of this mode of operation.

Dual Jarvik 2000 support was performed by Saito et al.(2011)[19]. Initially LVAD and RVAD speeds were set to 10 000 and 7 000 RPM respectively. As the minimum speed of the Jarvik 2000 pump is 8 000 RPM, a custom pump controller was manufactured in order to reach the lower RVAD speed. During the initial post-operative period, left and right pump speeds were adjusted frequently under the guidance of echocardiography. After extubation, the patient's PVR fell, resulting in a sudden increase in right pump flow rate. A reduction in RVAD speed to 6 000 RPM and an increase in LVAD speed to 11 000 RPM were required to reduce the onset of pulmonary oedema.

Saito et al. (2011) also performed biventricular support using a Terumo DuraHeart (centrifugal flow pump) as an LVAD and a Jarvik 2000 (axial flow pump) as an RVAD. After implantation, weaning off bypass was difficult because of the presence of RV suction. Normally RV suction would be mitigated by reducing RVAD speed, however this was impossible, because the RVAD was operated at the minimum pump speed for the Jarvik 2000. Weaning was therefore performed more slowly under the guidance of transoesphegol echocardiography with the aid of volume management and acute speed adjustments. More volume balancing issues occurred after extubation, which resulted in severe pulmonary congestion. It was thought that PVR was suddenly reduced after extubation, which lowered RVAD afterload (and therefore differential pressure). This resulted in an increase in right pump flow rate and therefore pulmonary congestion. It was relieved by increasing the LVAD speed from 1600 to

1900 RPM. This paper highlighted that one of the disadvantages of operating the RVAD below the design speed for LVAD use is that there is little to no reserve for speed reductions during RV suction events.

The first reported implantation of dual HeartWare HVADs clinically was by Strueber et al. (2010) [47]. Initially, the LVAD was operated at 3600 RPM and the RVAD at 2000 RPM, but speeds were later reduced to 3100 and 1900 RPM respectively. Pump flows were estimated by the pump controllers to be 4.5 - 5.5 $Lmin^{-1}$. Spontaneous breathing caused fluctuations in LAP, which peaked at the beginning of inspiration. A constant low flow alarm was present from the right pump controller; however echocardiography revealed that there was no regurgitant flow, so the estimated flow rate was deemed incorrect and therefore the alarm was turned off. The high LVAD speed suggests high energy input into the system, yet the flow estimations were within normal ranges. This indicates that either the vascular resistance may have been elevated or the flow rate estimate was incorrect.

Clearly the simplest method of adapting an LVAD to support pulmonary circulation is via reducing the right pump speed. This can be adjusted on a patient-by-patient basis. It must be noted, however, that operating the device at a low speed limits the capacity to further reduce pump speed in the event of RV suction. Additionally, hydrodynamically levitated impellers rely on sufficient speed to create a fluid film and thus may become unstable at these lower speeds. Whilst this issue is negated in mechanically/pivot supported impellers, the ensuing reductions in outflow pressure also potentially reduces the washout through the small impeller/casing clearances in the device, which in turn may increase the risk of thrombosis [65].

2.2.2 Mode 2: Operating both pumps at the same design speed

The previous section highlighted advantages and disadvantages to operating the RVAD at a lower speed than the LVAD. A second mode of operation is to set both pump speeds at identical design speeds. However, there is a discrepancy between pump theory and experimental/clinical observations.

Hetzer et al. (2010) speculated that operating both pumps at the same speed will result in different flow rates, due to different differential pressures across each device [48]. This is due to the significantly lower RVAD afterload, caused by much lower PVR (compared to systemic vascular resistance (SVR)). The right pump would therefore shift more volume than the left, resulting in overflow pulmonary oedema and/or RV suction. This mode appears to be dangerous to the patient, however evaluation of this mode would be beneficial in that it could establish the magnitude of potential complications if it were attempted.

The best example of the clinical use of this mode was when the HeartWare HVAD was used for isolated RV support [66]. Personal correspondence with the author revealed that the pump was operated at the design speed for LVAD use (2400-2800 RPM). There was no evidence of overflow pulmonary oedema

or RV suction, which seems to contradict the assumption of Hetzer and colleagues. However, the healthy LV may have accommodated increased pulmonary flow via the Frank-Starling mechanism.

Two experiments have investigated this mode using dual Jarvik 2000 LVADs, as part of a larger study. Kindo et al. (2004) implanted two Jarvik 2000s as a BiVAD into two calves for thirty days [67]. The pumps were implanted without bypass, and a custom controller was used to operate the RVAD across a lower range of set speeds. LVAD speed was kept constant throughout the 30 day study. For the majority of the 30 days the RVAD speed was kept below LVAD speed. On the final day, the effect of speed variations on pressures was investigated. Operating both devices at the same speed did not result in excessive LAPs or flow rates, and no pulmonary congestion was present. However, the authors report thrombus formation in the outflow graft of the RVAD. This may have acted as a flow-restrictor, preventing LV overflow. Furthermore, the speeds were changed in 15 minute intervals, which may have allowed enough time for the circulatory system to adapt to each change. Finally, ventricular contractility was not modified pharmacologically, which meant that the residual Frank-Starling mechanism of the LV could accommodate increases in right pump flow.

Radovancevic et al. (2003) performed an acute in-vivo study of biventricular support using dual Jarvik 2000 LVADs [68]. After implantation the heart was fibrillated to produce a worst case scenario for heart contractility. Both pumps were initially clamped and baseline haemodynamics were obtained. LVAD was unclamped first, then RVAD. Speed was gradually increased for both pumps until both were at the maximum (12000 RPM). Increasing RVAD speed with constant LVAD speed resulted in increased AoP, PAP and LAP. However all pressures and flows were kept within normal ranges for human cardiovascular support, with maximums of 100, 22 and 16 mmHg for AoP, PAP and LAP respectively. Flow rate at maximum speeds was only 4.5 $L.min^{-1}$. This low flow rate at high speeds might be as a result of high PVR or SVR, which could explain the lack of congestion.

In summary, the assumptions made by Hetzer and colleagues (2010) with respect to operating the right pump at its design speed are only sound if there is assumed to be little-to-no ventricular function, which may be the case during the initial post-operative period [48]. However, if the ventricular function recovers, then the native Frank-Starling response of the ventricles can compensate. In cases in which there is some ventricular function in conjunction with reduced afterload, the ventricles are able to eject blood through the semilunar valves in parallel to the pump flow, the quantity of which is dependent on ventricular preload. This may explain why Kindo et al. (2004) were able to operate both LVADs at their design speed without observing pulmonary or systemic venous congestion [67]. It also almost certainly explains why an LVAD can be used to support isolated RV failure, as discussed by Deuse et al. (2013) [66].

2.2.3 Mode 3: Operating the RVAD at design speed and restricting RVAD outflow diameter.

The previous section summarised the theoretical difficulties with attempting to operate the RVAD at its design speed because of the lower differential pressure across the pump. Mode 3 involves artificially increasing RVAD afterload by restricting the diameter of the RVAD outflow graft, effectively reducing pump flow to a normal level.

Hetzer et al. (2010) were the first to promote the concept of restricting the RVAD outflow graft when using a HeartWare HVAD as an RVAD. Their justification was that the HeartWare HVAD should be operated at its design speed to prevent impeller instability and thrombus formation inside the pump. However, as explained in the aforementioned section, this may result in LV overflow because of the low PVR. Restricting the RVAD outflow cannula increases the effective total PVR, thereby increasing the RVAD differential pressure and reducing pump flow (Figure 2.1) when operated at the design speed.

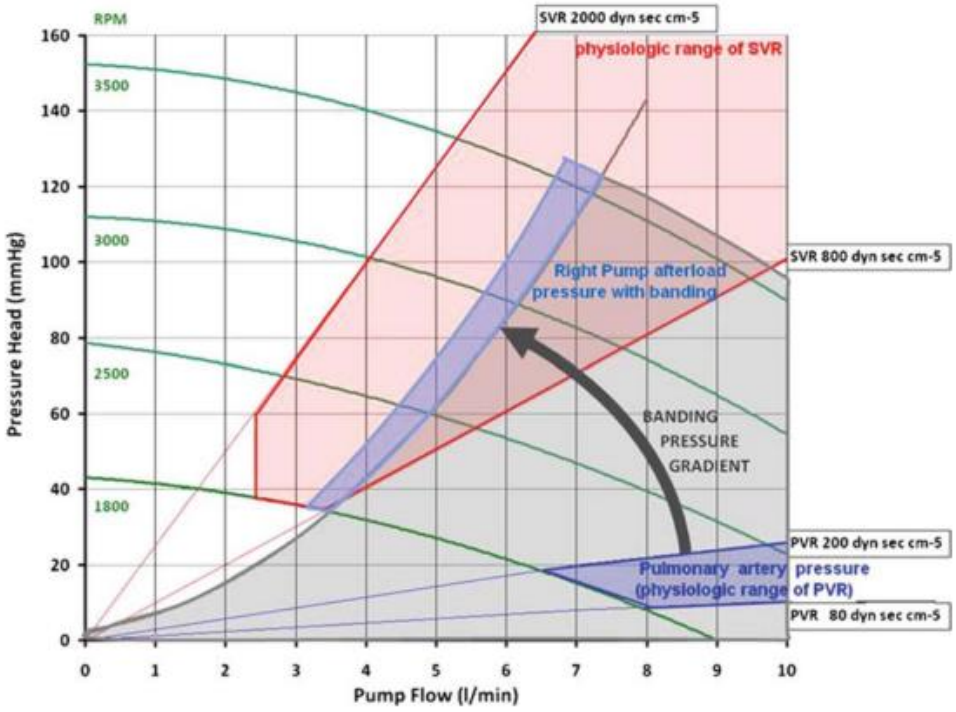

Figure 2.1: Effect of banding of the RVAD outflow cannula on the pump curve operation[48].

The authors implanted dual HVADs into 8 patients, with the 6 surviving patients successfully discharged. In-vitro investigations revealed that banding the RVAD outflow diameter to 5mm was sufficient to reduce RVAD flow to a sufficient level, so this was the diameter chosen for most patients. One patient required a banding diameter of 7mm due to elevated PVR. This indicates that one level of banding diameter is not suitable for all patients, and perhaps adjustable banding would be beneficial. Banding was facilitated before surgery by suturing a piece of graft with 6-0 Prolene over a 5-mm Hegar dilator bar (Figure 2.2).

Figure 2.2: Banding procedure as performed by Hetzer and colleagues [48] **using a 5mm dilator.**

Numerous investigations into the effect of banding of the HVAD outflow graft have been performed by Krabatsch and colleagues in 2011 [16], [17], [69].The effects of varying RVAD outflow diameter from 4 to 10mm were investigated in-vitro using a mock circulation loop. It was found that without banding and a normal level of PVR, the HVAD delivered between 6.5 and 8 $L.min^{-1}$of flow, much higher than the normal resting cardiac output of 5 $L.min^{-1}$. Normal flow rates were restored by restricting the outflow graft diameter.

The authors stated that in order for LVAD and RVAD to operate at the same speed, the effective PVR (graft resistance plus vessel resistance) must equal the total systemic resistance. The authors state that PVR is dynamic and unpredictable, and so a dynamic restriction to automatically adjust RVAD outflow cannula resistance might be suitable. Alternatively, dynamic PVR could be accommodated for by fixing the RVAD diameter at 6mm and adjusting RVAD speed. Since rotary VADs are operated at a constant speed, frequent speed changes would require regular interaction with a clinician.

Based on these successful in-vitro findings, Krabatsch and colleagues reported the implantation of dual HVADs into 17 patients [16]. Patients with normal PVR received a 5mm outflow graft banding diameter, whereas patients who presented with an elevated PVR received a 7mm banding. The authors reported a 50% survival at 6 months, which is comparable to recently published INTERMACS data for BiVAD patients [70]. The authors commented that PVR appeared to gradually decline in some patients, and that RVAD speed was reduced to accommodate. However, the length and rate of this decline is generally unpredictable. This highlights one of the difficulties of using a fixed banding diameter. The diameter chosen at the time of implantation must ensure that the new operating ranges for pump speed can accommodate the gradual decline of PVR.

Additional case reports by Loforte and colleagues [71], [72] and McGee et al. [49] confirm that the banding the RVAD outflow graft to 5mm when using dual HeartWare HVADs as a BiVAD is a safe method of adopting an LVAD for RV support. However, the diameter is dependent on each patient's PVR, which is dynamic and unpredictable. The inclusion of some system to automatically adjust the right pump output with changes in PVR may offer some benefit.

2.2.4 Comparisons

The previous sections summarised the clinical use of dual LVADs as a BiVAD, and the different modes of operation used by clinicians. However, these methods have only been experimentally compared once,

by Timms et al. (2011)[73]. In that study, a biventricular HF condition was simulated in a MCL and biventricular support provided by dual Medos DeltaStream pumps. LVAD and RVAD speeds were set to obtain normal systemic and pulmonary pressures and flow rates respectively. Then RVAD speed was varied from 500 to 4500 RPM in order to evaluate the sensitivity of speed variations on pulmonary pressures and flows. Then RVAD speed was set to the LVAD speed and the diameter of the RVAD outflow was adjusted (using a pinch valve) until normal pulmonary haemodynamics were obtained. Then RVAD outflow diameter was varied to evaluate the sensitivity of diameter variations on pulmonary pressures and flows.

The authors found that RVAD speed should be significantly lower than LVAD speed without banding (3500 vs. 4900). A banding diameter of 5.4mm was required to operate both pumps at 4900 RPM. The authors found that sensitivity of flow and pressure was highest when the RVAD flow exceeded LVAD flow, which occurred between RVAD speeds of 3200 - 4400 RPM or outflow diameters of 5.3- 6.5mm. This indicates that only a slightly incorrect RVAD speed or outflow diameter may result in excessive pulmonary flow which may lead to pulmonary congestion. Whilst this study did not use long-term implantable rotary LVADs, the results are still relevant as the Medos pumps are centrifugal pumps like the HeartWare HVAD.

2.2.5 Summary of Literature Review

In summary, there are three modes of operation of dual rotary LVADs that are used in clinic. Firstly, RVAD speed can be set lower than LVAD speed. This reduces the output of the right pump relative to the left, reducing the likelihood of pulmonary congestion. However, this means that the RVAD speed will be close to the minimum pump speed, leaving no reserve to further reduce speed in the event of ventricular suction. Additionally, operating below the design point increases the likelihood of thrombosis in the pump due to lower washout, and may affect the stability of pumps that rely on hydrodynamic forces to lift the impeller. The second option is to operate both pump speeds at the design point. Theoretically, operating the RVAD and LVAD at the same speed will result in excess pulmonary flow, possibly leading to congestion. However, this was not observed in in-vivo experiments using two axial flow pumps. The final method is to operate both pumps at the same speed in conjunction with banding of the right pump outflow graft, effectively reducing right pump output relative to left. This method requires consideration of both pump speed and banding diameter, and both should be adjusted depending on the patient's PVR.

Clearly there are advantages and disadvantages to each operating mode. Each mode will result in different patient haemodynamics, which should be characterised to provide clinicians with a more comprehensive understanding of dual LVAD support in the biventricular heart failure setting.

The aim of this study was to characterise each of these three modes using an in-vitro and a preliminary in-vivo model of biventricular heart failure. This investigation involved measuring the steady-state

effects of each operating mode on mean arterial pressure (MAP), LAP and mean systemic flow rate (MSQ) and determining if these values remained in clinically safe regions. Pump speed changes required to accommodate for dynamic variations in pulmonary vascular resistance, as may occur during straining, were also measured. Based on these results, recommendations were made for each operating mode and for the future development of biventricular support with two LVADs.

2.3 Hypothesis

The main hypothesis for this chapter is that none of the three modes of operation would be able to accommodate dynamic changes in the circulatory system without changes in either banding diameter or pump speed.

2.4 Methods

2.4.1 In-Vitro Evaluation

A physical five element Windkessel mock circulation loop (MCL) including systemic and pulmonary circulations was used for this study[74], [75]. In brief, ventricular systole was controlled through a series of electropneumatic regulators (ITV2030-012BS5, SMC Pneumatics, Tokyo, Japan) and 3/2 way solenoid valves (VT325-035DLS, SMC Pneumatics, Tokyo, Japan) to provide passively filled heart chambers and variable contractility, heart rate and systolic time. Heart rate and systolic time were maintained at 60 beats per minute and 35% respectively throughout this study. The inotropic state of each ventricle (contractility) was modified by changing the maximum regulator supply current each cardiac cycle, effectively a surrogate for changing the slope of the ESPVR. A Starling response was implemented in both left and right ventricles which actively controlled ventricular pressure (through electropneumatic regulator supply current) based on ventricular preload. This mechanism was developed in collaboration with Dr Shaun Gregory and details of its implementation and validation can be found in [76]. Briefly, this mechanism varied the magnitude of the ventricular air regulator voltage based on a logarithmic function of the end-diastolic ventricular volume. The new equation for regulator voltage is given in Equation (2.1).

$$V_{reg}(t) = \mathrm{V}_P(t).K_{starling}(t).K_{ven} \qquad (2.1)$$

where $V_{reg}(t)$ is regulator voltage, $V_P(t)$ is the time varying voltage waveform sent to the electropnuematic regulator in order to produce true ventricular pressure waveforms (details of which can be found in [74]), K_{ven} is a scalar that changes the magnitude of the waveform for RV or LV contractility, and $K_{starling}(t)$ scales the regulatory voltage based upon the current end-diastolic volume to simulate the Frank-Starling effect. $K_{starling}(t)$ is calculated at the end of diastole each cardiac cycle using Equation (2.2).

$$K_{starling}(t) = K_{sm1}.ln(K_{sm2}(EDV(t) + c_{EDV})) + c_{sm1} \quad (2.2)$$

Where *EDV(t)* is the ventricular end-diastolic volume (mL), K_{sm1} and K_{sm2}(mL^{-1}) set the sensitivity of the ESPVR, and c_{EDV} (mL) and c_{sm1} set the horizontal and vertical offset of the ESPVR respectively. These constants were adjusted for left and right ventricles to match the human ESPVRs presented by Guyton [77]. Further details of this mechanism and its validation can be found in [76]. The values of K_{ven}, K_{sm1}, K_{sm2}, C_{EDV} and C_{SM1} for three cases of heart function for left and right ventricles are given in Appendix A.

Mechanical check valves were used to simulate the mitral, aortic, tricuspid and pulmonary valves to ensure unidirectional flow throughout the circuit. Four independent Windkessel chambers were employed to simulate lumped systemic and pulmonary arterial and venous compliance. Socket valves (VMP025.03X.71, Convair Engineering, Epping, Australia) allowed easy manipulation of systemic and pulmonary vascular resistance respectively. The working fluid throughout this study was a water/glycerol mixture (60/40% by mass) with similar viscosity and density to that of blood.

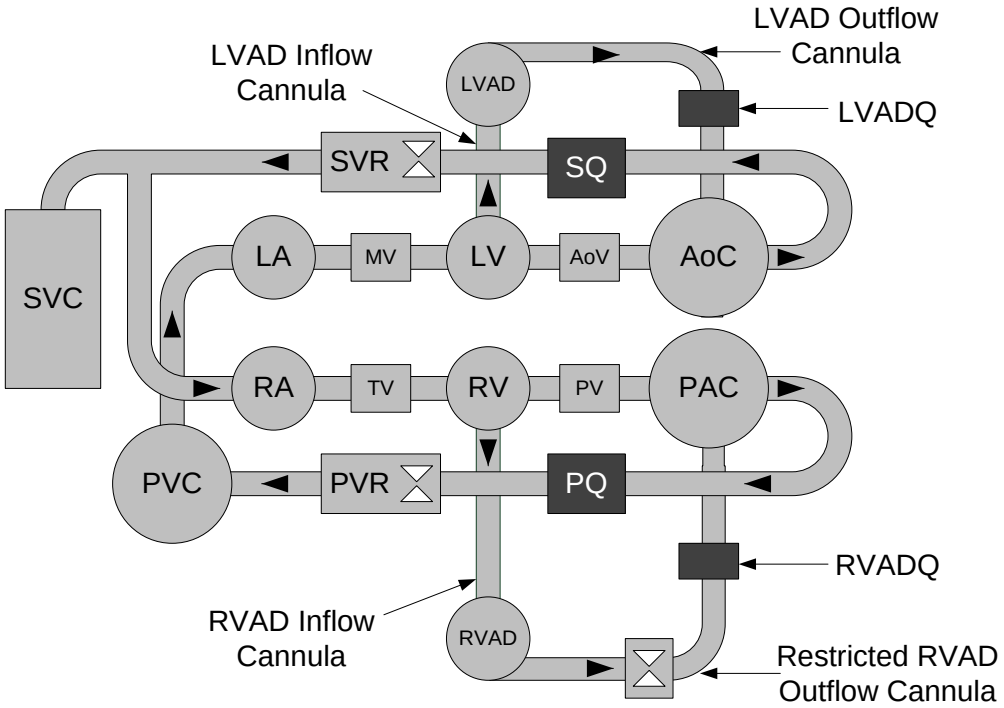

Figure 2.3: Schematic of the MCL setup for evaluation of aortic valve regurgitation with rotary biventricular support. LA - left atrium, MV - mitral valve, LV - left ventricle, AoV - aortic valve, AoC - aortic compliance chamber, SQ - systemic flow meter, SVR - systemic vascular resistance valve, SVC - systemic venous compliance chamber, RA - right atrium, TV - tricuspid valve, RV - right ventricle, PV - pulmonary valve, PAC - pulmonary arterial compliance chamber, PQ - pulmonary flow meter, PVR - pulmonary vascular resistance valve, PVC - pulmonary venous compliance chamber, LVAD - left ventricular assist device, LVADQ - left ventricular assist device flow meter, RVAD - right ventricular assist device, RVADQ - right ventricular assist device flow meter.

Two VentrAssist LVADs (Ventracor Ltd., Sydney, Australia) were used to provide biventricular circulatory support. Each pump was cannulated with inflow connected to the ventricle and outflow to the aorta (LVAD) and pulmonary artery (RVAD). Half-inch diameter tubing (Tygon 06408-18, Saint Gobain, Paris) was used for the outflow grafts. Pumps were operated using a custom-built breakout box which enabled a greater range of set speeds (1200 – 3500 RPM) compared with standard VentrAssist controllers.

Three experiments were performed to characterise each of the three operating modes. In the first experiment, steady state characteristics of all three modes were determined for a number of different heart and circulatory conditions. Three different combinations of left and right heart ventricular failure were simulated in the MCL (Table 2.1) by adjusting the maximum electrical supply current for each ventricle's electro-pneumatic regulator. Biventricular support was achieved using each of the three modes of operation. For mode 1, left and right pump speeds were set at 2800 and 2000 RPM respectively. For modes 2 and 3, both pumps were operated at 2400 RPM. In mode 3, the outflow restriction diameter was set at 6.5mm, which was determined prior to experimentation to be the optimum banding diameter for these speeds.

Table 2.1: Haemodynamic properties for each biventricular failure condition simulated in-vitro. LVF: level of left ventricular failure; RVF: level of right ventricular failure; LAP: left atrial pressure; MAP: mean aortic pressure; RAP: right atrial pressure; MPAP: mean pulmonary arterial pressure; MSQ: mean systemic flow rate; LVEDV; LV end diastolic volume; RVEDV: RV end diastolic volume. * indicates maximum ventricular volume.

Condition	LVF	RVF	LAP (mmHg)	MAP (mmHg)	RAP (mmHg)	MPAP (mmHg)	MSQ ($L.min^{-1}$)	LVEDV (mL)	RVEDV (mL)
1	Severe	Mild	14	51	9	19	2.5	270*	206
2	Mild	Severe	8	60	12	13	3	160	230
3	Severe	Severe	11	48	9	14	2.1	230	225

Each combination of contractility and operating mode were subject to three different settings of vascular resistance. Normal resistance was defined as PVR = 100 $dynes.s.cm^{-5}$and SVR = 1200 $dynes.s.cm^{-5}$, low resistance was defined as PVR = 40 $dynes.s.cm^{-5}$ and SVR = 600 $dynes.s.cm^{-5}$, and high resistance was defined as PVR = 160 $dynes.s.cm^{-5}$and SVR = 1800 $dynes.s.cm^{-5}$. Steady state values of MAP, LAP and MSQ were measured in each condition to assess the feasibility of each mode. Feasibility was defined as follows: LAP below 25 mmHg to prevent pulmonary congestion [78], MAP below 100mmHg to limit hypertension and mean systemic flow at 6 $L.min^{-1}$ to limit hyper flow. Hyper flow describes a state in which too much flow is delivered through the circulatory system.

In the second experiment, the relationship between RVAD outflow cannula resistance and RVAD speed for mode 3 was characterised. Firstly, a set of custom RVAD outflow restrictions were designed based on the FloWatch® Pulmonary Artery Banding System (FloWatch-PAB, EndoArt, Lausanne, Switzerland) [79] and manufactured using a 3-D printer (OBJET 24, Stratasys, MN, USA). These

restrictions ranged in cross-sectional area from 35.6mm^2 to 77.7mm^2(equivalent diameters of 6.73mm to 9.94mm) and were designed for quick placement around the RVAD outflow graft (Figure 2.4). Left and right pump speeds were set to those values determined for mode 1 before the smallest restriction was placed around the RVAD outflow graft. RVAD speed was then increased to restore PAP and RVAD flow (RVADQ) to their baseline values. This procedure was repeated for each restriction, thereby characterising the relationship between RVAD outflow graft diameter and pump speed.

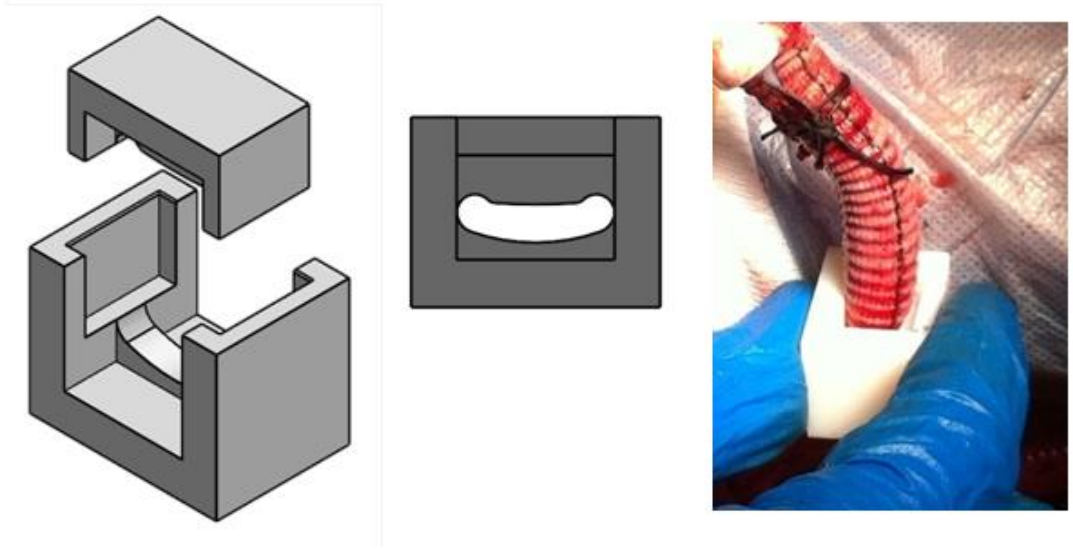

Figure 2.4: Example of a printed restriction used for dynamic variation of RVAD outflow graft diameter. The restriction consisted of two pieces (left) that combined around the graft (right) to reduce cross sectional area (middle).

In the third experiment, the effects of dynamic PVR changes with modes 1 and 3 were then evaluated. Biventricular HF condition 3 was simulated in the MCL with a PVR of 100 dynes.s.cm^{-5}, LVAD speed set at 2200 RPM, RVAD speed set at 2150 RPM (close to LVAD speed), and an initial RVAD outflow restriction of 7.77 mm. The PVR was increased to 200 dynes.s.cm^{-5} in a stepwise manner and the RVAD speed was altered until RVADQ was restored to the baseline condition. The test was then repeated but with changes in RVAD outflow restriction instead of speed, and for final PVR values of 300, 400, and 500 dynes.s.cm^{-5}.

2.4.2 In-Vivo Evaluation

Ethics approval was obtained from the Queensland University of Technology Animal Ethics Committee prior to experimentation (Approval Number 1100001052). One female sheep was used. After induction of general anaesthesia, the animal was intubated with a cuffed endotracheal tube and ventilation

commenced at 12 breaths/min. The animal was heparinised until an ACT > 480 s was achieved, at which point baseline arterial pressures and flow rates were recorded.

After a median sternotomy, two VentrAssists were implanted without cardiopulmonary bypass. The LVAD was implanted first, with the inflow cannula inserted in the left ventricular apex and secured using the VentrAssist sewing ring. The outflow cannula was connected to the ascending aorta with an end-to-side anastomosis. Both LVAD and RVAD outflow grafts (Gelweave, Terumo Cardiovascular Systems, Ann Arbor, MI) were approximately 30 cm long and 12 mm diameter. The pump was placed in an abdominal pocket. After implantation, the pump was switched on and speed set to restore arterial pressures to baseline.

After haemodynamics stabilised, the RVAD was implanted. The outflow graft was sutured to the pulmonary artery (PA) using an end-to-side anastomosis. An incision was then made in the RV free wall, and the inflow cannula was inserted and fed through the tricuspid valve into the right atrium (RA). This removed the risk of the interventricular septum occluding the tip of the inflow cannula. Based on previous work, the difference between RVAD inflow cannulation in-vitro and in-vivo isn't expected to affect the comparison between the in-vitro and in-vivo experiments [64].

The cannula was then secured using a purse-string suture, and the pump was switched on. The heart was then fibrillated, so there was no ejection through the semilunar valves. This greatly simplified the experiment. Left and right pump speeds were individually manipulated to maintain suitable systemic and pulmonary haemodynamics (MAP > 60mmHg, PAP ~ 20 mmHg, MSQ> 4 $L.min^{-1}$).

After haemodynamics settled, evaluation of the steady state performance of all three modes was performed, similar to the first in-vitro experiment. In the first experiment, only one contractility condition was assessed due to difficulties in maintaining consistent haemodynamics. Then, the relationship between RVAD outflow cannula restriction size and RVAD speed was characterised as per the second in-vitro experiment. The effect of transient increases in PVR were also evaluated in-vivo, but in a more simplified manner than performed in the third-vitro experiment. Step changes in PVR were achieved by tying a felt strip around the PA distal to the anastomosis site. The strip was manually tightened to increase PVR, and released to restore the condition to baseline. It is difficult to perform repeatable changes in PVR in-vivo, so in-vivo assessment of the relationship between RVAD speed and PVR changes was purely qualitative.

At the end of the experiment, the animal was euthanized using sodium pentobarbitone (295mg/mL at 0.5 mL/kg). The pumps and outflow cannulae were then explanted and examined for signs of thrombus formation.

2.4.3 Data Acquisition

In-vitro systemic and pulmonary flow rates were measured using magnetic flow meters (IFC010, KROHNE, Sweden). VAD flow rates were measured using ultrasonic flow probes (TS410-10PXL, Transonic Systems, NY, USA). Systemic and pulmonary pressures were monitored throughout using pressure transducers (PX181B-015C5V, Omega Engineering, Connecticut, USA). The MCL and VentrAssist breakout box were interfaced to a computer using dSPACE hardware (DS1103, dSPACE, MI, USA). All signals were sampled at 100 Hz.

In-vivo, a Swan-Ganz catheter (Swan-GanzCCOmbo, Edwards Lifesciences, Irvine, California, USA) was inserted prior to RVAD placement via the external left jugular vein to monitor pulmonary arterial pressure. Systemic arterial pressure was monitored via cannulation of the facial artery. Central venous pressure (CVP) was monitored at the jugular vein. Left and right VAD flows were recorded using flow probes (TS420-10PXL, Transonic Systems, NY, USA). Left and right atrial pressure were measured using indwelling catheters, and pump outflow pressures were measured using fluid-filled lines that were attached to tubing connectors at the pump outlet. Total pulmonary and systemic flow rates were measured by placing flow probes (MC20PAU and MC16PAU, Transonic Systems, NY, USA) around the pulmonary artery and ascending aorta respectively. Probes were placed downstream of the anastomoses in order to measure the combined flow produced by the pump and the ventricle.

2.5 Results

The MAP, LAP and MSQ for each resistance level, heart contractility and operating mode evaluated in-vitro are shown in Figure 2.5. Mode 1 resulted in LAP below 25mmHg for all levels of contractility and resistance. However, suitable MAP was only attainable during vasodilation; resulting in a flow rate above 7 $L.min^{-1}$.

Mode 2 resulted in high LAP for all cases except for mild left ventricular failure (LVF)/severe right ventricular failure (RVF) with vasodilation. The lower resistance of the pulmonary circulation lowered the differential pressure across the right pump, allowing more pulmonary flow than desired. The resulting fluid shift increased LAP. The combination of stronger LV contractility and vasodilation relieved this congestion.

In mode 3, restricting the RVAD outflow diameter to 6.5mm enabled both pumps to be operated at the same speed without elevating LAP. In addition, MAP was kept below 100mmHg and MSQ less than 6 $L.min^{-1}$. Even though the RVAD was operated at the same speed as in mode 2, the reduced RVAD diameter increased RVAD outflow cannula resistance, thus increasing the total effective pulmonary vascular resistance. The right pump was therefore able to produce flows below 6 $L.min^{-1}$.

In contrast to the in-vitro results, all 3 modes were achievable in-vivo with expected levels of LAP, MAP and MSQ (Table 2.2). The main difference between in-vitro and in-vivo results was that the

unrestricted RVAD outflow graft resistance was much higher in-vivo than in-vitro (observed to be between 20 and 40 dynes.s.cm^{-5} compared to 510 dynes.s.cm^{-5} in-vivo). The increased resistance was due to longer grafts, different material, formation of thrombus evenly along the outflow graft (discovered after post mortem examination) and additional resistance caused by the PA anastomosis. Increased resistance acted like a diameter restriction by increasing effective PVR, enabling the right pump to be operated at its design speed.

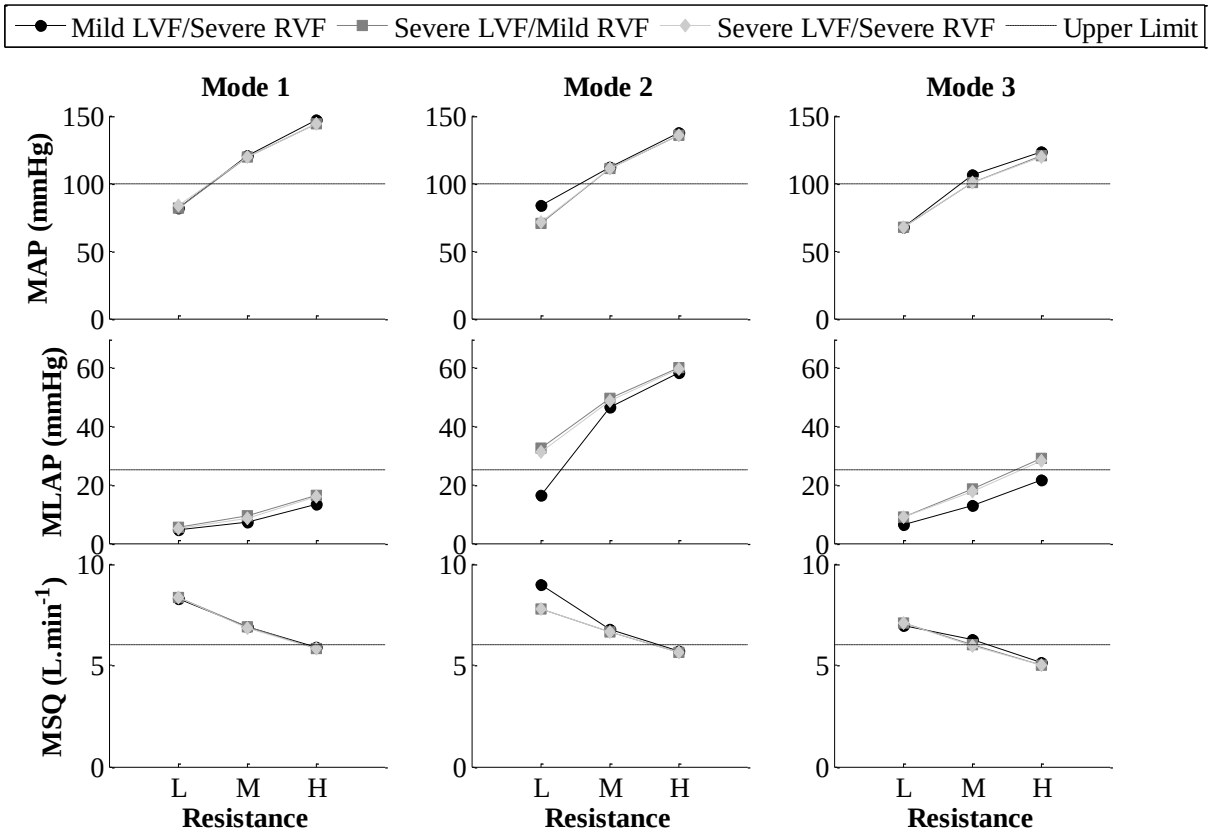

Figure 2.5: In-Vitro haemodynamics for three operating modes of dual left ventricular assist devices for different pulmonary and systemic vascular resistances (PVR and SVR) and contractilities. MAP: mean aortic pressure; LAP: left atrial pressure; MSQ: mean systemic flow; L: low resistance (PVR=40 dynes.s.cm^{-5} and SVR=600 dynes.s.cm^{-5}); M: medium resistance (PVR=100 dynes.s.cm^{-5} and SVR=1200 dynes.s.cm^{-5}); H: high resistance (PVR=160 dynes.s.cm^{-5} and SVR=1800dynes.s.cm^{-5}).

Table 2.2: Haemodynamics observed during in-vivo evaluation of three operating modes for dual left ventricular assist devices. LVAD: left ventricular assist device; RVAD: right ventricular assist device; MAP: mean aortic pressure; PAP; mean pulmonary arterial pressure; LAP: mean left atrial pressure; MSQ: mean systemic flow rate; $R_{outflow}$: resistance along the RVAD outflow cannula.

Operating Mode	LVAD Speed (RPM)	RVAD Speed (RPM)	Restriction Diameter (mm)	MAP (mmHg)	PAP (mmHg)	LAP (mmHg)	MSQ ($L.min^{-1}$)	$R_{outflow}$ ($dynes.s.cm^{-5}$)
1	2300	1800	None	85	18	9.0	5.5	510
2	2300	2300	None	83	18	9.0	6.0	514
3	2300	2300	8.1	81	17	8.0	6.0	1143

Figure 2.6 shows that the RVAD speed required to maintain RVADQ at 5 $L.min^{-1}$ increased exponentially with decreasing RVAD outflow diameter, both in-vitro and in-vivo, due to the progressive increase in afterload. The speeds required for each level of restriction were higher in-vivo than those observed in the MCL, again due to higher RVAD outflow graft resistance.

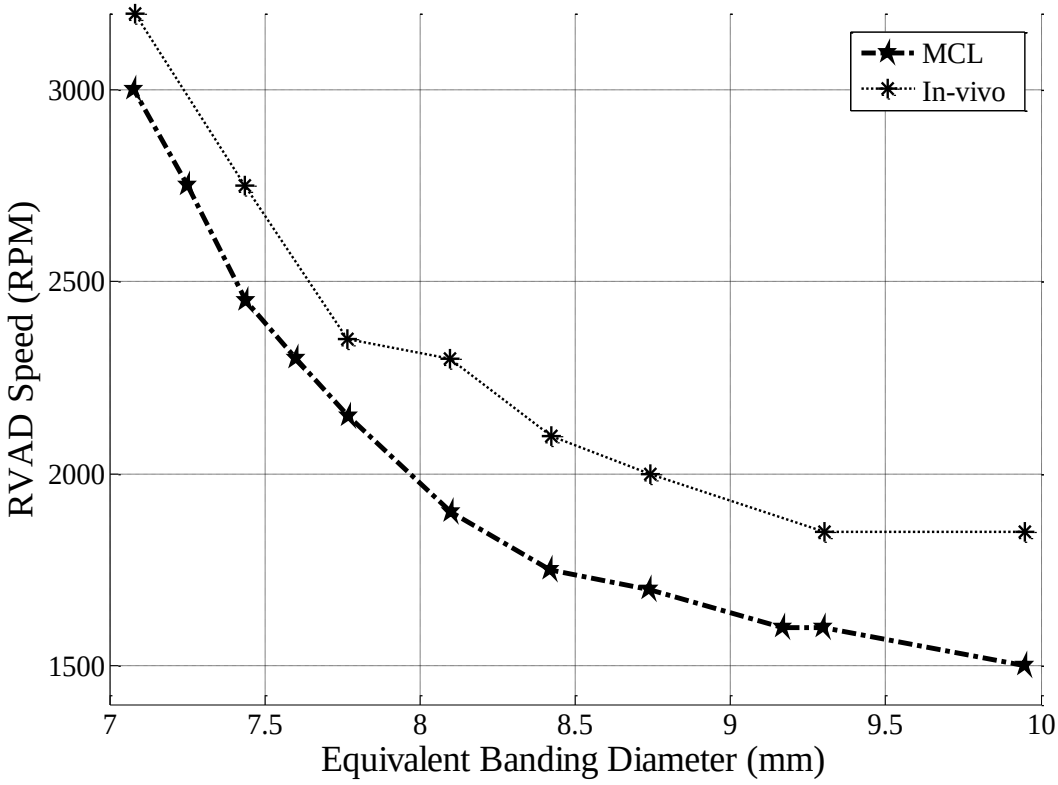

Figure 2.6: RVAD speed vs. equivalent outflow graft diameter for both in-vivo and in-vitro results. RVAD - Right ventricular assist device, MCL - Mock Circulation Loop.

During in-vitro simulations of elevated PVR, increased speed or outflow graft diameter were required to maintain pulmonary flow rate at 5 $L.min^{-1}$ (Table 2.3). This indicated that dynamic adjustments of pump speed or banding diameter may be beneficial to overcome elevated PVR, even transiently as occurs in a Valsalva manoeuvre. There was no change in required outflow diameter between 100 and

200 dynes.s.cm^{-5} because the next largest banding diameter was too large, increasing RVAD flow above 5 L.min^{-1}.

Table 2.3: Changes in outflow graft diameter (fixed RVAD speed) or RVAD speed (fixed outflow graft diameter) for modes 1 and 3 required to maintain normal pulmonary flow at various levels of pulmonary vascular resistance (PVR). *the next size of restriction produced flow rates greater than 5 L.min^{-1}, so restriction was left unchanged.

Mode 1	
PVR (dynes.s.cm^{-5})	**RVAD Speed (RPM)**
100	1400
200	1500
300	1600
400	1650
500	1750
Mode 3 (Fixed RVAD speed 2150 RPM)	
PVR (dynes.s.cm^{-5})	**Outflow Graft Diameter (mm)**
100	7.77
200	7.77*
300	7.93
400	8.10
500	8.42
Mode 3 (Fixed Outflow Graft Ø (7.77mm))	
PVR (dynes.s.cm-5)	**RVAD Speed (RPM)**
100	2150
200	2250
300	2300
400	2350
500	2400

The simplified version of the third experiment in-vivo showed that a change in pump speed was required to overcome increased PVR. Figure 2.7 shows an example of the speed changes required to overcome an increase in PVR, simulated in-vivo through restriction of the PA at approximately five seconds. After the increase in PVR from 375 to 425 dynes.s.cm^{-5}, the RVADQ reduced from 4.5 to 3.2 L.min^{-1}, before increasing slightly to 3.75 L.min^{-1} at 35 seconds. This may have been as a result of the tie around the PA slipping slightly. After 40 seconds, the RVAD speed was increased manually until the flow rate was restored to baseline levels (approximately 60 seconds).

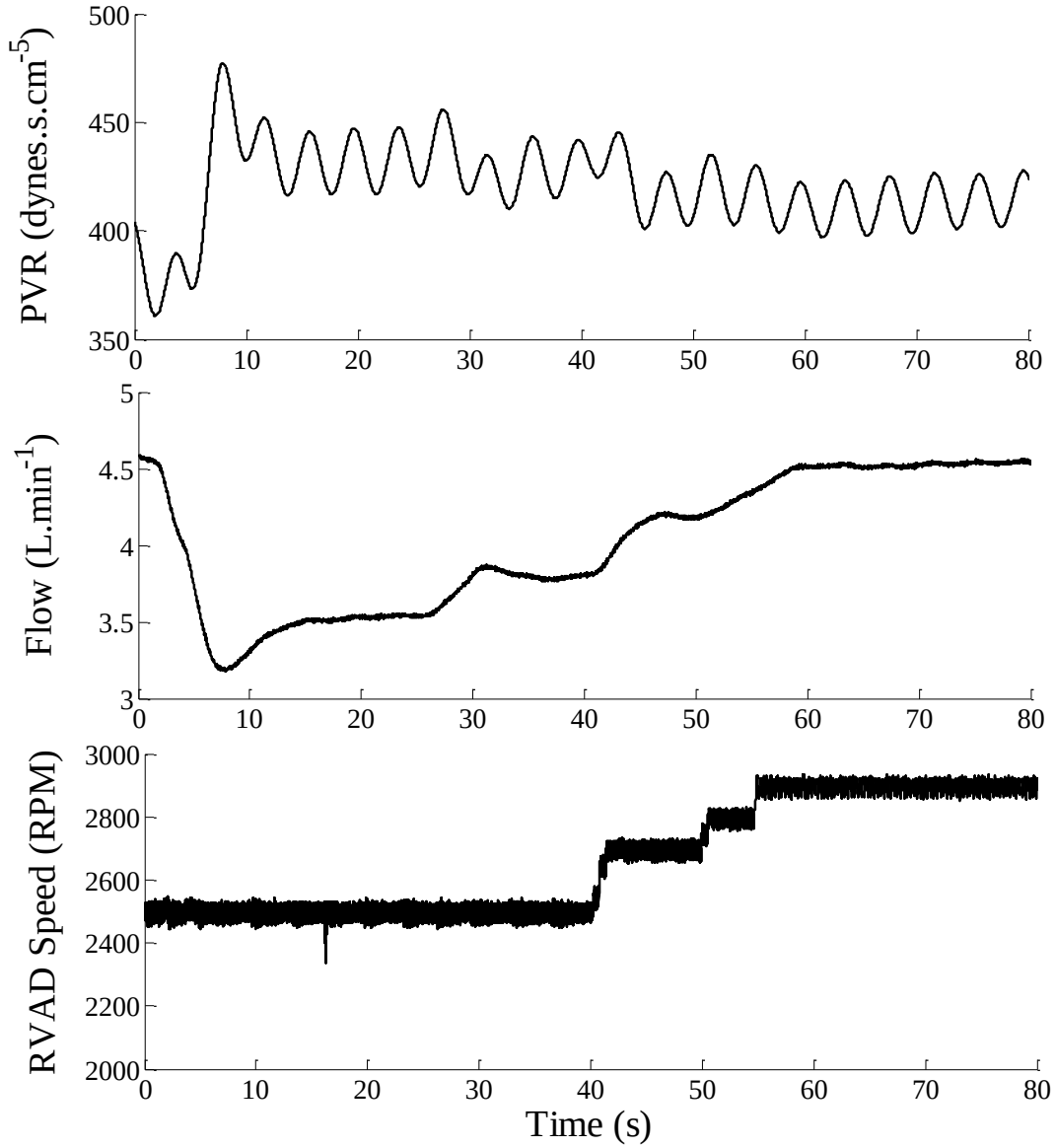

Figure 2.7: Pulmonary vascular resistance (PVR) (top), cardiac output (middle) and right ventricular assist device (RVAD) speed (bottom) during a restriction of the pulmonary artery.

2.6 Discussion

Krabatsch et al. (2011) [17] highlighted three primary challenges when using a HeartWare HVAD as an RVAD. These included reducing the output of the RVAD to prevent pulmonary congestion; shortening the inflow cannula to prevent septal obstruction; and finding an appropriate inflow cannulation site in the RV. Whilst the last two issues are pump and patient specific, the first challenge is applicable to all patients receiving dual LVAD therapy.

In our study, operating the right pump at a lower speed than the left pump (mode 1) reduced right pump output and therefore the likelihood of pulmonary congestion. Strueber et al. (2010)[47] used this mode to operate dual HVADs, setting the RVAD speed close to the design speed (2000 RPM) and the LVAD at an elevated 3600 RPM to mitigate pulmonary congestion. The authors achieved a suitable flow rate of 4.5-5 $L.min^{-1}$ however the high LVAD speed indicates excess energy input into the system. Our in-vivo experience was more similar to that of Saito et al. [19] who implanted dual Jarvik 2000 devices. They operated the LVAD at the design speed and the right pump at a speed lower than the minimum set by the manufacturer. It must be noted, however, that operating the device at a low speed limits the capacity to reduce pump speed in the event of RV suction. Additionally, hydrodynamically levitated impellers rely on sufficient speed to create a fluid film and thus may become unstable at these lower speeds. Whilst this issue is negated in mechanically/pivot supported impellers, the ensuing reductions in outflow pressure also potentially reduces the washout through the small impeller/casing clearances in the device, which in turn may increase the risk of thrombosis [65]. These results indicate that mode 1 is a suitable option for dual LVAD operation. However, there is a trade-off between obtaining normal haemodynamics and avoiding impeller instability and thrombus risk.

There are no reports of using mode 2 clinically, however it has been attempted in-vivo using dual Jarvik 2000 devices[67], [68]. These studies report similar results to those seen in our in-vivo trials, with thrombus formation in the RVAD outflow graft. In our study, this thrombus formation increased the outflow resistance by partially occluding the flow, effectively acting as a diameter restriction. This may have prevented pulmonary congestion or RV suction. Our in-vitro results, however, showed that without any restriction (thrombus or otherwise), mode 2 causes elevated LAP due to the lower right pump afterload. A moderate level of LV contractility can relieve theses high LAPs, which may explain how the HeartWare HVAD can be used for supporting isolated RV failure without causing pulmonary congestion [66].

Mode 3 artificially increases RVAD afterload via a reduction in the diameter of the right pump outflow graft, thus enabling the right pump to be operated at its design speed. In this study, the outflow diameter required to operate the RVAD at the same speed as the LVAD was between 6.5 and 7.8 mm in-vitro and 8.1mm in-vivo. These values are higher than the 5mm reported previously [17], [48], but are close to the 7mm suggested by Krabatsch et al. for patients with elevated PVR to maintain LV filling [16].

Elevated PVR was observed in our in-vivo trials (>400 dynes.s.cm^{-5}), possibly due to mechanical ventilation, which explains the need for a larger outflow diameter. Another point of difference between in-vitro and in-vivo experiments that may account for the different RVAD resistance is the different outflow graft materials.

Pulmonary vascular resistance increases transiently during straining, falls rapidly during extubation [18], and gradually recovers in hypertensive patients who undertake successful VAD therapy. Therefore it is important to determine what changes are required to either RVAD speed or banding diameter to accommodate for variations in PVR. After a step increase in PVR in-vitro, RVAD flow and LV filling reduced. Increased pump speed or outflow graft diameter were required to restore cardiac output and LAP. It can be inferred that the opposite is true for transient reductions in PVR. Whilst speed changes can be performed by the clinician, restrictions are difficult to adjust without reoperation because the outflow diameter is fixed. An implantable, transcutaneously adjustable restriction device, such as the FloWatch PAB suggested by Timms et al.(2011) [73], would be useful in this scenario. Clinicians could perform speed adjustments for small, acute changes in VAD flow, and adjust the RVAD outflow restriction after long-term PVR changes.

Ideally, both speed and restriction should be adjustable. Alternatively, a fixed restriction could be chosen which allows for sufficient increases and decreases in RBP speed to cope with variations in PVR. Ideally, the fixed restriction would allow the device to normally operate approximately halfway between minimum and maximum speeds. This would ensure that there is reserve available to lower speed during low PVR to prevent RV suction, and to increase speed during high PVR or exercise to prevent LV suction.

The results from this chapter clearly indicate that speed changes are necessary to maintain a suitable flow rate in response to changes in PVR if the banding is to remain constant. The use of a physiological control system, as opposed to clinical input, to control RVAD speed based on patient state would greatly benefit active patients by transiently changing speed in response to PVR changes.

2.7 Limitations and Future Work

There were a number of limitations with both the in-vitro and in-vivo experiments. Firstly, the MCL did not replicate any autoregulatory mechanisms beyond the Frank-Starling response. These autoregulatory mechanisms were potentially compromised in the in-vivo studies due to anaesthesia. Secondly, VentrAssist rotary LVADs were used both in-vitro and in-vivo. The VentrAssist was too large to be used as an RVAD, and had to be positioned outside the chest cavity. Additionally, the long VentrAssist inflow cannula was not ideal for RVAD support, as it had to be pushed through the RV wall, across the tricuspid valve and into the RA. Smaller pumps should be utilised for future long-term studies. Thirdly, the PVR changes induced in-vivo by tying a band around the PA were not necessarily

physiological. Future work should investigate whether pharmacological changes in PVR are more physiological and repeatable. Fourthly, only one animal experiment was performed, in which the heart was fibrillated. More than one animal is required to confirm the results presented in this thesis. Future work could involve investigating the degree that a functioning ventricle can assist with flow balancing. Finally, only PVR changes were performed in-vitro and in-vivo, which established the need for RVAD speed control. Whilst it can be inferred that changes in SVR would require changes in LVAD speed, experimental evidence is required to verify this assumption. This is addressed in the next chapter, in which an evaluation framework to assess rotary LVAD physiological control system performance is discussed.

2.8 Conclusions and Summary

This investigation characterised three modes of operation when using dual LVADs as a biventricular support system. The RVAD can be operated at a lower speed than the LVAD, however this may require operating the pump at a speed lower than recommended by the manufacturer, resulting in potential impeller instability and suboptimal washout within the device. Attempting to operate both pumps at the same speed is only possible in patients with high PVR, high LV contractility, or high RVAD outflow cannula resistance. However, if the RVAD outflow cannula is restricted to a diameter between 6.5 and 8.1 mm, suitable steady-state haemodynamics can be achieved while maintaining impeller stability and optimal device washout. RVAD speed adjustments or outflow diameter changes can accommodate for long term or transient variations in PVR, however the latter requires the use of an adjustable restriction mechanism. Due to the variable nature of heart contractility between patients and the time-varying nature of a patient's PVR, physiological control of dual rotary LVADs could be advantageous to ensure suitable cardiac outputs at all times.

This chapter highlighted that whilst the methods used clinically to operate dual rotary LVADs can provide stable steady-state haemodynamics, speed adjustments are required after changes in the circulatory system. The remainder of this thesis describes the development of such a control system, with the next chapter devoted to the description of the evaluation framework.

3 Control Evaluation Framework

The previous chapter highlighted that the three current modes of operation for dual rotary LVADs are sufficient to maintain steady state resting haemodynamics, provided that careful monitoring is provided by the clinician to prevent pulmonary oedema or ventricular suction. However, the dynamic nature of the circulatory system means that frequent changes in the speeds of both pumps may be required. A physiological control system that can automatically adjust pump speed in response to changes in the circulatory system may offer some benefit by reducing the patient's reliance in clinical input. The rest of this thesis will describe the development of a physiological control system for dual rotary LVADs.

In order to develop a suitable physiological control system for dual rotary LVADs, an evaluation framework must first be established. This can then be used to assess the performance of such a control system. This framework encompasses the testing apparatus used to evaluate the control system, the experimental protocols used to test the control system, and the metrics used to quantify the performance of a physiological control system.

This chapter describes the development of an evaluation framework for the testing of the control systems described in Chapters 4 and 5. It begins with a literature review, summarising all of the previously used methods for evaluation of physiological control systems. Following this is a description of the testing protocol that was used throughout this thesis to evaluate physiological control systems in-vitro. Then there is a description of the performance metrics used to quantify the performance of control systems evaluated throughout this thesis. Finally, both the patient scenarios and the performance metrics were validated against patient data presented in the literature.

The significance of the work in this chapter is that it presents a novel method of evaluating physiological control systems. It involves simulations of a series of common patient scenarios which enables the results to be analysed from both a clinical and engineering perspective. Also, the figures of merit presented in this chapter can be used to quantitatively compare control system performance. This is significant because currently there is no consistent method of assessing controllers, making it difficult to directly compare control systems from literature.

3.1 Aim

The aim of this chapter is to develop an evaluation framework for testing of physiological control systems. The specific objectives devised to meet this aim are:

- Review the literature regarding evaluation of physiological control systems.
- Design a series of automated test scenarios in the mock circulation loop that represent common patient activities.
- Propose a set of evaluation metrics for control performance that will be used in later chapters.

- Perform validation of both the patient scenarios and performance metrics.

3.2 Literature Review

In this section, the different evaluation techniques previously used to assess control system performance and the performance metrics used to quantify performance are discussed. A number of databases (Wiley Online Library, ScienceDirect and Google Scholar) were searched for articles related to the development of physiological control systems for pulsatile and rotary LVADs, BiVADs and TAHs. The search produced 62 peer reviewed publications. Each article was reviewed and the evaluation techniques, facilitation of the techniques and figures of merit were noted. Publications that did not discuss any control evaluation were then excluded from the search results.

3.2.1 Evaluation techniques

The two main functions of a feedback loop are set point tracking and regulation of the set point in the presence of disturbances to the system. Evaluation of physiological control system performance therefore should involve a disturbance to the plant and/or a variation in the set point. Investigators have previously employed a number of different evaluation techniques in order to meet this requirement. This section describes the different techniques used by authors to evaluate performance of their control systems. The popularity of these different methods is shown in Table 3.1, with each technique described in detail in the following subsections.

Table 3.1: Popularity of different evaluation techniques for rotary VAD control system assessment.

Evaluation Technique		Number of Controllers	References
Circulatory System Variation	Preload	13	[80]–[92]
	Afterload	20	[80], [81], [84], [86]–[88], [91]–[104]
	Contractility	4	[81], [83], [91], [105]
Control System Variation	Switch On	5	[86], [87], [106], [107]
	Target	5	[101], [108]–[111]
Patient Scenarios	Exercise	8	[91], [96], [106], [109], [112]–[115]
	Suction	2	[116], [117]

3.2.1.1 Circulatory System Variation

Control systems for rotary VADs should adjust pump speed to accommodate variations in the circulatory system. It follows then that evaluation could involve some variation of the circulatory system. The most common circulatory system variations performed are step or ramp changes in preload, afterload and contractility.

3.2.1.1.1 Preload

Changes in preload can be used to measure the preload sensitivity of a control system. The preload sensitivity of a healthy LV is between 0.19 and 0.24 L/min/mmHg [51], which enables it to adjust ventricular output to be proportional to venous return. Preload sensitivity of a VAD-assisted ventricle should be in this range in order to avoid ventricular suction, hence the importance of performing step changes in preload.

Preload changes have been performed by a number of investigators, however the facilitation of this change varies between authors. In in-silico studies, Moscato and colleagues simulated an instantaneous depletion and subsequent reinfusion of 0.45 L of blood [91]. Choi et al. (2001) reduced PVR from 133.33 to 26.67 dynes.s.cm^{-5} to reduce LV preload [80]. As Waters et al. [92] and Arndt et al. [83] lumped right heart and pulmonary circulatory elements together as a single pressure source, LV preload was changed simply by adjusting the value of this pressure source. Gwak and colleagues (2007, 2011) did not use a traditional lumped parameter model for evaluation, so these investigators empirically varied preload by changing the horizontal and vertical offset of their cost function for control optimisation [86], [87]. However, these variations in cost function were not validated against clinical data.

In MCL studies, Gwak et al. (2005) [85] used a hand-operated valve between the ventricle and pump inlet to control pump inlet flow in a left-side-only MCL. This is not a realistic scenario, because it simultaneously lowers pump inlet pressure whilst increasing ventricular preload. Gaddum and colleagues (2012) [89] increased circulatory volume in a biventricular MCL by shifting fluid from the systemic venous compliance chamber into the right atrium, increasing both left and right ventricular preloads. However the volume of fluid shift was not reported.

From these papers, it is clear that changes in preload are not consistent between authors. This makes it difficult to quantitatively compare controller performance directly from literature. Another observation is that changes in preload are more precisely facilitated in-silico than in-vitro, due to the use of hand valves in-vitro. The inclusion of electronically controlled valves in a MCL may improve the precision and repeatability of preload changes in-vitro.

3.2.1.1.2 Afterload

The most common method for control system assessment is to perform a step change in afterload. The native heart is considered to be afterload-insensitive, which ensures that cardiac output is maintained regardless of the arterial pressure. The VAD-assisted ventricle should also be afterload insensitive in order to obtain similar behaviour, hence the importance of performing this test.

Afterload changes are facilitated by adjusting the systemic arterial resistance in both numerical models and mock circulation loops. However, the magnitude, sign (i.e. increase or decrease) and duration of

this change differ between authors. In-silico, Wu et al. (2003) decreased total peripheral resistance by approximately 1333 dynes.s.cm-5 linearly over a 10 second period [93]. Moscato et al. (2010) reduced SVR from 1600 to 933.33 dynes.s.cm-5 in a step wise manner [91]. Choi and colleagues (2001) increased SVR from 1333 to 1600 dynes.s.cm-5, again using a step wise approach[80]. Ferreira et al. (2009) performed a step increase in SVR from 1333.33 to 2400 dynes.s.cm^{-5}. Waters et al. (1999) performed step reductions in SVR, ranging in size from 1 to 50% of the original value of 1280 dynes.s.cm^{-5}[92]. Simaan et al. (2009) performed a ramp increase in SVR from 1333 to 2666 dynes.s.cm^{-5} over a 5 second period[99]. Like their preload changes, Gwak and colleagues (2007, 2011) adjusted their cost functions empirically to mimic afterload changes [86], [87]. Both Faragallah et al. (2012) and Wang et al. (2012) halved systemic vascular resistance in a step wise manner from 1333 to 667 dynes.s.cm^{-5}[103], [104]. Interestingly, no clinical justification is provided for any of these changes, so the clinical relevance of the magnitude, sign and duration of these changes is unknown. Whilst no justification is presented for choosing step changes over ramp changes, step changes could be considered as a worst-case scenario.

Afterload changes in-vitro are not as precise or repeatable as those performed in-silico, as they are primarily implemented by manually adjusting valves. Systemic vascular resistance was adjusted using clamp valves by Choi et al. (2001) [80], Gwak and colleagues (2005) [85], Nishida and colleagues (1996)[97], Kosaka et al. (2003) [118] and Endo et al. (2002) [119]. It appears that these investigators did not attempt to control the SVR change to any specific value. Ohuchi et al. (2001) dropped the MAP from 100 to 40mmHg, although no description was given as to how this was facilitated [98]. More recently, Casas et al. (2007) performed pseudo random changes in SVR using a servo valve [120], indicating that controlled changes in SVR are possible. Khalil and colleagues (2008) attempted more controlled changes in SVR by manually adjusting clamp valves to increase SVR from 1440 to 1760 dynes.s.cm^{-5} and to increase PVR from 160 to 800 dynes.s.cm^{-5}. However, this SVR range was quite small compared to that observed clinically. Additionally, the accuracy and repeatability of manually adjusting clamp valves was not presented and may be quite low.

Changes in afterload in-vivo and in the clinic can be performed pharmacologically or mechanically. Beppu et al. (1997) increased afterload by gradually clamping the ascending aorta[108]. Nishida et al. (1996) similarly clamped the ascending aorta during clinical evaluation of their rotary pump control system for CPB [97]. Olegario et al. (2003) pharmacologically changed afterload by injecting 10mg of methoxamine hydrochloride [117]. Nishimura (1997) also used vasodilators and vasoconstrictors to adjust vascular resistance, however no details about drugs and dosage were provided [121]. Like the manual changes in the MCL, these changes are not as precise as those made in the numerical model.

Assessing control system performance by changing the afterload is the most common form of assessment. However, like preload changes, the facilitation of changes in afterload are not consistent

between authors, which makes it difficult to compare control systems directly from literature. Afterload changes are more precise and repeatable in-silico than in-vitro and in-vivo. This is primarily due to the use of hand-operated valves in MCLs and clamps/drugs in-vivo, which introduce human error. The incorporation of electropneumatic valves along with methods of accurately measuring vascular resistances should improve repeatability and precision of this type of test in-vitro. The only way to ensure precision and repeatability in-vivo is with experienced anaesthetists and other clinical staff.

3.2.1.1.3 Contractility

Changes in contractility are used to assess the response of a control system to ventricles that are recovering (increased contractility) or failing (decreased contractility). Additionally, changes in patient activity may also affect residual heart contractility. As changes in contractility are a regular occurrence physiological control systems must be able to respond accordingly to them.

Both Moscato et al. (2010) [91] and Arndt et al. (2007) [83] used step changes in contractility to assess their controllers in an in-silico environment, in an attempt to simulate an exercise state. These changes were implemented simply as changes in the ESPVR. In in-vitro simulations, Wu et al. (2007) [116] evaluated their controller using three different depressed values of LV contractility, facilitated by adjusting the output of the pneumatic control unit for their silicone ventricle. However no transitions between contractilities were performed. Endo et al. (2002) performed step changes in contractility at two minute intervals[119]. These changes were facilitated easily because a pulsatile pump was used as a model for the ventricle, which could be easily controlled to a specific contractility. In-vivo, Endo and colleagues (2000) induced global ischemia by clamping the base of the ascending aorta, reducing contractility for preliminary controller evaluation[122].

A step change in contractility could represent a transition from rest to exercise, or a sudden myocardial infarction. Simulating different contractilities as separate experiments simulates different patients and can be used to assess the control system's ability to accommodate inter-patient variability. However, like the other circulatory system variations there is no consistency between authors with respect to the magnitude, size and implementation of these variations.

3.2.1.2 Control System Variation

Making adjustments to the circulatory system can be difficult, especially in-vivo or in clinic. In contrast, characterising control system performance by adjusting controller settings is easy to perform regardless of the evaluation apparatus used. The two main methods of control system variation are switching on the controller and performing a step change in the target signal.

3.2.1.2.1 Switching on Controller

When physiological control systems are eventually utilised in clinic, it is more than likely that the pump will first be operated in constant speed mode. Operation will then be switched to physiological control

at the clinician's discretion after the patient has stabilised. Therefore, the behaviour of the control system during initial start-up should be known, and for this reason it has previously been used as an evaluation technique.

Giridharan et al. (2002) attempted to characterise this response by switching on the pump and control system at the same time, however the dynamic behaviour of the pump somewhat masked the effect of the control system [123]. A better approach was used by Choi et al. (2001), who switched on their control system after operating at a constant speed during in-vivo evaluation [80]. Gwak and colleagues (2007,2011) and Chang et al. (2010) evaluated their controllers in the same manner as Choi et al., but using a numerical model instead of an in-vivo model [86], [87], [124].

This technique is repeatable and can be performed easily regardless of the evaluation environment. However, evaluation should not be limited to just switching on the controller, as it does not give the users enough knowledge about the controller's interaction with the native circulatory system.

3.2.1.2.2 Step Change in Target

The conventional evaluation of control system performance is the step response test, from which time-domain characteristics such as rise time, settling time and overshoot can be measured (Figure 3.1). The step response test involves performing a step-wise change in the target signal for the controller. This is different from switching the controller on, as it isolates the effect of the control system from pump dynamics.

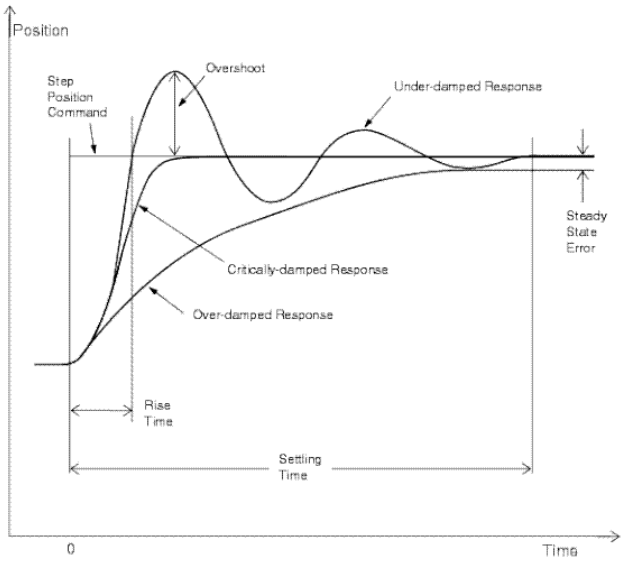

Figure 3.1: Some of the characteristics that can be obtained using a step response test [125]**.**

Alomari et al. (2011) used step changes in the target signal to assess their inlet-pressure controller[110]. Whilst it enabled time-domain evaluation, the authors neglected to highlight the effect of these step changes on the circulation. Additionally, while their controller did have a fast response time, the authors did not discuss whether these time-domain characteristics would be suitable for the human circulatory system. Saeed et al. (2010) varied the target flow of their constant-flow control system during in-vivo evaluation, and also measured the effect on LAP, CVP and total flow[126]. However, only steady-state results were obtained and no time domain analysis was reported.

Step response tests enable easy time-domain characterisation of a control system. However, suitable values for time-domain characteristics must be defined by the author for the results to be relevant. This requires knowledge of the transient characteristics of the human circulatory system in order to create a clinical context. Another downside of the step response test is that it can only be used for systems that rely on a fixed target value. Step response tests are difficult to perform on systems with varying target value, such as those presented in [91], [127], [128]. Finally, whilst tracking experiments are easy to perform, they cannot replace plant disturbances, as they do not provide an indication of how the control system will respond to common patient scenarios.

3.2.1.3 Patient Scenarios

The aforementioned evaluation techniques involve changes in single variables, either circulatory system or controller parameters. Changes in single variables are easy to perform and can provide time-domain characterisation of VAD physiological control systems as well as a low-level understanding of how these systems interact with the circulatory system. However, in practise it is rare that a circulatory parameter changes in isolation because of the complex nature of the circulatory system. Therefore, single parameter changes are not necessarily reflective of what happens during common patient scenarios. Evaluating the performance of a control system during a typical patient scenario results in a more clinically relevant assessment. The two main scenarios previously used for evaluation are exercise and ventricular suction.

3.2.1.3.1 Exercise

The most commonly simulated patient scenario for controller evaluation is exercise, and has been simulated in-silico and in-vitro. However, as shown in Table 3.2, differences arise as to how exercise has been simulated. This variation is due to the differences between evaluation apparatuses as well as the lack of a specific reference case for validation. However, from these papers, a state of exercise can be characterised by a decrease in SVR, and an increase in HR, venous return (due to increased action of the muscle pump) and contractility, all of which contribute to increased flow and arterial pressure. Interestingly, some investigators initiate exercise as a step change whereas others use a linear change in parameters over a ten second period (although no justification is given for this time scale). The step change could be considered as a worst-case scenario, and if the controller can be shown to handle this it could theoretically handle slower transitions to exercise, which are more realistic.

Table 3.2: Different methods of simulating an exercise condition using numerical models (NM) and mock circulation loops (MCLs) for the purpose of evaluating control systems. SVR - systemic vascular resistance; LVC - left ventricular contractility; RVC - right ventricular contractility; SVC - systemic venous compliance.

Author	Apparatus	Resting HR (BPM)	Exercise HR (BPM)	Transition	Other
Giridharan	NM	60	135	Start	SVR ↓ 33%
Giridharan	MCL	60	100	Step	None
Wu	NM	60	60	Ramp	SVR ↓ 35-50% Activate muscle pump
Moscato	NM	60	60	Step	SVC ↑
Karantonis	NM	70	150	Ramp	LVC ↑50% RVC ↑25% SVR ↓ 50%
		80	135		
		85	120		
		90	110		
Ferreria	NM	75	90	Step	SVR ↓ 20%
Bullister	MCL	60	99	Step	None
Lim	NM	60	95	Ramp	SVR ↓ 50% SVC fluid shift 500mL.

Exercise evaluation has also occurred in-vivo and in clinical evaluation of some controllers. Nakamura et al. exercised calves using treadmill tests, increasing the speed of the treadmill over 3 minute intervals, when evaluating pulsatile TAH control systems[129]. In the landmark clinical evaluation of their control system, Vollkron et al. [84] and Schima et al. [130] performed ergometric exercise of LVAD patients, monitoring electrocardiograms, CVP, RAP, LAP, PAP, AoP, LVAD flow and RV cardiac output. Assuming that the animal or patient is stable, functional and mobile, exercise based evaluation is simple to perform. However, instrumentation of the subject is difficult. Additionally, like all in-vivo and clinical evaluation it is an expensive and risky undertaking. The inter-patient variation means that a large number of patients must be evaluated in order to obtain statistical significance.

3.2.1.3.2 Induced Suction

Some investigators deliberately induced a state of ventricular suction in order to assess their control system's ability to mitigate this hazardous state. Wu et al. (2007), achieved this in-silico by initialising the pump speed at maximum level, causing suction, before switching the control system on [116]. For evaluation of RVAD component of a dual LVAD control system, Olegario et al. (2003) induced LV suction in-vitro and in-vivo by increasing the LVAD speed by 700 RPM[117]. Using this as a method of control system assessment requires accurate replication of ventricular suction, which is made complicated by the complex nature of rotary VAD-induced suction [56].

3.2.2 Combination of Evaluation Techniques

The previous section highlighted that there are a number of different evaluation techniques used by investigators to assess different aspects of physiological control system performance, with step changes

in afterload being the most common. One observation from this review is that investigators tend to only use only one or two of these techniques to characterise control system performance (Table 3.3). Only one author, Moscato et al. (2010)[91], evaluated their system using four different evaluation techniques. This trend of minimal evaluation is a current deficiency of control system evaluation. Only subjecting controllers to one type of test means that not all aspects of controller performance are characterised. Additionally, this minimal evaluation makes it difficult to directly compare control system performance from the literature. Consequently, if the early in-silico or in-vitro evaluation is not thorough enough, progression to in-vivo and clinical evaluation becomes difficult. Therefore, control systems should be subject to a number of different evaluation techniques in order to facilitate comparison and to thoroughly characterise the effect of the control system on the circulatory system.

Table 3.3: Number of evaluation techniques that control systems are subjected to in order to characterise control system performance.

Number of tests used to quantify performance	Number of controllers assessed in this manner
1	20
2	12
3	3
4	1

3.2.3 Performance Comparisons

The previous sections highlighted that one of the shortcomings of current evaluation methods was the tendency to subject systems to a single evaluation technique. Another shortcoming is the lack of comparisons with other physiological control systems, simulated healthy patients and/or VAD supported patients at constant speed during evaluation. Table 3.4 shows that the majority of control systems presented in literature are assessed in isolation. The end result of this isolated evaluation is that there is no point of comparison for all of these different control systems. Consequently, there is no way to directly compare control system performance from the literature. To improve upon this, investigators should subject other control systems to their evaluation framework.

Table 3.4 Types of benchmarks used for performance comparisons during control system evaluation

Benchmark Type	Number of controllers
Constant Speed	6
Healthy LV	4
Other Controller	6
None (Isolated Evaluation)	25

3.2.4 Summary of Literature Review

The purpose of the literature review was to identify evaluation techniques used by other authors in order to develop an evaluation framework for the control system evaluation used in this thesis. Evaluation techniques involve performing either single changes in variables or simulation of a patient scenario. Step changes in single variables, such as preload, afterload and contractility, allow for low-level characterisation of control system performance. However, these single variable changes are not reflective of what actually happens to the circulatory system during common patient scenarios. Patient scenarios, including exercise and deliberate induction of suction, are simulated because they are more reflective of scenarios that happen in clinic. They can also be induced easily in-vivo and in clinic, which makes in-silico and in-vitro results can be more easily validated. However, there has been no consistent method of simulating exercise.

One observation from the literature is that most investigators have only evaluated their control system by subjecting it to one or two evaluation techniques. Evaluation using more than two techniques would result in more through testing, the end result being a more robust control system. Additionally, most investigators evaluate their control system in isolation, without comparison to other physiological control system. Given the volume of VAD physiological control systems presented in the literature over the last two decades, a high-quality evaluation framework should involve quantitative comparisons to previous work. Therefore, a suitable evaluation framework must first be developed which can be used to quantitatively compare control systems previously presented in literature across a number of different patient scenarios.

3.3 Hypothesis

The main hypothesis of this chapter was to develop a repeatable evaluation framework for the assessment of VAD physiological control systems that quantifies their performance across a number of common patient scenarios.

3.4 Methods

An evaluation protocol for the assessment of control systems was developed. This section describes the selection of a testing apparatus, improvements made to this apparatus, descriptions of the testing scenarios used for evaluation, descriptions of the figures of merit used for performance evaluation and the validation procedure used for both scenarios and the figures of merit.

3.4.1 Testing Apparatus Selection

The testing apparatuses commonly used for control system evaluation were described in Chapter 1. Of these apparatuses, an MCL was chosen as the main evaluation apparatus for this thesis for a number of reasons. Firstly, using real VADs ensures that evaluation incorporates real-world limitations such as pump speed limits, turbulent flow and uncertain viscous flow behaviour in the pump. Whilst these can

be modelled numerically, their inclusion increases computation time of numerical models. Using an MCL for evaluation ensures the most realistic performance characterisation without resorting to the expense or risk of in-vivo or clinical trials. Secondly, most control system development occurs initially in the in-silico environment, and as such some evaluation is already performed in that environment. Controllers must be assessed in a different environment to remove biases associated with the developmental environment. Thirdly, the difficulties involved in modelling a pump in-silico would add unnecessary delays to the experiment, especially if pumps are already available for bench top testing.

The MCL designed and constructed by Timms and colleagues [74], [131] (described in section 2.4.1) was used for a number of reasons. Firstly, it is one of the only five-element Windkessel MCLs available worldwide. Five-element Windkessel models incorporate elements of characteristic resistance, arterial compliance, peripheral resistance, inertial component and venous compliance. Inclusion of these elements ensures accurate replication of ventricular and arterial pressure waveforms (Figure 3.2), making this apparatus appropriate for control system evaluation. Secondly, the MCL was designed by first developing a computer simulation of the loop. Pipe diameters and lengths were optimised within the simulation in order to replicate haemodynamics accurately [75]. Finally, this MCL is a biventricular MCL, making it suitable for evaluation of control systems for rotary BiVADs. In contrast, many other MCLs used for control system evaluation are left-sided only loops which makes them unsuitable for this thesis.

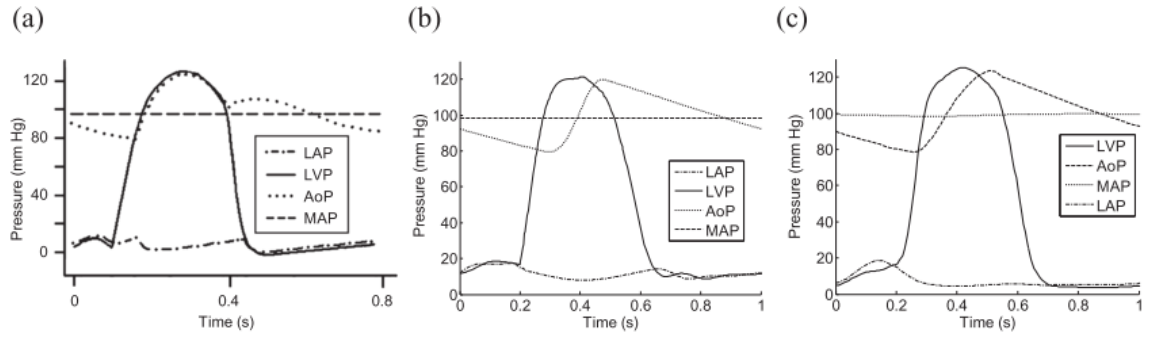

Figure 3.2: Comparison of systemic pressure traces between a natural (a), computer simulated (b) and that produced by an MCL (c). LVP - left ventricle pressure; LAP - left atrial pressure; AoP - aortic pressure; MAP - mean aortic pressure. [74]

3.4.2 Rotary Ventricular Assist Devices

In order to evaluate control systems for dual rotary pumps, two rotary LVADs were required. Two ex-vivo VentrAssist LVADs were donated by Professor Robert Salamonsen from the Alfred Hospital, enabling two devices to be used free-of-charge. While these devices are no longer used in clinic, they are still third-generation implantable centrifugal rotary LVADs and as such can be used to represent modern devices such as the HeartWare HVAD. It could be argued that the results in this thesis would be more clinically relevant if the experiments used a clinically available centrifugal pump. However,

the control objectives that are described in the next chapter are almost all pump-independent. Giridharan and Skliar established this by testing their control system using both axial and centrifugal pumps [106]. This means that the choice of pump does not have as much impact on performance as the selection of the control objective.

With the assistance of Professor Nigel Lovell from University of New South Wales and Dr Peter Ayre (Thorvascular Pty Ltd), these pumps were interfaced with the dSPACE 1103 data acquisition system, enabling both measurement and control of pump parameters. The VentrAssist LVAD DC motor uses a constant voltage source and a pulse width modulation (PWM) signal to control the current. The higher the duty cycle of the PWM signal, the higher the motor current and therefore the higher the pump speed. Using this information, a new PI speed controller was developed in the Matlab/Simulink environment (The Mathworks, Natick, MA), which was more responsive than the default speed controller available clinically. Additionally, access to the PWM duty cycle enabled all control systems developed in this thesis to directly control pump PWM duty cycle, rather than pump speed. This minimised the complexity of controllers developed in this thesis.

3.4.3 Evaluation Techniques

Patient scenarios were used to evaluate the control systems in this thesis, because they provide a clinical context for controller evaluation. The most common scenario from the literature was exercise, so this scenario was also utilised in this thesis. Two other scenarios, a postural change and a Valsalva manoeuvre, were also simulated. These two scenarios are commonly performed by discharged patients, with the Valsalva manoeuvre representing straining that occurs during lifting or defecation. Therefore, knowing the response of a physiological control system to these scenarios would be of significant value to patients and caregivers.

3.4.3.1 Postural Change

Changes in posture cause fluid shifts in the circulatory system. For example, moving from a lying to standing position causes fluid to move from the thorax into the lower limbs. This will result in a temporary reduction in venous return to the right atrium. The reason for simulating a transition from lying to standing is that the reduced venous return to the RA increases the risk of suction in the RV. It also increases the risk of suction in the LV, since a reduction RV inflow will eventually cause a reduction in LV inflow. Simulating this drop in venous return enables evaluation of a control system's preload sensitivity and therefore their ability to avoid suction.

Fluid shifts between the thorax and lower limbs were simulated by shifting 300 mL of fluid from the circulation into the systemic venous compliance (SVC) chamber. The SVC chamber is a realistic approximation of lower limb venous circulation because 60% of all venous blood lies in the veins of

the lower limbs. After shifting the fluid, the new state was held for 60 seconds, which allowed enough time for MCL haemodynamics to settle. The fluid was then shifted back into circulation.

Fluid shifting in the MCL was controlled by adjusting the air pressure in the SVC chamber. Reducing air pressure allows fluid to move into the SVC and decreases mean circulatory pressure (MCP) (emptying the MCL), whilst increasing air pressure moves fluid out of the SVC and increases MCP (filling the MCL).

Figure 3.3: Ball valves used to lower (large valve) and raise (small valve) circulatory volume in the MCL

This fluid shift was initially facilitated using manual ball valves (Figure 3.3). As described in the literature review of this chapter, the use of manual valves results in low repeatability, which lowers the quality of evaluation using volume changes. To improve repeatability, these manual valves were replaced with a combination of two normally closed (NC) solenoids and a high-pressure manual regulator, using the configuration shown in Figure 3.4. Filling and emptying were facilitated using the switching shown in Table 3.5.

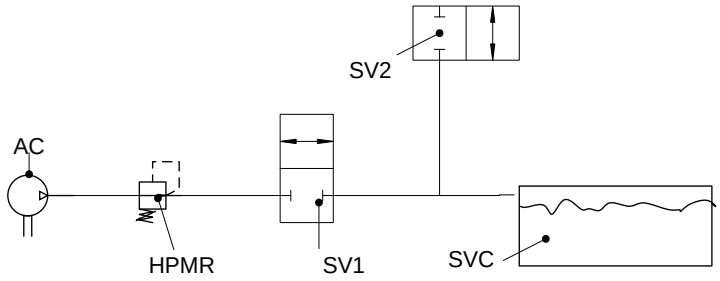

Figure 3.4: Solenoid valve configuration for filling and emptying. AC - compressed air supply; HPMR - high pressure manual regulatory; SV - solenoid valve; SVC - systemic venous compliance chamber.

Table 3.5: Solenoid valve settings for filling and emptying the MCL.

Mode	Solenoid Valve 1	Solenoid Valve 2
Filling	Open	Closed
Emptying	Closed	Open
Hold	Closed	Closed

Accurate fluid shifts were facilitated using closed loop control. The weight of fluid in the SVC was continuously measured using a digital scale (BW 4-20 Indicator, @Weight Pty Ltd, Melbourne, Australia). Fluid shifts were then automated using the control logic shown in Figure 3.5. The control logic was implemented using Simulink.

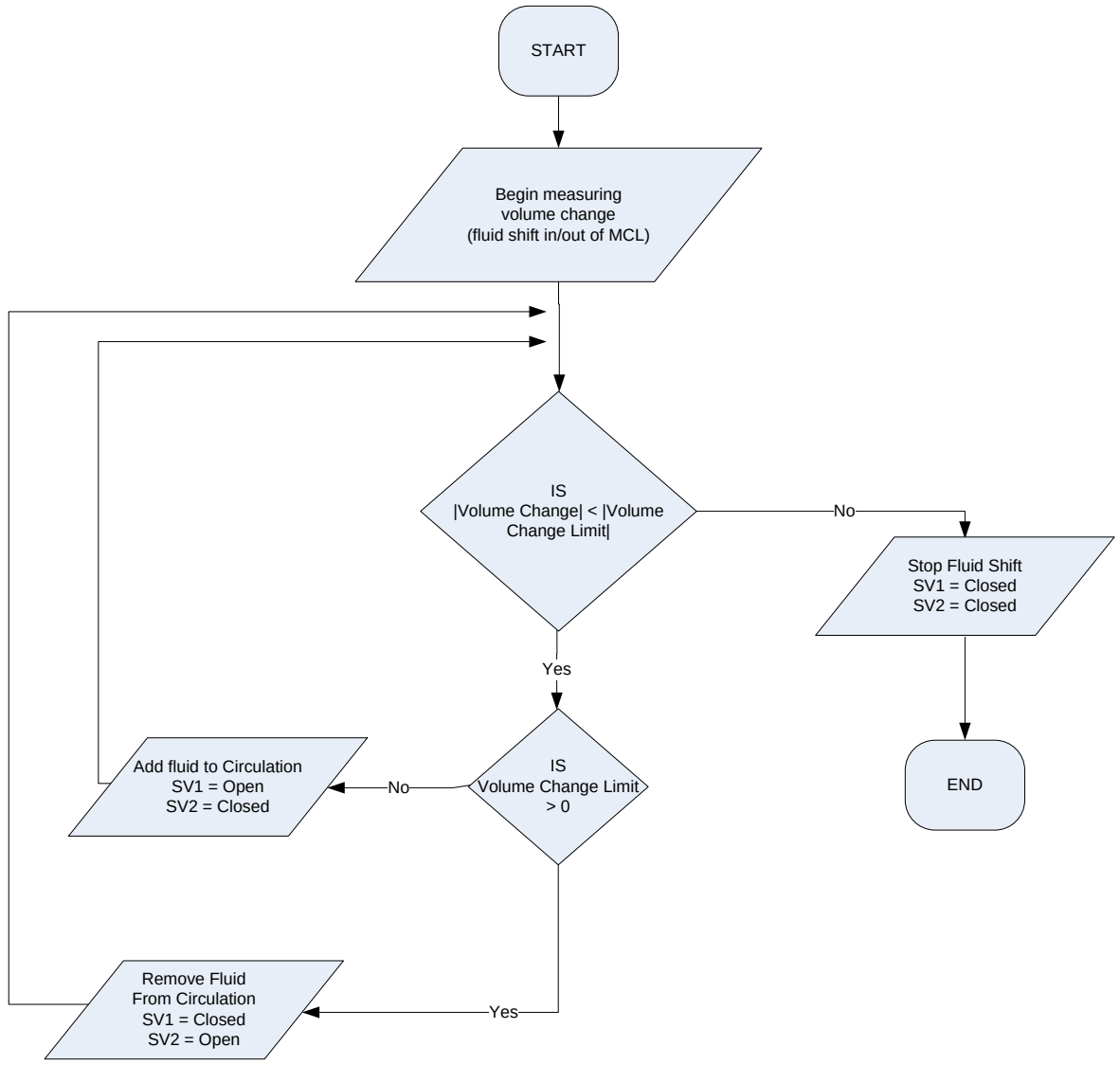

Figure 3.5: Control logic for controlled shifts of fluid in the MCL.

3.4.3.2 Valsalva manoeuvre

The Valsalva manoeuvre describes forced exhalation against a closed glottis. It is a simple action that can be performed easily by patients, and is sometimes used to assess heart function [132]. It is also representative of the straining that occurs during lifting, sneezing, coughing and defecation. The Valsalva manoeuvre has been shown to sharply reduce LV venous return. Therefore, evaluation of a control system's performance to this scenario is necessary to ensure the controller response is appropriate.

The Valsalva manoeuvre consists of four phases (Figure 3.6). The first phase, intrathoracic compression, compresses the heart chambers and augments output to the periphery. It also causes reduced diastolic filling and therefore reduced LV stroke volume. According to Lu and colleagues [133] this phase lasts for 1-2 heartbeats. The reduced LV output leads to the reduction in arterial pressure seen in Phase 2. The baroreflex (particular the sympathetic stimulation of venous tone and contractility) is then responsible for restoring arterial pressure. Phase 3, release of the Valsalva, is marked by a drop in arterial pressure, due to the sudden reduction in intracardiac pressure and stroke volume. Phase 4 describes the overshoot and recovery of the arterial pressure caused by the baroreflex.

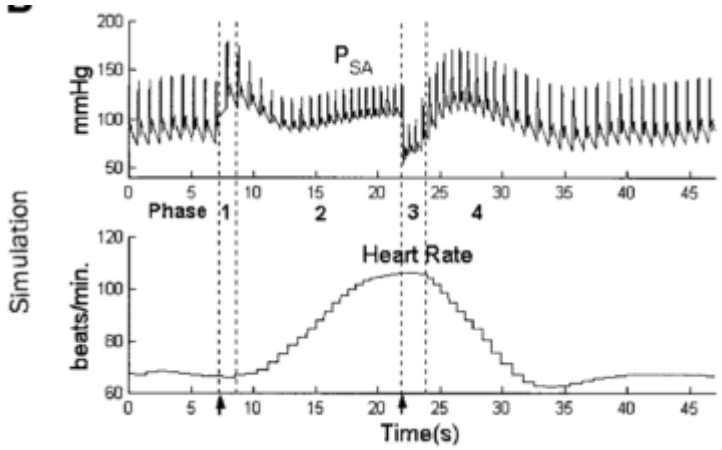

Figure 3.6: Arterial pressure and heart rate during a Valsalva manoeuvre, simulated using a numerical model of the cardiovascular and pulmonary systems [133]**. The four phases are noted here.**

From the previous description of the Valsalva manoeuvre, some simulation of breathing was required to be implemented in the MCL prior to implementing this scenario. Variation of intrathoracic pressure caused by breathing changes the external pressure on the ventricles, which results in changes to preload. Unfortunately, the MCL chambers were constructed from rigid polyvinyl chloride, making it impossible to apply an external compressive pressure. Therefore, breathing was simulated by pressurising the air in the pulmonary venous compliance (PVC) chamber, which pushed fluid from the PVC chamber into the left ventricle. This simulated the compression of the pulmonary capillaries that occurs during breathing, which squeezes additional fluid into the left atrium.

Table 3.6: Solenoid valve inputs required for each breathing state

Breathing State	3/2 Valve	2/2 Valve
Inhalation	ON	ON
Exhalation	OFF	ON
Hold	ON or OFF	OFF

This mechanism was implemented using a compressed air supply, high pressure manual regulator (ITV2030-012BS5, SMC Pneumatics, Tokyo, Japan), a 3/2 NC solenoid valve (VT325-035DLS, SMC Pneumatics, Tokyo, Japan) and a 2/2 NC

solenoid valve (VX2360-04-5D1, SMC Pneumatics, Tokyo, Japan) as per Figure 3.7. The configuration of solenoid valves enabled three states of operation: inhalation, exhalation and a hold mode (Table 3.6). Breathing was facilitated by switching the 2/2 valve ON and alternating the 3/2 valve between the ON and OFF positions. The default breathing rate was set at 10 breaths per minute. This pneumatic configuration was installed alongside the other MCL pneumatics. The manual regulator was adjusted until an inhalation of 3 seconds pushed most of the fluid out of the PVC chamber.

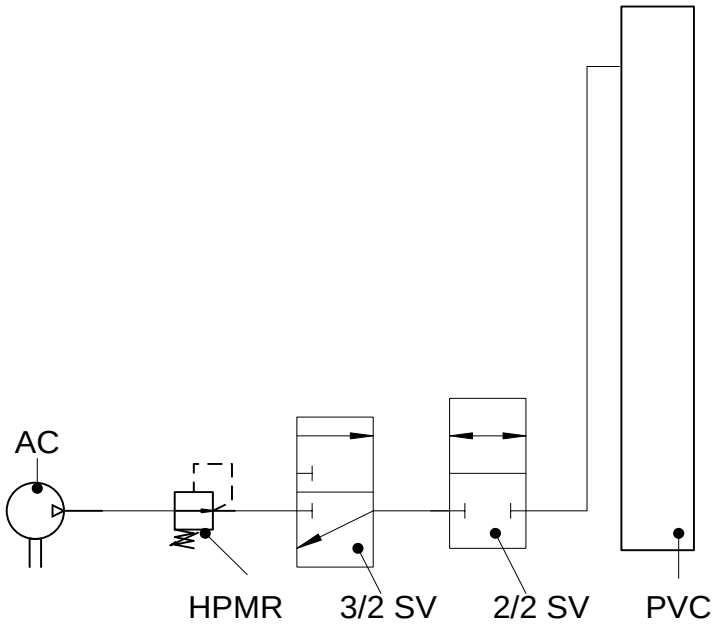

Figure 3.7: Pneumatic setup required for simulation of breathing in the MCL. AC - compressed air supply; HPMR - high pressure manual regulator; SV - solenoid valve; PVC - pulmonary venous compliance chamber.

Simulation of the Valsalva manoeuvre was simplified by only incorporating the changes in intrathoracic pressure and stroke volume. To replicate the increase in intrathoracic pressure (Phase 1), an inhalation was performed. Then the pulmonary venous compliance chamber (PVC), normally open to atmosphere to simulate the high compliance of the pulmonary circulation, was closed to atmosphere. This increased the LV diastolic filling and therefore the arterial pressure. The drop in LV diastolic filling and therefore arterial pressure (Phase 2) was simulated by increasing the PVR from 100 to 350 dynes.s.cm^{-5} two seconds after phase 1. To release the Valsalva manoeuvre, the PAC chamber was reopened to atmosphere (Phase 3) and PVR restored to the normal value of 100 dynes.s.cm^{-5} two seconds after the PAC was reopened (Phase 4).

The baroreflex is an important factor in the shapes of the of the arterial pressure waveforms during the Valsalva manoeuvre. However, a baroreflex simulation was omitted from the MCL for a number of reasons. The first reason was that in the situation in which dual LVADs are required, the reflex is either

absent or severely limited in its action due to pre-existing cardiovascular disease or the implantation procedure. This means that even if a reflex was able to be simulated in the MCL, its inclusion is not necessary relevant. Secondly, omission of the reflex should still produce realistic results, since it is the changes in intrathoracic pressure during the Valsalva manoeuvre (and consequently LV end-diastolic volume) that are of most concern, since reduced LV filling may result in LV suction. A baroreflex was not necessary to change preload in the MCL. Finally, incorporation of the baroreflex introduces another control loop into the system, increasing system complexity and may result in the masking of the behaviour of the physiological control systems. One effect of the omission of the baroreflex was that the heart rate did not vary during the Valsalva manoeuvre.

3.4.3.3 Exercise

Exercise encompasses any patient activity more intense than a resting state, requiring a higher cardiac output than rest. Discharged rotary VAD patients may exhibit slightly improved exercise performance a number of months after implantation compared to unsupported chronic HF patients and are therefore more active [134]. Salamonsen and colleagues found that the larger the pump flow increase in exercise the greater the patient's exercise capacity [135]. Therefore, a control system that can increase pump flow in exercise without draining the ventricles may be beneficial for patients. It was for this reason that an exercise scenario was chosen as part of the framework.

Further modifications to the MCL were required in order to increase cardiac output during exercise. Firstly, in a collaboration with Dr Shaun Gregory, the ventricular contraction mechanism was modified in order to better mimic the Frank-Starling behaviour of each ventricle. This mechanism was described in detail in section 2.4.1.

The second MCL modification ensured that increases in heart rate resulted in increased contractility. One limitation of the Timms' MCL was that increasing the heart rate resulted in less time to pneumatically compress the ventricles in systole and less time for the ventricles to passively fill in diastole. The result was that increasing the heart rate actually decreased cardiac output, which is the opposite of what happens in a normal heart. To compensate, the regulator voltage was increased in proportion to the increase in heart rate, effectively introducing the force-frequency relationship present in the native heart into the MCL. Equation (2.1) was modified to incorporate heart rate, producing Equation (3.1).

$$V_{reg} = \begin{cases} V_P(t).K_{starling}(t).K_{ven}\ ;\ HR\ \leq 60 \\ V_P(t).K_{starling}(t).(K_{ven} + (HR - 60)K_{HR})\ ;\ 60\ < HR < 90 \\ V_P(t).K_{starling}(t).(K_{ven} + 30K_{HR})\ ;\ HR\ \geq 90 \end{cases} \quad (3.1)$$

HR is the heart rate (BPM) and K_{HR} (min) is another contractility constant which affects the sensitivity of the contractility to heart rate. Values of K_{HR} for LV and RV for three different contractility conditions are given in Appendix A.

Finally, a variable systolic period was introduced into the MCL. The Timms' MCL initially required the user to set the percentage of time spent in systole during the cardiac cycle, and this was kept constant regardless of heart rate. However, the percentage of time spent in systole actually increases as heart rate increases [136]. Therefore, to more accurately represent states of exercise, this variation was incorporated into the MCL.

Systolic period was adjusted using the relationship defined by Vollkron and colleagues [136], shown in Figure 3.8 . Data were extracted from this figure using DataThief (B.Tummers, http://datathief.org) and imported into Matlab (The Mathworks, Natick, MA, USA). The relative time spent in systole (systolic ratio) during each heart beat was calculated for each heart rate. Linear regression was the used to quantify the relationship between HR (in BPM) and the systolic ratio (Equation (3.2)).

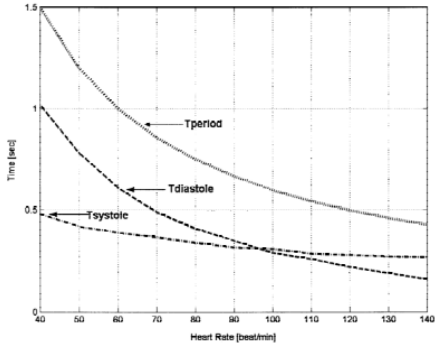

Figure 3.8: The effect of heart frequency on the duration of systolic and diastolic phases [136].

$$SystolicRatio = K_{SD}\,.HR + c_{SD} \tag{3.2}$$

The constants K_{SD} and c_{SD} were 0.0029 min and 0.2123 respectively, producing an R^2 value of 0.9963. Systolic time (in seconds), T_{sys}, was then determined by multiplying the ratio by the heart period (Equation (3.3)).

$$T_{sys} = \frac{60.SystolicRatio}{HR} \tag{3.3}$$

As highlighted in the literature review, exercise has been simulated in a number of different ways by other investigators. However, in each of these previous simulations, the primary haemodynamic characteristics of exercise were an increase in cardiac output and arterial pressure [20]. For this evaluation framework, cardiac output was increased by increasing the heart rate from 60 to 80 BPM, decreasing the SVR from 1300 to 800 dynes.s.cm^{-5} and decreasing the PVR from 100 to 40 dynes.s.cm^{-5}. The heart rate was only increased to 80 BPM because further heart rate increases did not increase

cardiac output. This was a limitation of this MCL. Replication of the muscle pump effects was achieved by shifting 700mL of fluid from the SVC into the RA, further augmenting cardiac output increases. N

During simulations of healthy ventricles, left and right ventricular contractility were increased by varying K_{sm1} from 0.387 to 0.403 for the LV and 0.199 to 0.256 for the RV, which increased both cardiac output and arterial pressure. However, exercise capacity is greatly reduced in heart failure, due to reduced contractile strength of the myocardium[20]. It was therefore assumed that in simulations of HF in the MCL, there was no capacity for the failed ventricles to further increase their output via sympathetic stimulation. Therefore, for simulations of HF patients exercising, K_{sm1} was not increased beyond the resting values. An atrial kick was also included to assist in shifting fluid across the atrioventricular valves. Atrial contraction was implemented in a manner similar to the ventricles, as described in [74]. The contractility (as represented by the maximum current sent to the electropneumatic regulators during systole) of the atria was varied manually until the atrial and ventricular pressures equalized at the end of ventricular diastole.

3.4.3.4 Combined Test Bed

The three patient scenarios were combined sequentially to produce a single test bed for control system evaluation. Combining each scenario provides a more complete story than each scenario alone. For example, after a scenario, if a control system that does not stabilise pump speed fast enough then it may affect its performance in the next scenario.

Beginning with a resting condition, each scenario was simulated consecutively. The loop was returned to a resting state between each scenario. A summary of the timing of the combined test bed, and the MCL settings that were adjusted for each event is given in Table 3.7.

Table 3.7 Settings for each patient scenario simulated in the MCL. PVR - pulmonary vascular resistance; SVR - systemic vascular resistance; HR - heart rate; RV - right ventricle; SVC - systemic venous compliance chamber; PVC - pulmonary venous compliance chamber; LV - left ventricle.

Scenario	Simulation Time (s)	Name	PVR (dynes.s.cm^{-5})	SVR (dynes.s.cm^{-5})	HR (BPM)	Circulation fluid shift
1	0	Rest	100	1300	60	--
2	60	Postural Change	100	1300	60	RV -> SVC (300mL)
3	120	Rest	100	1300	60	SVC -> RV (300mL)
4	180	Valsalva	350	1300	60	PVC -> LV (100mL)
5	240	Rest	100	1300	60	LV -> PVC (100mL)
6	300	Exercise	40	800	80	SVC -> RV (700mL)
7	360	Rest	100	1300	60	RV -> SVC (700mL)

3.4.4 Figures of Merit

As highlighted in the literature review, there is no consistent method of quantifying of the performance of physiological control systems for rotary VADs. It is essential to quantify control performance to provide a measurable point of comparison with other control systems during evaluation. Four different figures of merit (FOMs) were created in order to quantify four aspects of control system performance.

Firstly, the control system's ability to maintain appropriate resting haemodynamics was assessed by measuring the steady state mean aortic pressure, mean pulmonary arterial pressure and mean pulmonary and systemic flow during all resting states (Scenarios 1, 3, 5 and 7). In order to maintain appropriate end-organ perfusion as well as patient comfort, these parameters must remain within certain ranges. These ranges (Table 3.8) were selected after review of physiological textbooks and discussions with clinical staff at The Prince Charles Hospital.

Table 3.8: Appropriate ranges for control systems during rest to ensure end-organ perfusion.

Variable	Range
Mean aortic pressure	60-120 mmHg
Mean pulmonary arterial pressure	15-25mmHg.
Mean pulmonary flow rate	4.5-6 L.min^{-1}
Mean systemic flow rate	4.5-6 L.min^{-1}

A single performance metric, FOM_{REST} was used to quantify how well these 4 variables remained within these ranges (Equation (3.4))

$$FOM_{REST} = \frac{\sum_{i=1}^{i=N}(T_{i_{Safe}} - T_{i_{Unsafe}})}{N.T} \times 100\% \tag{3.4}$$

Where T_{iSafe} and $T_{iunsafe}$ represent the time (in seconds) spent by the *ith* variable in the safe and unsafe ranges respectively, N is the number of such variables (in this case N = 4) and T represents the total length of the simulation (in seconds). FOM_{REST} was calculated only during the resting scenarios, as pressures and flow may temporarily vary outside of these ranges safely during common patient scenarios.

Secondly, the control systems must not cause pulmonary or system venous congestion. Pulmonary congestion is especially harmful, as it causes oedema fluid to overwhelm the capacity of the interstitial space and flood the airways and alveoli [137]. Pulmonary and systemic congestion is prevented by maintaining LAP and RAP below the threshold of 25mmHg respectively [137], [138]. Maintaining pressures at 15mmHg was advised by Boston, Antaki and Simaan (2003) in order to improve the safety margin [59]. Therefore, we defined two regions for safe LAP and RAP operation. Atrial pressures below 15 mmHg were considered "good", between 15 and 25mmHg "average" and above 25mmHg was considered "Poor". To quantify congestion avoidance performance, Equation (3.5) was used.

$$FOM_{CONG} = \frac{(T_{Good} - T_{Poor})}{T} \times 100\% \tag{3.5}$$

Where T_{Good} is the time (in seconds) spent in the "Good" range, T_{poor} the time (in seconds) spent in the "Poor" range and T the total length of the simulation (in seconds). Spending significant time in the "Good" range results in a high positive score, whilst excessive time in the "Poor" region results in a negative score. "Average" performance results a score around zero. This score was calculated separately for systemic and pulmonary circulations.

Thirdly, as fewer suction events indicated better control system performance, the number of suction events were recorded as FOM_{SUC}. Suction events were simulated in the same manner as Lim [139], who defined the resistance between LV and pump inlet as a variable resistance R_{suc}. Under normal operation, R_{suc} is set to zero. When the LV volume below a threshold, R_{suc} increased exponentially, based on the difference between ventricular volume and a threshold. This approach was found to match the suction observed in the author's animal experiments than other approaches. Therefore, this approach was adopted for use in this MCL. Variable inflow cannula resistance in the LV and RV was achieved using socket valves (VMP025.03X.71, Alb. Klein Ohio, Plain City, OH) installed between the ventricles and VAD inlet ports. These valves were used to set the inflow cannula resistance as a function of ventricular volume, adapting the relationship used by Lim [139]. This relationship is described by Equation (3.6).

$$R_{suc} = \begin{cases} k_{s1}\left(e^{k_{s2}(V_{lv}-V_{th})}\right) V_{lv} < V_{th} \\ 0 \;\; V_{lv} \geq V_{th} \end{cases} \tag{3.6}$$

Values for the constants k_{s1} and k_{s2} were selected the same as presented by Lim and colleagues (0.5 $mmHg.s.mL^{-1}$ and $-1.3\ mL^{-1}$ respectively). The volume threshold V_{th} was set at 30mL, which was the minimum volume achievable in the MCL that enabled normal ventricle contractile behaviour.

A suction event was defined as closing of the suction solenoid valves, and was measured as events per second (Equation (3.7)).

$$FOM_{SUC} = \frac{N}{T} \tag{3.7}$$

N represents the total number of suction events and *T* the total simulation time in seconds. FOM_{SUC} was calculated separately for left and right ventricles.

Fourthly, the exercise performance was assessed by measuring the steady state LVAD, RVAD, systemic and pulmonary flow rates. An increase in total flow is desired during exercise, which would theoretically deliver more oxygen to the exercising muscles. It is also desirable that the increase in flow be primarily due to an increase in pump flow in order to reduce unnecessary strain on the ventricles.

With this in mind, FOM_{EX} (described in Equation (3.8)) was used to quantify the effective increase in flow during exercise.

$$FOM_{EX} = (\overline{Q_{exercise}} - \overline{Q_{rest}})^{\left\{\frac{\left(\overline{Q_{VAD\,exercise}}\right)}{\left(\overline{Q_{exercise}}\right)}\right\}} \tag{3.8}$$

Where $\overline{Q_{exercise}}$ and $\overline{Q_{VAD\,exercise}}$ represent the mean total and pump flows respectively during the whole duration of the exercise scenario (scenario 6), and $\overline{Q_{rest}}$ and $\overline{Q_{VAD\,rest}}$ represent the mean resting total and pump flows respectively. This FOM primarily rewards increases in total flow due to increases in pump flow. It also rewards controllers that increase flow quickly, as the mean exercise flow is calculated over the duration of the whole exercise scenario. (Note that whilst the other three FOMs are expressed as a percentage, FOM_{EX} is expressed in $L.min^{-1}$)

3.4.5 Validation and Repeatability Assessment

In order to use the test beds and FOMs, validation was required. The following section describes the validation methods used.

3.4.5.1 Patient Scenarios

Ten iterations of patient scenarios were simulated for two heart conditions (healthy and mild left ventricular failure), and both accuracy and repeatability were measured. Accuracy was assessed by measuring the steady state mean ± standard deviation of systemic and pulmonary arterial pressure and flow and left and right atrial pressures for all scenarios across all the tests and comparing these values to those presented in literature. Steady state was defined as the final ten seconds of each of the seven stages outlined in Table 3.7. Additionally, arterial pressure waveforms during the Valsalva manoeuvre were compared to those presented by Lu and colleagues, who simulated the Valsalva manoeuvre with and without a validated baroreflex in a numerical model [133].

Transient repeatability was assessed by calculating the correlation coefficients of key haemodynamic parameters (aortic, pulmonary arterial, left and right atrial pressures and systemic and pulmonary flow rates) between each of the ten iterations for each heart condition. The null hypothesis was that there was no correlation between any of the simulations. A p-value less than 0.05 was considered significant to reject the null hypothesis.

3.4.5.2 Figures of Merit

Validation of the four FOMs involved determining the range of values for each one. Some of the ranges could be inferred, while others had to be determined experimentally.

Validation of FOM_{REST} and FOM_{CONG} was performed by simulating 3 patient scenarios for three different heart conditions and obtaining the maximum and minimum values for each FOM. The VAD was not in place for these simulations. The best-case scenario was considered to be a healthy simulated patient. As the loop was previously validated using human data, simulation of a healthy patient was considered a realistic representation of human cardiovascular behaviour. Simulations of mild and severe left heart failure patients were used establish baselines for the worst-case scenarios.

Validation of FOM_{suc} was not required, because this metric only counts the number of times the suction valves close during a simulation. The best-case value for FOM_{suc} was considered to be zero, while there would be no upper limit.

Validation of FOM_{EX} involved measuring the increase in flow rate during the simulation of the healthy patient exercising, and using this as the upper limit. The lower limit was considered to be zero, indicating no contribution from the VAD during exercise.

3.4.6 Results

3.4.6.1 Test Bed Validation

Accuracy of the test bed simulation was assessed by comparing steady state haemodynamics with those observed in literature. For the healthy simulation, resting MAP, mean pulmonary arterial pressure (MPAP), MSQ and mean pulmonary flow rate (MPQ) were all within suitable ranges given in literature (Table 3.9). However, LAP and RAP were higher than these ranges at rest. All resting haemodynamics were similar across the four resting scenarios, indicating that the initial condition was able to be restored before the next patient scenario was simulated.

The changes in postural change for all variables were different to those reported in literature. MAP dropped by 8mmHg, whereas it should not have changed at all. The other parameters all fell, however these reductions were not as large as those reported in literature. In the Valsalva manoeuvre, the flow rate decreased and the pulmonary arterial pressures all increased, although these changes were not as high in magnitude as those reported in literature. However, the MAP, which was meant to stay constant, fell nearly ten percent. The aortic pressure waveforms produced during the Valsalva manoeuvre were compared with those generated by Lu and colleague, who simulated the Valsalva manoeuvre without the baroreflex (Figure 3.9). Whilst the time scales are different, it is obvious that the behaviour of arterial pressure is similar, and the 4 phases can be clearly identified.

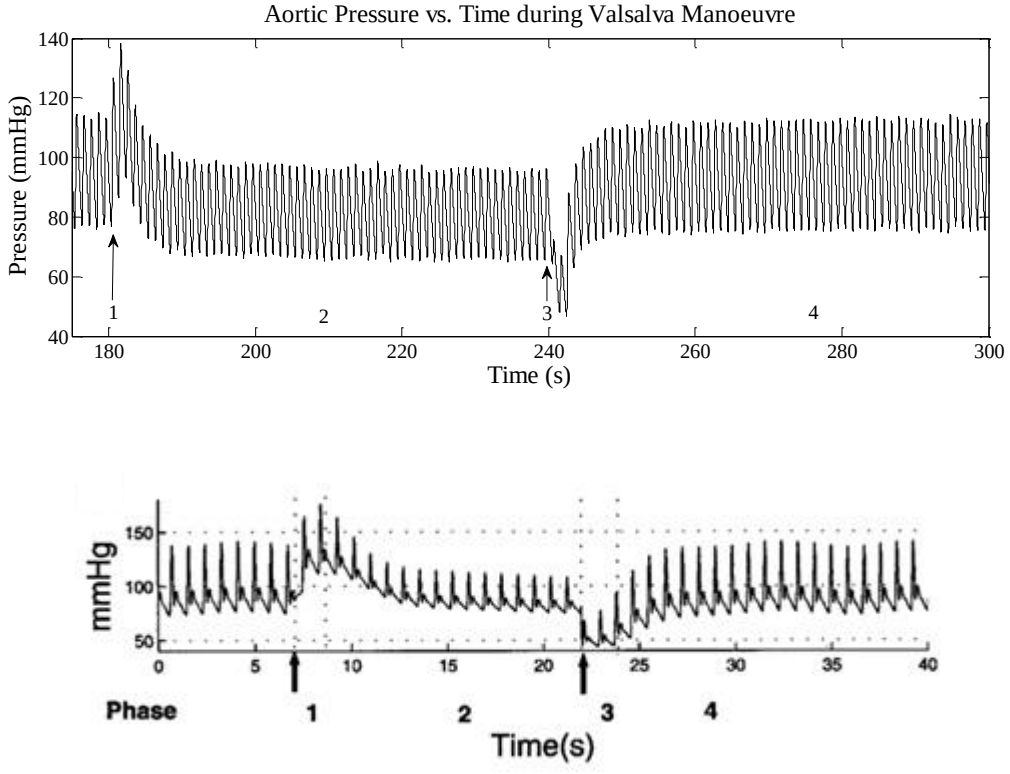

Figure 3.9: Aortic pressure during a simulated Valsalva manoeuvre, produced in the MCL (Top) and from a numerical model (bottom) produced obtained from literature [133]**. Both simulations were performed without a baroreflex present.**

During exercise, the MPAP, MLAP, MRAP and flows all increased, similar to that observed in literature. However, the MAP was unchanged. The MCL was able to revert back to the initial resting condition between scenarios, with all haemodynamics returning to within three percent of their initial values. However, the final resting state produced haemodynamics between five and ten percent lower than the initial values.

Table 3.9: Steady state haemodynamics in all scenarios for simulated healthy patients in the MCL

Parameter	Rest 1		Postural Change (% Change)		Rest 2 (% Change)	Valsalva (% Change)		Rest 3 (% Change)	Exercise (% Change)		Rest 4 (% Change)
	MCL	Literature	MCL	Literature		MCL	Literature		MCL	Literature	
MAP	95±2.2mmHg	100 mmHg [77], [140]	-8.6±0.3	1[141]	-1.3±0.5	-15.8±0.6	0	-2±0.5	-0.5±4.5	19-40[140], [141]	-5.5±0.7
MPAP	16±0.8 mmHg	15 mmHg [77]	-9.6±0.3	-33[141]	-1.6±0.3	51.4±3	252	-1±0.5	12.7±4.6	67[141]	-6.6±1.4
LAP	10±0.7 mmHg	1-5 mmHg [77]	-10.6±0.4	-111[141]	-1.9±0.4	-24.2±0.6	- -	-2.8±0.6	33.9±6.2	61[141]	-6.3±2.1
RAP	8±0.6 mmHg	-5 -0 mmHg [77]	-21.6±2	-157[141]	-2.7±1.3	11.6±3.1	- -	-2±1.5	57.9±11.1	33[141]	-9±7.4
MSQ	4.9±0.1L.min^{-1}	4.9-5.6 L.min^{-1} [77]	-7.3±0.2	-21[141]	-1.2±0.4	-18.5±0.5	-53.13	-1.9±0.5	74.7±7.6	60-76[140], [141]	-5.2±0.4
MPQ	4.8±0.1 L.min^{-1}	4.9-5.6 L.min^{-1}[77]	-7.5±0.4	-21[141]	-1±0.5	-18.9±0.6	-53.13	-1.6±0.6	78±8.6	60-76[140], [141]	-5.1±0.5

Table 3.10: Steady state haemodynamics in all scenarios for simulated mild left heart failure patients in the MCL

Parameter	Rest 1 (% Change)		Postural Change (% Change)		Rest 2 (% Change)	Valsalva (% Change)		Rest 3 (% Change)	Exercise (% Change)		Rest 4 (% Change)
	MCL	Literature	MCL	Literature		MCL	Literature		MCL	Literature	
MAP	72.3±8.4 mmHg	80-87 mmHg [140], [142], [143]	-7.4±0.6	0 [141]	-1.3±0.3	-11±0.6	- -	-1.7±0.2	3.2±0.4	0-32[140]–[143]	-5±0.7
MPAP	18.5±0.2 mmHg	15.9-31 mmHg [140]–[144]	-11.2±0.2	-15 - - 49[141], [144], [145]	-2±0.3	35.9±0.8	- -	-1.9±0.2	23.1±1	54-71[140], [142], [143]	-7.9±0.3
LAP	13.4±0.1 mmHg	11-19 mmHg [141]–[143]	-13.1±0.3	-74 [141]	-2.2±0.5	-25.1±0.5	- -	-3.2±0.3	39.5±1.2	63-94[142], [143]	-8.6±0.3
RAP	6.7±0.2 mmHg	4-8 mmHg [141]–[143]	-25.1±1.5	-105[141]	-4.2±0.4	15.9±1.3	- -	-3.6±0.6	48.4±4.8	63-175[141]–[143]	-14.9±5.3
MSQ	4±0L.min^{-1}	3.5-4.56 L.min^{-1}[140]–[143]	-5.5±0.7	-12.5[141]	-0.9±0.5	-13.7±0.6	- -	-1.4±0.2	83.2±1.1	60-88[141]–[143]	-3.9±0.8
MPQ	4±0 L.min^{-1}	3.5-4.5 L.min^{-1}6[140]–[143]	-6.1±1.1	-12.5[141]	-1.1±0.6	-14.2±0.4	- -	-1.2±0.7	86.3±0.8	60-88[141]–[143]	-4.3±0.5

For the mild left heart failure condition, all resting parameters except for MAP were within the ranges specified in literature (Table 3.10). Specifically, the LAP, PAP and RAP were elevated and MSQ and MPQ reduced compared to their healthy values, due to reduced LV function. MAP was lower than literature values, due to the lack of a baroreflex.

Like the healthy simulations, the haemodynamic changes for simulated mild left heart failure (MLHF) patients during the postural change simulation were of a smaller magnitude that those reported in literature. The main differences between MCL and literature observations were the left and right atrial pressures (-13% and -25% in the MCL and -74% and -105% from literature).

Validation of the Valsalva manoeuvre with MLHF was more complicated than the healthy case due to the fact the Lu and colleagues did not simulate a MLHF case without the baroreflex. Therefore, validation was performed using data from patients whose baroreflex was present. Figure 3.10 shows that there was a distinct difference in the systemic arterial pressure waveform for the mild LHF condition generated in the MCL compared to mild and severe heart failure waveforms from patients. There was no overshoot of arterial pressure during Phase 2, nor was there large variation in MAP in phases 2 and 4. This was primarily due to the lack of a baroreflex. Between heart failure and healthy simulations, the only similarity was that the percentage change in LAP was similar. This was to be expected, as the change in PVR was consistently 350 dynes.s.cm^{-5}.

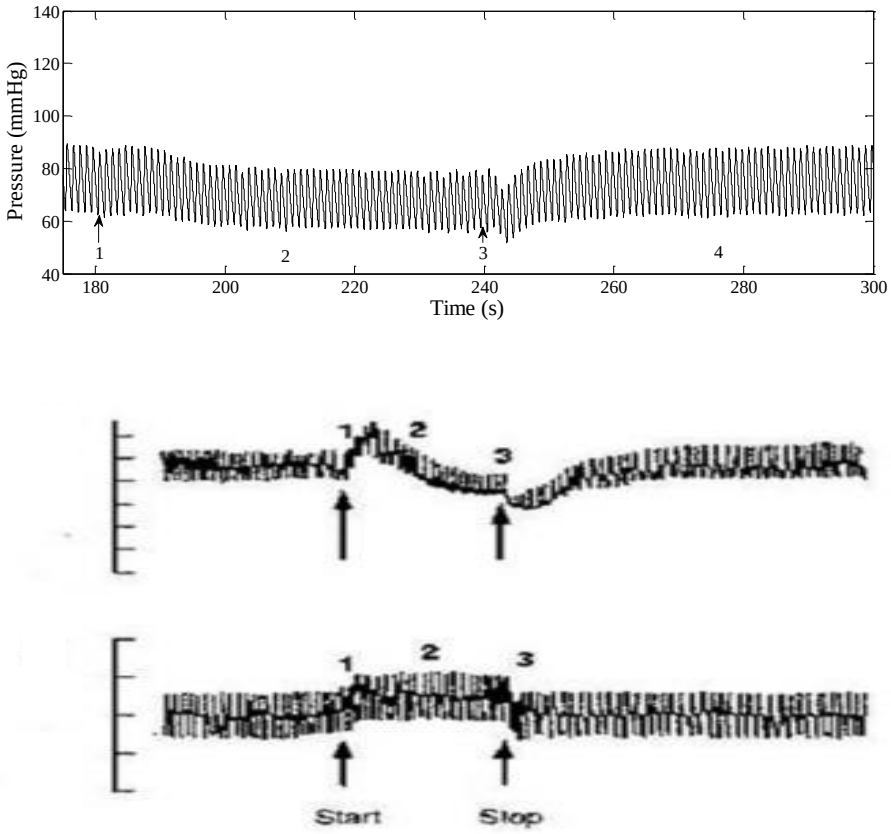

Figure 3.10: Arterial pressure trace during a simulated Valsalva manoeuvre of a patient with mild left hear failure (LHF) in the MCL (top), arterial pressure traces of patients with mild LHF (middle) and severe LHF (bottom) [146]**.**

In exercise, all variables increased, however only the flow rate increases were similar to literature. All other increases were below reported values. The total cardiac output during exercise was lower with lower LV contractility, due to reduced functional capacity of the ventricle (Figure 3.11, left). This led to higher LAP in exercise, as the weakened LV was not able to respond accordingly to increased venous return (Figure 3.11, right).

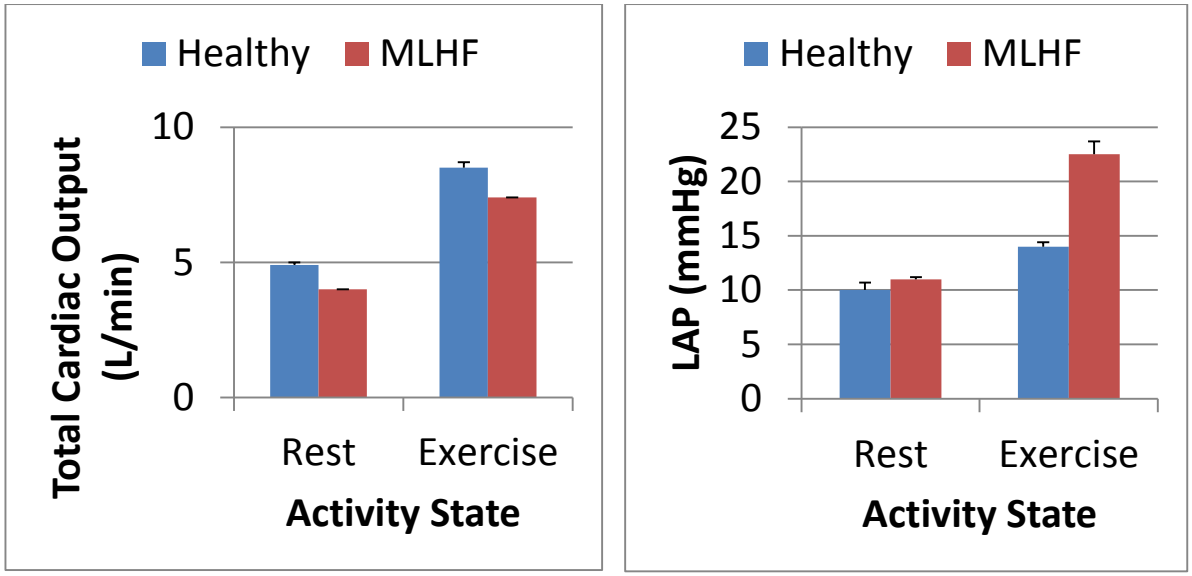

Figure 3.11: Total cardiac output (left) and left atrial pressure (right) during rest and exercise in the MCL simulations for two different heart conditions.

For assessment of transient repeatability, correlation coefficients were calculated between all of the ten tests. For the sake of readability, these coefficients are presented in Appendix B. All tests correlated positively with one another for all signals, indicating a high level of repeatability. Figure 3.12 shows the beat-to-beat mean LAP trace for all ten healthy simulations, and is a typical example of the differences between tests. From this figure, the only haemodynamic difference between signals was a vertical offset. This was due to small differences in initial priming volume of the MCL.

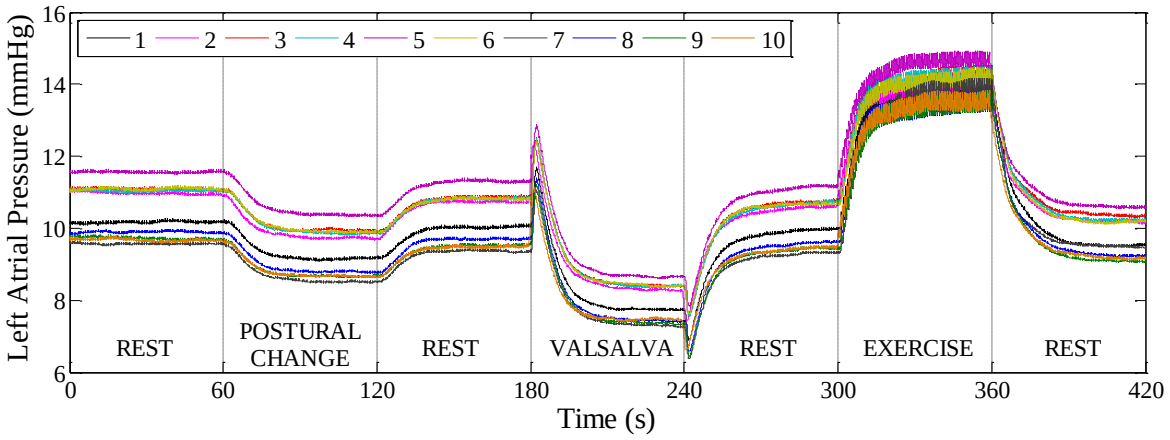

Figure 3.12: Left atrial pressure vs. time for 10 simulations of the test bed, showing the strong correlation between all signals.

3.4.6.2 FOM Validation

Table 3.12 shows the FOMs determined for all of the heart conditions evaluated. The FOM_{REST} and FOM_{CONG} scores for the healthy simulation were near-perfect, indicating that the four key

haemodynamics remained within safe regions. The scores for FOM_{REST} fell with decreasing heart failure, due to the reduced flow rate and higher LAP caused by the reduced ventricular contractility. The severe heart failure simulation produced an FOM_{REST} score of -45.9%, which indicates that 3 of the 4 variables were outside of the safe ranges for the whole duration of the scenario.

FOM_{CONG} -Left score for mild LHF was lower than that of the healthy simulation (83.4 vs. 94.6%), reflective of the increased LV volume caused by reduced heart contractility. This score decreased even further to 9% with severe heart failure, indicating that the LAP was between 15 and 25mmHg for nearly the entire simulation. The FOM_{CONG} -right score was unchanged with decreasing LV functionality, due to the unchanged RV contractility.

Table 3.11: Range of FOMs

		Worst	Best
FOM_{REST} (%)		2.7.±0.1	96.9±0.3
FOM_{CONG} (%)	**Left**	9.8±2.4	94.6±0.4
	Right	9.8±2.4	95.1±1.2
FOM_{SUC} (s^{-1})	**Left**	- -	0
	Right	- -	0
FOM_{EX} ($L.min^{-1}$)	**Left**	0	3.56±0.25
	Right	0	3.62 ±0.28

During the exercise in the healthy simulation, the cardiac output increased by 3.62 L/min, a suitable benchmark for the LV-assisted conditions. The heart failure conditions all resulted in higher increases in flow than the healthy test. This was due to higher stroke volume caused by greater LAPs. Despite this, the total cardiac output in exercise with heart failure was lower than that of the healthy simulation, due to the lower cardiac output during rest.

Table 3.11 shows the range and standard deviation of each of the FOMs based on the baseline conditions simulated in the MCL.

Table 3.12: Figures of merit for three different unassisted left heart failure conditions in the mock circulation loop.

Heart Condition	FOM_{REST}	FOM_{CONG}		FOM_{SUC}		FOM_{EX} Left			FOM_{EX} Right		
		L	R	L	R	CO (L/min)	VAD (L/min)	FOM (L/min)	CO (L/min)	VAD (L/min)	FOM
Healthy	95.3±0.5	94.6±0.4	95.1±1.2	--	--	3.56±0.25	N/A	3.56±0.25	3.62 ±0.28	N/A	3.62 ±0.28
MLHF	6.28±0.9	83.4±1.2	93.0±0.2	--	--	3.66±0.03	N/A	3.66±0.03	3.88±0.03	N/A	3.88±0.03
SLHF	-45.9±0.2	9.8±2.4	96.7±.1	--	--	4.13±0.06	N/A	4.13±0.06	4.31±0.07	N/A	4.31±0.07

3.5 Discussion

The aim of this chapter was to simulate a repeatable sequence of patient scenarios for the purpose of quantitative comparison of VAD physiological control systems. This chapter described an attempt to simulate three common patient scenarios in a five-element Windkessel MCL: postural change, Valsalva manoeuvre and exercise. All three scenarios were simulated for healthy and left heart failure conditions, and haemodynamics were compared to values reported in literature to assess accuracy.

All three scenarios simulated produced haemodynamics that were only somewhat similar to those presented in literature. A major reason for this was that there was no baroreflex in the mock circulation loop. Therefore, vascular resistance was controlled to be constant throughout each scenario. The change in MAP brought about by the change in posture would theoretically activate the baroreflex and cause increased heart rate, contractility, venous tone and systemic vascular resistance in order to restore MAP whilst maintaining cardiac output. As all of these elements were unchanged in the MCL, the reduction in MAP during the postural change and Valsalva manoeuvre was an expected result.

In all three scenarios, some of the haemodynamic changes were not as large in magnitude as those reported in literature. However, with the exception of MAP, all haemodynamic changes were in the correct direction. In the postural change, the atrial pressures did not fall as much as reported in literature due to their not being enough volume removed from the loop during the study. However, we found that rapid removal of fluid amounts larger than the 300 mL in this study transiently emptied the right atrium, causing temporary cessation of RV contractility, before the fluid redistributed. Slower fluid shifts may prevent this from occurring, enabling a larger volume of fluid to be shifted. This would require replacement of the solenoid valves used to control filling and emptying with electropneumatic regulators to enable more controlled fluid shifts.

In the exercise scenario, the MCL simulation had a similar increase in flow compared to literature, but the rises in pressure were not as high as those reported in literature. This may have been caused by not enough fluid being shifted from the SVC into the circulatory system.

Even though the simulated scenarios did not produce as large a variation in haemodynamics as reported in literature, it can be argued that these scenarios can still be used to assess control system performance. The simulated postural change, for example, reduced preload to the RV, which translated into reduced LV preload a few heart beats later. In the healthy simulation, the ventricles instantaneously accommodated for the reduced preload by reducing its output via the Frank-Starling mechanism. Normally the baroreflex would then activate a few seconds later. The few seconds before the baroreflex activates is a low ventricle volume state, and therefore a high risk for suction. Physiological controllers should mimic the initial Frank-Starling response of the ventricle by reducing pump flow and preventing suction. Therefore, the simulated postural change is still a valid test case for control performance

assessment. As for the Valsalva manoeuvre, this scenario caused lower LV volume but higher RV volume. This is a particularly valid test case for dual LVAD control, as the left pump would have to decrease speed and the right pump increase speed to accommodate.

Scenarios were simulated with a high degree of repeatability, as indicated by the high correlation between results. This was primarily due to the use of electronically-controlled pneumatic regulators, solenoid valves, pressure, flow and volume sensors which enabled precise control of resistance and circulatory volume. This is superior to other MCLs, as discussed in the literature review of this chapter, which adjusted preload and afterload using ball valves that were operated manually. This highlights that the MCL and test beds is precise enough for comparing VAD physiological control systems, and is a significant contribution of this thesis..

The pressure offset (as per Figure 3.12) between simulations were primarily caused by small differences in initial volume for each test. The loop was filled manually with fluid until the mean circulatory filling pressure was between 8 and 9mmHg. This small difference in pressure is enough to cause this variation between tests. This limitation could be overcome in the future by improving the active control of loop filling volume to ensure that the same volume of fluid is added each time. To compensate this shortcoming in the remainder of this thesis, extra care was given to ensure that the MCP prior to the beginning of each test was restored back to 8.5mmHg, and that all pressure transducers were correctly offset prior to each test.

In order to be able to quickly compare different control systems, quantitative performance metrics are required. In this chapter, metrics were proposed that covered four aspects of control system performance. These metrics were validated by using them to quantify the performance of unsupported left ventricles with three different levels of contractility. The results from this chapter provided context for each of the four performance metrics. Ideally, controllers evaluated later in this thesis could be considered "good" if their metrics are similar to those produced by the healthy heart. Conversely, "bad" controllers are those with scores close to those produced by the MLHF and SLHF simulations.

Based on the high repeatability of these tests, control testing in this thesis will only be performed once. It was assumed that the sample standard deviations measured for each FOM in this chapter are similar to the true standard deviations. Based on this assumption, the largest standard deviation for each FOM will be used as the standard deviation for all controller results presented later in this thesis, and will therefore be used to determine if the differences between results are significant.

There are a number of disadvantages to using the performance metrics presented in this chapter. Firstly, these FOMs are quite complex in their derivation and may not be easily understood at first glance by clinicians or engineers. Context is required in order for the reader to understand, for example, the relevance of a FOM_{REST} score of 6%. Another shortcoming was that FOM_{REST} lumped together 4

different haemodynamic signals together into one metric. It is not possible to determine which of the 4 signals are responsible for a poorly-performing result without further investigation into the resulting waveforms. However, the purpose of these metrics is not to provide detailed and thorough insight into control behaviour. Rather, the objective of these metrics is to quickly rank the performance of physiological control systems with respect to their ability to maintain resting haemodynamics, prevent congestion, avoid suction and increase flow during exercise. This will enable investigators to subject a number of control systems to the same evaluation protocol and then quickly determine which controllers are most appropriate and which should be disregarded. Further characterisation of control system performance could then be performed by the investigator at their discretion.

3.6 Limitations and Future Work

There were a number of limitations in this study. The first was that while a MCL offers numerous advantages over a NM, it is not as customisable. Secondly, whilst the pressure and flow sensors were correctly offset to zero at the start of each simulation, calibration was not performed as frequently. Future work should incorporate sensor recalibration on a regular basis. Thirdly, the model of ventricular suction was not validated due to time constraints. Given that a previously validated suction model was used (albeit in a numerical model), it was assumed that it would give a similar response in the MCL. However, the use of pneumatic regulators and a different volume threshold may have modified the suction behaviour. Future work should incorporate validation of this suction mechanism.

3.7 Conclusion and Summary

This chapter described the evaluation framework that can be used to assess the performance of physiological control systems for rotary VADs. This framework involved the simulation of three common patient scenarios in a mock circulation loop, and the creation of performance metrics to provide quantifiable information about control system performance. The scenarios were validated against haemodynamic data presented in the literature, and it was found that perfect replication of haemodynamics was difficult without implementation of a baroreflex. However, the scenarios are still useful for evaluation of control systems because they subject the systems to preload and afterload changes similar to those observed in clinic. The performance metrics were validated using simulations of healthy and heart failure patients, and will enable fast ranking of controller performance. However, they are not easily understood at first glance and as such may not be useable beyond quick comparison of control systems.

The purpose of this chapter was to describe the development and validation of a testing protocol for evaluation of control systems. In the context of this thesis, this protocol is essential to the development of any control systems for both single and dual rotary LVADs. It enabled thorough and quantifiable evaluation of control systems, which aids in identifying shortcomings and furthers development. This

protocol will be used in Chapter 4 in order to compare a number of LVAD control systems, and in Chapter 5 to assess the final dual LVAD control system.

4 LVAD Control System Development

The previous chapter outlined the evaluation framework that was required prior to the development of a dual LVAD control system. The next two chapters discuss the development of this system.

One method of developing a control system for dual LVADs is to adapt one of the many LVAD control systems previously reported. In order to select a suitable system for adaptation, a review of previously proposed control methods and their efficacy is required. However, as outlined in the previous chapter, direct comparison of controllers from the literature is difficult due to the inconsistent nature of evaluation. The aim of this chapter was to therefore experimentally compare the performance of a number of rotary LVAD physiological control systems. The results of this comparison will determine the most suitable LVAD control strategy, which may then be adapted for use in a BiVAD system.

The significance of this chapter is that it presents, for the first time, a thorough and quantitative comparison of a number of different rotary LVAD control systems previously presented in literature. Since the evaluation techniques for physiological control systems differs between authors, the controllers that are worth further investigation can only be speculated. The definitive results in this chapter provide a starting point for development of a control system for dual LVADs. Furthermore, results from this chapter can provide both clinicians and engineers with relevant information about the performance of well-known physiological control systems.

The chapter begins with a literature review, which summarises the previous work. A number of control systems from literature were then selected and implemented. Each control system was then subject to the test bed outlined in the previous chapter, and their performance measured using the figures of merit described in the previous section.

This chapter uses some information and descriptions from three publications. The first manuscript entitled "Evaluation of a morphological filter in mean cardiac output determination: application to left ventricular assist devices." was published in the scientific journal Medical and Biological Engineering and Computing (Volume 51 Issue 8, 891 – 899). The filter described in that publication was used to pre-process feedback signals. This publication is included in

Appendix E. The second manuscript, “Starling-like Flow Control of a Left Ventricular Assist Device; In Vitro Validation”, was published in Artificial Organs (38 (3), E46-56). This was a standalone evaluation of one of the control systems compared in this chapter, and I was the second author on this paper. The third publication, “Comparison of Linear and Non-Linear control of Flow and Pressure in a Rotary Left Ventricular Assist Device”, was submitted to the scientific journal "Medical and Biological Computing and Engineering" and at the time of the submission of this thesis is currently under review.

4.1 Aim

The aim of this chapter is to experimentally compare a number of control systems from literature and determine the best performing LVAD control system to be adapted into a BiVAD controller. The specific objectives devised to complete this aim are:

- Review the literature of physiological control systems.
- Identify suitable control systems for evaluation.
- Compare control systems using the framework established in the previous chapter.
- Select one or more control systems for development into a dual LVAD control system.

4.2 Literature Review

Development of a physiological control system for a rotary LVAD required detailed knowledge of the work previously done in this field. This section presents a review of literature on these topics and discusses the gaps in the field.

4.2.1 Structure of a physiological control system

Pump speed is conventionally adjusted by a clinician, which is referred to as an operator-in-the-loop approach (Figure 4.1). Clinicians make adjustments to pump speed based on observations of patient and pump parameters, including haemodynamic and biochemical markers. A physiological control system involves careful selection of objective and implementation that can remove the clinician out of the loop, which reduces patient dependence on clinical staff.

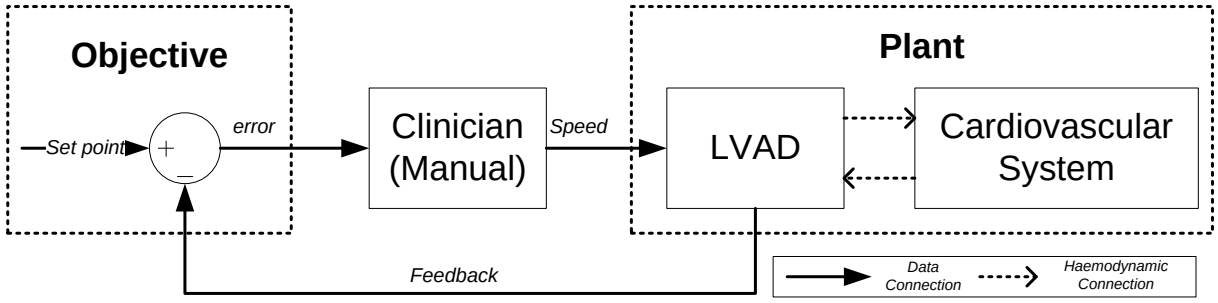

Figure 4.1: Conventional pump operation, using a clinician-in-the-loop

A physiological control system can be broken down into two components: a control objective and an implementation (Figure 4.2). The objective encompasses the selection of the controlled variable (usually one or more parameters from the pump or circulation) and the selection of the desired set point for this variable. Effectively the control objective describes the "physiological" aspect of physiological control, and should be based on strategies used by clinicians when operating LVADs manually. The implementation involves taking these clinically-based objectives and implementing some method to

automate pump speed changes. Effectively the implementation section could be considered as the "control" aspect of physiological control.

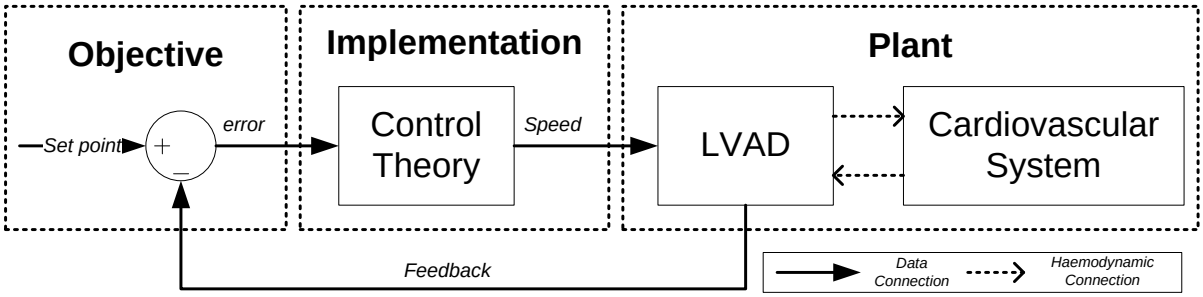

Figure 4.2: General structure of a physiological control system for a rotary LVAD and its interaction with the human body

4.2.2 Control Implementation

Automatic control has been integrated into numerous engineering applications, such as temperature control and cruise control for automobiles. A number of control theories and techniques are used across all of these applications. These theories and techniques are well understood. Most control objectives are independent of controller implementation, with the exception being those objectives that require optimisation of some function. This section is a brief summary of some of the more common implementations used for physiological control of rotary LVADs.

4.2.2.1 Proportional, Integral and Derivative Control

Perhaps one of the most popular control techniques is proportional-integral-derivative (PID) control. This linear control technique matches plant output to a target input by combining the raw, integral and derivative of the error signal (with respect to time) between target and measured plant output. The transfer function of a PID controller is shown in Equation (4.1).

$$G(s) = K_p + \frac{K_i}{s} + K_d s \tag{4.1}$$

The transient response of the system is affected by adjusting the three PID gains. Either K_d or K_i may be set to zero to produce a proportional-integral (PI) or proportional-derivative (PD) controller respectively. Numerous approaches are used for tuning PID gains, including analytical, heuristic, frequency response, optimisation and adaptive tuning methods [147]. For further information, the reader is directed to [148].

4.2.2.2 Fuzzy Logic

Fuzzy logic (FL) control is a non-linear control technique that is an implementation of the natural multi-variable logic that human beings perform every day. This control technique is suitable for plants that have unknown and/or complex characteristics that are difficult to model [149]. Briefly, FL control uses

FL theory to implement the linguistic control laws that govern human decision making. Input and output variables are defined and sets of linguistically labelled classes are used to describe the range of possible values. An example of a set of labelled classes to describe a controller error signal could be {"Negative", "Zero", "Positive"}. Fuzzification is the process of acquiring discrete input values and converting them into degrees of membership of one or more of these classes. A set of fuzzy rules is then defined which dictates the changes in output with changes in input. An example of a rule is "If error is Negative, controller output is Positive". After the fuzzification step, fuzzy inferencing is used to evaluate all of the fuzzy rules with respect to the degrees of membership to the fuzzy sets. Each fuzzy output now obtains a value corresponding to the degree that output action should be applied. For further detail, the reader is directed to [149], [150].

4.2.2.3 Extremum Seeking Control

Extremum seeking control, or ESC, adjusts control output (u) to reach the optimal point of some cost function l. This cost function may be related to some desired performance objective of the system that may be unknown and/or time varying. ESC can be thought of as a real-time optimisation algorithm for control purposes. The advantage of ESC is that it does not require *a priori* knowledge of the cost function, and can also be used for time-varying cost functions. A variation of ESC, slope-seeking control (SSC) maintains operation at a precise slope on this cost-function. Further details of the implementation of the ESC algorithms can be found in [82], [86].

4.2.3 Control Objectives

Physiological control systems automatically adjust pump speed in response to changes in one or more haemodynamic or pump variables in order to satisfy some clinical objective. This section presents a literature review of the different control objectives for rotary LVADs.

4.2.3.1 Differential Pressure

The differential pressure (ΔP) across a rotary blood pump refers to the difference in fluid pressure between the outlet and the inlet of the pump. The ΔP, or head (H), generated across a rotary pump depends upon the speed of the impeller and the flow rate of fluid through the device. The relationship between these three variables is commonly presented using an H-Q curve (Figure 4.3).

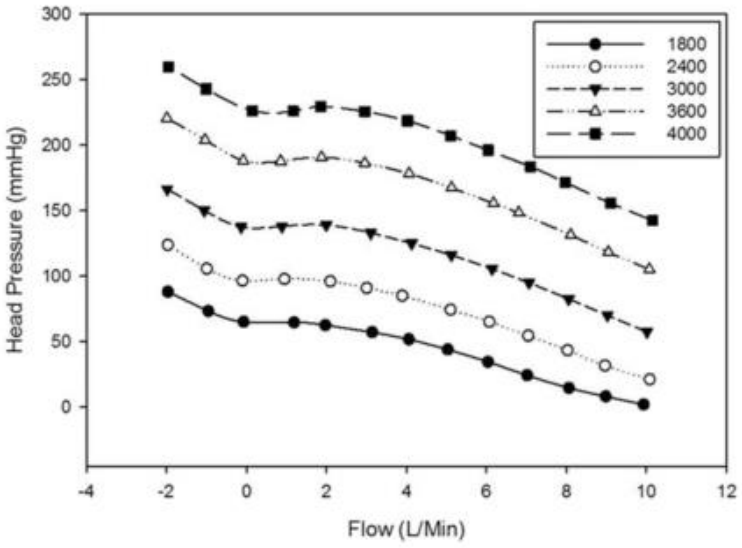

Figure 4.3: Example of a H-Q, showing the relationship between speed, flow and pressure in the HeartWare HVAD [151].

The justification for controlling ΔP, according to Giridharan and Skliar (2003) is that the native ventricle maintains a constant differential between the pulmonary veins and the aorta, and therefore the pump's control system should do likewise [152]. Waters and colleagues (1999) were the first to propose maintaining ΔP constant as a control strategy, and used proportional-integral (PI) control to maintain ΔP at 110mmHg [92]. Controller gains were chosen based on root locus analysis of the system's stability. The gains were selected such that any oscillation of ΔP caused by residual contractility did not result in oscillatory pump speed. Evaluation was performed using a lumped-parameter numerical model. The control system was subject to step changes in filling pressure (± 50mmHg) and systemic vascular resistance (1-50%), and the time taken for ΔP to return to the set-point was measured as a figure of merit. The settling time was found to be approximately 10 seconds.

The most significant investigations into ΔP control were performed by Giridharan and colleagues [106], [112], [123], [153]–[155]. These authors extended on the previous work by evaluating ΔP control of both axial and centrifugal pumps. Initially the authors used fixed gain PI control, with gains determined using an exhaustive numerical search in order to minimise the controller error and pump speed oscillations[123]. These gains resulted in a settling time of 30 seconds. The authors later used gain scheduling to reduce pump speed oscillations, but without any improvements in settling time [154]. Evaluation was performed by simulating a state of exercise using both a NM and an MCL, and comparisons were made with a pump operating at constant speed as well as a simulated healthy LV. During exercise simulations in-silico, ΔP control increased pump speed and restored cardiac output to a similar level as the healthy ventricle. In-vitro tests showed a similar response, however\ the controller was implemented with user-in-the-loop in-vitro, with the investigators manually changing pump speed to meet the control objective. Thus practical implementation of this algorithm has not been investigated.

Giridharan and colleagues extended the concept of ΔP control into maintaining the differential between the pulmonary vein and aorta (ΔP_{aopv}) constant[156]. The intention of the authors was to remove the systolic portion of LVP, and therefore truly maintain the difference between heart preload and afterload

to be constant. Another significant benefit of this approach is that this pressure difference is maintained regardless of cannula resistance. The authors used a mock circulation loop to assess the steady state validity of this control variable. Manual changes in pump speed were used. Qualitative comparisons were made with an unsupported LV, constant speed control and ΔP control, using a healthy LV, failing LV and asystolic LV. The authors concluded that ΔP_{aopv} control was able to consistently restore the steady state flow rate close to the baseline values during rest and exercise states, regardless of heart condition.

Maintaining ΔP constant increases the afterload and preload sensitivity of the pump equally. Therefore, independent changes in either of these variables will result in a corresponding change in pump flow, which may be advantageous. However, there are two disadvantages to this approach. Firstly, simultaneous changes in afterload and preload may not be accommodated for by the control system. Secondly, the native ventricle is preload sensitive but highly afterload insensitive. Therefore, making the LVAD-supported LV equally sensitive to both makes the system behave less like the native ventricle, potentially increasing the risk of hazardous events like ventricular suction. Whilst the exercise performance has been thoroughly assessed, the ability of this control system to avoid and/or handle suction has not been assessed at all.

4.2.3.2 Aortic pressure

Aortic pressure (AoP) is normally maintained by the baroreflex, which adjusts vascular resistance, venous tone, heart rate and contractility [133]. However, this mechanism may be diminished in heart failure, partly due to reduced ventricular contractility. Adjusting pump speed to maintain AoP would be able to compensate for a reduced baroreflex mechanism. This approach was proposed by Wu and colleagues as a primary control objective [93], [113], [116]. The authors identified that solely maintaining AoP constant without knowledge of the venous return may result in suction events, so they included constant ΔP control as a secondary objective. The reasoning behind this is that if afterload and pump differential pressure are constant, then by extension LVAD inlet pressure must be constant as well, which helps to avoid suction. The authors evaluated their system using both a NM and a MCL, with different evaluation protocols in each. In the NM evaluation, the authors performed a series of step changes in SVR, and then simulated a transition from rest to exercise. Exercise was simulated by increasing RV contractility and decreasing SVR. In the MCL, only changes in contractility were used to disturb the system. The authors assessed the performance of AoP control by comparing the changes in arterial pressure, total flow and left atrial pressure during each scenario obtained using their algorithm with those obtain from simulating healthy and chronic heart failure patients undergoing the same scenarios. The system exhibited settling times between 2 and 5 seconds for all disturbances, and was able to recover from suction in the MCL. This approach requires estimation or measurement of two pressures in order to prevent suction and maintain perfusion. This control strategy appears to be quite

beneficial; however its performance has only been compared to a healthy left ventricle and has not to compared to any other system

4.2.3.3 Constant Preload

One of the aims of physiological control of a rotary LVAD is to avoid ventricular suction. Control of LV end-diastolic pressure (LVEDP), or preload, to a set point is the most direct method of avoiding suction because it would maintain a constant level of fluid in the ventricle. Bullister et al. (2001, 2002) developed a control strategy based around maintaining LVEDP to a set point, and they utilised their own custom-made pressure sensor to measure LVEDP for feedback [115], [157]. The set point selection was automatically optimized to ensure that AoP remained at an appropriate level, whilst ensuring LVEDP remained within safe ranges. Integral control was used to implement this objective, whilst the addition of ventricular collapse and retrograde flow detection algorithms as outer control loops enhanced the safety of this control system. No details were given about the latter components.

The authors assessed the controller using a Donovan MCL[158]. Time-domain performance was assessed by starting with constant speed operation and then switching the control system on. Haemodynamic performance was assessed by simulating an exercise condition through an increase in heart rate. The controller's performance was assessed by observing the changes in LVEDP and arterial pressure during exercise. No comparison was performed with any other control system. The authors found that their system was able to reach the target LVEDP within 10 seconds. The control system was also found to automatically adjust the target LVEDP during increases in heart rate to ensure increased perfusion pressure during increased activity. No assessment of suction avoidance was performed, and no comparison was made to any other system.

More recently, Alomari et al.(2011) proposed sensorless control of inlet pressure to a constant value [110]. The authors used a dead-beat control algorithm, which used an autoregressive exogenous (ARX) model of the system to determine the required pump output in the shortest possible time. Evaluation was performed using an ARX model of pump and circulatory system. Assessment involved using square waves of various amplitudes, frequencies, means and duty cycles as the set point and calculating the maximum and minimum error between target and measured inlet pressure. Errors were kept between ± 0.92mmHg by the controller. The response time of the control system was rapid, with a nearly instantaneous rise time. However this system was not compared to anything else and its ability to respond to realistic patient scenarios was not assessed.

Maintaining pump preload constant could be a suitable approach for preventing suction. However, no authors have confirmed this assumption in their evaluations, nor has it been compared to other control systems. Additionally, selection of an appropriate set point for end-diastolic pressure is difficult because the LVEDP is not constant in the native human heart. Such a system would rely heavily on the user's

clinical experience. Finally, no pressure sensors are commercially available for use in rotary blood pumps (although some are in development) making practical implementation difficult [159], [160].

4.2.3.4 Pulsatility Control

Provided that the ventricle has some residual contractility, all haemodynamic signals will exhibit a sinusoidal-like characteristic, referred to as pulsatility (PI_x). The native Frank-Starling mechanism means that the strength of residual contraction (hence the amplitude of pulsatility) depends upon the left ventricular end-diastolic volume. This is shown in Figure 4.4, in which the pulsatility of the flow signal is shown to decrease as preload decreased due to an increase in pump speed. Therefore, pulsatility can be used as a surrogate for preload, negating the need for a pressure sensor on the pump inlet.

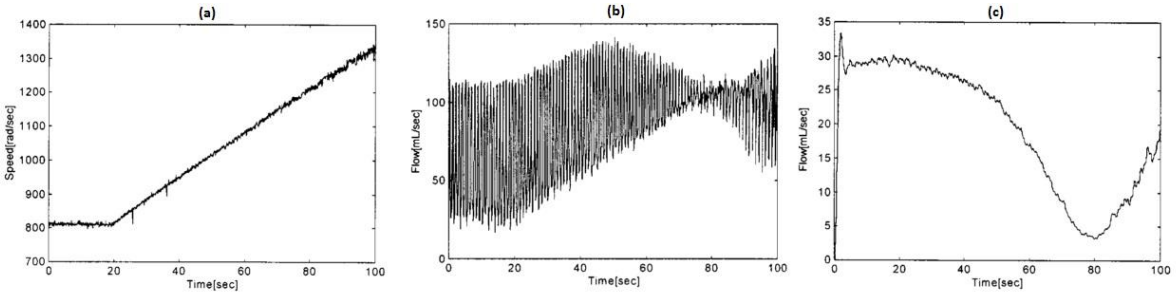

Figure 4.4: LVAD speed (a), flow (b) and flow pulsatility (c) during a speed ramp test [80]**.**

Choi et al. (2001) was the first to develop a control system whose aim was to maintain a constant level of pulsatility [80]. The authors implemented this algorithm using both fuzzy logic (FLC) and proportional-integral-derivative (PID) control. The authors defined pulsatility of flow (expressed in $L.min^{-1}$) as per Equation (4.2).

$$Pulsatility(t) = LP\left(\left|HP\left(Q_{LVAD}(t)\right)\right|\right) \tag{4.2}$$

Where HP and LP are 3rd-order Butterworth high-pass and low-pass filters with cut-off frequencies of 0.5 and 0.25 Hz respectively. Evaluation was performed in a NM, MCL and in a single acute animal experiment. Haemodynamic performance was evaluated using PVR and SVR step changes in the NM, SVR step changes in the MCL, and simply switching on the control system in the animal. Each test began with the pump operating at constant speed (the minimum pump speed), before switching the control system on. The response of the LVAD flow, atrial pressures and arterial pressure to changes in preload and afterload was observed. A qualitative comparison of time-domain performance was performed with PID control, in which the control system was switched on and the PI_x was monitored for undesirable characteristics (oscillations, slow settling time).

In the numerical model, the authors showed that their algorithm restored atrial pressures (6 – 8mmHg) and arterial pressures (90 – 120mmHg) at rest. The algorithm also increased pump flow during increased

venous return and increased afterload. The controller settling time was between 35 and 40 seconds, as interpolated from the graphs. Finally, the authors found that fixed-gain PID control performance was affected by contractility, whilst the FLC performance was not, suggesting that FLC is the preferred method of control implementation. This paper is the only comparison of PID and FLC implementation techniques for rotary LVAD control in the literature. The investigators also found that different set points were required for NM, MCL and animal studies [80].

One of the shortcomings of maintaining a constant PI_x is that PI_x is not a monotonic function of pump speed, as shown in Figure 4.4. PI_x decreases as speed increases until suction occurs, at which point PI_x increases again. Therefore there are two speeds that can produce the same PI_x, and one of these solutions is in a state of suction. To overcome this, Choi and colleagues (2005) found that the ratio between flow and pressure pulsatility (PI_{ratio}) changed significantly during ventricular suction, but was relatively constant when there was no suction regardless of the base level of residual contractility [95]. Thus they evaluated a new control objective that maintained the PI_{ratio} at a level just before suction occurs.

This control system was implemented using fuzzy logic control and evaluated using a NM. The system was subject to step changes in preload, afterload and ESPVR, and its performance was compared to that of a PI_x control system. They found that the PI_{ratio} objective was able to avoid suctions in all scenarios tested, whereas using the PI_x objective resulted in suction events when the ESPVR decreased.

Endo and colleagues (2002) investigated the use of motor current pulsatility to detect and avoid ventricular suction [119]. Current pulsatility was calculated as the difference between maximum and minimum divided by the beat-to-beat mean current every cardiac cycle and referred to as the index of current amplitude (ICA). The authors developed a controller that maintained ICA at 0.18, which was found to be always below the point of suction (Figure 4.5). The authors used a proportional controller which adjusted the speed in 50 RPM increments every 3 seconds. Evaluation was performed by subjecting the control system to changes in afterload and contractility in a MCL and observing the convergence time. The controller took 1 minute to converge to a new pump speed with each parameter change. Unlike flow pulsatility used by Choi et al., this sensorless feedback variable appears to be independent of changes in contractility. It still requires input by a clinician for the target ICA, which is not necessarily a concept easily understood by clinicians.

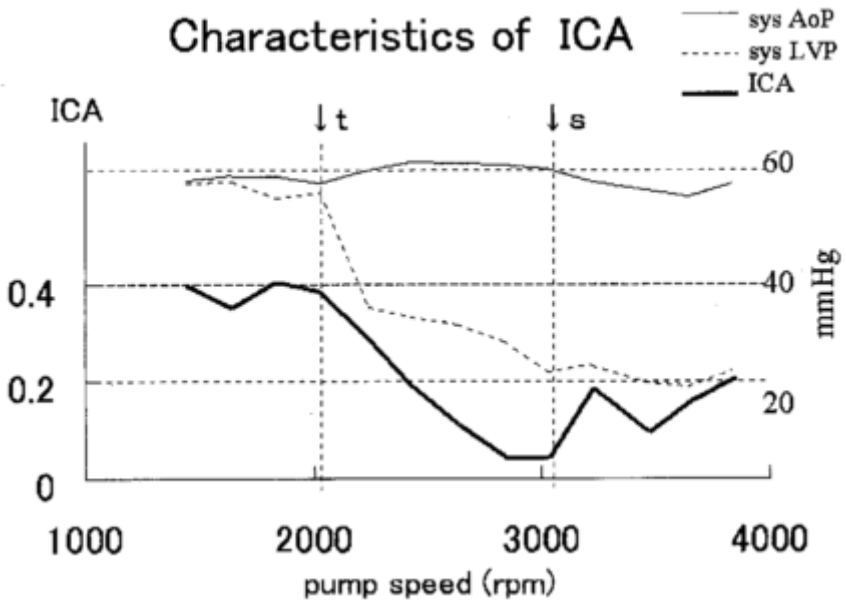

Figure 4.5: Index of current amplitude (ICA), or current pulsatility, with increased pump speed. t corresponds to cessation of aortic valve flow and s corresponds to the point at which suction occurred[119].

Using the pulsatility of an easily obtainable signal as a surrogate for preload is feasible and may be able to prevent suction. However, as the relationship between contractility and pulsatility differs between patients, the selection of an appropriate set point is difficult, and may require individual patient calibration. Additionally, the method of calculating pulsatility differs between authors.

4.2.3.5 Constant Flow

Clinicians may wish to treat their patient by operating the pump at a constant flow rate in order to ensure end organ perfusion. As outlined earlier, the flow rate through a rotary pump depends primarily on the speed and differential pressure across the pump. Changes in both preload and afterload can vary pump flow. A constant flow control algorithm adjusts pump speed to maintain a constant flow.

Constant flow control algorithms have been proposed for automatic control of rotary pumps used for cardio-pulmonary bypass (CPB) and for extracorporeal membranous oxygenation (ECMO) [94], [97]. Constant flow is suitable for these applications, as the patient is immobile and thus there is little variation in cardiac demand. Lim and colleagues (2011) proposed a method of controlling LVAD flow to a sinusoidal set point using non-invasive measurements [109]. It was implemented using deadbeat control, and assessed using a NM. Evaluation involved performing a step change in target flow, as well as simulating an exercise condition. The authors showed that this control approach could track target flow within ± 0.5L.min^{-1}, and that the controller could maintain flow rate in the exercise case. However, this required a manual increase in the target flow rate. This limits the application of this control system for active patients.

4.2.3.6 Frank-Starling Control of Pump Flow

The demand for blood flow varies depending on patient activity and heart condition, thus the set point in a flow controller must vary. The native ventricle varies flow automatically with preload due to the Frank-Starling mechanism; however this mechanism is diminished in failed ventricles. Therefore, direct mimicry of this mechanism using a physiological control system should improve preload sensitivity.

Maslen and colleagues (1998) were the first to propose a physiological control system that mimicked the Frank-Starling mechanism of the native ventricle[161]. This system was designed to vary pump flow rate in response to preload by adjusting the pump speed, forcing the pump to exhibit a flow-preload response similar to that shown in Figure 4.6. However, no implementation or evaluation of this controller was presented.

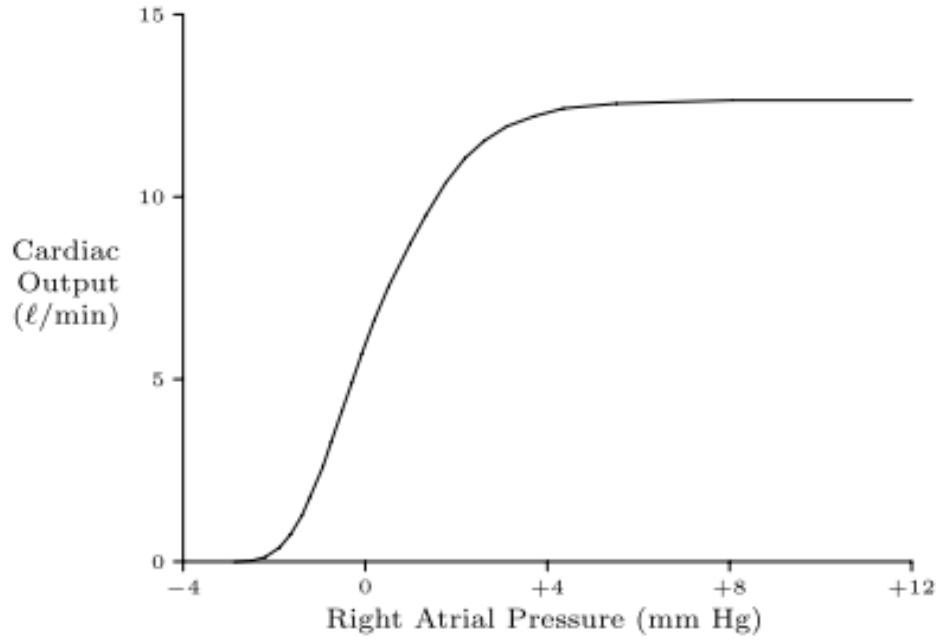

Figure 4.6: An example of the flow vs. preload response exhibited by the native ventricle that could be mimicked using physiological control [161]**.**

Salamonsen and colleagues (2012) described a Frank-Starling like control system that sets a target flow rate as a function of preload [127]. This controller used flow pulsatility (difference between maximum and minimum flow rate each cardiac cycle) as a surrogate for preload which eliminated the need for an implantable pressure sensor. The authors suggested that the relationship between beat-to-beat mean flow and flow amplitude should be maintained linear using a physiological control system (Figure 4.7). The paper explained the theory underlying such a controller but did not present evaluation of the control system in any format.

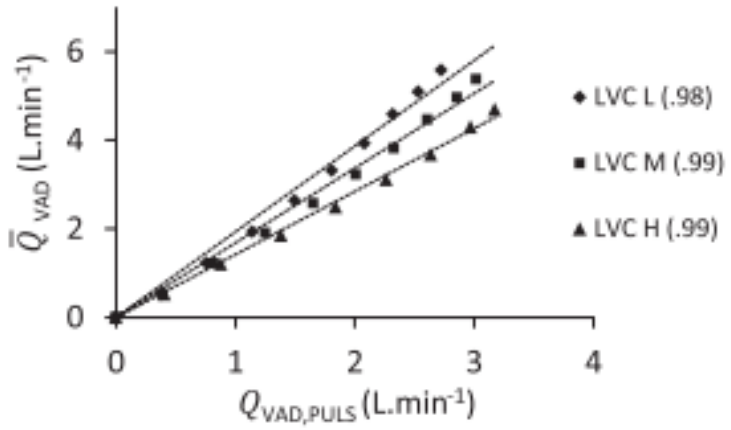

Figure 4.7: Starling-like relationship between mean flow (QVAD) vs. flow pulsatility (QVAD,PULS) for different levels of contractility [127]**.**

The authors highlighted that tracking a variable target flow rate is difficult, because the initial target flow rate post-disturbance is an over or underestimate of the final value of flow, especially with a steep relationship between target flow and pulsatility. This could result in a hyper sensitive control system that spends excessive time hunting for steady state. The authors proposed that after a system disturbance, the control system should predict the steady-state target flow rate and adjust speed to meet that, rather than using the instantaneous target flow rate determined using the linear relationship between flow and pulsatility. To implement this, the investigators proposed that the target flow rate should be determined using an arc drawn from the operating point to the target control line, rather than simply moving vertically from the operating point to the target control line. Two different arcs were proposed, one with its centre at the origin of the Cartesian plane and the other with its centre along the control line (Figure 4.8). However, as this was a theoretical paper, comparison of these approaches was not performed. One shortcoming of Salamonsen's approach is that flow amplitude is dependent on systolic pressure generated by the ventricle. This pressure varies not only with preload but also with changes in the inotropic state of the heart, such as those caused by changes in patient activity or with recovery or worsening of the baseline heart condition (Figure 4.7). Therefore, changes in activity or heart condition may be misinterpreted as preload changes, causing the control system to behave incorrectly.

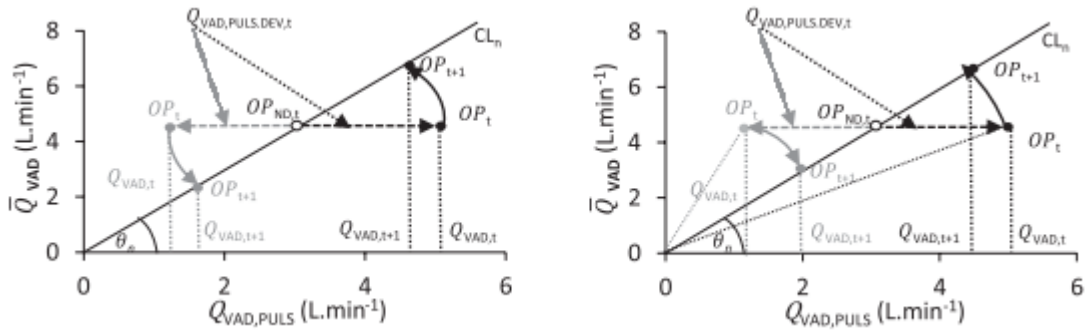

Figure 4.8: Calculation of steady state target flow rate using an arc centred about the control line (left) and about the origin of the Cartesian plane (right). OP - operating point; CL - control line; Q_{VAD} - pump flow; $Q_{VAD,PULS}$ - pump flow amplitude.

Gaddum and colleagues (2014) recently assessed the aforementioned control system in a mock circulation loop [128]. The target flow was calculated using the radial about the origin method (Figure 4.8, right). Evaluation consisted of step increases in filling pressure (to assess preload sensitivity), step decrease in PVR (to assess suction avoidance) and a simulated exercise state. The Starling-like control system was shown to have a higher preload sensitivity, better avoid suction and produce higher flow rates during exercise than constant speed control. However, this system was not compared to any other physiological control system, and the radial about the control line methodology was not assessed.

The flow control system developed by Moscato et al. automatically varied flow rate using a linear relationship between LVP and target flow[91]. The justification for this approach is that, assuming that the LVAD provides all flow during mechanical support, the afterload impedance that the LV sees can be approximated as the ratio of Q_{LVAD} and LVP. Maintaining constant afterload impedance therefore ensures that target QLVAD varies linearly with LVP, which itself is a function of LVEDP, inadvertently mimicking the Starling relationship between flow and preload.

Proportional-integral control was used to implement this algorithm. For the feedback variables, Q_{LVAD} was measured, and LVP was estimated using an extended Kalman filter utilising Q_{LVAD}, AoP and pump rotational speed as inputs. The authors evaluated this control system using a NM by perturbing the model in a number of ways, including exercise simulations, increased contractility, step changes in blood volume and step changes in afterload. During each disturbance, the authors compared the changes in afterload impedance as well as the changes in flow with changes in LVP for a controlled LVAD and for a LVAD operating at constant speed.

The authors found that maintaining constant afterload impedance improved the overall preload sensitivity of the LVAD system – the flow automatically varied with LVP, avoiding suction situations that otherwise occurred during constant speed operation. During the various scenarios, the maximum variation in afterload impedance with the constant speed controller was shown to be 26.3%, whereas there was no variation with the control system. The authors suggested that maintaining this impedance constant enabled controlled training of the ventricle and may lead to recovery of the ventricle. Long-term in-vivo testing is required to determine if this is the case. The settling time of the control system was approximately seven seconds. These investigators did not report any difficulties using a variable target flow rate, however the use of the Kalman filter may have damped the response of preload. Additionally, a pressure sensor is still required for AoP in order to estimate the LVP. Finally, another shortcoming of this study was that this controller was not compared with any other control systems.

A control system that mimics the native Frank-Starling relationship is the most direct way to improve preload sensitivity. Despite this, little work has been completed on this field, with no comparisons performed with other controllers. It is unknown whether LVEDP or pulsatility would be a more suitable measure of preload in this control system.

4.2.3.7 Flow Control Based on Systemic Vascular Resistance

Faragallah and colleagues (2012) [103] developed a control system that set the target flow rate based on the systemic vascular resistance. The SVR was estimated in real time using a 6th order NM, using 11 iterations of a Fibonacci optimisation sequence. This estimated SVR was then substituted into a model of a healthy unsupported patient to determine the required cardiac output. A second Fibonacci optimisation operation (10 iterations) was then used to adjust pump current until desired pump flow was reached. Evaluation was performed using a NM by reducing SVR by 50%, and comparing the steady state values of flow and motor current before and after the disturbance. The controller increased motor current to increase flow from 9.224 L/min to 11.912 L/min. Basing pump flow rate on a model of a healthy patient is a logical approach to this problem. However no comparison was performed with other controllers and no time domain performance was characterised. Additionally, the flow rates were much higher than the resting cardiac output of 5 L/min. No mention was made of the time it takes to complete each iteration of the Fibonacci optimisation, so the time-domain performance of this approach is unknown.

Wang and colleagues (2012) [104] extended the aforementioned concept by incorporating a suction detector, which interrupted the SVR control logic if suction was detected. Evaluation also involved a step change in SVR in the same NM as above. The suction detector correctly classified suction in 98.1% of cases. The rise time of the system was approximately 10 seconds, with a settling time between 15 and 20 seconds. Further evaluation of this system in a different evaluation environment is required to ensure that other haemodynamic pressures, including LAP and AoP, are not adversely affected.

4.2.3.8 First and Second Derivatives of Pump Parameters

Baloa et al. (2000) established that as pump speed increases, mean pump flow increases at a decreasing rate before reaching a plateau (or even decreasing) after suction occurs [111]. This can be seen in the top graph of Figure 4.9, which shows how the rate of change of pump flow rate with pump speed starts as a positive value, decreases to zero just before 12 kRPM (reportedly the point of suction), and becomes slightly negative. The rate of change of this curve is shown in the bottom graph of Figure 4.9, which falls below zero at the point of suction. Minimum flow and pulsatility of ΔP also exhibit similar behaviour [86], [87].

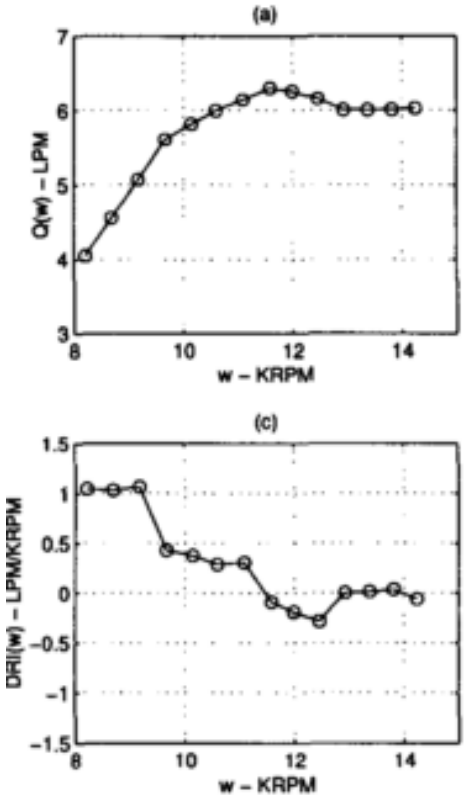

Figure 4.9: Pump flow (a) and first derivative of pump flow with respect to pump speed (b) during a speed ramp [111]**. The first derivative of pump flow falls below zero just prior to the point of suction at 12 kRPM, which may be useful as an indicator of suction.**

Researchers at the University of Pittsburgh were the first to develop control algorithms based around utilising the first derivative of the minimum flow each cardiac cycle ($Q_{LVADmin}$) with respect to pump speed as the feedback variable. The algorithm was first described by Chen et al. (2005) [162] , with further evaluation performed by Simaan et al (2009) [99]. These authors showed that the first derivative of $Q_{LVADmin}$ with respect to pump speed is positive when not in suction, and rapidly falls to a negative value when suction occurs (Figure 4.10). By maintaining this slope at zero, suction is avoided whilst providing the maximum amount of flow.

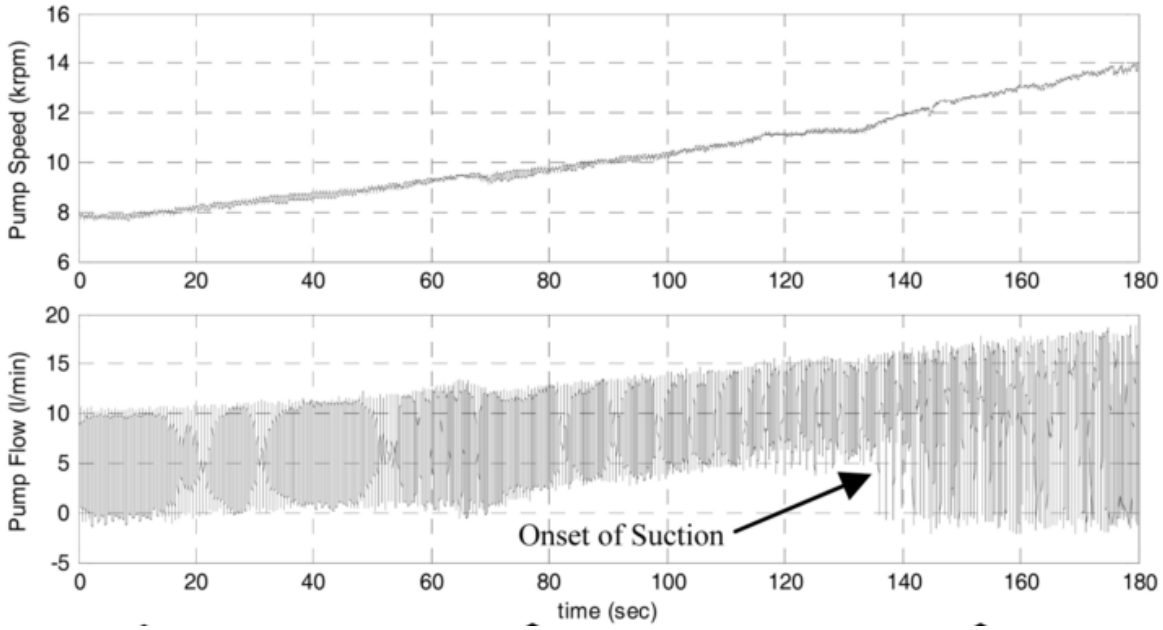

Figure 4.10: LVAD speed (top) and flow (bottom) during an in-vivo experiment, showing the change in minimum flow as suction occurs[99]**.**

The speed signal was updated using an integral controller, with the speed update rule shown in Equation (4.3).

$$\omega(k+1) = \omega(k) + c.\frac{dQ_{LVADmin}}{d\omega} \tag{4.3}$$

Where ω is pump rotational speed (RPM), k is the update sample, $Q_{LVADmin}$ is the minimum pump speed each cardiac cycle ($L.min^{-1}$) and c ($min^2.L^{-1}$) is the gain parameter used to control the rate of speed adjustment. Evaluation was performed using a NM. The perturbations were step changes in SVR, and its performance was compared to that of a controller that maintains maximum possible flow rate in [162], and ΔP control in [99]. The authors were primarily interested in comparing the control systems' ability to avoid suction. When comparing with ΔP control, the authors compared the steady state flow and arterial pressure at three levels of resistance. The authors also added noise to the flow signal to determine if noise impacted on the controller's ability to avoid ventricular suction. Suction frequency and severity were measured using two indices. The first was ρ, which was a percentage of the total time T (seconds) that the pump speed exceeded the speed at which suction was known to occur (Equation (4.4)).

$$\rho = \frac{\sum_{i=1}^{i=I} \Delta t_i}{T} \times 100 \tag{4.4}$$

Where Δt_i (seconds) is the ith interval over which pump speed exceeded suction speed, and I is the number of such intervals. The second index η measures the percentage average speed penetration into suction (Equation (4.5)).

$$\eta = \frac{\overline{\omega_s} - \omega_s}{\omega_s} \times 100 \tag{4.5}$$

Where ω_s is the suction speed (RPM), and $\overline{\omega_s}$ is the average speed over the intervals where suction occurs and is calculated using Equation (4.6).

$$\omega_s = \frac{\sum_{i=1}^{i=I} \int_{\Delta t_i} \omega(t) dt}{\sum_{i=1}^{i=I} \Delta t_i} \tag{4.6}$$

The authors found that $Q_{LVADmin}$ control algorithm avoided suction when the SVR increased by 50%. Interpolation from the figures in the paper revealed a settling time for pump speed of approximately 10 - 15 seconds using the noise-free signal. The main difference between $Q_{LVADmin}$ and ΔP control was that $Q_{LVADmin}$ control produced slightly higher arterial pressures and total flow rate for each level of resistance, which shows that this algorithm provides greater unloading of the ventricle. No comparison was made between the transient responses of these two controllers. Finally, the authors showed that the addition of noise (SNR < 20) into the feedback signal increased the number of and severity of suction events. Thus, the main disadvantage of this algorithm is that it relies on a high-fidelity flow probe or accurate noise-free estimation algorithms in order to measure the minimum LVAD flow.

Gwak (2007) used extremum seeking control (ESC) and slope seeking control (SSC) instead of integral control to adjust the pump speed until the peak of minimum flow vs. pump speed curve was reached[86]. This controller was evaluated using a NM by switching the controller on and observing the transient behaviour. The author found that the controller overshot the peak and did not return, resulting in sustained ventricular suction. This was because the cost function (i.e. slope of the minimum flow vs. pump speed curve) was not monotonically decreasing in the numerical model, making it difficult to locate the peak. To overcome this, the author replaced the entire NM with a cost-function obtained in-vivo. The transient response of both ESC and SSC was measured after switching on the controller. The ability to accommodate different patient scenarios was also evaluated, with the scenario variations simulated by changes in the shape of the in-vivo cost function. Overall, ESC exhibited more overshoot and oscillations than SSC. Slope seeking control was more stable than ESC, indicating that it is easier to maintain the first derivative close to (but not equal to) zero. Both options had settling times of 120-150 seconds. Both ESC and SSC systems using minimum flow were able to reduce pump speed to avoid ventricular suction. However, the settling times were long. Additionally, the replacement of a valid

numerical model with a cost function is a gross simplification of the circulatory system, and the variations in the cost functions were not validated against different patient scenarios, limiting the value of this study. The author also highlighted that SSC was preferable to ESC because the peak point of the cost function was close to the point of suction. As SSC kept the pumps speed just below the peak point, it operated with a large safety margin. However, determination of the optimal slope for each patient was not discussed.

A solution proposed both by Arndt et al. (2008,2010) and Gwak et al. (2011) to determine the optimal slope for a ΔP pulsatility vs. pump speed curve (Figure 4.11, top) was to use ESC to operate at the minimum of the first derivative of this curve i.e. locating where the second derivative is zero (Figure 4.11, bottom) [82], [83], [87]. Gwak and colleagues [87] compared this approach using ΔP pulsatility and minimum pump flow approaches, using a simplified NM for evaluation (previously described in [86]). Assessment involved switching the controllers on and measuring time until convergence. Variations in circulatory conditions were facilitated by adjusting the cost function used for the plant model. The authors found that ΔP pulsatility had a shorter settling time than using the minimum pump flow (300 vs. 1200 seconds). No evaluation was made against realistic patient scenarios, however, this controller is anticipated to be too slow to handle sudden changes in patient condition.

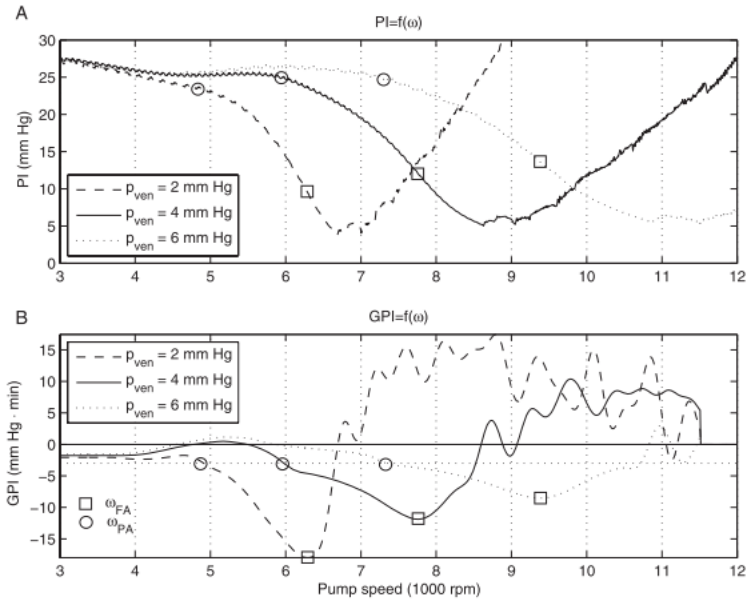

Figure 4.11: Pulsatility vs. Speed curves (A) and gradient of the pulsatility vs. speed curves (B) for three levels of preload[83]**.**

The controller developed by Arndt and colleagues (2008, 2010) was more complicated than that developed by Gwak et al. (2011). The controller had two modes of operation: partial assist and full assist (FA). In partial assist mode, the first derivative of pulsatility of ΔP (GPI) was kept constant at -2mmHg, at which point the aortic valve remained open. In FA mode, ESC was used to maintain the pump speed at the minimum of the GPI vs. speed curve. Implementation consisted of a cascaded control loop. The outer loop was responsible for maintaining GPI at a set point (for partial assist mode) or at the minimum (FA mode). The output of the outer loop was a desired pulsatility index, which was used as the input for the inner loop. The inner loop controlled pump speed to maintain the desired PI. The inner loop was tuned using internal model control to produce robust stability and performance for varying plant gains. The outer loop was controlled using integral

control, with the gain set at 1. Evaluation was performed using a LV-only NM, which simulated the pulmonary circulation with a single pressure source. The controller was subject to step changes in preload, transitions between FA and partial assist and sudden changes in contractility. Performance metrics included observing the settling time, the number of suction events that occurred and time to resolve suction events and restore normal operation. The response time of the inner loop was fast, with the PI restored to its initial value within 25 seconds, although this was reduced to 15 with the implementation of dedicated suction avoidance strategies[83]. The outer loop was much slower, with the system taking 500 seconds to switch from FA to partial assist mode. Settling time after switching on the outer loop was 2500 seconds. The authors argue that the long settling times for the outer loop are suitable because the inner loop is fast enough to avoid suction events, and that changes in the target GPI will mainly occur with changes in patient parameters, which happen over a long time scale. No comparison was performed with any other control system, nor was the controller evaluated outside of the in-silico environment.

4.2.3.9 Suction Avoidance

Ferriera, Boston and Antaki (2009) describe a method of control that relied on maintaining the pump speed as high as possible without inducing suction[96]. Discriminant analysis was used to combine 8 suction indicators into two discriminant scores, which represented whether the LV was in a state of no suction, moderate suction or severe suction. Fuzzy logic was then used to adjust pump speed based on these scores. Pump speed modifications were kept within ±5% of the current speed. Evaluation was performed using an LV-only NM. The controller was subjected to two simulated scenarios with three different levels of contractility. Exercise was simulated by performing step reductions in SVR and step increases in HR, and hypertension was simulated by a step increase in SVR. The settling time of the controller after switching on was approximately 110 seconds, and it reduced speed within 30 seconds of a suction event. The controller appeared quite conservative, but the maximum allowable speed change could be adjusted by the clinician to improve responsiveness. Interestingly, the pump speed actually decreased in exercise, which is the opposite of what is expected to occur. This indicates that the exercise simulation did not incorporate any increase in preload.

Numerous investigators have proposed algorithms for detecting and classifying ventricular suction events [55], [163]–[168]. However, as these systems do not adjust pump speed based on the detection of suction, they do not satisfy the definition of a physiological control system and as such will not be discussed here.

4.2.3.10 Motor Current

Pump motor current is attractive for use as a feedback control variable because it can be obtained non-invasively, without the need for implanting different sensors. Nishimura and colleagues (1997) [121] controlled a centrifugal blood pump at a constant motor current, which increased pump speed when ΔP

rose. Evaluation was performed in-vivo using nine adult male sheep. Constant speed operation was used for two sheep and constant current control was used in seven sheep. In the sheep with current control, rotational speed corresponded positively with ΔP and inversely correlated with pump flow. Current control reduced the amount of flow fluctuations over a thirty minute period whilst sheep were upright in a cage. Maintaining a constant flow by way of current control is good for bypass applications. However, some flow variation is required to avoid ventricular suction and accommodate variations in cardiac demand.

4.2.3.11 Multi-objective Control

Multi-objective control (MOC) strategies involve combining two or more control objectives into a single controller. Gwak et al. (2005) proved the feasibility of MOC by combining a suction prevention controller with a venous-return matching controller [85]. The suction prevention controller first determined the ratio between the powers of the first and second harmonic (HSI), which was found to decrease during suction, and kept this to a constant value. The venous return controller (VRI) maintained the first derivative of pump flow with respect to speed close to zero. Final speed output of the control system was the weighted average of two separate PI controllers. Evaluation was performed using a LV-only MCL. The system's response time was assessed by performing step changes in preload and afterload, facilitated by manual adjustments of needle valves. The two components of this MOC strategy were tested separately before being combined. Individually the VRI had rise times of 10-15 seconds, whilst the combined controller had a rise time of 30-35 seconds. HSI control did not change the pump speed at all on its own. When combined, the VRI controller saturated to the upper limit whilst the HSI controller reached a low pump speed. The weighted average of the two prevented excessive pump flow.

One of the most successful MOC strategies was proposed by Vollkron and colleagues (2005) [84]. This system consists of four logical units that interacted to adjust flow with cardiac demand as well as alleviate suction events (Figure 4.12).

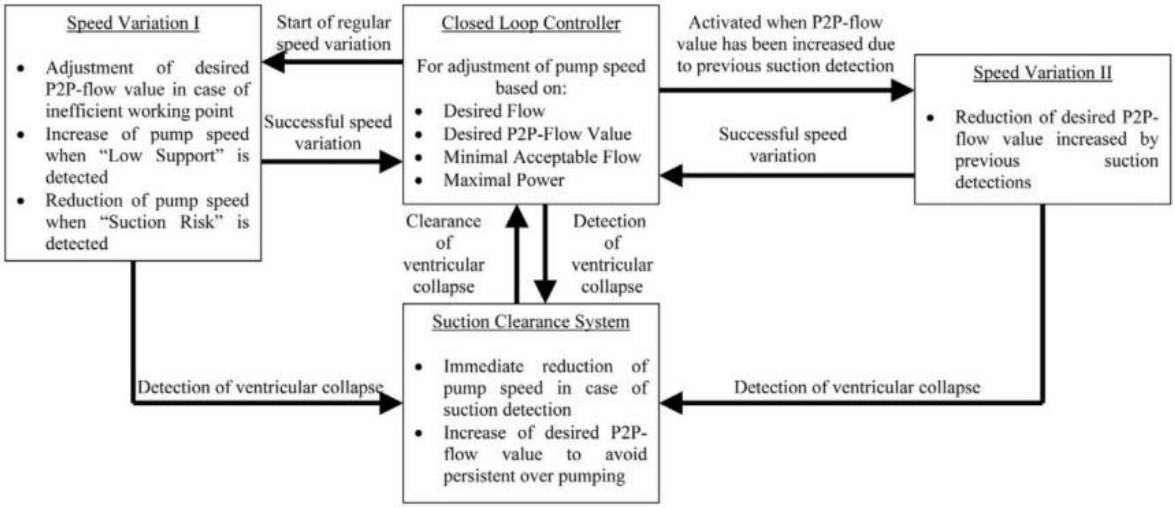

Figure 4.12: Multi-objective control proposed by Vollkron et al. (2005) [84]

The closed loop controller adjusted pump speed based on four different control objectives: maintaining a desired flow rate (set based on HR), maintaining a desired flow pulsatility, ensuring a minimal acceptable flow and limiting pump power to a preset maximum. Each objective was weighted using gains, and combination was performed using minimum and maximum operations (Figure 4.13).

An integral controller was used to adjust pump speed. Evaluation was performed in a MCL and in a clinical study. In the MCL, the controller was subjected to step changes in HR, aortic pressure, LV pressure, LA pressure, systemic flow and stroke volume. However, no evaluation results were presented.

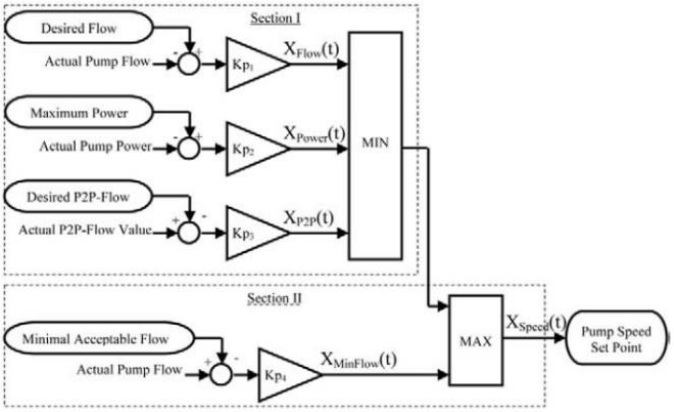

Figure 4.13: Closed loop control using four different control strategies [84]

In the clinic, 15 patients were tested in as many as 4 different settings, including the intensive care unit, standard ward, rehabilitation bicycling, and spiroergometry. The controller was compared to constant speed operation. The controller remained stable across HR from 100 to 220 BPM. There was a significant increase in pump flow during exercise with the control system compared to manual operation. Patients reported subjective improvements in comfort with the automatic control system. This system is the only rotary LVAD physiological control system to have undergone clinical evaluation. It is a landmark study which highlights the benefits that physiological control can offer rotary LVAD patients. However, the controller gains and settings were not mentioned in any of their publications.

More recently, Karantonis and colleagues (2010) proposed a MOC system that relied on the input from an accelerometer combined with HR as an indicator of patient activity level [169]. This formed part of a 6-level hierarchical controller, which meets the following objectives (in order)

1. Pump power must remain below a certain threshold.
2. A minimum pump flow must always be achieved
3. Upon detection of ventricular suction, pump speed must be reduced.
4. A minimum pulsatility must always be achieved.
5. Peak ΔP must remain within a specified range.
6. Speed to be controlled according to ALI.

No mention was made as to how the objectives were implemented or combined. Evaluation was performed using a NM. A transition from rest to exercise was simulated by slowly ramping LV and RV contractility, HR and SVR over a 55 second period. This was performed for three different levels of contractility. Cardiac output was measured before and after exercise, and speed pulsatility was used as a measure of suction avoidance. The MOC was compared to constant ΔP, constant PI and constant speed control systems. The results showed that whilst ΔP control produced the highest increase in flow during exercise, it also produced the lowest PI which suggests it has the highest risk of suction. In contrast, the MOC increased pump flow whilst still avoiding ventricular suction. This paper highlights the benefits of combining objectives. However, the accelerometer input was only simulated. Additionally, the final pump speed depended on heart contractility, with lower speeds observed with weaker hearts. This is the opposite of what is expected in clinic. Since there was no assessment of control using solely the accelerometer signal, its benefit is unknown.

Kosaka and colleagues (2003) investigated controlling pump speed to keep both pump flow and differential pressure within ±20% of an operating point. They also incorporated a suction handling component, which sharply drops pump speed if an adverse event is detected. In-vitro analysis revealed that this approach could maintain pump flow during increases in afterload. However, it took the controller 50 seconds to recover from a state of suction, which seems like an excessive amount of time.

Multi-objective control systems are a feasible approach to combining the benefits of two or more control systems, simultaneously addressing shortcomings of individual control strategies. However, the more systems that are incorporated into a MOC, the more complex the final control system is. Careful consideration must be given to the switching between different control systems. Of the MOCs presented in this literature review, only Gwak et al. [85] and Vollkron et al. [84] gave details as to how they managed the interaction between the different objectives.

4.2.4 Summary of Literature Review

In summary, physiological control systems consist of two components: a control objective, which compares feedback from the VAD and/or patient to some set points, and the control implementation, which automatically adjusts pump speed in order to meet the control objective. The two main control implementations, PID and FL control, have been widely used in VAD control yet only compared in one study. Extremum seeking control is only applicable for control objectives that involving finding the minimum of some variable.

A number of different control objectives have been presented in literature that range in complexity from single variable control systems to multi-objective approaches. Some of these control systems may be suitable for adaptation into controllers for dual LVADs as BiVADs. However, experimental comparison is required to more thoroughly evaluate these control systems. Multi-objective control systems combine the benefits of a number of different control objectives into one system. However, these systems are complex and little detail is given in the literature regarding the combination of these algorithms. A simpler control algorithm that behaves in a physiological way similar to the native heart and that naturally avoids hazardous states would be more preferable than a complex MOC. Finally, physiological control systems can either use implantable sensors to measure pressure and/or flow, or estimate these values using pump parameters. The accuracy of estimation algorithms may have some effect on controller performance.

The main finding from this review is that while there has been a significant volume of research into the field of LVAD control, it is difficult to determine the "best" performing control systems by direct examination of the literature. Therefore, there is no simple way to determine which algorithms would be best for adaptation into BiVAD control. The remainder of this chapter will describe the evaluation of a number of controllers from literature, in order to determine the most suitable candidates for rotary BiVAD control.

4.3 Hypothesis

The main hypothesis of this chapter is to evaluate a number of LVAD physiological control systems in a thorough and proper manner in order to determine the most suitable control system

4.4 Methods

4.4.1 Control Algorithms

Control systems selected for comparison included most of the systems previously described in the literature review and some of their variations, as listed in Table 4.1. These systems were chosen based on their popularity in the literature, and the fact that enough information was provided in their respective publications to implement them in the evaluation framework.

Table 4.1: Control systems compared using the testing protocol developed in Chapter 3

Strategy	Author
Constant ΔP	Giridharan
Constant Afterload Impedance	Moscato
Starling-like control	Salamonsen
Constant QLVAD	Casas
Constant LVEDP	Bullister/AlOmari

All controllers were implemented using Simulink (The Mathworks, Natick, MA). For each system, PI control was used. Gains were tuned using an optimisation procedure with the intention of giving all control systems the same dynamic response. This approach ensured that differences in control system performance were solely due to differences in strategy, not due to differences in tuning or PI gains. The optimisation procedure is described in detail in Appendix D.

With the exception of the ΔP and Starling-like controllers, all of the aforementioned controllers had only one configuration and thus implementation was simple. Two configurations of the ΔP controller was evaluated. The first, ΔP, was the original concept proposed by Giridharan, and used the difference in pressure between the inlet and outlet of the pump. The second, ΔP_{aolv}, was a modified version that utilised the pressure difference between the LV and aorta, thereby including the pressure drop across the cannulae as well. The Starling-like control system proposed by Salamonsen and colleagues had two different methods of calculating a target flow rate (Figure 4.8) - radial about a control line (RACL) or radial about the x-intercept (RAXI). These two methods are described in further detail in Appendix C, and both were evaluated in this study. Additionally, the original description of Starling-like control of an LVAD by Maslen and colleagues [161] used preload or LAP to set a target flow rate. To evaluate this original approach, pulsatility was substituted with LVEDP in Salamonsen's approach, and both RACL and RAXI methods were evaluated. Therefore, four different configurations of the Starling-like control system were evaluated in this study.

Finally, it was assumed that all of the control systems were implemented using pressure and flow sensors where necessary, as opposed to using estimation techniques. This assumption was made in order to only compare the efficacy of the control objectives in isolation. Estimation algorithms increase the complexity of control systems and may mask elements of the control objective's behaviour.

4.4.2 Signal Conditioning

All signals were filtered in order to remove the native heartbeat. Without removal of the heartbeat, the control signal sent to the pump would unnecessarily oscillate at the same frequency. This extra controller effort may result in increased power consumption, leading to shorter battery life.

Filtering of signals for select frequency removal is traditionally performed using a linear filter. These filters require a trade-off between response time and stop-band attenuation. The higher the attenuation, generally the slower the response time of the filter. For LVAD control applications, the signal should be free of artefacts caused by the heartbeat but also be responsive enough to accommodate for sudden

changes in state, caused by coughing, sneezing or postural changes. As an alternative to linear filters, a non-linear morphological filter (MF) was developed to obtain the mean beat-to-beat signal for control purposes.

A full description and evaluation of the morphological is presented in Appendix E, and can also be found in [170]. Briefly, the filter involved firstly performing real time morphological opening and closing on the signal *x (t)* using a flat structuring element $\boldsymbol{B}$. These processes yielded the beat-to-beat minimum and maximum of the signal respectively. The mean was then determined as a weighted average of the maximum and minimum. (Equation (4.7)).

$$y(t) = w.(x(t) \bullet \boldsymbol{B}) + (1 - w).(x(t) \circ \boldsymbol{B}) \tag{4.7}$$

Where the symbols • and ∘ denote morphological closing and opening respectively, and $0 < w < 1$, which can be adjusted to accommodate different waveform shapes. For pressure and flow signals, *w* was set at 0.33, based on the clinically standard equation for calculating MAP from systolic and diastolic pressures.

4.4.3 Evaluation

Evaluation was performed using the framework outlined in the previous chapter. A severe left heart failure condition was simulated in the MCL and the ventricle supported using a VentrAssist LVAD. Initial pump speed was set at 2300 RPM, which restored all systemic haemodynamics to the same values as those in the healthy simulations presented in Chapter 3. For each control system, the target variable and other controller settings were selected in order to produce the same initial pump speed of 2300 RPM. The controller gains, target variables and other controller settings are summarised in Table 4.2. Note that a butterworth filter was utilised for Moscato et al.'s control system, because it was difficult to make this controller work using the MF.

Table 4.2: Summary of all control system settings used in this study.

Controller	Target Variable/Control Parameters	Value	KP	KI	Filter
ΔP	Pump Differential Pressure	100 mmHg	18 RPM.mmHg^{-1}	21 RPM.mmHg^{-1}.s^{-1}	MF
ΔP_{aolv}	LV-Aorta Differential Pressure	75 mmHg	16 RPM.mmHg^{-1}	14 RPM.mmHg^{-1}.s^{-1}	MF
Moscato	Afterload Impedance	0.5 mmHg.mL.s^{-1}	59 RPM.min.L^{-1}	81 RPM.min.L^{-1}	BW
Constant Flow	Pump Flow	4.25 L.min^{-1}	0.06 PWM.min.L^{-1}	0.04 PWM.min.L^{-1}	MF
Constant LVEDP	Left Ventricular End-diastolic pressure	5.75 mmHg	0.06 PWM.mmHg^{-1}	0.04 PWM.mmHg^{-1}	MF
Starling Preload RACL	K_{sc1}	0.447			
	K_{sc2}	0.894 L.min^{-1}.mmHg^{-1}	0.06 PWM.min.L^{-1}	0.04 PWM.min.L^{-1}	MF
	a	5.5 mmHg			
Starling Preload RAXI	K_{sc}	2 L.min^{-1}.mmHg^{-1}	0.06 PWM.min.L^{-1}	0.04 PWM.min.L^{-1}	MF
	a	5.5 mmHg			
Starling Pulsatility RACL	K_{sc1}	0.447			
	K_{sc2}	0.894	0.06 PWM.min.L^{-1}	0.04 PWM.min.L^{-1}	MF
	a	5.5 L.min^{-1}			
Starling Pulsatility RAXI	K_{sc}	2	0.06 PWM.min.L^{-1}	0.04 PWM.min.L^{-1}	MF
	a	5.5 L.min^{-1}			

Each control system, as well as constant speed control was subject to the sequence of patient scenarios presented in Chapter 3. Pressure and flow transducers were all re-zeroed and the MCP restored to 8.5mmHg prior to the evaluation of each controller. Figures of merit were calculated for each control system and compared. As no repetition was performed, differences in figures of merit were considered significant if they were greater than the maximum standard deviation determined in Chapter 3. These deviations are presented in Table 4.3. The controllers that produced the best performance across all four performance metrics were then selected for further development into a dual LVAD control system, as discussed in Chapter 5.

Table 4.3: Deviations of figures of merit as determined in Chapter 3

	FOM_{REST}	FOM_{CONG}		FOM_{SUC} -L	FOM_{SUC} -R	FOM_{EX}
		L	R	s^{-1}	s^{-1}	Left
Deviation	±0.6	±2.4	±1.2	--	--	±6.4

4.5 Results

Table 4.4: FOMs for each LVAD control system evaluated in the evaluation framework

Controller	FOM_{REST} (%)	FOM_{CONG} (%)		FOM_{SUC}	FOM_{EX} (L/min)		Score
		L	R	(s^{-1})	Total Flow Increase	Pump Flow Increase	
Constant Flow	95.71	87.66	95.42	0.32	1.95	0.21	1.22
Constant LVEDP	93.55	97.76	93.78	0.09	3.5	2.94	2.93
Constant Speed	97.38	86.42	94.95	0.12	2.48	1.62	2.14
Constant ΔP_{aolv}	96.56	99.67	94.64	0.74	3.43	2.63	2.81
Constant ΔP	96.99	87.77	96.20	0.08	2.58	2.03	2.09
Afterload Impedance	95.63	89.20	95.32	0.25	2.64	1.89	2.1
Starling (preload) RACL	93.65	99.09	93.66	0.00	3.54	3.1	3.05
Starling (preload) RAXI	92.37	97.97	93.75	0.02	3.47	3.03	2.97
Starling (pulsatility) RACL	91.17	95.72	93.47	0.52	3.37	1.37	2.25
Starling (pulsatility) RAXI	93.45	94.60	93.40	0.46	3.69	2.85	3.27

The four FOMs for each controller tested are shown in Table 4.4. All controllers exhibited similarly good behaviour at rest, as reflected by the high FOM_{REST} scores. There were some small differences in FOM_{REST} scores which were greater than the maximum standard deviation (0.6%) observed in Chapter 3, indicating that they were significant. The range of FOM_{REST} was 91.17% (Starling (pulsatility) RACL) to 97.38% (Constant Speed), which was close to the healthy heart simulation (95.3%) and much higher than the untreated heart failure simulations (6.28% and -45.9% for MHF and SHF respectively).

There was a distinct difference between FOM_{CONG} scores for the left atrium between controllers. Only constant LAP, constant ΔP_{aolv}, and all of the Starling-like controllers produced an FOM_{CONG}-Left score equal to or greater than that of the healthy LV (94.6%). The other controllers produced FOM_{CONG}-Left scores between 86.42 and 89.2%, significantly lower than the aforementioned controllers and only slightly better than the MLHF simulation (83.4%). The response of each control system to exercise had the most effect on FOM_{CONG} -L. Constant LVEDP control, ΔP_{aolv} and all of the Starling controllers increased pump speed from 2300 RPM to above 2700 RPM during exercise, which maintained LAP below 15mmHg, hence the good FOM_{CONG} -L scores (Figure 4.14). The other controllers did not increase speed sufficiently to relieve LAP, as reflected by their reduced FOM_{CONG} -L. All of the FOM_{CONG} -R scores were high and similar to those produced in the unassisted LHF simulations, indicating that the controllers had no negative effects on RAP.

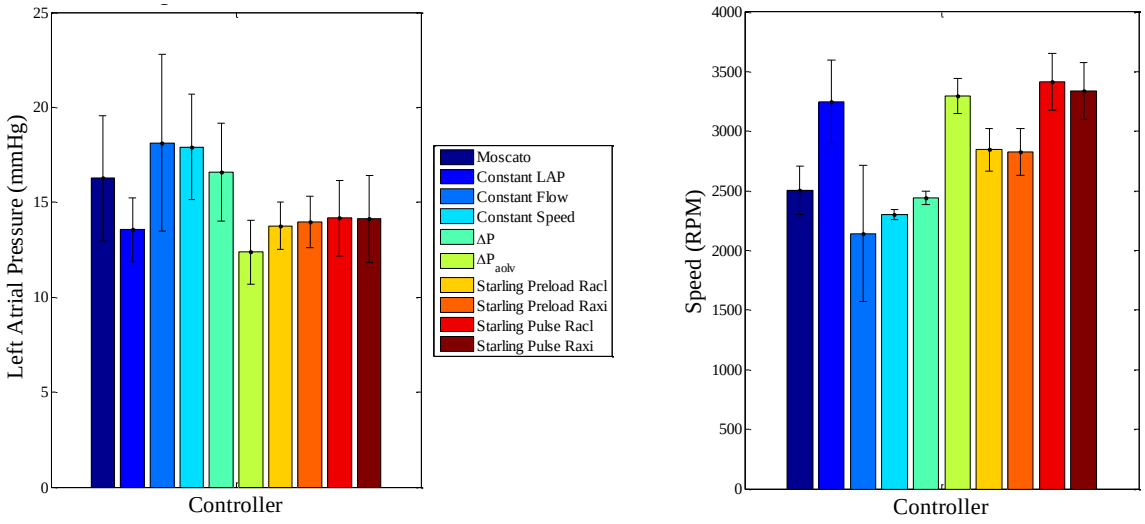

Figure 4.14: Mean LAP (left) and pump speeds (right) during exercise for the different control systems.

The main difference between control system performances was with regards to suction handling and avoidance. Only one controller (Starling Preload RACL) completely avoided all states of suction. This controller successfully reduced flow sufficiently quickly in response to the drops in preload caused by the postural change and Valsalva manoeuvre. Only Starling Preload RAXI, constant ΔP and constant P_{in} had less than 0.1 events per second. The suction events produced by these controllers were shorter

and less severe than the others, indicating that these controllers could recover quickly from suction events.

Sustained, unresolvable suction was observed with some of the controllers that controlled flow rate. If flow rate did not drop sufficiently quickly in response to changes in preload, suction occurred. These suction events caused further reduction in flow rate. This resulted in a positive error between the target flow rate set by the flow controllers and the measured flow rate, to which the controller responded by further increasing pump speed. This exacerbated the suction condition, further reducing flow, which led to further increases in pump speed (Figure 4.15). This cycle continued until pump speed reached the upper limit. Since these controllers could not escape suction events, suction events continued throughout the duration of the simulated scenarios. This may have affected the performance of these controllers during exercise.

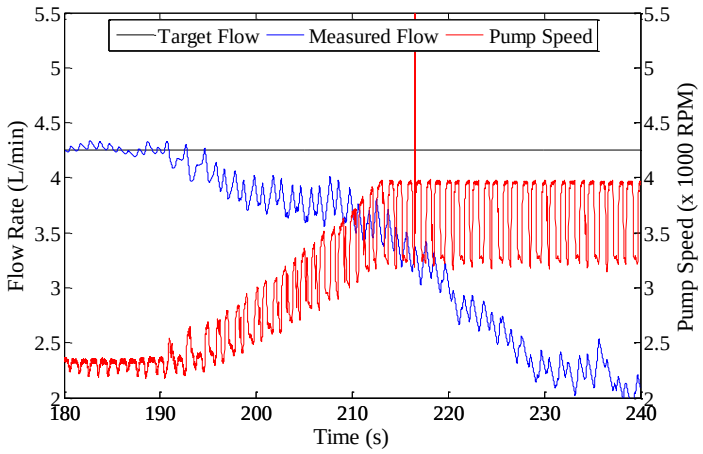

Figure 4.15: Pump flow rate and speed for the constant flow control system during the Valsalva manoeuvre.

Maintaining a constant LVEDP caused unresolvable suction during the exercise scenario for two reasons. Firstly, LVEDP was significantly elevated during exercise, to which the controller responded by increasing pump speed. However, the target LVEDP was not reached even after reaching maximum speed. This led to suction events, even though the LAP was nearly 15mmHg. These suction events occurred just before the start of the isometric relaxation phase of the cardiac cycle, when the ventricular volume was low but pressure high. Once diastole began the suction events were relieved. However, constant LVEDP control did not cause suction during the low preload in the postural change and Valsalva manoeuvres.

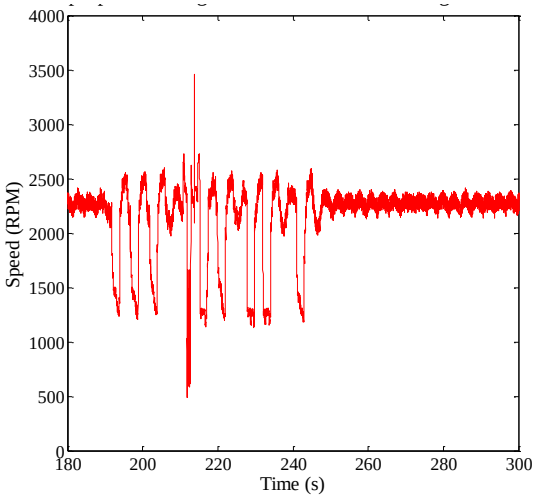

Figure 4.16: Pump speed during the Valsalva manoeuvre using ΔP control.

Both differential pressure controllers caused suction, with better suction handling exhibited by ΔP control. This was because activation of the suction valves caused the pump inlet pressure to fall sharply and LV pressure to rise. This sharply increased ΔP each event but kept ΔP_{aolv} relatively constant. Therefore, the ΔP controller sharply lowered pump speed with each suction event whilst ΔP_{aolv} kept speed constant. Whilst ΔP control dropped speed with each suction event, effectively shortening the width of each event, it kept speed constant during preload reductions that preceded suction and was therefore not able to prevent suction from occurring (Figure 4.16).

The exercise performance of all controllers varied significantly. The best performing control systems in exercise were the Starling Preload RACL, Starling Preload RAXI and Constant LVEDP control. The two Starling controllers increased pump speed to 2800 RPM, which increased pump flow without causing suction events in exercise. The constant LVEDP controller increased flow to the maximum speed, which resulted in suction events. However, the severity of these events was not enough to significantly reduce total flow.

The worst performing controllers during exercise were those that did not sufficiently increase pump flow (Figure 4.17). This was due to either a small or zero increase in pump speed (for constant speed, afterload impedance and constant ΔP control) or by sustained severe suction from previous patient scenarios (Starling Pulsatility controllers).

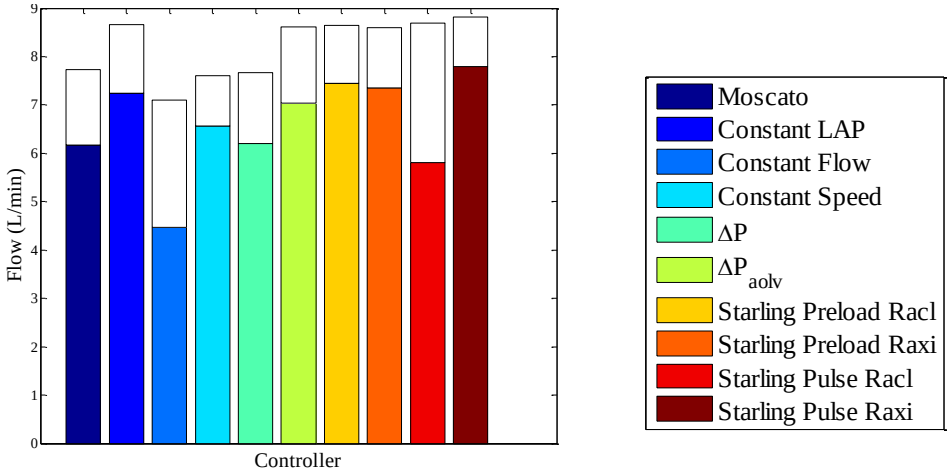

Figure 4.17: Systemic and pump flow rates during exercise for each of the different controllers. Coloured bards represent pump flow rate; white bars represent aortic valve flow.

4.6 Discussion

The key finding from this comparison of physiological control systems was that Starling control using preload and the RACL method was the best performing system with respect to all aspects evaluated. This control system not only produced suitably appropriate resting haemodynamics, but prevented any suction events from occurring. This was due to prompt reductions in pump speed when preload dropped, in combination with pump speed increases during exercise that increased flow without over-pumping. This is the first time a Frank-Starling control system has been evaluated with respect to three different patient scenarios, and the results have highlighted the advantages of this system over other types of control systems. Based on these findings, the Starling Preload RACL controller should be further investigated for use in a BiVAD system.

However, this evaluation has also highlighted that one of the disadvantages of flow-based controllers is their ability to exacerbate ventricular suction conditions. Lower average pump flow caused by sustained ventricular suction in conjunction with a target flow that was not low enough to avoid suction led to the controller increasing pump speed in order to compensate what appeared to be a positive controller error. This exacerbated the suction condition, which may be relieved by a sustained reduction in pump speed, suspended controller action and/or infusion of fluid to raise the patient's circulatory volume. Even though the successful Starling controller configuration avoided states of suction in this evaluation, the fact that it relies on control of pump flow means that it too is vulnerable to this phenomenon. The inclusion of a suction-detection and avoidance algorithm into the control system is required to prevent this from occurring.

In order to validate the results in this study, individual control system results should be compared to those published by the original investigators. The two differential pressure controllers presented by Giridharan and colleagues, ΔP and ΔP_{aolv}, exhibited higher pump flows in exercise than constant speed control, with ΔP_{aolv} producing higher flows than ΔP. These results align with those initially presented by Giridharan in [112], [152]. Additional findings from this study were that the differential pressure control strategies did not reduce pump speed sufficiently in response to a change in preload to prevent ventricular suction. This implies that this control approach should not be used as a primary control objective.

Constant flow control was the worst performing control strategy in this evaluation. It did not drop pump speed to prevent suction and exacerbated suction conditions. It also produced the worst exercise performance. These results indicate that maintaining a constant pump flow rate at all costs is not a viable control objective. Casas et al. (2007) proposed that this control objective can ensure suitable end-organ perfusion regardless of the patient's SVR [120]. However, the results from this study suggest that the disadvantages of this control system greatly outweigh this potential advantage in patients with varying cardiac demand.

Maintaining a constant LVEDP using an LVAD physiological control system proved to be one of the better performing control strategies. Bullister and colleagues did not perform any suction-avoidance assessment [115], so no direct comparison can be made. Maintaining a constant LVEDP effectively produces an infinite preload sensitivity, which supports its case as being a suitable control strategy. The performance of this controller was marred by the occurrence of ventricular suction during exercise, which occurred because the pump speed increased to the upper limit. This occurred because the LVEDP increased to approximately 13mmHg during exercise and was not able to return to the baseline level of 5.75mmHg, despite maximum speed being reached. This is reflective of the fact that LVEDP is not rigidly fixed in a healthy patient, and it could therefore be argued that it is not physiological to do so with a pump. This shortcoming could be overcome by setting a different target LVEDP for exercise. These results indicate that this simple approach can avoid suction and increase flow during exercise and thus should also be considered for control of dual LVADs.

The afterload impedance based control presented by Moscato et al. is effectively another form of Starling-like control in that it varies pump flow with pump preload (LVP). However of all the Starling controllers, this approach had the worst overall result. The changes in pump flow with venous return were not large enough in magnitude to prevent suction events, and the flow increase in exercise was not as high as the other Starling-like controllers. This may have been due to the use of LVP rather than LVEDP. Another reason for the poor performance was that Moscato's controller was slower to change pump flow rate than the other Starling controllers. This was due to the use of a 3-Windkessel model to calculate target flow, as well as a 3rd order Butterworth filter. The other Starling controllers used a

morphological filter to determine the beat-to-mean values of LVEDP and flow rate, which has been shown to be more responsive that Butterworth filters [170]. Another reason for the poor performance may have been the use of a different afterload impedance compared to the original paper (0.5 vs. 1 $mmHg.mL.s^{-1}$). However, this afterload impedance was required in order to obtain suitable initial resting haemodynamics in this MCL.

4.7 Experimental Limitations and Future Work

There were a number of limitations in this experiment which should be addressed in future experiments. Firstly, only a number of control systems were compared. Notable omissions included work by Arndt et al. [82], [83], Vollkron and colleagues [84], Choi et al. [80], [95] and Gwak et al. [86], [87]. These controllers were omitted because their complexity, in conjunction with insufficient detail of controller parameters in their published descriptions, made it difficult to implement them in this experimental setup within the time frame. Comparisons with these untested systems may require collaboration with the initial investigators in future studies.

The second limitation of this study was that it was assumed that all feedback variables were measured using accurate and reliable sensors. This assumption was necessary in order to assess the efficacy of each control objective in isolation. Both pressure and flow sensors were required, and for long term use these sensors need to have high accuracy and low drift. Currently there are no commercially available pressure sensors that meet this criteria, although there are some in development [159], [160]. Flow sensors are an available alternative, as one is incorporated into the HeartAssist 5 LVAD [171]. Therefore, the assumption that sensors were available is not reflective of the current situation in clinic. Further investigation is required to determine whether the use of flow [172] and/or pressure [110] estimation algorithms instead of sensors affects the performance of these control systems.

Finally, no repetition was performed of the results. The repeatability of the MCL was already established in the previous chapter, so it was assumed that repeating experiments in this chapter was redundant.

4.8 Conclusion and Summary

The aim of this chapter was to compare and contrast a number of physiological control systems for rotary LVADs in order to determine which systems could be adapted into a control system for dual rotary LVADs. Using the testing protocol described in the previous chapter, a thorough and detailed comparison of control systems was performed. It was found that Frank-Starling like control produced the best all-round performance, and thus was used as the basis of a dual LVAD control system in the next chapter. However, this control system does rely on the implantation of flow and pressure sensors, which are not available for long term clinical use. Additionally, some LVAD controllers were missing from the comparison stage due to insufficient information from the literature.

As the aim of this thesis was to develop a control system for dual rotary LVADs, knowledge of the current state of single LVAD control systems was required. Knowing which approaches worked best for LVAD control enabled selection of appropriate systems for further development into a BiVAD system. This stage streamlined the development process of the BiVAD control system described in the next chapter.

5 BiVAD Control

The previous chapter described the comparison of a number of rotary LVAD physiological control systems. The result was that the Starling-like control systems produced significantly better performance than other control systems. The next challenge is to identify methods of modifying this LVAD controller into a suitable control system for dual LVAD use.

This chapter describes the adaptation of this control mechanism into a dual LVAD control system. The chapter begins with a review of the literature encompassing dual LVAD control systems, which highlights that a number of different approaches could be used for this adaptation process. These different methods are assessed using the evaluation framework described in Chapter 3, which enabled selection of an appropriate control method.

The significance of this chapter is that it presents a novel physiological control system for dual LVADs. This system is shown to be better than other dual LVAD control systems through thorough quantitative evaluation methods. The use of quantitative methods for evaluation as well as comparisons with other control systems ensure that this novel control system is an improvement upon other methods previously presented in literature.

The work completed in this chapter has been published as a manuscript entitled "Physiological control of dual rotary pumps as a biventricular assist device using a master/slave approach" in the scientific journal Artificial Organs (Published Online 21st April 2014). The methods, results and discussion of this chapter were taken directly from that publication. The introduction was extended to provide the reader with more background information. The results and discussion sections were further expanded to include comparisons of different slave control systems

5.1 Aim

The aim of this chapter is to develop a control system for dual rotary LVADs based on the LVAD physiological control system selected at the end of Chapter 4. The specific objectives devised to meet this aim were as follows:

- Review the literature regarding evaluation of physiological control systems.
- Identify a number of possible approaches for control of dual rotary pumps in series.
- Implement these approaches in an in-vitro testing environment.
- Evaluate each approach using the framework established in Chapter 3.

5.2 Literature Review

Prior to development of a control system for dual LVADs, knowledge of previous work was required. The following section is a summary of the physiological control systems for dual LVADs previously proposed in literature. Unlike the review in Chapter 4, this review includes both pulsatile and rotary pump control methods, and control methods for TAHs as well as BiVADs. This is because the issue of balancing left and right flow rates applies to both pulsatile and rotary blood pumps, regardless of whether they are used for TAH or BiVAD applications.

5.2.1 Pulsatile Pump Control

Most clinically available pulsatile VADs, such as the Thoratec PVAD, can operate on a fill-to-empty mode. In this mode of operation, the pump only ejects when the blood volume in the device reaches a minimum level. This ensures that the outflow of the pump matches the inflow, making the device preload sensitive. When using two pulsatile pumps as a BiVAD or as a TAH, both devices are operated in the fill-to-empty mode, which helps to balance flows [173]. The Syncardia TAH, which consists of two pulsatile pumps, also operates using a similar fill-to-empty mode [174]. In addition to the physiological control systems used by these commercially available devices, other investigators have presented more complicated methods of physiological control.

Nakamura et al. (1999) proposed control of a pneumatic TAH using mixed venous oxygen saturation (SVO_2) [129]. Left pump flow rate was set as a linear function of SVO_2 and right pump flow rate was set as 90% of left pump output to prevent pulmonary venous congestion and to account for bronchial shunt flow. This system was evaluated in-vivo by implanting a TAH into a sheep and recovering the animal. The animal was exercised using a treadmill, the speed of which was increased from 1 to 6 km/h over 6 stages of 3 minutes each. The final stage was continued until the calf collapsed. The controller resulted in higher pump flows during exercise compared to constant flow control, however there was no difference in total exercise duration. Settling time of the system was approximately 1 minute. Clearly SVO_2 is a good indicator for cardiac demand and can be used as a guide to increase pump output. However in this study SVO_2 was only measured every 5 seconds, which is a slow sampling rate. Additionally, SVO_2 cannot be used as an indicator for ventricular suction.

Previous work by Abe and colleagues investigated control of dual pulsatile pumps for both TAH and BiVAD applications [175], [176]. In both applications, the investigators designated one pump as the master and the other the slave. The control system for the master pump in both applications was based on 1/R control, which set the cardiac output as a function of the SVR. At each time step, the flow rate of the master pump was set using Equation (5.1).

$$CO = (AoP_{set} - RAP_{set}).\frac{Q}{(AoP - RAP)} + CP.BW.(AoP - AoP_{set}) \quad (5.1)$$

Where CO is the desired cardiac output ($L.min^{-1}$), Q is the measured cardiac output ($L.min^{-1}$), BW is the body weight of the sheep (kg), CP is an animal-specific constant ($L.min^{-1}.kg^{-1}.mmHg^{-1}$), AoP and RAP the aortic and right atrial pressures respectively (mmHg) and AoP_{set} and RAP_{set} were the desired values for AoP and RAP respectively (mmHg). The CO of the master was varied by changing the beat rate and keeping stroke volume (SV) constant.

For the TAH approach [175], the left pump was set as the master and the right pump the slave. The SV of the right pump was programmed to balance the left and right atrial pressures, using Equation (5.2).

$$LAP = a_{slave}.RAP + b_{slave} \quad (5.2)$$

Where a_{slave} was set to 1 and b_{slave} (mmHg) set to the difference in static pressure head between left and right atria. Evaluation was performed in-vivo using 10 goats. Seven goats had their ventricles removed and two pulsatile pumps implanted. Three goats were instrumented but otherwise healthy and used as controls. Of the seven TAH animals, four had 1/R control and three used constant SV and beat rate (i.e. constant flow control). Animals were recovered and data recorded continuously for at least 21 days (up to 340), during which they undertook everyday scenarios as well as treadmill tests. There was no statistically significant difference in flow rates between natural heart group and 1/R group. With 1/R control, CO varied throughout each 24 hour period in a similar manner to normal circadian rhythm, with lower flow in rest and higher flows in standing and eating. Constant flow control resulted in elevated AoP and RAP compared to natural heart group. In exercise there were similar increases in CO between 1/R control and the natural heart groups, although the 1/R control group exhibited 30 second delay between exercise commencing and the pump flow rate changing. Clearly this approach showed benefits for control of dual pulsatile pumps by making them respond similar to the native heart. However, there was a strong dependence on sensor fidelity, with the control system no longer working once pressure sensors became obstructed. The delay of 30 seconds after the onset of exercise was also slow. No justification was presented for the choice of using the left pump as master and right pump as slave.

For biventricular assistance, Abe and colleagues (2000) used a similar control scheme but set the right pump as master [176]. The left pump, as slave, was set to maintain LAP below 10mmHg. Driving pressure was updated every 2 seconds, with a new target flow rate calculated every 6 seconds. This was a more precise update interval than the TAH controller. After implantation, the PA was clamped off to produce total RV assistance, whilst the aorta was partially clamped to provide partial LV assistance. The authors claim that this was because the 1/R control strategy does not work when the LVAD is providing full assistance. The algorithm was tested in 5 goats, with support durations ranging from 13 to 75 days. The pulse rate of the devices was compared to that of the residual ventricles, and found to always be higher than the native heart. However, the changes in VAD pulse rate mirrored those of the

native ventricle, indicating synchronicity with the native control mechanisms. Whilst flow balancing was achievable with this controller, there was no inherent method of avoiding RV suction. In addition, no comparisons were performed with other control mechanisms.

Saito and colleagues (2003) developed a multi-objective control system for using dual undulation pumps as a TAH [177]. The undulation pump is a continuous-flow volume-displacement pump which can produce continuous flow, continuous flow with pulsatility or totally pulsatile flow. The 7 control objectives were (in order of priority):

1. Controlling pump speed to a set point using PWM control of pump current.

2. Pulsatility mode, which switches between a high and low PWM duty cycles to simulate systole and diastole.

3. Anti-suction mode, which drops PWM duty cycle to the diastolic value if suction is detected in systole.

4. PRD control, which maintains the product of systolic PWM and systolic/diastolic ratio (PRD) constant.

5. Emergency control, which lowers the target PRD if inlet pressures fall below -20mmHg, and increases target PRD if inlet pressures rise above 20mmHg.

6. LAP control, in which the left pump sets the PRD to maintain LAP constant at 4mmHg using an integral controller.

7. 1/R control, as described above, for the right pump.

The investigators kept goats alive for up to 62 days with this control system, and all suction events were resolved within two "beats". However, no comparison was performed with any other control mode, nor was any mention made of the control logic used to combine all 7 control systems.

In summary, all of the physiological control systems for dual pulsatile pumps are master/slave style controllers, with one pump's control system dependant on the other. They appear to have all been assessed in-vivo.

5.2.2 Rotary Pump Control Strategies

Rotary VADs produce a continuous flow of blood, and cannot be operated in a fill-to-empty mode like pulsatile VADs. This makes it difficult to automatically balance flow rates. Therefore the development of a physiological control system is more important for dual rotary LVADs.

All of the aforementioned control strategies for pulsatile BiVAD and TAH were evaluated in an in-vivo environment and appeared offer some benefit over normal pulsatile pump operation. However, control of dual rotary LVADs is more challenging due to the lower preload sensitivity of rotary pumps [51]. There have been two types of approaches used to control dual LVADs, both of which involve separate control systems for each approach. In the first approach, the two control systems are completely independent from each other. In the second approach, one control system takes the role of master and the other slave, which introduces some dependency between the controllers. The following section summarises the different control systems for dual rotary LVADs for both TAH and BiVAD.

5.2.2.1 Independent Control Systems

Khalil and colleagues (2008) designed a flow-based control system for dual HeartAssist 5 pumps [102]. The strategy was for each pump to maintain its flow rate constant using integral control. Equations of pump flow were derived from first principles, and the unknown variables were determined using frequency analysis of the pumps in a mock circulation loop. In-vitro evaluation revealed that constant flow was maintained during variations in SVR and PVR. However, this control system did not consider any strategies for suction avoidance, nor did it incorporate any mechanism to automatically adjust flow during exercise. Additionally, attempting to maintain a constant flow is not a suitable approach for active patients, given the results presented in the previous chapter. Finally, this study assumed that there was no bronchial flow, which is not a clinically relevant assumption for a system that relies on maintaining constant pump flow rates.

Gaddum et al. (2012) used two independent Starling-like control systems for control of dual VADs [89]. Each pump's control system varied its flow rate with preload, similar to those systems proposed by Salamonsen et al.[127] and Moscato et al. [91]. This controller was implemented with two independent PID controllers, with the gains tuned manually. Evaluation involved shifting fluid from the SVC to the RA and measuring the preload sensitivity and rise and settling times. Whilst this approach increased LV and RV preload sensitivity to 0.28 and 0.2 L/min/mmHg respectively, some coupling between the two systems was observed. Increased flow from the RVAD increased LV preload, causing increased LVAD flow. This in turn raised RV preload, causing further increased RVAD flow. The effects of the interaction are reflected in the oscillations present in the RVAD flow signal. It took nearly 60 seconds for these oscillations to disappear (Figure 5.1). The interaction between these two independent control systems was more pronounced when using constant inlet pressure control, in which both pump speeds continuously increased and did not appear to settle. While these results are promising, the evaluation was simplistic and the coupling of the two pumps must be addressed before further implementation.

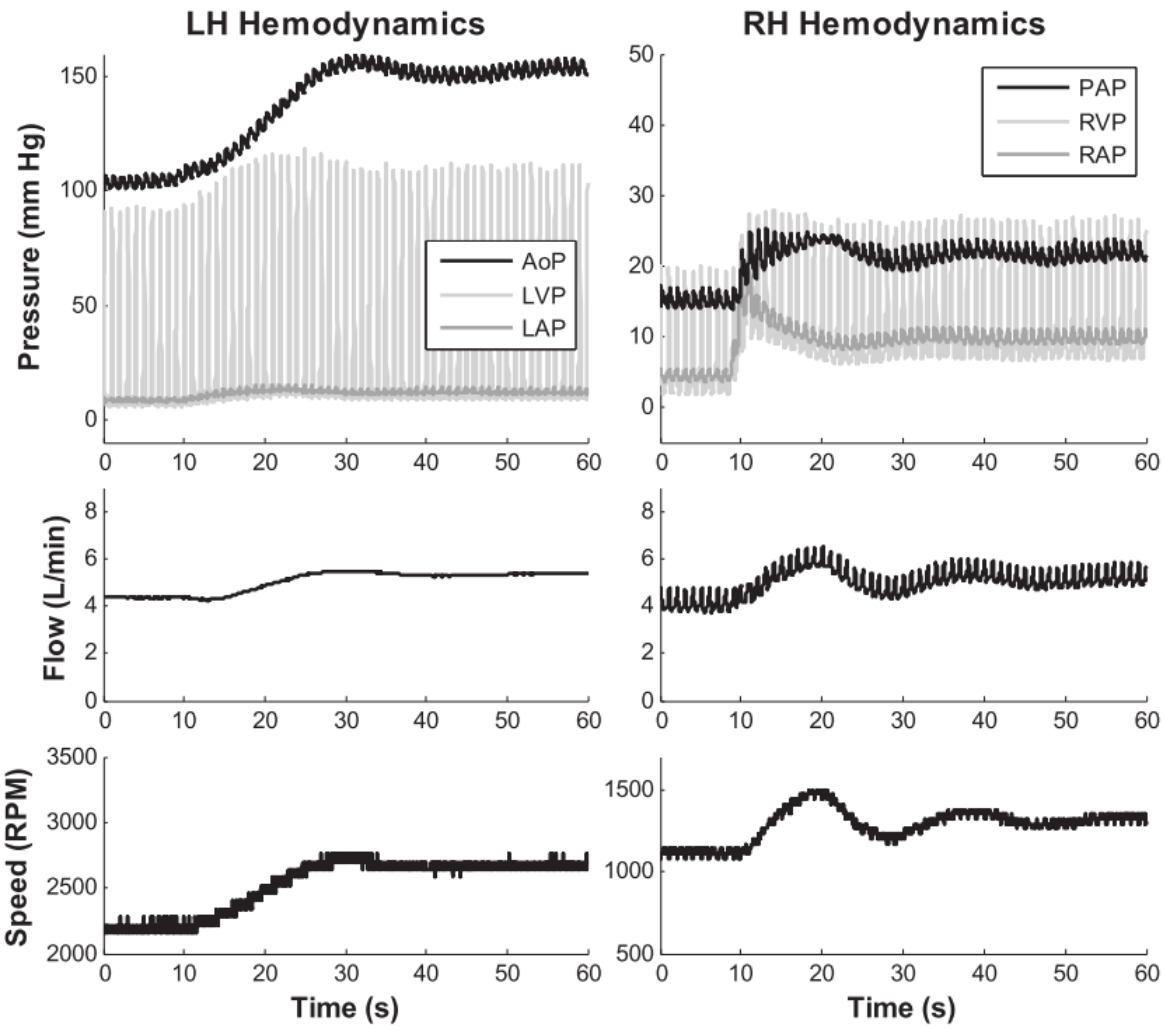

Figure 5.1: Response of dual independent Starling-like control systems to an increase in right atrial pressure [89].

5.2.2.2 Master/Slave Control Systems

Olegario and colleagues (2003) [117] extended the work of Abe and colleagues by using a master/slave approach for control of dual RBPs as a TAH. The left pump was set as the master, and controlled using 1/R control previously described. The right pump was the slave, and controlled to maintain LAP constant. Evaluation was performed in-vitro and in-vivo using two Capiox centrifugal blood pumps (Terumo Corp., Tokyo, Japan). In the MCL, only the right pump slave control system was evaluated, with the left pump operated at constant speed. Evaluation involved inducing suction by increasing left pump speed by 700 RPM, and observing the right pump speed changes. It took 60 seconds for the LAP to recover after the left pump speed increase. Some oscillation of LAP was observed, possibly due to overshoot of the right pump controller.

In-vivo, the pumps were implanted alongside the native heart and the heart stopped with electrical current. The MCL study was repeated first, with the left pump speed increased by 2000 RPM. The settling time of the slave controller was faster (approximately 10 s), however right pump speed exhibited

oscillatory behaviour. 1/R control was then switched on, and some right pump speed and flow oscillation was still present. However, arterial pressure was still maintained. In the animal study, the authors found that the system was able to prevent left atrial suction. However, oscillatory behaviour of right pump speed was present, because the RVAD controller was trying to maintain preload to a constant value. Preload in a healthy person is not strictly constant - it varies with circadian rhythm. Therefore, it is not physiological to maintain a constant LAP, which may be why the oscillatory behaviour was present. The inclusion of a tolerance into the controller may have eased this oscillatory behaviour without causing hazardous effects on the human body. Another shortcoming of this controller was that there was no method of avoiding RA suction.

Endo and colleagues (2000) [122] used a master/slave control system to control two mixed-flow pumps as a BiVAD. The master was the left pump, and was set to maintain a constant LV preload using the ICA (previously described in section 4.2.3.4). The RVAD was controlled to match the LVAD flow rate. This strategy was implemented with the user-in-the-loop, with the operator manually adjusting pump speeds to meet the objectives. Evaluation was performed in-vivo using 5 piglets, and involved clamping the base of the aorta to develop global ischemia, then gradually recovering the heart using nitric oxide or defibrillation. The right pump was able to be weaned off completely as the heart recovered using this control strategy. However, no practical implementation of this system was discussed. Like Olegario's controller, there was also no method of avoiding or recovering from RV suction.

Another master/slave control system was proposed by Siess in a patent for control of two rotary VADs when used as a BiVAD [178]. In this system, the LVAD was considered master and kept flow rate constant. The RVAD, as slave, maintained a flow rate that was 90% of the LVAD flow rate. If the LVAD flow rate changed, the RVAD flow would automatically change to remain 90% of the LVAD flow rate. However, no evaluation was presented.

5.2.3 Summary of Literature Review

The two main approaches to controlling dual rotary LVADs are to use two identical and independent control systems, or making one control system dependent on the other (commonly referred to as a master/slave configuration). Early work controlling dual pulsatile pumps using master/slave configurations was relatively successful, however this success has not yet been achieved with rotary pumps. This may be due to the comparatively lower preload sensitivity of rotary pumps.

Controlling two rotary LVADs placed in a series circuit has proven challenging. The interaction between left and right pumps due to their inherent coupling makes selecting the control strategy difficult. It appears that any system that involves maintaining one or both atrial pressures or preloads constant has strong coupling between left and right pumps, which results in instability if not handled correctly. Interestingly, the successful strategies employed in dual pulsatile pump control (1/R control

master control and preload-matching slave control) have not yet been employed to control dual rotary pumps.

Like LVAD control, evaluation of dual rotary pump control has involved simulating one patient scenario or circulatory system change, which is not thorough enough to characterise performance. Additionally, with the exception of Gaddum et al. [89], no dual LVAD control systems have been evaluated against other control systems.

Given the success of the Starling-like control systems (as shown in the previous chapter), they are a suitable candidate for dual LVAD control. Based on the literature review, a master/slave implementation of the Frank-Starling system would be most appropriate in order to reduce the negative effects of the coupling between left and right pumps and therefore create a stable system. However, there are two key unknowns. Firstly, there have been a number of different slave control systems presented in the literature, all evaluated in different ways, making it difficult to determine the most appropriate slave controller for this application. Secondly, it is not obvious whether the left or right pump should be the master. The aim of this chapter is to investigate these two unknowns in order to determine the best-performing approach for control of dual rotary LVADs.

5.3 Methods

Controller assessment was performed using the MCL previously described in Chapter 3. A severe heart failure patient was simulated, and biventricular support achieved by connecting two VentrAssist LVADs (VentraCor, Sydney, Australia) in a BiVAD configuration. The inflow cannulation sites were the ventricles, while outflow cannulation site was the aorta (for left pump) and pulmonary artery (for right pump). The outflow graft of the RVAD was not banded, which meant that under normal conditions of SVR and pulmonary vascular resistance (PVR), the RVAD speed was lower than LVAD speed.

The most successful LVAD control system from the previous chapter, preload-based Starling control using RACL, was adapted for use in a dual LVAD system. This adaptation involved developing a master/slave control system, with the Starling-like control system being used as a master. The controller settings for the master were the same as those outlined in Chapter 4 and in Appendix C. For reference, the master control system calculated the target flow rate (Q_{VADM_target}) using Equation (5.3).

$$Q_{VADM\_target} = Q_{VADM}(1 - K_{sc1}) + K_{sc2}(P_{inM} - a) \quad (5.3)$$

Where Q_{VADM_target} is the target flow rate of the master controller ($L.min^{-1}$), Q_{VADM} is the measured flow rate through the master pump ($L.min^{-1}$), P_{inM} the measured pump inlet pressure (mmHg), a the inlet pressure offset (mmHg), K_{sc1} and K_{sc2} ($L.min^{-1}.mmHg^{-1}$) are based on the desired preload sensitivity of the pump, and are set the same as described in Appendix C (0.447 and 0.894 $L.min^{-1}.mmHg^{-1}$).

A total of 8 different master/slave approaches were compared in this experiment (Table 5.1), with their results compared to constant speed operation, dual independent Starling-like controllers and dual constant LVEDP controllers. The 8 approaches consist of four different slave controllers, as well as designating either the LVAD or RVAD as the master pump.

Table 5.1: Different master slave control approaches evaluated in this chapter.

Controller Combination	LVAD Control System	RVAD Control System
1		Match Pressures (Slave)
2	Starling-Like	Match Flows (Slave)
3	(Master)	Constant Slave Preload (Slave)
4		Constant Master Preload (Slave)
5	Match Pressures (Slave)	
6	Match Flows (Slave)	Starling-Like
7	Constant Slave Preload (Slave)	(Master)
8	Constant Master Preload (Slave)	

The first slave controller (Controllers 1 and 5) varied the end-diastolic ventricular pressure of the slave pump (P_{EDS}) linearly with the end diastolic pressure of the master pump (P_{EDM}). This approach was first proposed by Abe and colleagues [175]. The implementation was similar to the master controller, except that Q_{VAD} was substituted with P_{EDS} in order to obtain the target slave inlet pressure (P_{EDS_target}), as per Equation (5.4).

$$P_{EDS\_target} = P_{EDS}(1 - cos(tan^{-1} K_{slave})) + (P_{EDM} - c)\, sin(tan^{-1} K_{slave}) \quad (5.4)$$

Where P_{EDS_target} (mmHg) is the target end-diastolic pressure for the slave pump, P_{EDS} is the measured end-diastolic pressure for the slave pump (mmHg), P_{EDM} is the measured end-diastolic pressure for the master pump (mmHg), c is the horizontal offset for the control line (mmHg) and K_{slave} (unitless) is the sensitivity of the controller. The constants K_{slave} and c were set to 2 and 7.63mmHg respectively in order to obtain the same resting haemodynamics described earlier in this thesis. P_{EDS_target} was limited to the range 3 - 25mmHg to prevent suction and venous congestion respectively. Equations (5.3) and (5.4) are generic descriptions of the master/slave (MS) control system. Table 5.2 shows the actual variables used for left/right or right/left MS configurations.

Table 5.2: Variables used for the two different master/slave configurations. EDP - End-diastolic pressure; QVAD - ventricular assist device flow; LVEDP - left ventricular EDP; RVEDP - right ventricular EDP; QLVAD - Left VAD flow rate; QRVAD - Right VAD flow rate.

Master/Slave Combination	P_{EDM}	EDP_S	Q_{VAD}
Left/Right	LVEDP	RVEDP	Q_{LVAD}
Right/Left	RVEDP	LVEDP	Q_{RVAD}

The second slave controller's (Controllers 2 and 6) objective was to set the flow rate of the slave VAD ($Q_{VADStarget}$) to be a fraction of the master VAD flow rate (Q_{VADM}), based on the controller proposed by Siess [178]. This was implemented as per Equation (5.5). The constant α was set at 0.9 when LVAD was master, and 1.1 when RVAD was master. This follows the assumption made by Siess that LVAD flow should be 10% greater than RVAD flow.

$$Q_{VADS_{target}} = \alpha . Q_{VADM} \tag{5.5}$$

The third slave controller (Controllers 3 and 7) that was evaluated maintained the preload of the slave controller constant and was assessed because of its simple implementation. The target preloads were selected in order to obtain the same base haemodynamics described earlier. These targets were 3.5mmHg for LVAD master/RVAD slave (Controller 3), and 9.0 mmHg for RVAD master/LVAD slave (Controller 7).

The fourth and final slave control system (Controllers 4 and 8) evaluated in this investigation maintained the preload of the master controller constant. This approach was initially proposed by Olegario and colleagues in 2003 [117]. The target preloads were selected in order to obtain the same base haemodynamics described earlier. These targets were 9.0mmHg for RVAD slave (Controller 4), and 3.5mmHg for LVAD slave (Controller 8).

Both master and slave control systems automatically adjusted the PWM duty cycle of their respective pumps each time step in order to maintain the target flow and inlet pressure respectively. For each pump, if the difference between measured and target value was less than 5% of the target value, no changes were made to the duty cycle. If the difference was greater than 5%, the duty cycle was adjusted using proportional-integral (PI) control. The PI gains were tuned using the same Quasi-Newtonian optimisation process used in the previous chapter, described in detail in Appendix D. Controller gains are given in Table 5.3.

Table 5.3: PI control gains for each of the dual LVAD controllers tested

Controller Number	LVAD Controller	RVAD Controller	Left Pump Gains		Right Pump Gains	
			KP	KI	KP	KI
1	Starling-Like (Master)	Match Pressures (Slave)	0.064	0.0389	0.056	0.0215
2		Match Flows (Slave)	0.0508	0.0498	0.0532	0.0507
3		Constant Slave Preload (Slave)	0.0940	0.0442	0.0615	0.0108
4		Constant Master Preload (Slave)	0.0725	0.0498	0.0953	0.0111
5	Match Pressures (Slave)	Starling-Like (Master)	0.1137	0.0346	0.0735	0.0224
6	Match Flows (Slave)		0.0485	0.0744	0.0461	0.0714
7	Constant Slave Preload (Slave)		0.1108	0.0160	0.0778	0.1270
8	Constant Master Preload (Slave)		0.0953	0.0111	0.0725	0.050
9	Starling Control	Starling Control	0.0552	0.0349	0.0938	0.03940
10	Constant Preload	Constant Preload	0.064	0.0389	0.056	0.0215

As per Chapter 4, a non-linear morphological filter, which used mathematical morphology to estimate the beat-to-beat mean of a signal using the minimum and maximum values each cardiac cycle, was used to smooth all feedback signals. Further details of this filter and its derivation can be found in Appendix E.

For controller evaluation, the evaluation protocol was the same as that described in Chapter 3 and used in Chapter 4. For comparative purposes, two different dual independent controllers (dual Frank-Starling-like (Controller 9) and dual constant preload controllers (Controller 10)) presented by Gaddum et al. (2012) [89] were also evaluated. These control systems were tuned using the aforementioned Quasi-Newtonian optimisation method, and the controller gains are given in Table 5.3. Dual constant speed controllers were also evaluated, in order to provide perspective with the current mode of operation used in clinic. In order to represent a patient with elevated circulatory volume, evaluation of constant speed control was performed at both a normal mean circulatory filling pressure (MCFP) of 8mmHg, and a MCFP of 11mmHg [179]. Pump speeds and independent control settings were adjusted to obtain the same resting haemodynamics as the MS controller.

5.4 Results

Table 5.4 shows the four figures of merit for each combination of left/right and right/left master/slave combinations. From these results, only preload-matching slave controllers (1 and 5) were able to maintain a FOM_{REST} score at 100%, indicating that these controllers were able to restore resting haemodynamics after each scenario. Of these two controllers, only the left/right combination maintained a high FOM_{CONG} score, indicating that it is better at avoiding pulmonary congestion. The left/right combination also had the least number of suction events and the second highest FOM_{EX} score. Therefore, this combination had the best all round performance.

Figure 5.2 shows the performance of Controller 1 across all scenarios. The master controller varied target flow according to changes in preload. It decreased flow (4.8 to 3.5 $L.min^{-1}$) during the postural

change to prevent suction. It initially decreased flow during the Valsalva manoeuvre, but then returned to baseline within 15 seconds. Finally, it increased flow significantly in exercise (4.8 to 8.5 $L.min^{-1}$) in response to increased venous return. Measured LVAD flow did not reach the target flow in exercise because the LVAD pump speed had reached the upper limit. Otherwise, the measured flow tracked the target flow accurately. The slave controller effectively maintained right ventricular end diastolic pressure (RVEDP) between 3 and 5 mmHg during rest, postural change and the Valsalva manoeuvre. During exercise, the target RVEDP increased in response to the increased venous return. Noise was present in both target signals, but otherwise the measured signals were stable.

Table 5.4: Figures of merit for all combinations of master and slave control systems

Controller Number	LVAD Controller	RVAD Controller	FOM_{REST}	FOM_{CONG} (%)		FOM_{SUC} (s^{-1})		FOM_{EX}					
				Left	Right	Left	Right	Left ($L.min^{-1}$)			Right ($L.min^{-1}$)		
								ΔSQ	ΔLVADQ	Score	ΔPQ	ΔRVADQ	Score
1	Frank-Starling (Master)	Preload Matching	100	95.13	98.40	0.01	0.00	4.69	4.27	4.33	4.24	3.93	3.98
2		Flow Matching	42.40	92.38	99.63	0.05	0.00	4.95	3.99	4.32	4.67	3.69	4.08
3		Constant RVAD preload	63.11	75.56	99.86	0.07	0.06	6.54	4.43	5.19	6.51	5.75	5.94
4		Constant LVAD preload	80.10	99.43	95.46	0.06	0.00	3.44	3.08	3.17	2.79	-0.42	1.56
5	Preload Matching	Frank-Starling (Master)	100	73.19	99.87	0.03	0.02	6.48	4.33	5.12	6.53	6.42	6.34
6	Flow Matching		100	80.43	98.30	0.01	0.03	4.05	1.41	2.77	3.42	2.54	2.97
7	Constant RVAD preload		93.61	77.54	99.85	0.04	0.03	6.65	4.58	5.30	6.61	6.49	6.40
8	Constant LVAD preload		97.07	84.22	99.87	0.04	0.05	2.31	-4.21	0.21	2.25	1.42	1.91

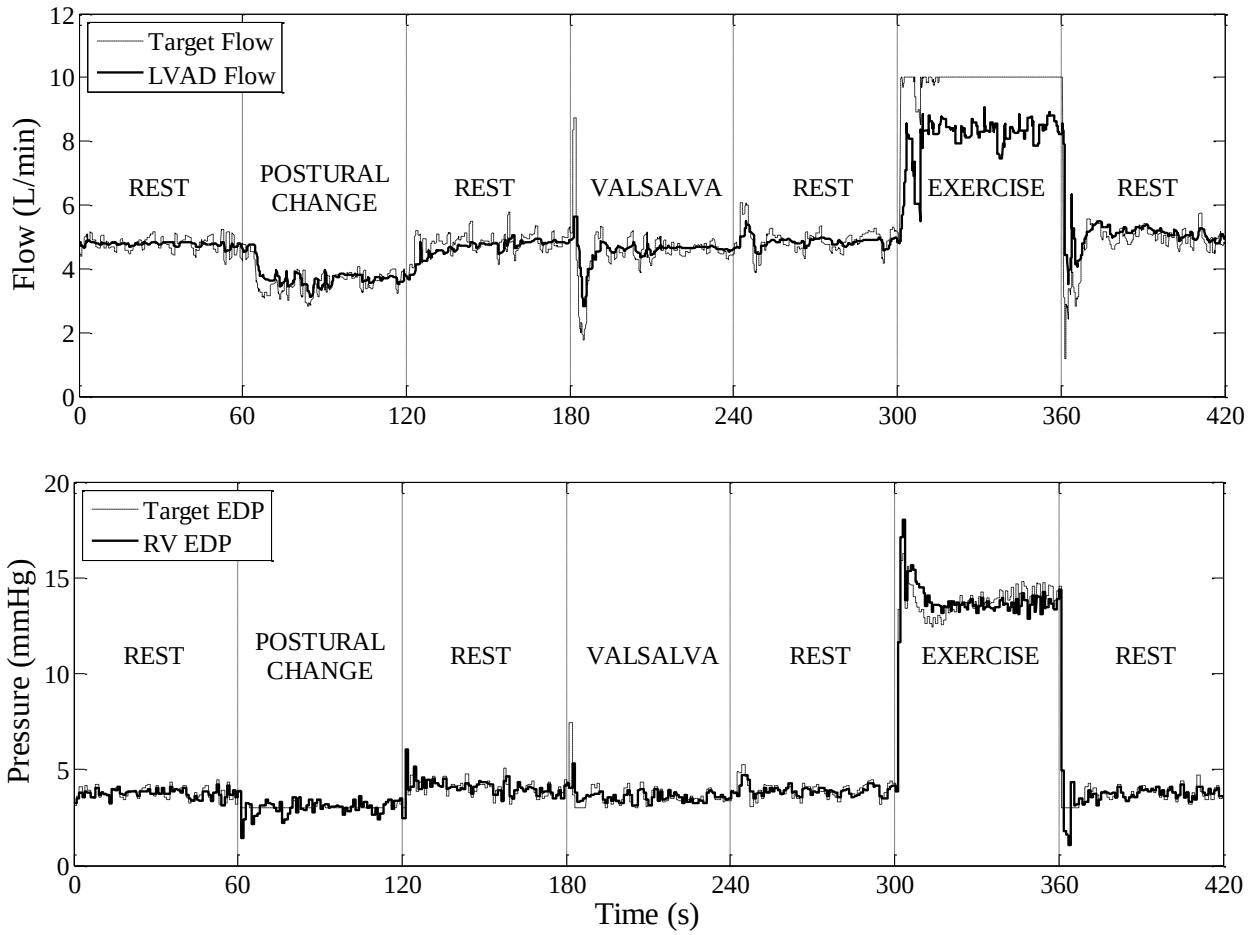

Figure 5.2: Target and measured LVAD flow (top) and target and measured right ventricular end diastolic pressure (bottom) as produced by the left/right master/slave control system.

Table 5.5 shows the performance metrics for the two best performing master-slave systems as well as the other controllers assessed for comparison. Sufficiently high arterial pressures and cardiac outputs were maintained during rest scenarios in all control systems and with constant speed control. The left/right MS control system produced fewer suction events than constant speed control (0.01 s^{-1} vs. 0.15 s^{-1}). An example of how the MS control system actively avoided suction during the Valsalva manoeuvre is shown in Figure 5.3. In this scenario, left ventricular (LV) venous return fell due to increased PVR. Constant speed control resulted in a fall in LV volume, and consequently suction events, because there was no decrease in LVAD flow. A similar drop in LV volume occurred with constant speed and high MCP (not shown), however the higher initial circulatory volume prevented suction. In contrast, the MS controller prevented suction by adjusting pump speeds. During reduced LV venous return, both the target flow rate of the master control system and the target inlet pressure of the slave system decreased. The LVAD speed decreased and the RVAD speed increased to match the new target values. The resulting reduction in LVAD speed prevented over-pumping from the LV, whilst the increase in RVAD speed overcame the increased PVR to assist with maintaining LV volume.

Table 5.5: Results from all control systems subjected to common patient scenarios in the mock circulation loop.

Controller	FOM_{REST} (%)	FOM_{CONG} (%)		FOM_{SUC} (s^{-1})		FOM_{EX} (L.min-1)	
		Left	Right	Left	Right	Left	Right
1	100	95.13	98.40	0.01	0	4.33	3.98
5	100	73.19	99.87	0.04	0.02	5.12	6.34
Constant Speed (Normal MCP)	100	95.49	97.87	0.15	0	2.09	1.92
Constant Speed (High MCP)	100	95.31	91.33	0	0	2.15	1.71
2x Independent (Constant EDP)	80	77.92	99.95	0	0.01	4.91	5.53
2 x Independent (Frank Starling)	100	76.32	99.89	0.04	0.05	5.41	6.49

Approximate time domain behaviour of the MS controller can be determined from Figure 5.3. All speed changes occurred within 2 seconds of perturbations. Both pump speeds exhibited 2% settling times of 10 seconds. The LVAD speed exhibited minor oscillations due to residual ventricle contractility. Chattering was present in the RVAD speed, which was due to the small level of noise in the target signal.

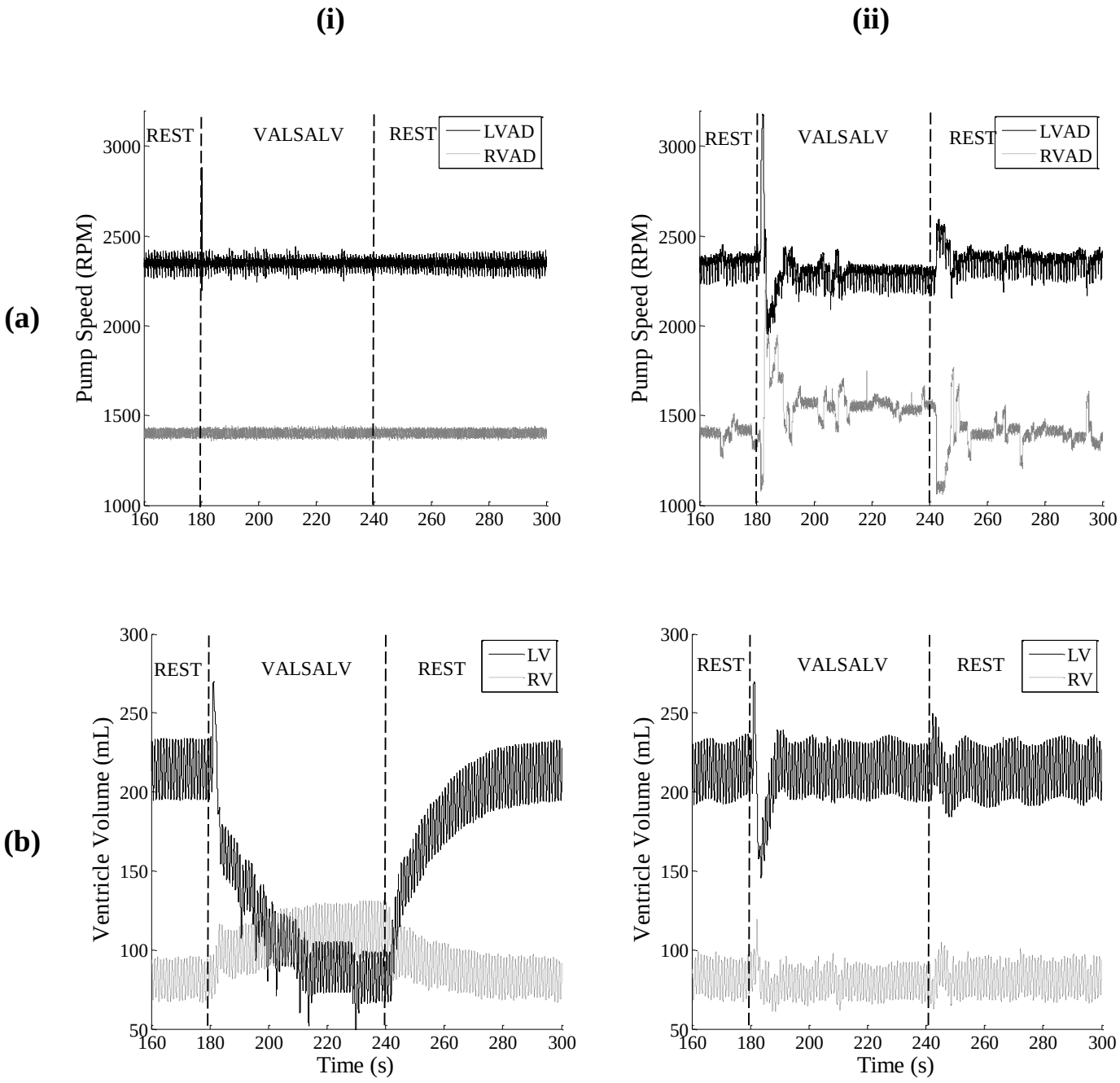

Figure 5.3: (a) Pump speeds and (b) ventricular volumes for (i) constant speed operation and (ii) left/right master/slave control system during the simulated Valsalva Manoeuvre. LVAD - left ventricular assist device; RVAD - right ventricular assist device; LV - left ventricle; RV - right ventricle;

In all systems, the maximum LVEDP and RVEDP occurred during the exercise scenario (Table 5.5). Both independent control systems and the right/left MS system resulted in excessively high LVEDP during exercise, resulting in high FOM_{cong} scores, which is indicative of pulmonary congestion. In this scenario, increased venous return to both ventricles caused all control systems to increase both LVAD and RVAD speeds. Left pump speed reached the upper limit of 3200 RPM, at which point there was no

further capacity to unload the LV. Figure 5.4 shows that the controller strategies that caused pulmonary congestion kept increasing RVAD speed above 3000 RPM, because the target values for the RVAD control system had not yet been reached. This caused RVAD flow to exceed LVAD flow (Figure 5.5), which led to overfilling of the LV. In contrast, the left/right MS system adjusted RVAD speed to match the LVEDP and RVEDP, regardless of LVAD speed. In this case the RVAD speed remained at 2072 RPM, preventing overfilling of the LV.

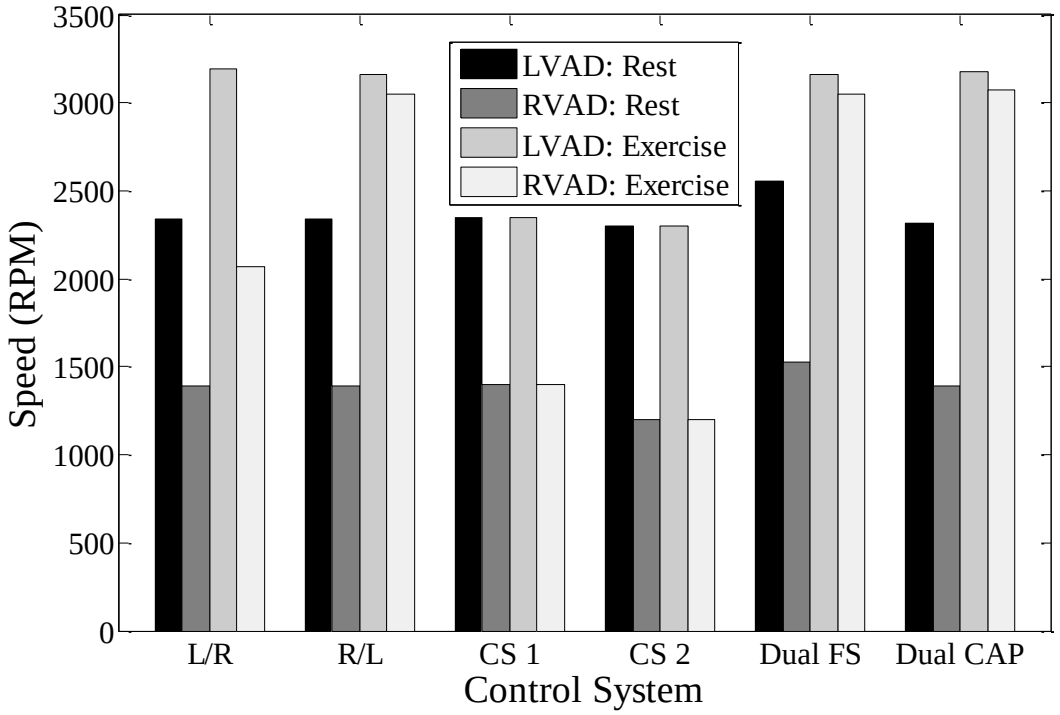

Figure 5.4: Pump speeds at rest and at exercise for each control system. L/R - left/right master/slave; R/L - right/left master/slave; CS 1 - constant speed (CVP 8mmHg); CS 2 - constant speed (CVP 11 mmHg); FS - Frank-Starling control; CAP - constant atrial pressure control.

Constant speed control did not cause high LVEDPs in any scenario. However, as shown in Figure 5.5, CO was lower in exercise with constant speed control compared to MS control (8.3 vs. 10 $L.min^{-1}$). Furthermore, the contribution of pump flow to total flow with constant speed control (approximately 73%) was lowest, whilst MS control was highest (93-97%). This indicates that MS control placed less strain on the ventricles than constant speed control during exercise.

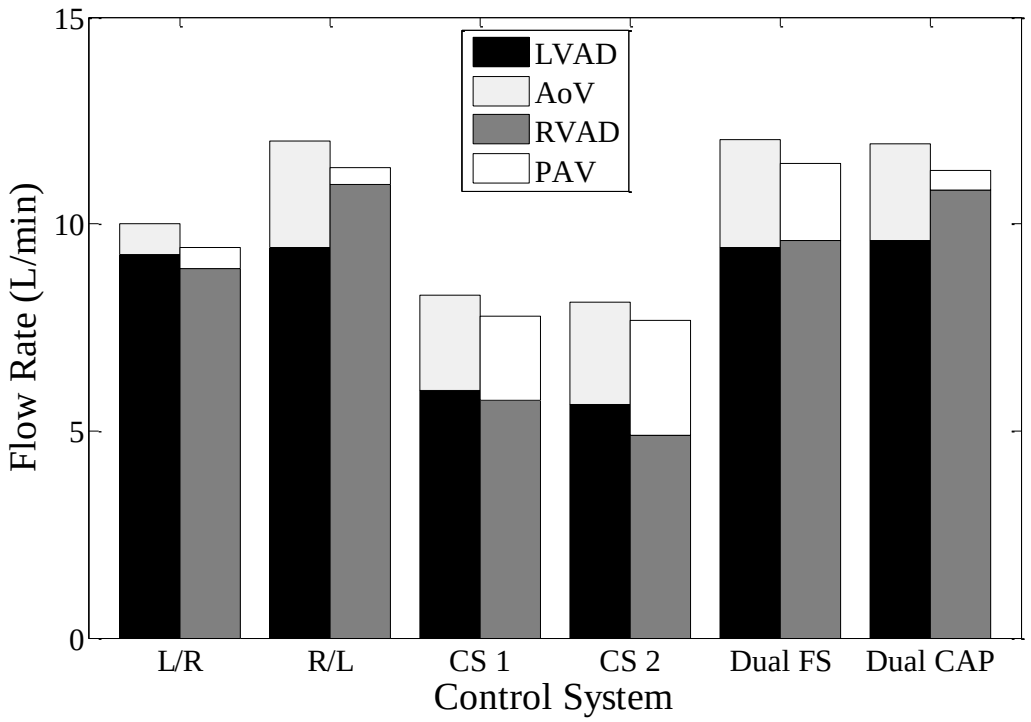

Figure 5.5: Flow rates through LVAD, RVAD, aortic valve and pulmonary valve during exercise scenario for each control system.

Using the right pump as the master resulted in higher cardiac output during exercise when compared to the left pump (12.06 vs. 10.1 L.min^{-1}). However, right/left MS caused more suction events across all scenarios. This indicates that the target flow rate set by the Starling controller was not low enough during low preloads. A linear relationship between flow and preload might not be suitable for RVAD Starling control.

5.5 Discussion

Of the 8 different combinations of master and slave control systems evaluated in this experiment, the LVAD master and the preload-matching RVAD slave controller (Controller 1) had the best overall performance. This system was adept at reducing suction events during reduced venous return, especially when compared to constant speed control. This was primarily due to the slave controller's ability to avoid both left and right ventricle suction. It could increase speed to fill the opposite ventricle, or decrease speed to prevent suction of the corresponding ventricle. This is an advantage over slave controllers that maintain the preload of one ventricle constant [117], as this would leave the other ventricle vulnerable to suction.

The successful MS slave system avoided pulmonary vascular congestion in all scenarios, which is one of the most difficult challenges of dual BiVAD operation [19]. Frequent speed changes that are induced by an automatic control system increase the likelihood of unbalancing systemic and pulmonary circulatory volumes. Using RVAD as slave meant that RVEDP was dependent on LVEDP. When LVAD pump speed reached the upper limit during exercise, the slave control system maintained the balance between LVEDP and RVEDP. In contrast, independent control systems increased the speed of both pumps to maximum levels in exercise, irrespective of the preload in the opposite ventricle. This resulted in the RVAD overfilling the LV. Therefore, there are clear advantages of this MS control system over dual independent Frank-Starling control systems.

Previous investigations into the MS relationship between LVAD and RVAD have assumed that the LVAD should be the master, without providing experimental evidence [175]. In this study, we compared both left/right and right/left MS configurations for our system. The left/right MS combination produced the fewest suction events and the lowest risk of pulmonary congestion, thus verifying the previous assumption. The Frank-Starling relationship between RVADQ and RVEDP for the right/left MS system was not sensitive enough at low preloads, resulting in an increase in suction events. Additionally, the support capacity of the LVAD during exercise was limited once the maximum LVAD speed was reached. This led to excessive LVEDP which is indicative of pulmonary congestion. Therefore there are obvious benefits to using the LVAD as the master.

In our study, the RVAD outflow cannula was not restricted, thus the RVAD speed was inherently lower than the LVAD speed. However, as outlined in Chapter 2, restriction of the RVAD outflow cannula is sometimes performed in clinic in order to operate the RVAD at the design speed for LVAD use [48]. With both pumps operating at similar speeds, it is difficult to determine which pump would reach the upper limit first during the simultaneous speed increases observed in exercise. However, left/right MS control should still work in this scenario. For instance, during exercise, if RVAD speed reached the upper limit first, the LV venous return will no longer increase. The LVAD Frank-Starling control

system, which sets flow based on preload, will then maintain LVAD flow rate in response to the stable venous return. Therefore, no LV suction or RV overfilling should occur.

It is advised to keep the circulatory volume of LVAD patients higher than normal in order to reduce the likelihood of suction events[179]. This was confirmed in our study, as elevated MCP during constant speed control resulted in zero suction events. In comparison, the left/right MS control system only produced 6 suction events at a normal level of MCP by maintaining ventricular volume. This indicates that suction events can be avoided without relying on volume-loading, a clear advantage of MS over constant speed operation. Further experimentation in-vivo is required to verify this finding.

5.6 Experimental Limitations and Future Work

One of the limitations of the master/slave system is the reliance on three sensors (2 pressure and 1 flow). Currently there are no commercially available long-term implantable pressure sensors. However there are low drift sensors under development [159] which may be incorporated into LVADs in the near future. Flow probes are an available alternative, as one is incorporated into the design of the HeartAssist 5 LVAD [171]. Further investigation is required to determine whether the MS system can use flow [172] and/or pressure [110] estimation algorithms instead of sensors.

Another limitation of this study was that the only implementation technique investigated was dual PI control systems. PI controllers were used for their simplicity in their implementation and to minimise steady state error. Additionally, only a simple implementation was required to assess the feasibility of different control strategies. PID controllers may have produced a faster response, however they would have increased the number of variables for optimisation from 4 to 6, increasing the optimisation time. Additionally, PI and PID controllers are linear, while the BiVAD and circulatory system is non-linear, which means that they may not be the most optimal control implementation. More complex non-linear multivariable control approaches, such as self-organising multivariable fuzzy logic control, may offer some benefit. They have previously been used for control of anaesthesia [180]. Future work could involve investigating if there any possible benefits offered by more complex control algorithms when compared to simpler PI and PID control systems.

5.7 Conclusion and Summary

In this chapter, a novel MS control system was developed by thoroughly comparing a number of different master/slave controllers. The most successful controller combined a Frank-Starling like control system for the LVAD and a preload-matching controller for the RVAD. Under in-vitro evaluation, the MS system produced fewer suction events than constant speed control, did not cause pulmonary congestion and increased cardiac output without placing extra strain on the ventricle. This controller was more adept at balancing ventricular volumes than dual independent control systems. The LVAD was also established to be the preferred master pump instead of the RVAD, primarily due to its

improved ability to prevent pulmonary congestion. However, this control system relies on pressure and flow sensors to operate. Limitations in this experiment include only using linear PI control and only performing each test once.

6 Conclusions

The aim of this thesis was to design and evaluate a physiological control system for a dual rotary LVAD system operating as a BiVAD. You will recall that in the introduction, four objectives were devised to help meet this aim. These objectives were

- Investigate the different operating modes of dual rotary LVADs as a BiVAD that have previously been presented in literature.
- Develop an evaluation framework for in-vitro assessment of physiological control systems.
- Develop a physiological control system for a rotary LVAD control system and evaluate using the evaluation framework.
- Modify the rotary LVAD physiological control system into a BiVAD physiological control system and assess using the evaluation framework.

With respect to the first objective, a review of the literature revealed that there are three different operating modes for dual rotary LVADs that are currently used in clinic: operating the left pump at a higher speed than the right pump, operating both pumps at their design speed, and restricting the outflow diameter of the right pump. These three modes were characterised in-vitro using a mock circulation loop. It was found that the RVAD can be operated at a lower speed than the LVAD, however this may require operating the pump at a speed lower than recommended by the manufacturer (1400-1800 RPM), resulting in potential impeller instability and suboptimal washout within the device. Attempting to operate both pumps at the same speed is only possible in patients with high PVR, high LV contractility, or high RVAD outflow cannula resistance. However, if the RVAD outflow cannula is restricted to a diameter between 6.5 and 8.1 mm, suitable steady-state haemodynamics (systemic flow rate 5 $L.min^{-1}$, MAP 90mmHg and LAP less than 25mmHg) can be achieved while maintaining impeller stability and optimal device washout. RVAD speed adjustments (increase between 250 and 350 RPM for a PVR increase of 400 $dynes.s.cm^{-5}$) or outflow diameter changes (increase of 0.65mm for the same PVR increase) can accommodate for long term or transient variations in PVR, however the latter requires the use of an adjustable restriction mechanism. Due to the variable nature of heart contractility between patients and the time-varying nature of a patient's PVR, physiological control of dual rotary LVADs could be advantageous to ensure suitable cardiac outputs at all times.

With respect to the second objective, a new evaluation framework for the assessment of physiological control systems for rotary blood pumps was developed. This was required, because a review of the literature revealed that previous evaluation techniques have been inconsistent between authors, nor were they thorough enough to characterise physiological control system behaviour across a number of different scenarios. Additionally, this inconsistency makes comparison between different control systems difficult when using the literature alone. The evaluation framework developed in this thesis addresses the lack of thoroughness by simulating three common patient scenarios in a mock circulation

loop. It also involved the creation of performance metrics to provide quantifiable information about control system performance and to facilitate fast control system comparisons. The scenarios were validated against haemodynamic data presented in the literature, and it was found that perfect replication of haemodynamics was difficult without implementation of a baroreflex. However, the scenarios were still useful for evaluation of control systems because they subjected the systems to preload and afterload changes similar to those observed in clinic. The performance metrics were validated using simulations of healthy and heart failure patients, and enable fast ranking of controller performance. However, they are not easily understood at first glance and as such may not be useable beyond quick comparison of control systems.

The testing scenarios developed in this thesis were used to determine the most physiologically suitable control system for a single LVAD, which met the criteria for the third objective of this thesis. A review of the literature revealed that there has been a significant volume of research into physiological control of single rotary LVADs, but not as much in the area of dual LVAD control. Some of the findings from single LVAD control could potentially be used in the area of dual LVAD control. However, it was found that direct comparisons between controllers was not possible due to the inconsistent evaluation frameworks used by authors. Therefore a quantitative experimental comparison of a number of different control systems was performed using the testing protocol described in the previous chapter. It was found that Frank-Starling like control produced the best all-round performance, and thus was used as the basis of a dual LVAD control system in the next chapter. It produced zero suction events (compared to 0.12 s^{-1} caused by constant speed control), kept left atrial pressure below 25mmHg for nearly all of the total simulation time, and increased pump flow in exercise by 3.1 $L.min^{-1}$ (compared to 1.62 $L.min^{-1}$ with constant speed control). However, this control system does rely on the implantation of flow and pressure sensors, which are not available for long term clinical use. Additionally, some LVAD controllers were missing from the comparison stage due to insufficient information from the literature. Despite these shortcomings, it was decided that the Frank-Starling control system was suitable for adaptation into a dual LVAD physiological control system.

With respect to the final objective, a novel master/slave control system was developed which utilised the Frank-Starling control system as a foundation. A number of different combinations of master and slave were assessed using the evaluation protocol developed in this thesis. The most successful controller combined a Frank-Starling like control system for the LVAD and a preload-matching controller for the RVAD. Under in-vitro evaluation, this MS system produced fewer suction events than constant speed control, did not cause pulmonary congestion and increased cardiac output without placing extra strain on the ventricle. This controller was more adept at balancing ventricular volumes than dual independent control systems. The LVAD was also established to be the preferred master pump instead of the RVAD, primarily due to its improved ability to prevent pulmonary congestion. However,

this control system relies on pressure and flow sensors to operate. Limitations in this experiment include only using linear PI control and only performing each test once.

6.1 Thesis Contributions

Each of the four experimental chapters in this thesis contributed to the literature. Firstly, the comparison of three different operating modes for dual LVADs provided details as to which circumstances would be best suited for each of the three operating modes. Another contribution from this work was that it showed, using both in-vitro and in-vivo methods, that changes in pump speed would be required to accommodate changes in vascular resistance, something that could be achieved using a physiological control system. Secondly, this thesis highlighted the inconsistencies in the literature with respect to the evaluation of physiological control systems for rotary blood pumps, and proposed a new thorough and quantitative method of evaluating these systems. Thirdly, this quantitative evaluation protocol was used to compare nine different physiological control systems and rank their performance with respect to suction avoidance, pulmonary congestion avoidance and their ability to increase flow during exercise. This work not only validated the work done by other investigators but also provided a new perspective on previous work. The experimental evidence produced during this stage was strong enough to support the decision to adapt Frank-Starling control from single LVAD to dual LVAD control. All of these contributions led to the design and evaluation of a novel master/slave control system, which was shown to be able to balance flows in all scenarios evaluated.

6.2 Thesis Limitations

There were a number of limitations in this study. In Chapter 2, the MCL did not replicate any autoregulatory mechanisms beyond the Frank-Starling response. Additionally these autoregulatory mechanisms were potentially compromised in the in-vivo studies due to anaesthesia. This means that the behaviour of the control system may be different when used in a recovery animal or in clinic. Secondly, VentrAssist rotary LVADs were used both in-vitro and in-vivo. The VentrAssist was too large to be used as an RVAD, and had to be positioned outside the chest cavity. Additionally, the long VentrAssist inflow cannula was not ideal for RVAD support, as it had to be pushed through the RV wall, across the tricuspid valve and into the RA. Smaller pumps should be utilised for future long-term studies. The VentrAssist is also no longer used clinically, which puts into question the clinical relevance of this study. However, as it is a third generation centrifugal LVAD its behaviour is similar to that of other third generation pumps (such as the HeartWare HVAD).Thirdly, the PVR changes induced in-vivo by tying a band around the PA were not necessarily physiological. Future work should investigate whether pharmacological changes in PVR are more physiological and repeatable. Finally, only PVR changes were performed in-vitro and in-vivo, which established the need for RVAD speed control. Whilst it can be inferred that changes in SVR would require changes in LVAD speed, experimental evidence is required to verify this assumption. Finally, only one animal study was performed. More

animals are required in order to determine if the discrepancies between MCL and in-vivo results observed in this experiment are significant.

In Chapter 3, whilst the MCL offers numerous advantages over a NM, it is not as customisable and therefore limited the detail with which scenarios could be evaluated. Secondly, whilst the pressure and flow sensors were correctly offset to zero at the start of each simulation, calibration was not performed as frequently. Thirdly, the model of ventricular suction was not validated due to time constraints. Given that a previously validated suction model was used (albeit in a numerical model), it was assumed that it would give a similar response in the MCL. However, the use of pneumatic regulators and a different volume threshold may have modified the suction behaviour. Future work should incorporate validation of this suction mechanism.

In Chapter 4, the biggest limitation was that only a number of control systems were compared. Notable omissions included work by Arndt et al. [82], [83], Vollkron and colleagues [84], Choi et al. [80], [95] and Gwak et al. [86], [87]. These controllers were omitted because their complexity, in conjunction with insufficient detail of controller parameters in their published descriptions, made it difficult to implement them in this experimental setup within the time frame. Comparisons with these untested systems may require collaboration with the initial investigators in future studies. The second limitation of this study was that it was assumed that all feedback variables were measured using accurate and reliable sensors. This assumption was necessary in order to assess the efficacy of each control objective in isolation. Both pressure and flow sensors were required, and for long term use these sensors need to have high accuracy and low drift. Currently there are no commercially available pressure sensors that meet this criteria, although there are some in development [159], [160]. Flow sensors are an available alternative, as one is incorporated into the HeartAssist 5 LVAD [171]. Therefore, the assumption that sensors were available is not reflective of the current situation in clinic. Further investigation is required to determine whether the use of flow [172] and/or pressure [110] estimation algorithms instead of sensors affects the performance of these control systems. Finally, no repetition was performed of the results. The repeatability of the MCL was already established in the previous chapter, so it was assumed that repeating experiments in this chapter was redundant. However, given the benefit of hindsight, the results presented in this chapter could be held with more confidence had repetition been performed.

In Chapter 5, one limitation of this study was that the only implementation technique investigated was dual PI control systems. PI controllers were used for their simplicity in their implementation and to minimise steady state error. Additionally, only a simple implementation was required to assess the feasibility of different control strategies. PID controllers may have given a faster response, however they would have increased the number of variables for optimisation from 4 to 6, increasing the optimisation time. Additionally, PI and PID controllers are linear, while the BiVAD and circulatory system is non-linear, which means that they may not be the most optimal control implementation. More

complex non-linear multivariable control approaches, such as self-organising multivariable fuzzy logic control, previously used for control of anaesthesia [180], may offer some benefit. Another limitation is that only one heart condition was evaluated, and the constants in the controller equations were only set for that condition. No work was performed to evaluate the system for different heart contractilities.

6.3 Future Work

The following areas are ideas as to how this work could be extended in the future by other researchers. Firstly, more in-vivo studies into characterisation of the three operating modes of dual LVADs could be performed, with the aim of establishing the differences between in-vivo and in-vitro results. Secondly, the evaluation framework could be extended by the inclusion of a simulation of the baroreflex and other autoregulatory features. This would aid in advanced performance assessment of physiological control systems and provide a more realistic picture of what might happen in the clinic. Thirdly, comparison of even more controllers could be performed, not only using systems that were omitted from this thesis but also incorporating pressure and flow estimation strategies and suction detection and avoidance algorithms. Fourthly, control systems could be compared using different models of LVADs, particularly those that are currently used in clinic. Fifthly, the only control theory technique used in this thesis was proportional integral control. Given the use of fuzzy logic control in the past, future work could involve investigating the use of fuzzy logic in both single and dual LVAD Starling-like control. Sixth, the ideal time domain characteristics of physiological control systems for rotary VADs are unknown. Future work could involve characterising the time domain response of the healthy heart to changes in preload in order to set a "gold standard" for future physiological control systems to reach. Finally, a hugely novel area of future work will be to migrate physiological control system evaluation out of the laboratory and into clinical trials.

7 References

[1] "Causes of Death, Australia, 2010," Australian Bureau of Statistics, 2012.

[2] "Cardiovascular disease: Australian facts 2011.," Australian Institute of Health and Welfare, Canberra, 2011.

[3] D. Lloyd-jones, R. J. Adams, T. M. Brown, et al., "Heart Disease and Stroke Statistics — 2010 Update. A Report From the American Heart Association," *Circulation*, vol. 121, pp. e46–e215, Feb. 2010.

[4] P. A. Heidenreich, J. G. Trogdon, O. A. Khavjou, et al., "Forecasting the Future of Cardiovascular Disease in the United States: A Policy Statement From the American Heart Association," *Circulation*, vol. 132, no. 8, pp. 933–944, Mar. 2011.

[5] L. Excel, V. Marion, K. Hurst, et al., "Australia and New Zealand Organ Donation Registry 2012 Report," Adelaide, SA, 2012.

[6] E. Rose, A. Gelijns, A. Moskowitz, et al., "Long-Term Use of A Left Ventricular Assist Device for End Stage Heart Failure," *N Engl J Med*, vol. 345, no. 20, pp. 1435–1443, 2001.

[7] R. E. Hershberger, D. Nauman, T. L. Walker, et al., "Care processes and clinical outcomes of continuous outpatient support with inotropes (COSI) in patients with refractory endstage heart failure.," *J. Card. Fail.*, vol. 9, no. 3, pp. 180–187, Jun. 2003.

[8] A. Shiose, K. Nowak, D. J. Horvath, et al., "Speed modulation of the continuous-flow total artificial heart to simulate a physiologic arterial pressure waveform.," *ASAIO J.*, vol. 56, no. 5, pp. 403–409, May 2010.

[9] M. S. Slaughter, J. G. Rogers, C. A. Milano, et al., "Advanced Heart Failure Treated with Continuous-Flow Left Ventricular Assist Device," *N Engl J Med*, vol. 361, no. 23, pp. 2241–2251, Dec. 2009.

[10] S. G. Drakos, L. Janicki, B. D. Horne, et al., "Risk Factors Predictive of Right Ventricular Failure After Left Ventricular Assist Device Implantation," *Am J Cardiol*, vol. 105, no. 7, pp. 1030–1035, 2010.

[11] J. R. Fitzpatrick, J. R. Frederick, W. Hiesinger, et al., "Early Planned Institution of Biventricular Mechanical Circulatory Support Results in Improved Outcomes Compared with Delayed Conversion of a Left Ventricular Assist Device to a Biventricular Assist Device," *J Thorac Cardiovasc Surg*, vol. 137, no. 4, pp. 971–977, 2009.

[12] R. L. Kormos, J. J. Teuteberg, F. D. Pagani, et al., "Right ventricular failure in patients with the HeartMate II continuous-flow left ventricular assist device: incidence, risk factors, and effect on outcomes.," *J. Thorac. Cardiovasc. Surg.*, vol. 139, no. 5, pp. 1316–24, May 2010.

[13] J. C. Matthews, T. M. Koelling, F. D. Pagani, et al., "The Right Ventricular Failure Risk Score: A Pre-Operative Tool for Assessing the Risk of Right Ventricular Failure in Left Ventricular Assist Device Candidates," *J Am Coll Cardiol*, vol. 51, no. 22, pp. 2163–2172, 2008.

[14] E. V Potapov, A. Loforte, Y. Weng, et al., “Experience with over 1000 Implanted Ventricular Assist Devices,” *J Card Surg*, vol. 23, no. 3, pp. 185–194, 2008.

[15] S. Lee, F. Kamdar, R. Madlon-Kay, et al., “Effects of the HeartMate II Continuous-Flow Left Ventricular Assist Device on RV Function,” *J. Hear. Lung Transplant.*, vol. 29, no. 2, pp. 209–15, Sep. 2010.

[16] T. Krabatsch, E. Potapov, A. Stepanenko, et al., “Biventricular circulatory support with two miniaturized implantable assist devices,” *Circulation*, vol. 124, no. 11, pp. S179–S186, Sep. 2011.

[17] T. Krabatsch, E. Hennig, A. Stepanenko, et al., “Evaluation of the HeartWare HVAD centrifugal pump for right ventricular assistance in an in vitro model.,” *ASAIO J.*, vol. 57, no. 3, pp. 183–187, Mar. 2011.

[18] S. Saito, T. Sakaguchi, S. Miyagawa, et al., “Biventricular support using implantable continuous-flow ventricular assist devices,” *J. Hear. Lung Transplant.*, vol. 30, no. 4, pp. 475–478, Apr. 2011.

[19] S. Saito, T. Sakaguchi, and Y. Sawa, “Clinical report of long-term support with dual Jarvik 2000 biventricular assist device,” *J. Hear. Lung Transplant.*, vol. 30, no. 7, pp. 845–847, Jul. 2011.

[20] A. C. Guyton, *Textbook of Medical Physiology*. London: W.B. Saunders, 1971.

[21] R. E. Klabunde, *Cardiovascular Physiology Concepts*. Baltimore: Lippincott Williams & Wilkins, 2004.

[22] D. Timms, “A review of clinical ventricular assist devices.,” *Med. Eng. Phys.*, vol. 33, no. 9, pp. 1041–1047, Nov. 2011.

[23] “Human Circulatory System,” *Revision World*, [Online]. Available: http://revisionworld.co.uk/a2-level-level-revision/biology/physiology-transport/human-circulatory-system. .

[24] E. H. Starling and M. B. Visscher, “The regulation of the energy output of the heart,” *J. Physiol.*, vol. 62, no. 3, pp. 243–261, Mar. 1927.

[25] S. Akselrod, O. Oz, M. Greenberg, et al., “Autonomic response to change of posture among normal and mild-hypertensive adults: Investigation by time-dependent spectral analysis,” *J. Auton. Nerv. Syst.*, vol. 64, no. 1, pp. 33–43, 1997.

[26] S. H. Kubo and R. J. Cody, “Circulatory autoregulation in chronic congestive heart failure: Responses to head-up tilt in 41 patients,” *Am. J. Cardiol.*, vol. 52, no. 5, pp. 512–518, 1983.

[27] A. Kantrowitz, “Origins of intraaortic balloon pumping,” *Ann. Thorac. Surg.*, vol. 50, no. 4, pp. 672–674, Oct. 1990.

[28] M. Krishna and K. Zacharowski, “Principles of intra-aortic balloon pump counterpulsation,” *Contin. Educ. Anaesthesia, Crit. Care Pain*, vol. 9, no. 1, pp. 24–28, Feb. 2009.

[29] H. Parissis, A. Soo, and B. Al-Alao, “Intra aortic balloon pump: literature review of risk factors related to complications of the intraaortic balloon pump.,” *J. Cardiothorac. Surg.*, vol. 6, no. 1, p. 147, Jan. 2011.

[30] O. H. Frazier, R. D. Dowling, L. A. Gray Jr, et al., “The total artificial heart: Where we stand,” *Cardiology*, vol. 101, no. 1–3, pp. 117–121, 2004.

[31] H. Tsukui, J. J. Teuteberg, S. Murali, et al., “Biventricular assist device utilization for patients with morbid congestive heart failure: a justifiable strategy.,” *Circulation*, vol. 112, no. 9 Suppl, pp. I65–72, Aug. 2005.

[32] T. Yamane, “The Present and Future State of Nonpulsatile Artificial Heart Technology,” *J Artif Organs*, vol. 5, pp. 149–155, 2002.

[33] R. J. Gordon, B. Quagliarello, and F. D. Lowy, “Ventricular assist device-related infections.,” *Lancet Infect. Dis.*, vol. 6, no. 7, pp. 426–437, Jul. 2006.

[34] E. J. Birks, M. H. Yacoub, N. R. Banner, et al., “The role of bridge to transplantation: should LVAD patients be transplanted?,” *Curr. Opin. Cardiol.*, vol. 19, no. 2, pp. 148–153, Mar. 2004.

[35] T. J. Myers, T. Khan, and O. H. Frazier, “Infection Complications Associated with Ventricular Assist Systems,” *ASAIO J*, vol. 46, no. 6, pp. S28–S36, 2000.

[36] T. W. Costantini, J. H. Taylor, and G. J. Beilman, “Abdominal complications of ventricular assist device placement.,” *Surg. Infect. (Larchmt).*, vol. 6, no. 4, pp. 409–418, Jan. 2005.

[37] L. W. Miller, F. D. Pagani, S. D. Russell, et al., “Use of a continuous-flow device in patients awaiting heart transplantation.,” *N Engl J Med*, vol. 357, no. 9, pp. 885–896, Aug. 2007.

[38] F. D. Pagani, L. W. Miller, S. D. Russell, et al., “Extended mechanical circulatory support with a continuous-flow rotary left ventricular assist device.,” *J. Am. Coll. Cardiol.*, vol. 54, no. 4, pp. 312–321, Jul. 2009.

[39] A. McDiarmid, B. Gordon, N. Wrightson, et al., “Hemodynamic, Echocardiographic, and Exercise-Related Effects of the HeartWare Left Ventricular Assist Device in Advanced Heart Failure.,” *Congest. Heart Fail.*, vol. 19, no. 1, pp. 11–15, Jan. 2013.

[40] R. Krishnamani, D. DeNofrio, and M. A. Konstam, “Emerging ventricular assist devices for long-term cardiac support,” *Nat Rev Cardiol*, vol. 7, no. 2, pp. 71–76, 2010.

[41] N. Moazami, K. Fukamachi, M. Kobayashi, et al., “Axial and centrifugal continuous-flow rotary pumps: a translation from pump mechanics to clinical practice.,” *J. Hear. Lung Transplant.*, vol. 32, no. 1, pp. 1–11, Jan. 2013.

[42] D. P. Mulloy, C. M. Bhamidipati, M. L. Stone, et al., “Orthotopic heart transplant versus left ventricular assist device: A national comparison of cost and survival.,” *J. Thorac. Cardiovasc. Surg.*, vol. 145, no. 2, pp. 566–574, Feb. 2013.

[43] S. Westaby, O. H. Frazier, and A. Banning, “Six Years of Continuous Mechanical Circulatory Support,” *N Engl J Med*, vol. 355, pp. 325–327, 2006.

[44] D. Timms, J. Fraser, M. Hayne, et al., “The BiVACOR Rotary Biventricular Assist Device: Concept and In Vitro Investigation,” *Artif. Organs*, vol. 32, no. 10, pp. 816–819, 2008.

[45] D. Saeed, S. Shalli, H. Fumoto, et al., “In Vivo Evaluation of Zirconia Ceramic in the DexAide Right Ventricular Assist Device Journal Bearing,” *Artif Organs*, vol. 34, no. 6, pp. 512–516, 2010.

[46] O. H. Frazier, T. J. Myers, and I. Gregoric, “Biventricular assistance with the Jarvik FlowMaker: a case report.,” *J. Thorac. Cardiovasc. Surg.*, vol. 128, no. 4, pp. 625–626, 2004.

[47] M. Strueber, A. L. Meyer, D. Malehsa, et al., “Successful use of the HeartWare HVAD rotary blood pump for biventricular support,” *J Thorac Cardiovasc Surg*, vol. 140, no. 4, pp. 936–937, 2010.

[48] R. Hetzer, T. Krabatsch, A. Stepanenko, et al., “Long-term biventricular support with the heartware implantable continuous flow pump.,” *J Hear. Lung Transpl.*, vol. 29, no. 7, pp. 822–824, 2010.

[49] E. C. McGee, U. Ahmad, D. Tamez, et al., “Biventricular Continuous Flow VADs Demonstrate Diurnal Flow Variation and Lead to End-Organ Recovery,” *Ann. Thorac. Surg.*, vol. 92, no. 1, pp. e1–3, Jul. 2011.

[50] J. N. Kirkpatrick, S. E. Wiegers, J. E. Rame, et al., “Imaging Use of Echocardiography to Optimize Left Ventricular Assist Devices,” *US Cardiol.*, vol. 7, no. 2, pp. 11–15, 2010.

[51] R. F. Salamonsen, D. G. Mason, and P. J. Ayre, “Response of rotary blood pumps to changes in preload and afterload at a fixed speed setting are unphysiological when compared with the natural heart.,” *Artif Organs*, vol. 35, no. 3, pp. E47–53, Mar. 2011.

[52] K. Fukamachi, A. Shiose, A. Massiello, et al., “Preload sensitivity in cardiac assist devices.,” *Ann. Thorac. Surg.*, vol. 95, no. 1, pp. 373–80, Jan. 2013.

[53] K. Reesink, A. Dekker, T. Van der Nagel, et al., “Suction Due to Left Ventricular Assist: Implications for Device Control and Management,” *Artif Organs*, vol. 31, no. 7, pp. 542–549, 2007.

[54] A. Tanaka, M. Yoshizawa, P. Olegario, et al., “Detection and Avoiding Ventricular Suction of Ventricular Assist Devices,” 2005, pp. 402–405.

[55] M. Vollkron, H. Schima, L. Huber, et al., “Development of a Suction Detection System for Axial Blood Pumps,” *Artif Organs*, vol. 28, no. 8, pp. 709–716, 2004.

[56] M. Vollkron, P. Voitl, J. Ta, et al., “Suction events during left ventricular support and ventricular arrhythmias.,” *J. Hear. Lung Transplant.*, vol. 26, no. 8, pp. 819–25, Aug. 2007.

[57] T. N. H. Drews, M. Loebe, M. J. Jurmann, et al., “Outpatients on mechanical circulatory support.,” *Ann. Thorac. Surg.*, vol. 75, no. 3, pp. 780–5; discussion 785, Mar. 2003.

[58] T. Krabatsch, M. Schweiger, A. Stepanenko, et al., “Mechanical circulatory support-results, developments and trends.,” *J. Cardiovasc. Transl. Res.*, vol. 4, no. 3, pp. 332–339, Jun. 2011.

[59] J. R. Boston, J. F. Antaki, and M. A. Simaan, “Hierarchical control of heart-assist devices,” *Robot. Autom. Mag. IEEE*, vol. 10, no. 1, pp. 54–64, 2003.

[60] E. Lim, S. Dokos, S. L. Cloherty, et al., “Parameter-optimized model of cardiovascular-rotary blood pump interactions,” *IEEE Trans. Biomed. Eng.*, vol. 57, no. 2, pp. 254–266, 2010.

[61] H. Suga, K. Sagawa, and a. a. Shoukas, “Load Independence of the Instantaneous Pressure-Volume Ratio of the Canine Left Ventricle and Effects of Epinephrine and Heart Rate on the Ratio,” *Circ. Res.*, vol. 32, no. 3, pp. 314–322, Mar. 1973.

[62] H. Suga and K. Sagawa, “Instantaneous Pressure-Volume Relationships and Their Ratio in the Excised, Supported Canine Left Ventricle,” *Circ. Res.*, vol. 35, no. 1, pp. 117–126, Jul. 1974.

[63] H. Suga and K. Sagawa, “Models of Cardiac Contraction,” *Simulation*, vol. 27, no. 5, pp. 181–184, Nov. 1976.

[64] S. D. Gregory, M. J. Pearcy, J. Fraser, et al., “Evaluation of Inflow Cannulation Site for Implantation of Right-Sided Rotary Ventricular Assist Device.,” *Artif. Organs*, vol. 37, no. 8, pp. 704–711, 2013.

[65] W.-K. Chan and Y.-W. Wong, “A Review of Leakage Flow in Centrifugal Blood Pumps,” *Artif Organs*, vol. 30, no. 5, pp. 354–359, 2006.

[66] T. Deuse, J. Schirmer, M. Kubik, et al., “Isolated permanent right ventricular assistance using the HVAD continuous-flow pump.,” *Ann. Thorac. Surg.*, vol. 95, no. 4, pp. 1434–1436, 2013.

[67] M. Kindo, B. Radovancevic, I. D. Gregoric, et al., “Biventricular Support With the Jarvik 2000 Ventricular Assist Device in a Calf Model of Pulmonary Hypertension,” *ASAIO J*, vol. 50, no. 5, pp. 444–450, 2004.

[68] B. Radovancevic, I. D. Gregoric, D. Tamez, et al., “Biventricular Support with the Jarvik 2000 Axial Flow Pump: A Feasibility Study,” *ASAIO J*, vol. 49, no. 5, pp. 604–607, 2003.

[69] T. Krabatsch, A. Stepanenko, M. Schweiger, et al., “Alternative technique for implantation of biventricular support with HeartWare implantable continuous flow pump.,” *ASAIO J*, vol. 57, no. 4, pp. 333–335, 2011.

[70] J. K. Kirklin, D. C. Naftel, R. L. Kormos, et al., “Second INTERMACS annual report: more than 1,000 primary left ventricular assist device implants.,” *J Hear. Lung Transpl*, vol. 29, no. 1, pp. 1–10, 2010.

[71] A. Loforte, P. L. Della Monica, A. Montalto, et al., “HeartWare third-generation implantable continuous flow pump as biventricular support: mid-term follow-up.,” *Interact. Cardiovasc. Thorac. Surg.*, vol. 12, no. 3, pp. 458–460, 2011.

[72] A. Loforte, A. Montalto, P. L. Della Monica, et al., “Biventricular support with the HeartWare implantable continuous flow pump: an additional contribution.,” *J. Hear. Lung Transplant.*, vol. 29, no. 12, pp. 1443–1444, Dec. 2010.

[73] D. Timms, E. Gude, N. Gaddum, et al., “Assessment of right pump outflow banding and speed changes on pulmonary hemodynamics during biventricular support with two rotary left ventricular assist devices.,” *Artif Organs*, vol. 35, no. 8, pp. 807–813, 2011.

[74] D. L. Timms, S. D. Gregory, N. A. Greatrex, et al., “A compact mock circulation loop for the in vitro testing of cardiovascular devices.,” *Artif Organs*, vol. 35, no. 4, pp. 384–391, 2011.

[75] S. Gregory, N. Greatrex, D. Timms, et al., “Simulation and Enhancement of a Cardiovascular Device Test Rig,” *J. Simul.*, vol. 4, pp. 34–41, 2010.

[76] S. D. Gregory, M. Stevens, D. Timms, et al., “Replication of the Frank-Starling response in a mock circulation loop.,” in *Annual International Conference of the IEEE Engineering in Medicine and Biology Society*, Boston, MA, 2011, vol. 2011, pp. 6825–6828.

[77] A. C. Guyton and J. E. Hall, *Textbook of Medical Physiology*. Philadelphia, Pennsylvania: Elseiver Inc., 2006.

[78] A. C. Guyton and A. W. Lindsey, “Effect of Elevated Left Atrial Pressure and Decreased Plasma Protein Concentration on the Development of Pulmonary Edema,” *Circ. Res.*, vol. 7, no. 4, pp. 649–657, Jul. 1959.

[79] A. F. Corno, P. Fridez, L. K. von Segesser, et al., “A new implantable device for telemetric control of pulmonary blood flow.,” *Interact. Cardiovasc. Thorac. Surg.*, vol. 1, no. 1, pp. 46–49, 2002.

[80] S. Choi, J. E. Antaki, R. Boston, et al., “A sensorless approach to control of a turbodynamic left ventricular assist system,” *IEEE Trans. Control Syst. Technol.*, vol. 9, no. 3, pp. 473–482, 2001.

[81] S. Choi, J. R. Boston, and J. F. Antaki, “Hemodynamic Controller for Left Ventricular Assist Device Based on Pulsatility Ratio,” *Artif Organs*, vol. 31, no. 2, pp. 114–125, 2007.

[82] A. Arndt, P. Nüsser, K. Graichen, et al., “Physiological Control of a Rotary Blood Pump With Selectable Therapeutic Options: Control of Pulsatility Gradient,” *Artif Organs*, vol. 32, no. 10, pp. 761–771, 2008.

[83] A. Arndt, P. Nüsser, and B. Lampe, “Fully Autonomous Preload-Sensitive Control of Implantable Rotary Blood Pumps,” *Artif Organs*, vol. 34, no. 9, pp. 726–735, 2010.

[84] M. Vollkron, H. Schima, L. Huber, et al., “Development of a reliable automatic speed control system for rotary blood pumps,” *J Hear. Lung Transpl*, vol. 24, no. 11, pp. 1878–1885, 2005.

[85] K.-W. Gwak, M. Ricci, S. Snyder, et al., “In vitro evaluation of multiobjective hemodynamic control of a heart-assist pump,” *ASAIO J*, vol. 51, no. 4, pp. 329–335, 2005.

[86] K.-W. Gwak, “Application of extremum seeking control to turbodynamic blood pumps.,” *ASAIO J.*, vol. 53, no. 4, pp. 403–409, 2007.

[87] K.-W. Gwak, J. F. Antaki, B. E. Paden, et al., “Safety-enhanced optimal control of turbodynamic blood pumps.,” *Artif. Organs*, vol. 35, no. 7, pp. 725–32, Jul. 2011.

[88] S. Weber, K. Doi, A. L. Massiello, et al., “In Vitro Controllability of the MagScrew Total Artificial Heart System,” *ASAIO J*, vol. 48, no. 6, pp. 606–611, 2002.

[89] N. R. Gaddum, D. L. Timms, M. Stevens, et al., “Comparison of Preload-Sensitive Pressure and Flow Controller Strategies for a Dual Device Biventricular Support System,” *Artif Organs*, vol. 36, no. 3, pp. 256–265, 2012.

[90] S. D. Gregory, D. Timms, N. R. Gaddum, et al., “In vitro evaluation of a compliant inflow cannula reservoir to reduce suction events with extracorporeal rotary ventricular assist device support.,” *Artif. Organs*, vol. 35, no. 8, pp. 765–72, Aug. 2011.

[91] F. Moscato, M. Arabia, F. M. Colacino, et al., “Left Ventricle Afterload Impedance Control by an Axial Flow Ventricular Assist Device: A Potential Tool for Ventricular Recovery,” *Artif Organs*, vol. 34, no. 9, pp. 736–744, 2010.

[92] T. Waters, P. Allaire, G. Tao, et al., “Motor Feedback Physiological Control for a Continuous Flow Ventricular Assist Device,” *Artif Organs*, vol. 23, no. 6, pp. 480–486, 1999.

[93] Y. Wu, P. Allaire, G. Tao, et al., “An Advanced Physiological Controller Design for a Left Ventricular Assist Device to Prevent Left Ventricular Collapse,” *Artif Organs*, vol. 27, no. 10, pp. 926–930, 2003.

[94] F. Casas, A. Orozco, W. A. Smith, et al., “A fuzzy system cardio pulmonary bypass rotary blood pump controller,” *Expert Syst. Appl.*, vol. 26, no. 3, pp. 357–361, 2004.

[95] S. Choi, J. R. Boston, and J. F. Antaki, “An investigation of the pump operating characteristics as a novel control index for LVAD control,” *Int. J. Control. Autom. Syst.*, vol. 3, no. 1, pp. 100–108, 2005.

[96] A. Ferreira, J. R. Boston, and J. F. Antaki, “A Control System for Rotary Blood Pumps Based on Suction Detection,” *IEEE Trans. Biomed. Eng.*, vol. 56, no. 3, pp. 656–665, 2009.

[97] H. Nishida, T. Nishinaka, M. Endo, et al., “Clinical Application of a Newly Developed Autoflow Control System for the Terumo Centrifugal Pump: From External Control to Built-in Direct Control,” *Artif. Organs*, vol. 20, no. 6, pp. 625–631, 1996.

[98] K. Ohuchi, D. Kikugawa, K. Takahashi, et al., “Control Strategy for Rotary Blood Pumps,” *Artif Organs*, vol. 25, no. 5, pp. 366–370, 2001.

[99] M. A. Simaan, A. Ferreira, C. Shaohi, et al., “A Dynamical State Space Representation and Performance Analysis of a Feedback-Controlled Rotary Left Ventricular Assist Device,” *IEEE Trans. Control Syst. Technol.*, vol. 17, no. 1, pp. 15–28, Jan. 2009.

[100] K. Gwak, M. Ricci, S. Snyder, et al., “In vitro evaluation of multiobjective hemodynamic control of a heart-assist pump,” *ASAIO J*, vol. 51, no. 4, pp. 329–335, 2005.

[101] R. Kosaka, K. Yanagi, T. Sato, et al., “Operating Point Control System for a Continuous Flow Artificial Heart:In Vitro Study,” *ASAIO J.*, vol. 49, no. 3, pp. 259–264, May 2003.

[102] H. A. Khalil, D. T. Kerr, M. A. Franchek, et al., “Continuous flow total artificial heart: modeling and feedback control in a mock circulatory system.,” *ASAIO J*, vol. 54, no. 3, pp. 249–55, 2008.

[103] G. Faragallah, Y. Wang, E. Divo, et al., “A new control system for left ventricular assist devices based on patient-specific physiological demand,” *Inverse Probl. Sci. Eng.*, vol. 20, no. 5, pp. 721–734, 2012.

[104] Y. Wang, G. Faragallah, E. Divo, et al., “Feedback control of a rotary left ventricular assist device supporting a failing cardiovascular system,” in *American Control Conference*, 2012, no. 3, pp. 1137–1142.

[105] Y. Wu, P. Allaire, G. Tao, et al., “Modeling, Estimation and Control of Cardiovascular Systems with a Left Ventricular Assist Device,” Portland, 2005, pp. 3841–3846.

[106] G. A. Giridharan and M. Skliar, “Control Strategy for Maintaining Physiological Perfusion with Rotary Blood Pumps,” *Artif Organs*, vol. 27, no. 7, pp. 639–648, 2003.

[107] Y. Chang and B. Gao, “A global sliding mode controller design for an intra-aorta pump.,” *ASAIO J.*, vol. 56, no. 6, pp. 510–6, 2010.

[108] T. Beppu, K. Seo, Y. Imai, et al., “An Automatic Flow Controller for a Centrifugal Blood Pump,” *Artif Organs*, vol. 21, no. 7, pp. 630–634, 1997.

[109] E. Lim, A.-H. H. Alomari, A. V Savkin, et al., “A method for control of an implantable rotary blood pump for heart failure patients using noninvasive measurements.,” *Artif. Organs*, vol. 35, no. 8, pp. E174–E180, Aug. 2011.

[110] A.-H. H. Alomari, A. V Savkin, P. J. Ayre, et al., “Non-invasive estimation and control of inlet pressure in an implantable rotary blood pump for heart failure patients.,” *Physiol. Meas.*, vol. 32, no. 8, pp. 1035–1060, 2011.

[111] L. A. Baloa, J. R. Boston, M. A. Simaan, et al., “Control of rotary heart assist devices,” in *Proceedings of the 2000 American Control Conference. ACC (IEEE Cat. No.00CH36334)*, 2000, vol. 5, pp. 2982–2986.

[112] G. A. Giridharan, G. M. Pantalos, K. J. Gillars, et al., “Physiologic Control of Rotary Blood Pumps: An In Vitro Study,” *ASAIO J.*, vol. 50, no. 5, pp. 403–409, 2004.

[113] Y. Wu, “Adaptive Physiological Speed/Flow Control of Rotary Blood Pumps in Permanent Implantation Using Intrinsic Pump Parameters,” *ASAIO J*, vol. 55, no. 4, pp. 335–339, 2009.

[114] D. M. Karantonis, E. Lim, D. G. Mason, et al., “Noninvasive Activity-based Control of an Implantable Rotary Blood Pump: Comparative Software Simulation Study,” *Artif. Organs*, vol. 34, no. 2, pp. E34–E45–E34–E45, 2010.

[115] E. Bullister, S. Reich, and J. Sluetz, “Physiologic control algorithms for rotary blood pumps using pressure sensor input,” *Artif Organs*, vol. 26, no. 11, pp. 931–938, 2002.

[116] Y. Wu, P. E. Allaire, T. Gang, et al., “Modeling, Estimation, and Control of Human Circulatory System With a Left Ventricular Assist Device,” *Control Syst. Technol. IEEE Trans.*, vol. 15, no. 4, pp. 754–767, 2007.

[117] P. S. Olegario, M. Yoshizawa, A. Tanaka, et al., “Outflow Control for Avoiding Atrial Suction in a Continuous Flow Total Artificial Heart,” *Artif Organs*, vol. 27, no. 1, pp. 92–98, 2003.

[118] R. Kosaka, K. Yanagi, T. Sato, et al., “Operating Point Control System for a Continuous Flow Artificial Heart:In Vitro Study,” *ASAIO J.*, vol. 49, no. 3, pp. 259–264, May 2003.

[119] G. Endo, K. Araki, M. Oshikawa, et al., “A Safe Automatic Driving Method for a Continuous Flow Ventricular Assist Device Based on Motor Current Pulsatility:In Vitro Evaluation,” *ASAIO J*, vol. 48, pp. 83–89, 2002.

[120] F. Casas, N. Ahmed, and A. Reeves, “Minimal sensor count approach to fuzzy logic rotary blood pump flow control.,” *ASAIO J*, vol. 53, no. 2, pp. 140–146, 2007.

[121] K. Nishimura, T. Tsukiya, T. Akamatsu, et al., “Control of the pressure flow relationship with a magnetically suspended centrifugal pump in a chronic animal experiment.,” *ASAIO J*, vol. 43, no. 5, pp. M553–M556, 1997.

[122] G. Endo, K. Araki, M. Oshikawa, et al., “Control Strategy for Biventricular Assistance with Mixed-Flow Pumps,” *Artif Organs*, vol. 24, no. 8, pp. 594–599, 2000.

[123] G. A. Giridharan, M. Skliar, D. B. Olsen, et al., “Modeling and control of a brushless DC axial flow ventricular assist device.,” *ASAIO J.*, vol. 48, no. 3, pp. 272–289, 2002.

[124] Y. Chang and B. Gao, “A global sliding mode controller design for an intra-aorta pump.,” *ASAIO J*, vol. 56, no. 6, pp. 510–516, 2010.

[125] A. SmartMotion, (2010, September 29), “Tuning Analysis Tools: Step and Frequency Response,” *Adept SmartMotion Developer’s Guide*, [Online]. Available: http://www1.adept.com/main/ke/data/controller/smartmotion_developer/TH_Tuning.html. .

[126] D. Saeed, A. L. Massiello, S. Shalli, et al., “Introduction of fixed-flow mode in the DexAide right ventricular assist device,” *J. Hear. Lung Transplant.*, vol. 29, no. 1, pp. 32–36, 2010.

[127] R. F. Salamonsen, E. Lim, N. Gaddum, et al., “Theoretical Foundations of a Starling-Like Controller for Rotary Blood Pumps.,” *Artif Organs*, vol. 36, no. 9, pp. 787–796, 2012.

[128] N. R. Gaddum, M. C. Stevens, E. Lim, et al., “Starling-like Flow Control of a Left Ventricular Assist Device; In Vitro Validation,” *Artif Organs*, vol. 38, no. 3, pp. E46–56, Mar. 2014.

[129] M. Nakamura, T. Masuzawa, E. Tatsumi, et al., “The Development of a Control Method for a Total Artficial Heart Using Mixed Venous Oxygen Saturation,” *Artif Organs*, vol. 23, no. 3, pp. 235–241, 1999.

[130] H. Schima, M. Vollkron, U. Jantsch, et al., “First clinical experience with an automatic control system for rotary blood pumps during ergometry and right-heart catheterization.,” *J. Heart Lung Transplant.*, vol. 25, no. 2, pp. 167–173, Feb. 2006.

[131] D. L. Timms, M. Hayne, A. Galbraith, et al., “A Complete Mock Circulation Loop for the Evaluation of Left- Right- and Bi- Ventricular Assist Devices,” *Artif Organs*, vol. 29, no. 7, pp. 564–571, 2005.

[132] M. J. Zema, B. Restivo, T. Sos, et al., “Left ventricular dysfunction--bedside Valsalva manoeuvre,” *Br. Heart J.*, vol. 44, no. 5, pp. 560–569, 1980.

[133] K. Lu, J. W. Clark, F. H. Ghorbel, et al., “A human cardiopulmonary system model applied to the analysis of the Valsalva maneuver,” *Am J Physiol Hear. Circ Physiol*, vol. 281, no. 6, pp. H2661–H2679, 2001.

[134] L. Compostella, N. Russo, T. Setzu, et al., “Exercise Performance of Chronic Heart Failure Patients in the Early Period of Support by an Axial-Flow Left Ventricular Assist Device as Destination Therapy.,” *Artif. Organs*, vol. 38, no. 5, pp. 366–373, May 2013.

[135] R. F. Salamonsen, V. Pellegrino, J. F. Fraser, et al., “Exercise studies in patients with rotary blood pumps: cause, effects, and implications for starling-like control of changes in pump flow.,” *Artif. Organs*, vol. 37, no. 8, pp. 695–703, Aug. 2013.

[136] M. Vollkron, H. Schima, L. Huber, et al., “Interaction of the cardiovascular system with an implanted rotary assist device: simulation study with a refined computer model,” *Artif Organs*, vol. 26, no. 4, pp. 349–359, 2002.

[137] R. Drake and M. Doursout, “Pulmonary edema and elevated left atrial pressure: four hours and beyond,” *Physiology*, vol. 17, pp. 223–226, 2002.

[138] J. W. Crowell, “Mechanical and Physiological Aspects,” in *Practice of Medicine*, 6th ed., J. A. Spittel, Ed. Hagerstown: Harper & Row, 1979, p. 39.

[139] E. Lim, “Characterization of cardiovascular-rotary blood pump interaction,” UNSW, Sydney, 2010.

[140] K. Meyer, R. Hajric, S. Westbrook, et al., “Hemodynamic responses during leg press exercise in patients with chronic congestive heart failure,” *Am. J. Cardiol.*, vol. 83, no. 11, pp. 1537–1543, 1999.

[141] H. E. Refsum, J. Eritsland, and O. K. Müller, “Excessive exercise ventilation in moderate left heart dysfunction. Influence of postural changes in central haemodynamics and blood gases.,” *Clin. Physiol.*, vol. 21, no. 2, pp. 141–149, Mar. 2001.

[142] L. Jacquet, O. Vancaenegem, A. Pasquet, et al., “Exercise capacity in patients supported with rotary blood pumps is improved by a spontaneous increase of pump flow at constant pump speed and by a rise in native cardiac output.,” *Artif. Organs*, vol. 35, no. 7, pp. 682–690, Jul. 2011.

[143] D. Mancini, R. Goldsmith, H. Levin, et al., “Comparison of Exercise Performance in Patients With Chronic Severe Heart Failure Versus Left Ventricular Assist Devices,” *Circulation*, vol. 98, no. 12, pp. 1178–1183, Sep. 1998.

[144] J. Gibbs, J. Keegan, C. Wright, et al., “Pulmonary artery pressure and activities in chronic heart failure,” *J. Am. Coll. Cardiol.*, vol. 15, no. 1, pp. 52–61, 1990.

[145] D. Raeside, G. Chalmers, and J. Clelland, “Pulmonary artery pressure variation in patients with connective tissue disease: 24 hour ambulatory pulmonary artery pressure monitoring,” *Thorax*, vol. 53, no. 10, pp. 857–862, Oct. 1998.

[146] G. M. Felker, P. S. Cuculich, and M. Gheorghiade, “The Valsalva maneuver: a bedside ‘biomarker’ for heart failure.,” *Am. J. Med.*, vol. 119, no. 2, pp. 117–122, Feb. 2006.

[147] K. H. Ang, G. Chong, and Y. Li, “PID control system analysis, design, and technology,” *IEEE Trans. Control Syst. Technol.*, vol. 13, no. 4, pp. 559–576, Jul. 2005.

[148] N. S. Nise, “Design via Root Locas,” in *Control Systems Engineering*, 6th ed., Hoboken, NJ: John Wiley and Sons, Inc., 1996, pp. 482–486.

[149] D. McNeill and P. Freiberger, *Fuzzy Logic*. New York: Simon & Schuster, 1993.

[150] E. Mamdani, “Application of fuzzy logic to approximate reasoning using linguistic synthesis,” *Comput. IEEE Trans.*, vol. C–26, no. 12, pp. 1182–1191, Dec. 1977.

[151] J. A. LaRose, D. Tamez, M. Ashenuga, et al., “Design concepts and principle of operation of the heartware ventricular assist system,” *ASAIO J*, vol. 56, no. 4, pp. 285–289, 2010.

[152] G. A. Giridharan and M. Skliar, “Control Strategy for Maintaining Physiological Perfusion with Rotary Blood Pumps,” *Artif. Organs*, vol. 27, no. 7, pp. 639–648, 2003.

[153] G. A. Giridharan, S. C. Koenig, M. Mitchell, et al., “A Computer Model of the Pediatric Circulatory System for Testing Pediatric Assist Devices,” *ASAIO J*, vol. 53, no. 1, pp. 74–81, 2007.

[154] G. A. Giridharan and M. Skliar, “Nonlinear Controller for Ventricular Assist Devices,” *Artif Organs*, vol. 26, no. 11, pp. 980–984, 2002.

[155] G. A. Giridharan and M. Skliar, “Physiological Control of Blood Pumps Using Intrinsic Pump Parameters: A Computer Simulation Study,” *Artif. Organs*, vol. 30, no. 4, pp. 301–307, 2006.

[156] G. Giridharan, G. Pantalos, S. Koenig, et al., “Achieving physiologic perfusion with ventricular assist devices: comparison of control strategies,” in *Proceedings of the 2005 American Control Conference*, Portland, OR, 2005, pp. 3823–3828 vol. 6.

[157] E. Bullister, S. Reich, P. D’Entremont, et al., “A Blood Pressure Sensor for Long-Term Implantation,” *Artif Organs*, vol. 25, no. 5, pp. 376–379, 2001.

[158] F. M. Donovan, “Design of a hydraulic analog of the circulatory system for evaluating artificial hearts.,” *Biomater. Med. Devices. Artif. Organs*, vol. 3, no. 4, pp. 439–449, 1975.

[159] R. W. Troughton, J. Ritzema, N. L. Eigler, et al., “Direct left atrial pressure monitoring in severe heart failure: long-term sensor performance.,” *J. Cardiovasc. Transl. Res.*, vol. 4, no. 1, pp. 3–13, 2011.

[160] B. Fritz, J. Cysyk, R. Newswanger, et al., “Development of an Inlet Pressure Sensor for Control in a Left Ventricular Assist Device,” *ASAIO J*, vol. 56, no. 3, pp. 180–185, 2010.

[161] E. H. Maslen, G. B. Bearnson, P. E. Allaire, et al., “Feedback Control Applications in Artificial Hearts,” *IEEE Control Syst. Mag.*, vol. 18, no. 6, pp. 26–34, 1998.

[162] S. Chen, J. F. Antaki, M. A. Simaan, et al., “Physiological control of left ventricular assist devices based on gradient of flow,” in *Proceedings of the 2005 American Control Conference*, Portland, OR, 2005, pp. 3829–3834.

[163] M. Vollkron, H. Schima, L. Huber, et al., “Advanced Suction Detection for an Axial Flow Pump,” *Artif Organs*, vol. 30, no. 9, pp. 665–670, 2006.

[164] D. M. Karantonis, N. H. Lovell, P. J. Ayre, et al., “Classification of Physiologically Significant Pumping States in an Implantable Rotary Blood Pump: Effects of Cardiac Rhythm Disturbances,” *Artif. Organs*, vol. 31, no. 6, pp. 476–479, 2007.

[165] O. Voigt, R. J. Benkowski, and G. F. Morello, “Suction detection for the MicroMed DeBakey Left Ventricular Assist Device,” *ASAIO J*, vol. 51, no. 4, pp. 321–328, 2005.

[166] A. Ferreira, S. Chen, M. A. Simaan, et al., “A discriminant-analysis-based suction detection system for rotary blood pumps.,” in *Annual International Conference of the IEEE Engineering in Medicine and Biology Society.*, New York, 2006, vol. 1, pp. 5382–5.

[167] D. M. Karantonis, S. L. Cloherty, N. H. Lovell, et al., “Noninvasive detection of suction in an implantable rotary blood pump using neural networks,” *Int. J. Comput. Intell. Appl.*, vol. 7, no. 3, pp. 237–247, 2008.

[168] A. Yuhki, E. Hatoh, M. Nogawa, et al., “Detection of Suction and Regurgitation of the Implantable Centrifugal Pump Based on the Motor Current Waveform Analysis and its Application to Optimization of Pump Flow,” *Artif Organs*, vol. 23, no. 6, pp. 532–537, 1999.

[169] D. M. Karantonis, E. Lim, D. G. Mason, et al., “Noninvasive activity-based control of an implantable rotary blood pump: comparative software simulation study.,” *Artif. Organs*, vol. 34, no. 2, pp. E34–E45, 2010.

[170] M. C. Stevens, A. P. Bradley, S. J. Wilson, et al., “Evaluation of a morphological filter in mean cardiac output determination: application to left ventricular assist devices.,” *Med. Biol. Eng. Comput.*, vol. 51, no. 8, pp. 891–899, Aug. 2013.

[171] G. P. Noon, D. L. Morley, S. Irwin, et al., “Clinical experience with the MicroMed DeBakey ventricular assist device,” *Ann Thorac Surg*, vol. 71, no. 3, pp. S133–138, 2001.

[172] M. Granegger, F. Moscato, F. Casas, et al., “Development of a pump flow estimator for rotary blood pumps to enhance monitoring of ventricular function.,” *Artif. Organs*, vol. 36, no. 8, pp. 691–699, 2012.

[173] E. Sorensen, “Ventricular-Assist Devices and Total Artificial Hearts,” *Biomed. Instrum. Technol.*, vol. 41, no. 5, p. 385, 2007.

[174] J. G. Copeland, F. a Arabia, P. H. Tsau, et al., “Total artificial hearts: Bridge to transplantation,” *Cardiol. Clin.*, vol. 21, no. 1, pp. 101–113, Feb. 2003.

[175] Y. Abe, T. Chinzei, K. Mabuchi, et al., “Physiological control of a total artificial heart: conductance-and arterial pressure-based control,” *J. Appl. Physiol.*, vol. 84, no. 3, pp. 868–876, 1998.

[176] Y. Abe, T. Chinzei, T. Isoyama, et al., “Analysis of Hemodynamic Response with 1/R Control on Biventricular Bypass Goat,” *Artif. Organs*, vol. 24, no. 4, pp. 312–315, Apr. 2000.

[177] I. Saito, T. Chinzei, Y. Abe, et al., “Progress in the control system of the undulation pump total artificial heart,” *Artif Organs*, vol. 27, no. 1, pp. 27–33, 2003.

[178] T. Siess, “Intracardiac pump device,” US6139487, 31-Oct-2000.

[179] M. S. Slaughter, F. D. Pagani, J. G. Rogers, et al., “Clinical management of continuous-flow left ventricular assist devices in advanced heart failure.,” *J. Heart Lung Transplant.*, vol. 29, no. 4 Suppl, pp. S1–39, 2010.

[180] Q. Lu and M. Mahfouf, “Multivariable self-organizing fuzzy logic control using dynamic performance index and linguistic compensators,” *Eng. Appl. Artif. Intell.*, vol. 25, no. 8, pp. 1537–1547, Dec. 2012.

[181] E. Lim, S. Dokos, R. F. Salamonsen, et al., “Numerical optimization studies of cardiovascular-rotary blood pump interaction.,” *Artif. Organs*, vol. 36, no. 5, pp. E110–24, May 2012.

[182] R. C. Gonzalez and R. E. Woods, *Digital Image Processing (3rd Edition)*. Prentice Hall, 2007, p. 976.

8 Appendix A

Constants for MCL settings

The following tables contain the values used to simulate various degrees of heart failure (as well as exercise) in the mock circulation loop used in this thesis. These constants relate to the equations found in Chapter 2 (Equations (2.1) and (2.2)) and Chapter 3 (Equation (3.1)).

8.1 Left Ventricle

Constant	Unit	Healthy	Mild Heart Failure	Severe Heart Failure	Healthy Exercise
K_{ven}	- -	2.2	2.2	2.2	2.2
K_{sm1}	- -	0.39	0.29	0.29	0.40
K_{sm2}	mL^{-1}	1	1	1	1
C_{EDV}	mL	0.00	300.00	200.00	0.00
C_{sm1}	- -	-0.54	-0.54	-0.54	-0.54
K_{HR}	Min	0.023	0.012	0.012	0.023

8.2 Right Ventricle

Constant	Unit	Healthy	Mild Heart Failure	Severe Heart Failure	Healthy Exercise
K_{ven}	- -	5	5	5	5
K_{sm1}	- -	0.20	0.16	0.13	0.26
K_{sm2}	mL^{-1}	1	1	1	1
C_{EDV}	mL	70.00	0.00	100.00	100.00
C_{sm1}	- -	-0.10	-0.10	-0.10	-0.10
K_{HR}	Min	0.043	0.017	0.017	0.043

9 Appendix B

Repeatability Testing Results for Test Bed Simulations.

As described in section 3.4.5.1, the repeatability of the evaluation protocol was assessed. This was achieved by simulating the sequence of patient scenarios (postural change, Valsalva manoeuvre and exercise) ten times each for two levels of ventricular contractility. To quantify the repeatability, a number of haemodynamic signals were recorded and compared.

Comparison was performed using Matlab (The Mathworks, Natick, MA). The built-in function *corrcoef* was used to determine repeatability. This function takes a set of signals and determines the correlation between each pair of signals. This function produces two outputs. The first is an array of correlation coefficients. This coefficient is a number between -1, which implies strong negative linear correlation between two signals, and 1, which implies that there is strong positive correlation between two signals. Zero implies no correlation between the two signals. The whole matrix then shows the correlation coefficient for each pair of signals. The second output is a matrix of p-values, which is the probability that there is no correlation between a pair of signals. A p-value less than 0.05 indicates that the two signals are statistically correlated. Both of these matrices are mirrored about the major diagonal.

In the context of this study, strong positive correlation indicates that two signals are tracking each other over time, indicating high repeatability. The following tables show the results of performing the correlation testing on a number of haemodynamic signals (mean systemic arterial pressure, mean pulmonary arterial pressure, mean left atrial pressure, mean right atrial pressure, mean systemic flow rate and mean pulmonary flow rate) for all ten tests and for two levels of left ventricular contractility. The result is a pair of 10 x 10 matrices for each haemodynamic variable, showing the correlation coefficient and p-value between each signal. The major diagonal is left blank, since a signal will always be 100% correlated with itself.

All of the p-values for each pair of signals for every variable are all less than 0.05, indicating that there is strong repeatability between each of the ten tests.

9.1 Healthy Left Ventricle

Mean Arterial Pressure

Correlation Coefficient										
Test Number	1	2	3	4	5	6	7	8	9	10
1	- -	0.91	0.92	0.91	0.85	0.92	0.99	1	1	0.99
2	0.91	- -	0.99	0.99	0.98	0.99	0.87	0.89	0.91	0.91
3	0.92	0.99	- -	1	0.98	1	0.87	0.90	0.91	0.89
4	0.91	0.99	1	- -	0.99	1	0.86	0.89	0.90	0.88
5	0.85	0.98	0.98	0.99	- -	0.98	0.80	0.82	0.85	0.84
6	0.92	0.99	1	1	0.98	- -	0.87	0.89	0.91	0.90
7	0.99	0.87	0.87	0.86	0.80	0.87	- -	0.99	0.99	0.99
8	1	0.89	0.90	0.89	0.82	0.89	0.99	- -	0.99	0.99
9	1	0.91	0.91	0.90	0.85	0.91	0.99	0.99	- -	0.99
10	0.99	0.91	0.89	0.88	0.84	0.90	0.99	0.99	0.99	- -

P-value (< 0.05 indicates correlation is present)										
Test Number	1	2	3	4	5	6	7	8	9	10
1	- -	0	0	0	0	0	0	0	0	0
2	0	- -	0	0	0	0	0	0	0	0
3	0	0	- -	0	0	0	0	0	0	0
4	0	0	0	- -	0	0	0	0	0	0
5	0	0	0	0	- -	0	0	0	0	0
6	0	0	0	0	0	- -	0	0	0	0
7	0	0	0	0	0	0	- -	0	0	0
8	0	0	0	0	0	0	0	- -	0	0
9	0	0	0	0	0	0	0	0	- -	0
10	0	0	0	0	0	0	0	0	0	- -

Mean Pulmonary Arterial Pressure

Correlation Coefficient										
Test Number	1	2	3	4	5	6	7	8	9	10
1	- -	0.99	0.99	1	0.99	0.99	1	1	1	1
2	0.99	- -	1	1	1	1	0.98	0.99	0.99	0.99
3	0.99	1	- -	1	1	1	0.99	1	0.99	0.99
4	1	1	1	- -	1	1	0.99	1	0.99	0.99
5	0.99	1	1	1	- -	1	0.98	0.99	0.99	0.99
6	0.99	1	1	1	1	- -	0.99	1	0.99	0.99
7	1	0.98	0.99	0.99	0.98	0.99	- -	1	1	0.99
8	1	0.99	1	1	0.99	1	1	- -	1	1
9	1	0.99	0.99	0.99	0.99	0.99	1	1	- -	1
10	1	0.99	0.99	0.99	0.99	0.99	0.99	1	1	- -

P-value (< 0.05 indicates correlation is present)										
Test Number	1	2	3	4	5	6	7	8	9	10
1	- -	0	0	0	0	0	0	0	0	0
2	0	- -	0	0	0	0	0	0	0	0
3	0	0	- -	0	0	0	0	0	0	0
4	0	0	0	- -	0	0	0	0	0	0
5	0	0	0	0	- -	0	0	0	0	0
6	0	0	0	0	0	- -	0	0	0	0
7	0	0	0	0	0	0	- -	0	0	0
8	0	0	0	0	0	0	0	- -	0	0
9	0	0	0	0	0	0	0	0	- -	0
10	0	0	0	0	0	0	0	0	0	- -

Mean Left Atrial Pressure

Correlation Coefficient										
Test Number	1	2	3	4	5	6	7	8	9	10
1	- -	0.99	1	1	0.99	1	0.99	1	1	0.99
2	0.99	- -	1	1	1	1	0.98	0.99	0.99	0.99
3	1	1	- -	1	1	1	0.99	1	0.99	0.99
4	1	1	1	- -	1	1	0.99	1	1	0.99
5	0.99	1	1	1	- -	1	0.97	0.99	0.99	0.99
6	1	1	1	1	1	- -	0.98	1	0.99	0.99
7	0.99	0.98	0.99	0.99	0.97	0.98	- -	0.99	0.99	0.99
8	1	0.99	1	1	0.99	1	0.99	- -	1	0.99
9	1	0.99	0.99	1	0.99	0.99	0.99	1	- -	0.99
10	0.99	0.99	0.99	0.99	0.99	0.99	0.99	0.99	0.99	- -

P-value (< 0.05 indicates correlation is present)										
Test Number	1	2	3	4	5	6	7	8	9	10
1	- -	0	0	0	0	0	0	0	0	0
2	0	- -	0	0	0	0	0	0	0	0
3	0	0	- -	0	0	0	0	0	0	0
4	0	0	0	- -	0	0	0	0	0	0
5	0	0	0	0	- -	0	0	0	0	0
6	0	0	0	0	0	- -	0	0	0	0
7	0	0	0	0	0	0	- -	0	0	0
8	0	0	0	0	0	0	0	- -	0	0
9	0	0	0	0	0	0	0	0	- -	0
10	0	0	0	0	0	0	0	0	0	- -

Mean Right Atrial Pressure

Correlation Coefficient										
Test Number	1	2	3	4	5	6	7	8	9	10
1	- -	0.98	1	0.99	0.96	0.98	0.98	1	1	0.98
2	0.98	- -	0.98	0.98	0.98	0.98	0.94	0.97	0.98	0.99
3	1	0.98	- -	0.99	0.96	0.99	0.98	1	1	0.98
4	0.99	0.98	0.99	- -	0.98	1	0.96	0.99	0.99	0.98
5	0.96	0.98	0.96	0.98	- -	0.98	0.91	0.95	0.96	0.98
6	0.98	0.98	0.99	1	0.98	- -	0.94	0.97	0.99	0.98
7	0.98	0.94	0.98	0.96	0.91	0.94	- -	0.99	0.98	0.96
8	1	0.97	1	0.99	0.95	0.97	0.99	- -	1	0.98
9	1	0.98	1	0.99	0.96	0.99	0.98	1	- -	0.98
10	0.98	0.99	0.98	0.98	0.98	0.98	0.96	0.98	0.98	- -

P-value (< 0.05 indicates correlation is present)										
Test Number	1	2	3	4	5	6	7	8	9	10
1	- -	0	0	0	0	0	0	0	0	0
2	0	- -	0	0	0	0	0	0	0	0
3	0	0	- -	0	0	0	0	0	0	0
4	0	0	0	- -	0	0	0	0	0	0
5	0	0	0	0	- -	0	0	0	0	0
6	0	0	0	0	0	- -	0	0	0	0
7	0	0	0	0	0	0	- -	0	0	0
8	0	0	0	0	0	0	0	- -	0	0
9	0	0	0	0	0	0	0	0	- -	0
10	0	0	0	0	0	0	0	0	0	- -

Mean Systemic Flow Rate

Correlation Coefficient										
Test Number	1	2	3	4	5	6	7	8	9	10
1	- -	1	1	1	1	1	1	1	1	1
2	1	- -	1	1	1	1	0.99	1	1	1
3	1	1	- -	1	1	1	1	1	1	1
4	1	1	1	- -	1	1	1	1	1	1
5	1	1	1	1	- -	1	0.99	0.99	0.99	1
6	1	1	1	1	1	- -	1	1	1	1
7	1	0.99	1	1	0.99	1	- -	1	1	1
8	1	1	1	1	0.99	1	1	- -	1	1
9	1	1	1	1	0.99	1	1	1	- -	1
10	1	1	1	1	1	1	1	1	1	- -

P-value (< 0.05 indicates correlation is present)										
Test Number	1	2	3	4	5	6	7	8	9	10
1	- -	0	0	0	0	0	0	0	0	0
2	0	- -	0	0	0	0	0	0	0	0
3	0	0	- -	0	0	0	0	0	0	0
4	0	0	0	- -	0	0	0	0	0	0
5	0	0	0	0	- -	0	0	0	0	0
6	0	0	0	0	0	- -	0	0	0	0
7	0	0	0	0	0	0	- -	0	0	0
8	0	0	0	0	0	0	0	- -	0	0
9	0	0	0	0	0	0	0	0	- -	0
10	0	0	0	0	0	0	0	0	0	- -

Mean Pulmonary Flow Rate

Correlation Coefficient										
Test Number	1	2	3	4	5	6	7	8	9	10
1	- -	1	1	1	1	1	1	1	1	1
2	1	- -	1	1	1	1	1	1	1	1
3	1	1	- -	1	1	1	1	1	1	1
4	1	1	1	- -	1	1	1	1	1	1
5	1	1	1	1	- -	1	1	1	1	1
6	1	1	1	1	1	- -	1	1	1	1
7	1	1	1	1	1	1	- -	1	1	1
8	1	1	1	1	1	1	1	- -	1	1
9	1	1	1	1	1	1	1	1	- -	1
10	1	1	1	1	1	1	1	1	1	- -

P-value (< 0.05 indicates correlation is present)										
Test Number	1	2	3	4	5	6	7	8	9	10
1	- -	0	0	0	0	0	0	0	0	0
2	0	- -	0	0	0	0	0	0	0	0
3	0	0	- -	0	0	0	0	0	0	0
4	0	0	0	- -	0	0	0	0	0	0
5	0	0	0	0	- -	0	0	0	0	0
6	0	0	0	0	0	- -	0	0	0	0
7	0	0	0	0	0	0	- -	0	0	0
8	0	0	0	0	0	0	0	- -	0	0
9	0	0	0	0	0	0	0	0	- -	0
10	0	0	0	0	0	0	0	0	0	- -

9.2 Mild Left Heart Failure

Mean Arterial Pressure

Correlation Coefficient										
Test Number	1	2	3	4	5	6	7	8	9	10
1	- -	0.99	0.99	0.99	0.99	0.99	1	1	0.99	0.99
2	0.99	- -	0.99	0.99	0.99	1	0.99	0.99	0.99	0.99
3	0.99	0.99	- -	1	1	0.99	1	1	0.99	1
4	0.99	0.99	1	- -	1	0.99	0.99	1	0.99	1
5	0.99	0.99	1	1	- -	0.99	1	0.99	0.99	1
6	0.99	1	0.99	0.99	0.99	- -	0.99	0.99	0.99	1
7	1	0.99	1	0.99	1	0.99	- -	1	0.99	1
8	1	0.99	1	1	0.99	0.99	1	- -	0.99	0.99
9	0.99	0.99	0.99	0.99	0.99	0.99	0.99	0.99	- -	0.99
10	0.99	0.99	1	1	1	1	1	0.99	0.99	- -

P-value (< 0.05 indicates correlation is present)										
Test Number	1	2	3	4	5	6	7	8	9	10
1	- -	0	0	0	0	0	0	0	0	0
2	0	- -	0	0	0	0	0	0	0	0
3	0	0	- -	0	0	0	0	0	0	0
4	0	0	0	- -	0	0	0	0	0	0
5	0	0	0	0	- -	0	0	0	0	0
6	0	0	0	0	0	- -	0	0	0	0
7	0	0	0	0	0	0	- -	0	0	0
8	0	0	0	0	0	0	0	- -	0	0
9	0	0	0	0	0	0	0	0	- -	0
10	0	0	0	0	0	0	0	0	0	- -

Mean Pulmonary Arterial Pressure

Correlation Coefficient										
Test Number	1	2	3	4	5	6	7	8	9	10
1	- -	1	1	1	1	1	1	1	1	1
2	1	- -	1	1	0.99	1	0.99	0.99	1	1
3	1	1	- -	1	0.99	1	0.99	0.99	1	1
4	1	1	1	- -	1	1	1	1	1	1
5	1	0.99	0.99	1	- -	1	1	1	0.99	1
6	1	1	1	1	1	- -	1	1	1	1
7	1	0.99	0.99	1	1	1	- -	1	0.99	1
8	1	0.99	0.99	1	1	1	1	- -	1	1
9	1	1	1	1	0.99	1	0.99	1	- -	1
10	1	1	1	1	1	1	1	1	1	- -

P-value (< 0.05 indicates correlation is present)										
Test Number	1	2	3	4	5	6	7	8	9	10
1	- -	0	0	0	0	0	0	0	0	0
2	0	- -	0	0	0	0	0	0	0	0
3	0	0	- -	0	0	0	0	0	0	0
4	0	0	0	- -	0	0	0	0	0	0
5	0	0	0	0	- -	0	0	0	0	0
6	0	0	0	0	0	- -	0	0	0	0
7	0	0	0	0	0	0	- -	0	0	0
8	0	0	0	0	0	0	0	- -	0	0
9	0	0	0	0	0	0	0	0	- -	0
10	0	0	0	0	0	0	0	0	0	- -

Mean Left Atrial Pressure

Correlation Coefficient										
Test Number	1	2	3	4	5	6	7	8	9	10
1	- -	1	1	1	1	1	1	1	1	1
2	1	- -	1	1	1	1	1	1	1	1
3	1	1	- -	1	1	1	1	1	1	0.99
4	1	1	1	- -	1	1	1	1	1	1
5	1	1	1	1	- -	1	1	1	1	1
6	1	1	1	1	1	- -	1	1	1	1
7	1	1	1	1	1	1	- -	1	1	1
8	1	1	1	1	1	1	1	- -	1	1
9	1	1	1	1	1	1	1	1	- -	1
10	1	1	0.99	1	1	1	1	1	1	- -

P-value (< 0.05 indicates correlation is present)										
Test Number	1	2	3	4	5	6	7	8	9	10
1	- -	0	0	0	0	0	0	0	0	0
2	0	- -	0	0	0	0	0	0	0	0
3	0	0	- -	0	0	0	0	0	0	0
4	0	0	0	- -	0	0	0	0	0	0
5	0	0	0	0	- -	0	0	0	0	0
6	0	0	0	0	0	- -	0	0	0	0
7	0	0	0	0	0	0	- -	0	0	0
8	0	0	0	0	0	0	0	- -	0	0
9	0	0	0	0	0	0	0	0	- -	0
10	0	0	0	0	0	0	0	0	0	- -

Mean Right Atrial Pressure

Correlation Coefficient										
Test Number	1	2	3	4	5	6	7	8	9	10
1	- -	0.95	0.99	0.94	0.97	0.93	0.98	0.99	0.93	0.98
2	0.95	- -	0.96	0.94	0.94	0.99	0.96	0.96	0.99	0.96
3	0.99	0.96	- -	0.96	0.98	0.95	0.99	1	0.94	0.99
4	0.94	0.94	0.96	- -	0.96	0.95	0.98	0.96	0.95	0.99
5	0.97	0.94	0.98	0.96	- -	0.94	0.98	0.98	0.94	0.98
6	0.93	0.99	0.95	0.95	0.94	- -	0.96	0.95	1	0.96
7	0.98	0.96	0.99	0.98	0.98	0.96	- -	0.99	0.95	1
8	0.99	0.96	1	0.96	0.98	0.95	0.99	- -	0.95	0.99
9	0.93	0.99	0.94	0.95	0.94	1	0.95	0.95	- -	0.96
10	0.98	0.96	0.99	0.99	0.98	0.96	1	0.99	0.96	- -

P-value (< 0.05 indicates correlation is present)										
Test Number	1	2	3	4	5	6	7	8	9	10
1	- -	0	0	0	0	0	0	0	0	0
2	0	- -	0	0	0	0	0	0	0	0
3	0	0	- -	0	0	0	0	0	0	0
4	0	0	0	- -	0	0	0	0	0	0
5	0	0	0	0	- -	0	0	0	0	0
6	0	0	0	0	0	- -	0	0	0	0
7	0	0	0	0	0	0	- -	0	0	0
8	0	0	0	0	0	0	0	- -	0	0
9	0	0	0	0	0	0	0	0	- -	0
10	0	0	0	0	0	0	0	0	0	- -

Mean Systemic Flow Rate

Correlation Coefficient										
Test Number	1	2	3	4	5	6	7	8	9	10
1	- -	1	1	1	1	1	1	1	1	1
2	1	- -	1	1	1	1	1	1	1	1
3	1	1	- -	1	1	1	1	1	1	1
4	1	1	1	- -	1	1	1	1	1	1
5	1	1	1	1	- -	1	1	1	1	1
6	1	1	1	1	1	- -	1	1	1	1
7	1	1	1	1	1	1	- -	1	1	1
8	1	1	1	1	1	1	1	- -	1	1
9	1	1	1	1	1	1	1	1	- -	1
10	1	1	1	1	1	1	1	1	1	- -

P-value (< 0.05 indicates correlation is present)										
Test Number	1	2	3	4	5	6	7	8	9	10
1	- -	0	0	0	0	0	0	0	0	0
2	0	- -	0	0	0	0	0	0	0	0
3	0	0	- -	0	0	0	0	0	0	0
4	0	0	0	- -	0	0	0	0	0	0
5	0	0	0	0	- -	0	0	0	0	0
6	0	0	0	0	0	- -	0	0	0	0
7	0	0	0	0	0	0	- -	0	0	0
8	0	0	0	0	0	0	0	- -	0	0
9	0	0	0	0	0	0	0	0	- -	0
10	0	0	0	0	0	0	0	0	0	- -

Mean Pulmonary Flow Rate

Correlation Coefficient										
Test Number	1	2	3	4	5	6	7	8	9	10
1	- -	1	1	1	1	1	1	1	1	1
2	1	- -	1	1	1	1	1	1	1	1
3	1	1	- -	1	1	1	1	1	1	1
4	1	1	1	- -	1	1	1	1	1	1
5	1	1	1	1	- -	1	1	1	1	1
6	1	1	1	1	1	- -	1	1	1	1
7	1	1	1	1	1	1	- -	1	1	1
8	1	1	1	1	1	1	1	- -	1	1
9	1	1	1	1	1	1	1	1	- -	1
10	1	1	1	1	1	1	1	1	1	- -

P-value (< 0.05 indicates correlation is present)										
Test Number	1	2	3	4	5	6	7	8	9	10
1	- -	0	0	0	0	0	0	0	0	0
2	0	- -	0	0	0	0	0	0	0	0
3	0	0	- -	0	0	0	0	0	0	0
4	0	0	0	- -	0	0	0	0	0	0
5	0	0	0	0	- -	0	0	0	0	0
6	0	0	0	0	0	- -	0	0	0	0
7	0	0	0	0	0	0	- -	0	0	0
8	0	0	0	0	0	0	0	- -	0	0
9	0	0	0	0	0	0	0	0	- -	0
10	0	0	0	0	0	0	0	0	0	- -

10 Appendix C

This appendix describes the Frank-Starling control system used in Chapter 4 and as the master control system in Chapter 5. It describes three different methods of calculating a target flow rate for a given measured preload/pump inlet pressure.

10.1 Starling-like Control Descriptions

A Frank-Starling control approach was used for LVAD control. This approach directly mimics the native preload-sensitivity of the ventricle. Direct mimicking of the native ventricular function should ensure pump and ventricular output matches cardiac demand. The fundamental principle of Starling control involves setting a target pump flow rate based on preload. LVAD inlet pressure was used as a direct measure of pump preload, and it was assumed that a sensor was available to do measure this. This simplified the development of the control system.

Guyton defines the relationship between flow and preload as sigmoid [20]. However, for this control system a linear relationship between pump flow and preload was used as it was simpler to implement. Upper and lower limits on flow were added to prevent excessive flow and back flow respectively. Figure 10.1 shows the relationship between pump flow and preload that will be maintained by the control system.

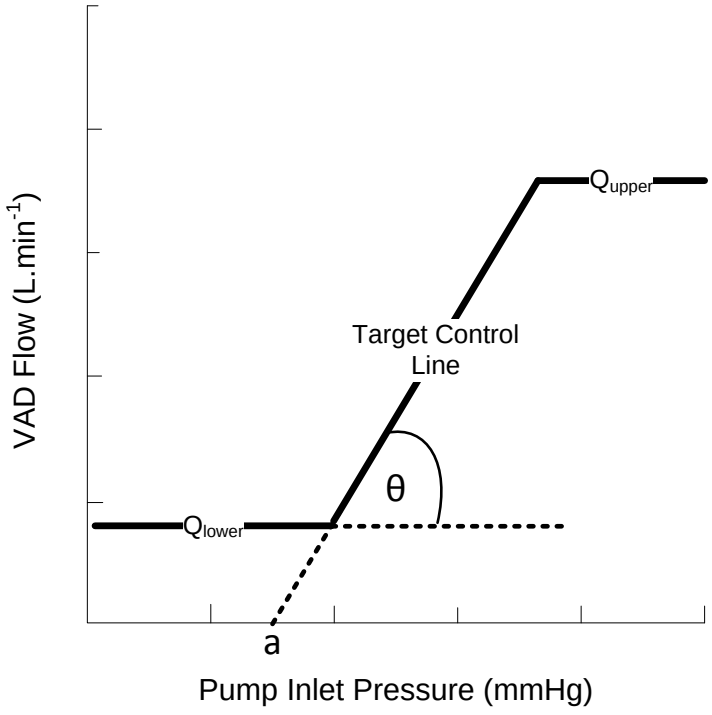

Figure 10.1: Target control line for the Starling-like control system for rotary LVAD control.

At each time step, the current values of pump inlet pressure (P_{in}) and VAD flow (Q_{meas}) were measured, which defined the current operating point. The target flow for that operating point was calculated, and

the speed of the pump adjusted to minimise the error between target and measured flow. Three different methods could be used for calculating the target flow, as described by Salamonsen and colleagues (2012) [127].

10.1.1 Vertical Flow Target

The first method, vertical flow target (VFT), is the most straightforward, and is shown in Figure 10.2. The target flow rate was located vertically from the operating point towards the target line (Equation (10.1)).

$$Q_{VFT} = K_{sc}(P_{in} - \mathrm{a}) \tag{10.1}$$

Where K_{sc} (L.min^{-1}.mmHg^{-1}) is the magnitude of the slope and a is the horizontal offset of this slope. These constants were set at 2 L.min^{-1}.mmHg^{-1} and 5.5 mmHg respectively, which resulted in normal cardiac output, systemic and pulmonary arterial pressures (5 L.min^{-1}, 90-100mmHg and 18-20mmHg respectively) at rest.

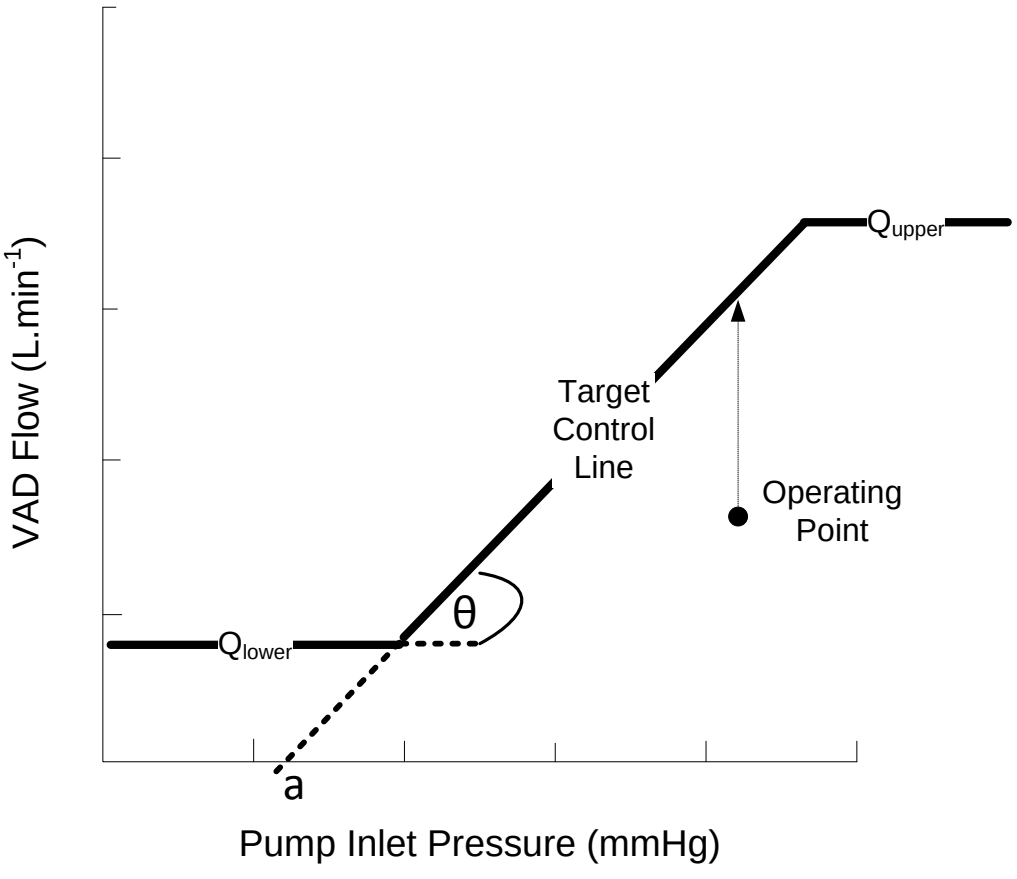

Figure 10.2: Calculation of target flow using the vertical target flow calculation

Vertical flow target is the most logical and straightforward calculation. However, the initial estimate for target flow using Equation (10.1) may over- or underestimate the final steady-state value as the operating point moves closer to the target control line. This is because as speed changes, both preload

and flow change, so the movement of the operating point is never vertical. This overestimation may result in overshoot of the control line, and consequently longer settling times. Higher values of K_{sc} accentuate this effect, producing high variation in target flow for small variations in P_{in}, resulting in the operating point continually "hunting" for its steady state. For these reasons, vertical flow error was not evaluated in this thesis. Instead, two more complex approaches were investigated – Radial flow about the X-Intercept and Radial Flow about the Target Control Line.

10.1.2 Radial Flow about X-Intercept

Target flow calculated radially about the x-intercept (RAXI), uses an arc drawn from the operating point to the target control line (Figure 10.3). The arc has its centre located at the x-intercept of the control line, and the error is calculated using Equation (10.2).

$$Q_{TRAXI} = \sin\left(\tan^{-1} K_{sc}\right)\sqrt{(P_{in} - a)^2 + \left(Q_{meas}\right)^2} \tag{10.2}$$

Where Q_{meas} represents the measured VAD flow, and all other constants as previously described. This method predicts a target value that is closer to the final steady-state value on the target control line. It also accommodates for steeper slopes in that small variations in P_{in} are damped by the Q_{meas} term.

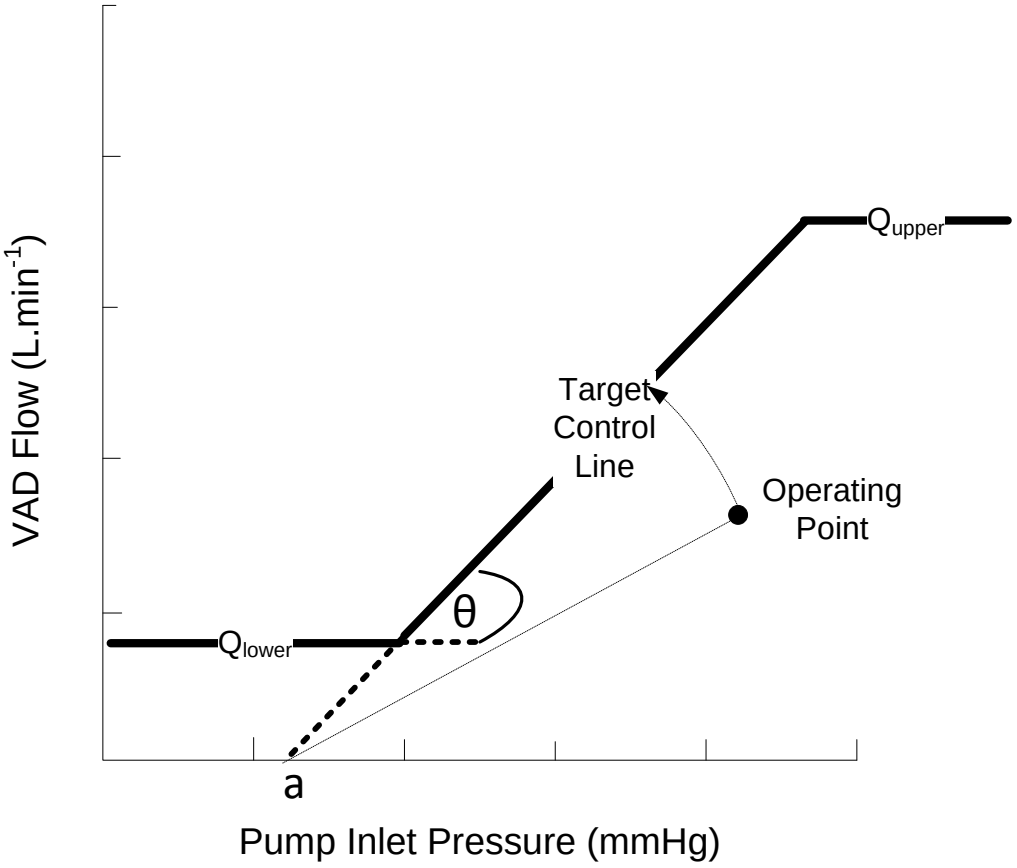

Figure 10.3: Calculation of target flow using radial about the x-intercept (TRAXI) method.

10.1.3 Radial Flow About the Target Control Line

The final method, target flow radial about the control line (RACL) is similar to RAXI but uses an arc with its centre located on the target control line, horizontally from the operating point (Figure 10.4). Equation (10.3) is used to determine the target flow rate. Like RAXI, this method sets a target flow rate close to the final steady state value on the control line, and accommodates for steep slopes.

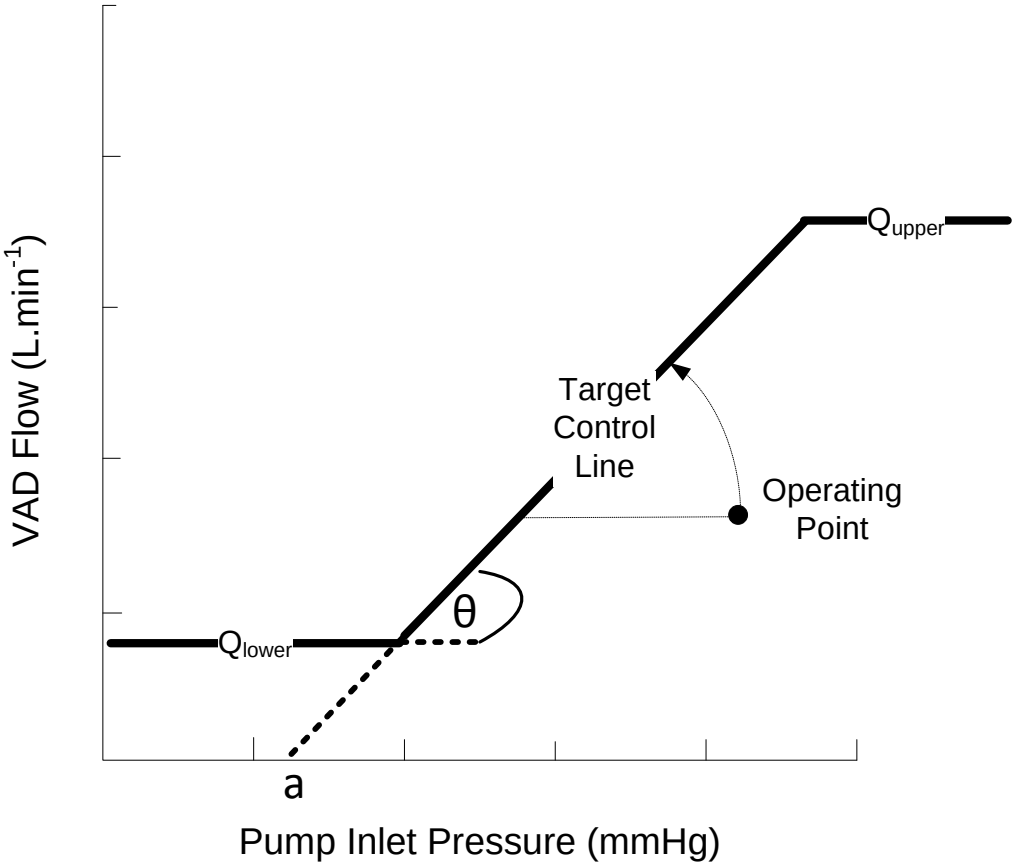

Figure 10.4: Calculation of target flow using radial about the control line (RACL) method.

$$Q_{TRACL} = Q_{meas}(1 - K_{sc1}) + \mathrm{K_{sc2}}(\mathrm{P_{inM}} - \mathrm{a}) \quad (10.3)$$

Where K_{sc1} and K_{sc2} (L.min^{-1}.mmHg^{-1}) are related to the slope K_{sc} by equations 10.4 and 10.5

$$K_{sc1} = cos\ (tan^{-1}\ K_{sc}) \quad (10.4)$$

$$K_{sc2} = sin\ (tan^{-1}\ K_{sc}) \quad (10.5)$$

Since K_{sc} was set at 2 L.min^{-1}.mmHg^{-1}, K_{sc1} and K_{sc2} were set as 0.447 and 0.894 L.min^{-1}.mmHg^{-1} respectively.

11 Appendix D

11.1 Optimisation Loop

Tuning of the gains (K_p and K_i) of the PI control implementation for each system was performed using Quasi-Newtonian optimisation. Optimisation was chosen as the tuning method because the complexity and time-varying nature of the cardiovascular system made tuning via traditional control design methods, such as pole placement, difficult.

A numerical model of the cardiovascular system was used to optimise the control gains[181]. A patient with severe LHF patient was simulated, and left pump support initiated with speed set at 2100 RPM. The Quasi-Newtonian tuning loop was then started. The goal of the optimisation loop was to determine the set of gains **k** that minimised the objective function S(**k**) (Equation (11.1))

$$S(\boldsymbol{k}) = \int_{t0}^{t1} \left(\frac{Q_{meas}(t) - Q^*(t)}{Q_{target}(t)} \right)^2 dt \tag{11.1}$$

Where Q*(t) is the desired, or ideal, controller response.

11.2 Ideal System Response

The ideal system response Q*(t) was represented as a second-order system, with a rise time of 1 second to ensure responsive tracking and a ten percent overshoot as a suitable compromise for the fast response. The general form of a second order transfer function is shown in Equation (11.2)

$$G(s) = \frac{\omega^2}{s^2 + 2\zeta\omega s + \omega^2} \tag{11.2}$$

Where ζ is the damping ratio and ω the natural frequency. The overshoot of a second order transfer function can be determined using Equation (11.3).

$$OS\% = 100\ \mathrm{e}^{-\zeta \frac{\pi}{\sqrt{1-\zeta^2}}} \tag{11.3}$$

Given an overshoot as a design specification, the damping ratio can be calculated by rearranging Equation (11.3), producing Equation (11.4).

$$\zeta = \frac{\ln\left(\frac{OS\%}{100}\right)}{\sqrt{\pi^2 + \ln^2 \frac{OS\%}{100}}} \tag{11.4}$$

The rise time of a second order system can be determined using Equation (11.5).

$$t_r = \frac{1}{\omega}\left(\frac{1}{\sqrt{1-\zeta^2}}\right)(\pi - \tan^{-1}\left(\frac{\sqrt{1-\zeta^2}}{\zeta}\right)) \quad (11.5)$$

Rearranging, the natural frequency of the system can be determined using Equation (11.6).

$$\omega = \frac{1}{t_r}\left(\frac{1}{\sqrt{1-\zeta^2}}\right)(\pi - \tan^{-1}\left(\frac{\sqrt{1-\zeta^2}}{\zeta}\right)) \quad (11.6)$$

Substituting the design specifications (overshoot 10% and rise time 1 second) into Equations (11.4) and (11.6) produced the transfer function of the ideal system response, shown in Equation (11.7)."

$$\frac{Q^*(s)}{Q_{target}(s)} = \frac{7.462}{s^2 + 3.23s + 7.462} \quad (11.7)$$

This was converted to a discrete transfer function in order to make a direct comparison with the discrete PI control system. Transformation was performed using Matlab with a sampling period of 1 second. The resulting discrete transfer function is given in Equation (11.8)

$$\frac{Q^*(z)}{Q_{target}(z)} = \frac{z + 0.2747}{z^2 + 0.2352z + 0.03957} \quad (11.8)$$

11.3 Optimisation Loop

S(**k**) was determined for a step reduction in target output over a time period of 30 seconds.

The optimisation loop consisted of the following steps.

1. Initial simulation.

    i. A patient with severe LHF was simulated and supported with an LVAD operating at constant speed.

    ii. The FS control system was turned on at t = 30 seconds, using an initial guess for the gains ($\mathbf{X_0} = [K_{p0}\ K_{i0}]$).

    iii. At t =60 seconds, the target flow rate of the FS control system was decreased by 20% in a step wise manner. The system was given 30 seconds to settle. S($\mathbf{X_0}$) was determined for this step response.

2. Calculate $S'(\boldsymbol{X_0}) =$

    i. Vary K_p by 5%.

    ii. Repeat step 1 after substituting in this new gain.

    iii. Calculate S_1, and change in S using Equation (11.9).

$$\frac{\partial S}{\partial K_p} = \frac{S_1 - S_0}{K_{p1} - K_{p0}} \tag{11.9}$$

    iv. Return the varied gain back to its original value, then repeat i - iii with all gains.

    v. Calculate the approximate gradient of the system ($S'(\boldsymbol{X_0})$) at the original set of gains using Equation (11.10).

$$S'(\boldsymbol{X_0}) \approx \frac{\Delta S_0}{\Delta \boldsymbol{X}} = \frac{\partial S}{\partial K_p} + \frac{\partial S}{\partial K_i} \tag{11.10}$$

3. Calculate second gain set using Equation (11.11) and apply to the controller.

$$\boldsymbol{X_1} = \boldsymbol{X_0} + -X_{step}\boldsymbol{H_1}\big(S'(\boldsymbol{X_0})\big) \tag{11.11}$$

Where X_{step} = 0.05 and $\mathbf{H_1}$is an *n x n* identity matrix, where *n* is the number of gains being optimised (in this example, *n* = 2).

4. Repeat Step 3 using $\mathbf{X}_1$ to calculate $S'(\boldsymbol{X_1})$

5. Determine new set of gains using Equation (11.12).

$$\boldsymbol{X_{k+1}} = \boldsymbol{X_k} + -X_{step}\boldsymbol{H_{k+1}}\left(S'(\boldsymbol{X_k})\right) \tag{11.12}$$

where

$$\boldsymbol{H_{k+1}} = \left(\boldsymbol{I} - \left(\frac{\boldsymbol{y}\Delta\boldsymbol{X^T}}{\boldsymbol{y^T}\Delta\boldsymbol{X}}\right)\right)^T \boldsymbol{H_k}\left(\boldsymbol{I} - \left(\frac{\boldsymbol{y}\Delta\boldsymbol{X^T}}{\boldsymbol{y^T}\Delta\boldsymbol{X}}\right)\right) + \left(\frac{\Delta\boldsymbol{X}\Delta\boldsymbol{X^T}}{\boldsymbol{y^T}\Delta\boldsymbol{X}}\right)$$

and

$$\boldsymbol{y} = S'(\boldsymbol{X_{k+1}}) - S'(\boldsymbol{X_k})$$

6. Repeat steps 5 and 6 until $\mathbf{S'(X_k)}$, $\mathbf{S(X_k)}$ or $|\mathbf{\Delta X}|$ falls below a defined threshold, or until maximum number of iterations is reached.

The parameters used for the optimisation process are given in Table 11.1.

Table 11.1: Parameters used for optimisation process.

Parameter	Value
$S'(X_k)$ Threshold	0.1
$S(X_k)$ Threshold	0.01
$\lvert\Delta X\rvert$ Threshold	0.5
Max iterations	20

12 Appendix E

Morphological Filter Description

This appendix contains a description of the morphological filter used to condition all signals prior to use in the physiological control systems described in this thesis. This description was published in the journal *Medical and Biological Engineering and Computing* in 2013, in Volume 51 Issue 8.

Briefly, signal conditioning was required for all feedback signals before their use in a physiological control system. Ideally, the pulsatile component of the signal caused by residual heart contractility should be removed without attenuating other clinically significant components or damping sharp changes in signal magnitude. Generally, linear or non-linear filters can be used. Linear filters (such as Butterworth filters) require a trade-off between response time and attenuation. Additionally, the have higher requirements for bit precision than some non-linear filters. Therefore, it was decided that a non-linear filtering approach should be utilised.

There are a number of different non-linear approaches that could be used. Morphological filters were chosen because of their previous use in processing other biological signals as well as their relatively simple computation requirements. More detail of the structure of a morphological filter and its implementation can be found in this appendix, as well as in [182].

Evaluation of a Morphological Filter in Mean Cardiac Output Determination: Application to Left Ventricular Assist Devices

Michael Charles Stevens[1,2]

Andrew P. Bradley[2]

Stephen J Wilson[2]

David Glen Mason[2]

1. Innovative Cardiovascular Engineering and Technology Laboratory, The Prince Charles Hospital, Brisbane, QLD, Australia

2. School of Information Technology and Electrical Engineering, University of Queensland, Brisbane, QLD, Australia.

Corresponding Author

Michael Stevens

School of Information Technology and Electrical Engineering, University of Queensland, Brisbane, QLD, Australia.

m.stevens2@uq.edu.au

Total Word Count: 5714

Abstract Word Count: 176

Number of Figures: 7

Number of Tables: 2

Abstract

A morphological filter (MF) is presented for the determination of beat-to-beat mean rotary left ventricular assist device (LVAD) flow rate, measured using an implanted flow probe. The performance of this non-linear filter was assessed using LVAD flow rate (Q_{LVAD}) data sets obtained from in-silico and in-vivo sources. The MF was compared with a 3rd order Butterworth filter (BWF) and a 10-second moving average filter (MAF). Performance was assessed by calculating the response time and steady state error across a range of heart rates and levels of noise. The response time of the MF was 3.5 times faster than the MAF, 0.5 seconds slower than the BWF, and had a steady state error of 2.61%. It completely removed pulsatile signal components caused by residual ventricular function, and tracked sharp transient changes in Q_{LVAD} better than the BWF. The use of a two-stage MF improved noise immunity compared to the single-stage MF. This study showed that the good performance characteristics of the non-linear MF make it a more suitable candidate for embedded real-time processing of Q_{LVAD} than linear filters.

Keywords

Morphological filter; Ventricle-Assist Device; Cardiac Output; Signal Processing

Abbreviations

MF: Morphological Filter; LVAD: Left Ventricular Assist Device; Q_{LVAD}: Left Ventricular Assist Device Flow Rate; SE: Structuring Element; IIR: Infinite Impulse Response; BWF: Butterworth filter; FIR: Finite Impulse Response; R_{sa}: Systemic Arterial Resistance; t: Time; BPM: Beats Per Minute; f_c: Cut-off Frequency; MAF: Moving Average Filter; RMSSSD: Root Mean Squared Steady State Difference;

Introduction

Rotary left ventricular assist devices (LVADs) mechanically support patients with left ventricular failure whilst they await a heart transplant. Continuous measurement of LVAD flow rate (Q_{LVAD}) by an implantable sensor may aid with the clinical management of these patients, and may also be required in future for feedback control of pump speed [8]. Flow sensors are currently incorporated into one type of LVAD [5]. Online filtering of signals obtained from these implantable sensors is necessary to obtain beat-to-beat mean Q_{LVAD} in real-time.

A requirement of a signal filter for Q_{LVAD} is to attenuate the pulsatile components of the flow signal (caused by residual heart contractility) to obtain beat-to-beat mean flow. A suitable filter must achieve this without attenuating other clinically significant signal components or damping sharp transient changes in signal magnitude. Obtaining a responsive beat-to-beat mean flow will allow clinicians to make appropriate decisions quickly regarding pump speed settings, which will obviously be beneficial to the patient. Additionally, attenuation of the heartbeat removes undesirable modulation, which makes it easier to design feedback control systems. Such control systems may reduce ventricular suction events [8] which may improve patient quality of life. An additional challenge is to minimise the computational complexity of the filter, enabling the use of low-power consumption embedded processors. Possible filters for this application can be broadly classified into two main categories: linear or non-linear filters.

Linear filters have previously been used to remove baseline drift and noise from ECG measurements [6]. However, it can be shown that these filters distort the QRS and ST complexes. This impedes the detection of QRS complex and consequently reduces the discriminatory power of any diagnostic system in which the filter is used [9]. Morphological filters (MFs) were shown to better preserve these complexes than linear filters due to their inherent ability to better preserve signal morphology [1]. An additional advantage of MFs is that they are computationally simple and have lower requirements for bit precision than linear filters. The successful use of MFs in filtering one type of biosignal, as described above, in conjunction with their implementation advantages, encourages their

use as a filter for Q_{LVAD}. To our knowledge, MFs have not yet been applied to biosignal processing applications other than ECG.

The aim of this study was to develop and evaluate a MF for the measurement of mean beat-to-beat Q_{LVAD}. Flow data generated in-silico and obtained from an in-vivo experiment were filtered using a MF, and the result compared to two linear filters.

Methods

Morphological Filters

MFs utilise mathematical morphology, of which the fundamental operations are erosion and dilation. These operations involve shifting a structuring element (SE) of a specified shape and size along the time dimension of a signal and at each time step either subtracting (eroding) or adding (dilating) the SE to the signal. Morphological opening (erosion then dilation) of a 1-D signal can be interpreted as moving the SE along a 1-D data set from underneath, and the resulting signal is the set of highest points reached by the structuring element, producing a set of local minima [9]. In the opposite manner, morphological closing (dilation then erosion) of the signal passes the SE through the data set from above, resulting in a set of lowest points reached by the element, producing a set of local maxima. For a more detailed description of mathematical morphology, see [2].

The MF algorithm used in this study estimated the mean y of the signal x in the following manner. Firstly, closing and opening operations with a flat structuring element B were performed simultaneously. The beat-to-beat mean flow was then determined by the weighted average of the closing and opening operations (Equation 1).

$$y = w.(x \bullet B) + (1-w).(x \circ B) \quad (1)$$

Where the symbols • and ∘ denote morphological closing and opening respectively, and $0 < w < 1$, which can be adjusted to accommodate different waveform shapes. Opening and closing operations were implemented using the fast implementation of 1-D time-series morphological filtering proposed by Wang and He (1994) to reduce computational complexity [12].

For implementation in embedded processors, comparisons and addition operations are favoured over multiplication due to faster (single clock cycle) instruction times and the universal implementation of these operations in processor hardware. An additional consideration when selecting a processor is the bit precision required for each operation – the higher the precision, typically the higher the power requirements and cost of the microcontroller. Using the aforementioned MF approach, at each time step only two comparisons, two multiplications and one addition are performed, independent of structuring element length [12]. The few arithmetic operations required and the reliance on comparison operators means that the requirement for bit depth is small. Only a small amount of internal memory is required to store the result of the comparison from the previous time step, and 8-bit implementation would be sufficient.

In contrast, the implementation of linear filters requires higher bit precision. For infinite impulse response (IIR) filters, the resultant pole location after hardware implementation may be different to the desired pole location due to quantisation, resulting in alterations in either resonant frequency or bandwidth [4]. Additionally, limit cycles (oscillatory behaviour when no input is present) may occur because of the rounding operation as a result of a low bit resolution. As an example, Figure 1 shows a comparison of the frequency and step responses of a third order low-pass Butterworth filter (BWF) implemented with different levels of bit precision. Twelve-bit precision resulted in a non-unity gain in the pass-band, producing an undesirable step response. Sixteen-bit precision was required to obtain desired filter characteristics (to within 0.5 dB).

Finite impulse response (FIR) filters are inherently stable and their coefficients do not require as high precision as IIR filters. However, a higher order FIR filter is required to obtain the same characteristics as an equivalent IIR filter. Additionally, the accumulation operation requires a reasonable amount of bit resolution to prevent overflow. Specifically, an extra bit of precision is required every time the result in the accumulator is doubled.

Having established that the requirements for bit precision and computational complexity are lower for MFs than for IIR and FIR filters, the next step is to determine if the non-linear behaviour of MFs is advantageous when determining beat-to-beat mean Q_{LVAD}.

Filter Evaluation

We assessed the suitability of a MF for filtering Q_{LVAD} using Simulink (The Mathworks, Natick, MA) so that the proposed algorithm could be tested in a simulated environment. The evaluation procedure involved subjecting Q_{LVAD} data to the MF and two other linear filters (Figure 2) and comparing the response time and steady-state error between them. Two different Q_{LVAD} data sets were used. The first was generated from a numerical model of the cardiovascular system (in-silico) and the second obtained from an acute non-recovery animal experiment (in-vivo). Generating data in-silico enabled evaluation of the filter across a range of different heart rates and noise levels. The in-vivo data were used to evaluate the MF using a true Q_{LVAD} signal, obtained from an implantable flow probe, which contained realistic pulsatile signal components.

Source Data: In-Silico

A lumped parameter model of a rotary LVAD and cardiovascular system [3] was used to generate the first set of Q_{LVAD} data for filter comparison. A patient with severe left ventricular failure was simulated, and left ventricular mechanical support provided by a VentrAssist LVAD (Ventracor, Sydney, Australia). Severe left ventricular failure was simulated by reducing the end-systolic left ventricular elastance from the normal healthy value of 3.54 mmHg/mL to 1.06 mmHg/mL. All other model parameters were kept at the healthy values as specified in [3]. LVAD speed was set at 2600 RPM in order to produce normal haemodynamics: mean arterial pressure of 100mmHg and a total cardiac output of approximately 5 L/min. Simulations were performed using Simulink (The Mathworks, Natick, MA).

To simulate a change in pump flow, a step change in systemic arterial resistance (R_{sa}) was performed. This simulated the dilation of arterial blood vessels that may occur during exercise. The pump speed was unchanged. The simulation protocol was as follows: the simulation commenced at

time t = 0, with the pump switched off and cannula occluded. At t = 10 second, the pump was switched on at a speed of 2600 RPM. At t = 60 seconds, the R_{sa} was decreased from 0.74 mmHg.s/mL to 0.56 mmHg.s/mL. Then at t = 120 seconds the initial value was restored. Total simulation time was 180 seconds. The protocol was repeated over a range of heart rates from 30 to 120 beats per minute (BPM), generating a set of Q_{LVAD} data encompassing a typical range of heart rates. For each heart rate, systolic fraction was automatically adjusted with heart rate using the relationship described by Vollkron et al. (2002) [11].

To evaluate the robustness of the MF to noise, normally distributed noise was added to the signal and the above protocol repeated. The magnitude of this noise was varied from 2.5% to 70% of the maximum flow signal, producing a range of signal-to-noise (SNR) ratios encompassing 6.6 to 35.6dB.

Source Data: In-Vivo

Haemodynamic data were acquired as part of an ongoing in-vivo evaluation of blood pumps using ovine models at the Medical Engineering and Research Facility located at The Prince Charles Hospital (Brisbane, Queensland, Australia). Animals were treated in accordance with the *Australian Code of Practice for the Care and Use of Animals for Scientific Purposes* (Code of Practice) and the *Animal Care and Protection Act* (Qld). Ethics approval was obtained prior to the experiment from the Animal Ethics Committee of the Queensland University of Technology (Ethics Approval Number 1100001052).

A single acute non-recovery ovine experiment was performed. After anesthetizing the sheep, a VentrAssist LVAD (Ventracor, Chatswood, Australia) was implanted into the left ventricle. The pump speed was set initially to maintain normal haemodynamics as described in the aforementioned section. After the sheep was stabilised, pump speed was increased to 2800 RPM. Controlled changes in flow were then produced by performing step reductions in pump speed: first, from 2800 to 2400 RPM, then from 2400 to 2000 RPM.

In the experiment, Q_{LVAD} was measured using an ultrasonic flow-Doppler probe (TS410-10PXL, Transonic Systems, Ithaca, NY, USA). Data were sampled at 100Hz using dSPACE 1103 data acquisition hardware (Ceanet Pty Ltd, Sydney, Australia).

Filter Implementation

The MF was implemented with a flat SE with a width of 201 elements. At a sampling frequency of 100Hz, this SE covered 2 seconds of input data. This width ensured that for all the evaluated heart rates, the window would always encompass at least one heartbeat. As this was an initial investigation into using a MF for determination of mean beat-to-beat Q_{LVAD}, the weighting constant *w* was fixed at 0.33 as per conventional calculations of mean arterial pressure that use the maximum and minimum arterial pressures [7]. This weighting factor assumes a triangular waveform shape, which is a reasonable approximation for Q_{LVAD}.

In an attempt to improve noise immunity, a two-stage MF was also evaluated using the in-silico data set. This filter consisted first of a noise-removing MF section (of the same structure as the proposed beat-to-beat MF, but with different parameters) cascaded with the single-stage beat-to-beat MF previously described. The noise-removal MF used a flat SE with a width of 21 elements, chosen to remove high frequency noise without causing significant signal delays. Weighting factor *w* was set at 0.5, since it was assumed that the noise was equally spread around the mean. Note that while a MF was used as the noise-removal stage, other non-linear filters, such as a median filter, could be used instead.

The performance of the MF was compared to two low-pass linear filters. For linear filters, correct selection of filter order and cut-off frequency requires consideration of the trade-off between response time and stop-band attenuation. A low cut-off frequency (f_c) would ensure attenuation of all pulsatile signal components, but would be slow to respond to transient changes. A higher cut-off frequency speeds up response time but at the cost of reduced attenuation of pulsatile components. For this reason we designed two linear filters that highlighted this trade-off: a low-order BWF and a long window MAF. Table 1 shows the order, cut-off frequency and attenuation across a range of frequencies for these two filters. Both filters were implemented with a sampling frequency of 100Hz.

The BWF an example of an IIR filter, whose characteristics include efficient implementation and a mildly non-linear phase response. For this study a 3rd-order filter with a cut-off frequency (f_c) of 0.5 Hz was selected. A low order was chosen for simple implementation and f_c was chosen to attenuate pulsatile components caused by the heartbeat without compromising response time. The MAF is an example of a FIR filter, whose characteristics include guaranteed stability and a linear phase response. For this study, a long averaging window (10 seconds) was used, in order to completely remove the pulsatile components of the signal for all heart rates. This MAF filter has been previously implemented during a clinical trial of rotary LVAD feedback control mechanisms [8, 10].

Performance Evaluation

Comparison was performed by calculating the response time of each filter, and the root mean squared steady state difference (RMSSSD) between MF, BWF and the MAF. Conventional frequency domain analysis techniques were not used in this study to make comparisons because these techniques are only suitable for the linear filters (BWF and MAF).

The response time was defined as the time required for the filtered signal to move from 10 to 90% of final value after a step change in R_{sa} (in-silico) or speed (in-vivo)). For the in-silico data, the response times across all heart rates were expressed as mean ± standard deviation. Comparisons between each filter were made using Student's t-test, performed using Matlab (The Mathworks, Natick, MA). A p-value less than 0.05 was considered significant.

The RMSSSD between the MF and the MAF was used as a measure of MF accuracy. The MAF had zero steady state error due to its high order and low f_c, so its use as a benchmark is reasonable. The RMSSSD was calculated over a 30 second period, 30 seconds after the change in flow, to ensure that the MAF had settled, and was calculated separately for both the increase and decrease in resistance. The RMSSSD was determined for all heart rates using the in-silico data, using both the clean signal and all noisy signals. The noise immunity of the single-stage MF, two-stage MF and BWF was assessed by comparing the RMSSSD (expressed as mean ± standard deviation).

Results

In-Silico

Figure 3 shows the mean response times of each filter for both the decrease and increase in R_{sa} for all different heart rates using the clean in-silico data. Statistically significant differences between two filters are marked with an asterisk. The only difference in response time between the MF and the BWF was during the reduction in R_{sa}, in which the BWF was 0.5 seconds faster. The response time of the MAF was nearly 3.5 times slower than the MF and BWF. Interestingly the response time of the BWF depended on the change in resistance, whilst the response times of the MF and MAF did not.

Figure 4 shows that the MF and BWF both exhibited very low RMSSSD for heart rates less than 40 BPM. For heart rates between 40 and 115 BPM, the BWF was more accurate than the MF. The maximum RMSSSD was 2.6% at 70 BPM. The heart rate at which maximum RMSSSD occurred for the MF increased as R_{sa} decreased.

A section of the Q_{LVAD} waveform at a heart rate of 70 BPM is shown in Figure 5. The MF over-estimated the beat-to-beat mean Q_{LVAD}, which was the reason its RMSSSD was higher than the BWF. All pulsatile signal components were removed by the MF. In contrast, the BWF did not completely attenuate the pulsatile component, which was the main contributor to its RMSSSD value.

Figure 6 shows the RMSSSD for the singe stage MF, the two stage MF and the BWF, for each level of SNR during the decreased R_{sa}. As the SNR decreased, the RMSSSD of all filters increased. The RMSSSD of the single stage MF increased exponentially as SNR decreased, reaching a maximum of 14.6±5.7% at an SNR of 6.6 dB. The two-stage MF exhibited noise immunity similar to that of the BWF, and improved upon the single stage MF by reducing the RMSSSD to 4.22± 0.6 % at the lowest SNR.

In-Vivo

Figure 7 shows the pump flow rate obtained in-vivo, processed using the three different filtering techniques. The initial flow rate was 6.5 L/min when the pump was operated at 2800 RPM.

Approximately 38 seconds later, Q_{LVAD} reduced, coinciding with the first reduction in speed. At approximately 110 seconds after the commencement of the experiment, Q_{LVAD} reduced again, coinciding with final speed reduction.

Table 2 shows the response time and RMSSSD for each filter, evaluated using the data set obtained in-vivo, for the two changes in speed. It is difficult to compare the in-vivo and in-silico results directly due to the differing nature of these two experiments, however some general observations can be made. Like the in-silico results, both MF and BWF produced faster response times than the MAF. Unlike the in-silico results however, the MF had a faster rise time than the BWF. The RMSSSD differed depending on the LVAD speed, however more data sets are required to determine if this was significant. The RMSSSD obtained in-vivo was higher than the RMSSSD obtained from the clean in-silico data at the same heart rate (120 BPM) however this may just be due to the presence of noise in the acquired signal. The MF tracked the flow signal better than the BWF during the sharp transient drops in flow that occurred when the speed changed (at 38 and 110 seconds). Both the MF and the BWF exhibited oscillations at a frequency of 0.2Hz, the same frequency as the mechanical ventilator used to support the animal.

Discussion

MFs are attractive as implantable biosignal processors due to their low requirements for bit precision and low computational complexity, provided they are responsive and accurate. The purpose of this study was to establish that using a MF to filter Q_{LVAD} can remove pulsatile signal components without attenuating transient changes or compromising accuracy. These results showed that the MF produced similar response times to a low-pass 3rd-order BWF using in-silico and in-vivo data, was flat during steady state and maintained a RMSSSD lower than 2.7% with a clean signal. To our knowledge this is the first report of the use of a non-linear filter for the filtering of Q_{LVAD}.

Evaluation using the clean in-silico data highlighted the advantages of using a non-linear filter to obtain beat-to-beat mean Q_{LVAD}. The non-linear MF removed pulsatile components of the signal, whilst having a fast response time and low steady state error. In contrast, linear filter design requires a compromise between response time and stop-band attenuation. The low-order BWF used in this study was responsive to changes in flow, but could not completely attenuate pulsatile components of the signal. Additional filtering would be required to remove the pulsatile component before this signal could be used in a feedback control system, otherwise the controller output may also oscillate. Complete attenuation of the pulsatile signal was achieved with the MAF, but at the cost of a slower response time due to a lower f_c. The non-linear MF exhibited the advantages of both types of linear filters evaluated and thus may be used to obtain a responsive, accurate and pulsatile-free Q_{LVAD} signal suitable for monitoring or feedback control.

The MF exhibited the same response time as the BWF for a decrease in R_{sa} when assessed with the in-silico data, but was 0.5 seconds slower in response to an increased R_{sa}. This indicates that the change in Q_{LVAD} with a change in R_{sa} may exhibit hysteresis. However, because the difference in rise times is so small this phenomenon is not likely to be noticed in the clinical environment.

The MF was compared with a MAF that was previously utilised in the only feedback control system for a rotary LVAD to have undergone clinical evaluation [8, 10]. Whilst those authors did not report any difficulties with the slow response time of this filter, the results from our study suggest that

the substitution of the MAF with a MF would result in a more responsive flow signal being fed to any feedback control system. This would improve control performance without any increase in bit precision.

It was observed that the RMSSSD of the MF varied with heart rate. The variation with heart rate may be explained by the fact that the systolic fraction (relative time spent in systole each cardiac cycle) increases with heart rate [11]. This will have an impact on the shape of the Q_{LVAD} waveform. The MF algorithm assumes that the waveform shape is fixed, and so as heart rate (and therefore systolic period) changed, the accuracy of the estimated mean also changed. However, the maximum RMSSSD was only 2.6%, which was acceptable. If further improvement in RMSSSD is required then a method of adapting *w* in Equation 1 with changes in beat-to-beat interval would have to be investigated.

The beat-to-beat mean Q_{LVAD} signal must be immune to noise, so that clinicians can accurately monitor end-organ perfusion, and so the performance of any feedback control system is not compromised. Our results showed that the RMSSSD of the single-stage beat-to-beat MF was vulnerable to noise with a SNR of less than 25dB. However, the accuracy of the two-stage MF, which consisted of a noise-removal component in addition to the beat-to-beat MF, was immune to high levels of noise. The addition of the second stage comes at the cost of increased computational complexity: at each time step the two-stage MF performed four comparisons, two additions and three multiplications (since the weighting factor in the noise-removal stage is 0.5). However, the two-stage MF still required fewer total multiplication operations than the 3rd order BWF used in this study, which required seven multiplication operations each time step. Note that while a MF was used as the noise-removal stage, other types of non-linear filters could also be used.

Evaluation using the data obtained in-vivo again confirmed the benefits of using the non-linear MF to obtain beat-to-beat mean Q_{LVAD}. The MF was just as responsive as the BWF, was able to remove the pulsatile signal components, did not attenuate the low-frequency pulse due to the mechanical ventilation and had low steady state error. An additional advantage of the MF was its ability to track sharp transient changes in flow better than either of the linear filters. This was because the low-pass linear filters attenuated high-frequency signal components, which included the transient changes in flow

observed in the in-vivo data. The MF filter however responded very quickly to the sharp drop in minimum flow and therefore produced a more realistic beat-to-beat mean Q_{LVAD}. Whilst this may not provide immediate advantages to a clinician monitoring LVAD flow, it may be beneficial for feedback control of Q_{LVAD}. Another advantage of the MF over conventional linear filters is that removal of the periodic noise caused by the heartbeat from the feedback signal simplifies controller design significantly and also reduces unnecessary oscillations in the pump control signal that would be present if pulsatility remained.

Only the single-stage MF was used to process the in-vivo data. While there was some noise present in the signal, it was not of a high enough magnitude to reduce accuracy. Despite the good noise immunity of the single-stage MF, we suggest that a two-stage filter be used for processing Q_{LVAD} in real time due to the unknown nature of noise.

The MF presented here can remove pulsatility from the Q_{LVAD} signal, which may simplify the feedback signal when used to directly control Q_{LVAD}. This simplifies controller design while also eliminating unnecessary oscillations in the pump control signal that would otherwise be present if pulsatility remained in the feedback signal. However, some proposed control algorithms, such as that presented by Schima et al. (2004) [8], utilize the pulsatility as a measure of preload. If pulsatility needs to be isolated, the MF algorithm proposed in this study could be modified to obtain a responsive measure of the pulsatility in the following manner. The MF calculates local minima and maxima (by performing simultaneous opening and closing operations) of the pulsatile waveform each time step. The pulsatility can then be calculated by subtracting the minimum from the maximum each cardiac cycle. This calculation could be performed in conjunction with Equation 1 each cardiac cycle without dramatically increasing computational complexity, since it is only a single addition operation.

In this study, we have evaluated the performance of the MF using data generated in-silico and in-vivo. Both data sources offer distinct advantages. The in-silico environment contained a large number of easily modifiable parameters and can create reproducible results. This enabled us to assess the MF thoroughly. However, these signals are only simulated approximations of the true Q_{LVAD}

waveform. The in-vivo data set was an example of a true Q_{LVAD} signal, and its inclusion in this paper shows the advantages of the MF are applicable outside of the in-silico environment. We acknowledge that the experimental conditions were different between the in-silico and in-vivo data and as such direct comparisons cannot be made between them. To accommodate for this, the MF was always compared to the same two linear filters for each data set.

Stability of any filter is an important characteristic, and should be ensured before implementation. The non-linear nature of the MF meant that traditional pole-zero analysis could not be performed to determine stability. However, like an FIR filter, the MF does not utilize any feedback. Therefore, it is inherently stable. Also, there was no instability observed in these experiments, which indicates that this filter is stable. Furthermore, unlike an IIR filter, the stability of the MF is not affected by reducing the bit precision. Reductions in bit precision would only result in a more quantized output; however this is not an issue as we do not foresee any reason to reduce the bit precision of the MF below that of the input signal.

There are some limitations associated with using a non-linear filter. Firstly, there is a lack of theoretical tools that can predict the performance of non-linear filters, and therefore their characteristics must largely be determined empirically. Secondly, the MF algorithm in this study effectively relied on determining the maximum and minimum flow each heartbeat. Therefore, this filter can only update at most once per heartbeat. If the filtered signal is utilised for a feedback control mechanism then this places some limitation on the sampling frequency of the controller.

This was an initial investigation of the benefits of MF to obtain mean beat-to-beat Q_{LVAD}. Future work will involve investigating how to adapt the weighting factor w in Equation 1 to ensure maximum accuracy, perhaps by responding to changes in the beat-to-beat interval. Additionally, future studies will investigate how the effects of the non-linearities of the MF would affect the complexity of a physiological control system. However, since the MF simplifies the feedback signal by removing the pulsatile component, we do not anticipate that it will increase the system complexity.

MFs have previously been established as a suitable means for removing noise and baseline drift from ECG signals. They are also advantageous in that their low computational complexity and low requirements for bit precision make them simple to implement on implantable embedded processors, which encourages their use in other biosignal applications. In this paper we evaluated the suitability of MFs to filter Q_{LVAD} signals obtained from an implantable flow probe. The MF completely attenuated pulsatile signal components and was able to track sharp transient changes in flow. This combination of characteristics cannot be achieved with a linear filter, whose design requires compromise between response time and attenuation. Due to the advantages of simpler implementation, low minimum bit precision, fast response time, noise immunity and low steady-state error, the MF proposed in this study can be used in place of a low pass linear filter to process the signal from an implantable LVAD flow sensor. This will result in a responsive, stable and accurate signal that can be used for monitoring by clinicians or utilised in a feedback control system. Whilst this study focused on obtaining a beat-to-beat mean Q_{LVAD}, these results indicate that a MF could also be applied to finding the mean, maxima or minima of other biosignals, such as arterial pressure.

Acknowledgements

The authors wish to acknowledge the financial support provided by the Experienced Researcher Grant (MS2011-27) and Novice Researcher Grant (NR2011-02), both provided by The Prince Charles Hospital Foundation.

References

1. Chu CH, Delp EJ (1989) Impulsive noise suppression and background normalization of electrocardiogram signals using morphological operators. IEEE Trans. Biomed. Eng. 36, 2, pp. 262–73.

2. Gonzalez RC, Woods RE (1992) Digital Image Processing. Addison-Wesley Longman Publishing Co., Inc., Boston, MA, pp. 518-560.

3. Lim E, Dokos S, Cloherty SL, Salamonsen RF, Mason DG, Reizes JA, Lovell NH (2010) Parameter-optimized model of cardiovascular-rotary blood pump interactions. IEEE Trans. Biomed. Eng. 57, 2, pp. 254–266.

4. Mulgrew B, Grant P, Thompson J (1999) Digital Signal Processing: Concepts and Applications. Palgrave Macmillan, Houndmills, Basingstoke, Hampshire, pp. 146-149.

5. Noon GP, Morley DL, Irwin S, Abdelsayed S V, Benkowski RJ, Lynch BE (2001) Clinical experience with the MicroMed DeBakey ventricular assist device. Ann Thorac Surg. 71, 90030, pp. S133–138.

6. Pahlm O, Sörnmo L (1984) Software QRS detection in ambulatory monitoring — a review. Medical & Biological Engineering & Computing. 22, 4, pp. 289–297.

7. Rogers J (1999) Cardiovascular physiology part 1. Update in Anaesthesia. 10, pp. 2–8.

8. Schima H, Vollkron M, Benkowski B, Morello G, Quittan M, Hiesmayr M, Wolner E, Wieselthaler G (2004) An automatic speed adaptation system for implantable rotary blood pumps and its clinical evaluation. J Heart Lung Transpl. 23, 2, Supplement 1, pp. S108–S108.

9. Sun Y, Chan K, Krishnan SM (2002) ECG signal conditioning by morphological filtering. Computers in Biology and Medicine. 32, 6, pp. 465–79.

10. Vollkron M, Schima H, Huber L, Benkowski R, Morello G (2005) Development of a reliable automatic speed control system for rotary blood pumps. J Heart Lung Transpl. 24, pp. 1878–1885.

11. Vollkron M, Schima H, Huber L, Wieselthaler G (2002) Interaction of the cardiovascular system with an implanted rotary assist device: simulation study with a refined computer model. Artif Organs. 26, 4, pp. 349–359.

12. Wang D, He D-C (1994) A fast implementation of 1-D grayscale morphological filters. IEEE Trans. on Circuits and Systems II: Analog and Digital Signal Processing. 41, 9, pp. 634–636.

Figures

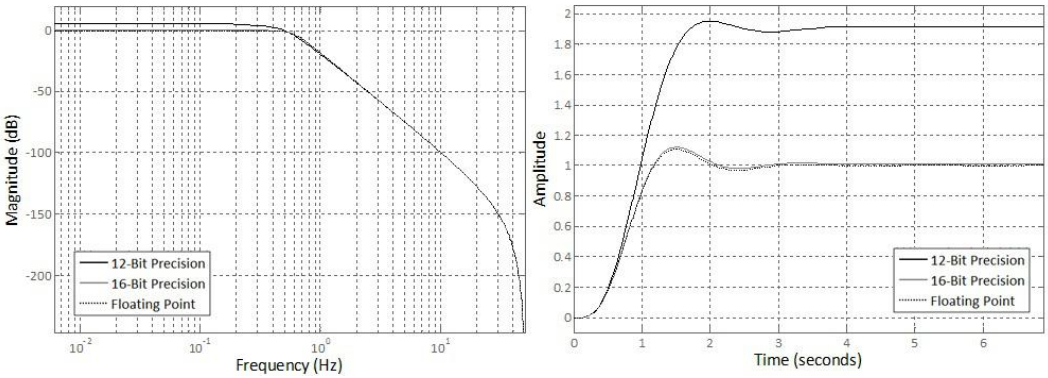

Fig 1 Comparison of the Bode magnitude plot (left) and step response (right) for 12 and 16 bit precision implementations of a 3rd order low-pass Butterworth filter.

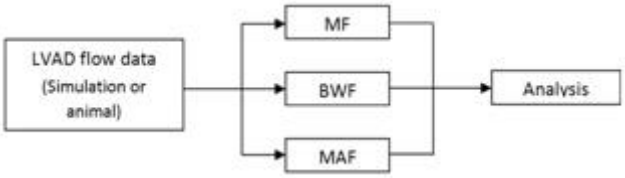

Fig 2 Schematic of the filter evaluation framework. Source data was generated in-silico and obtained from in-vivo studies.

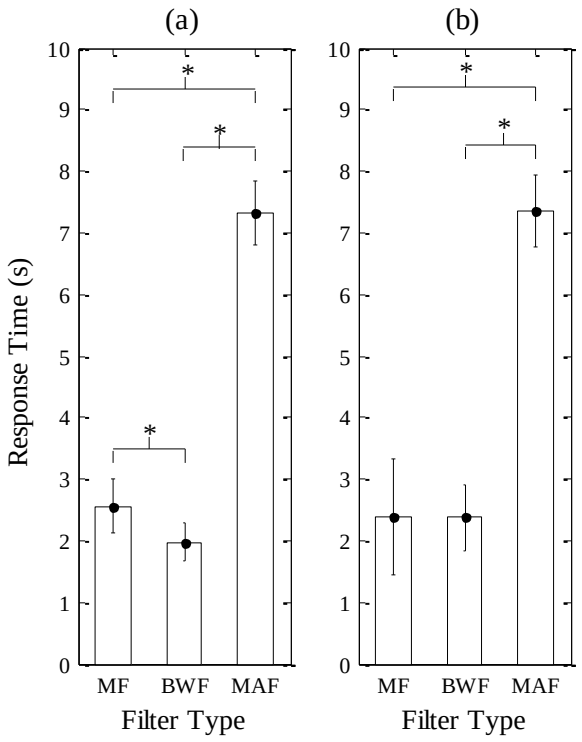

Fig 3 Mean ± SD response time of the clean LVAD flow signal after a step decrease (a) and a step increase (b) in systemic arterial resistance using three different filters for fixed heart rates between 30 and 120 BPM.

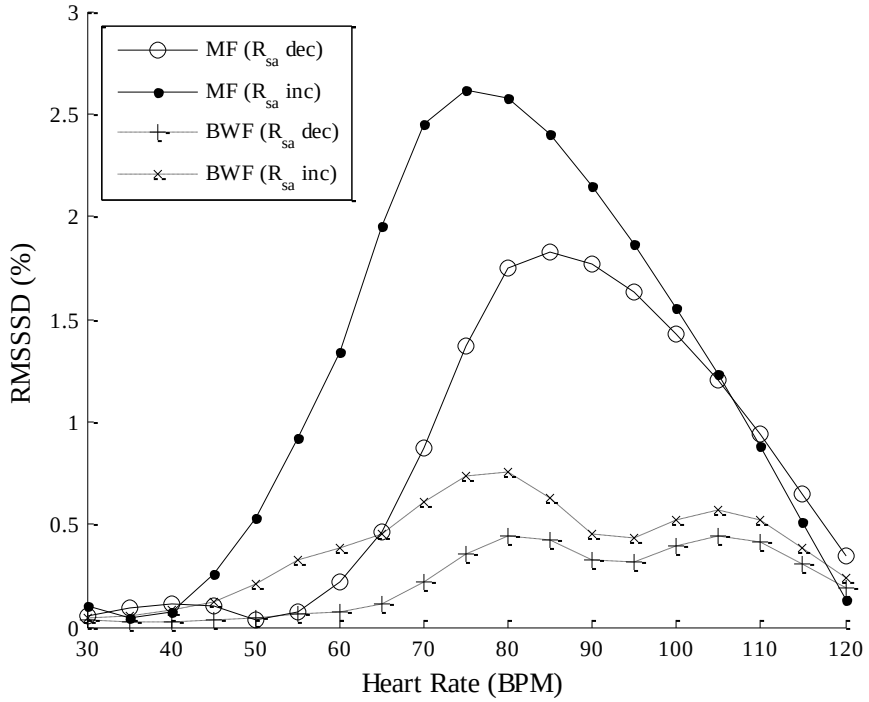

Fig 4 RMSSSD between the MF and the MAF, and between BWF and MAF for normal and low systemic arterial resistance (R_{sa}) over a range of heart rates.

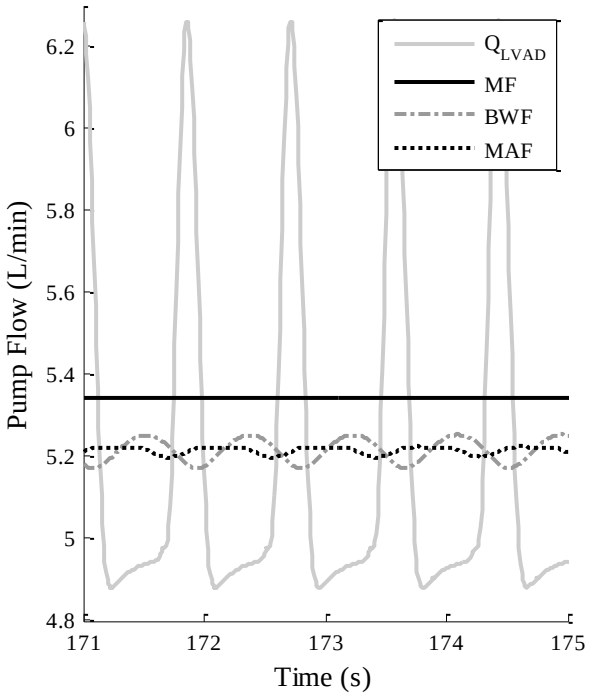

Fig 5 Segment of QLVAD waveform, filtered using the three different filtering techniques under evaluation.

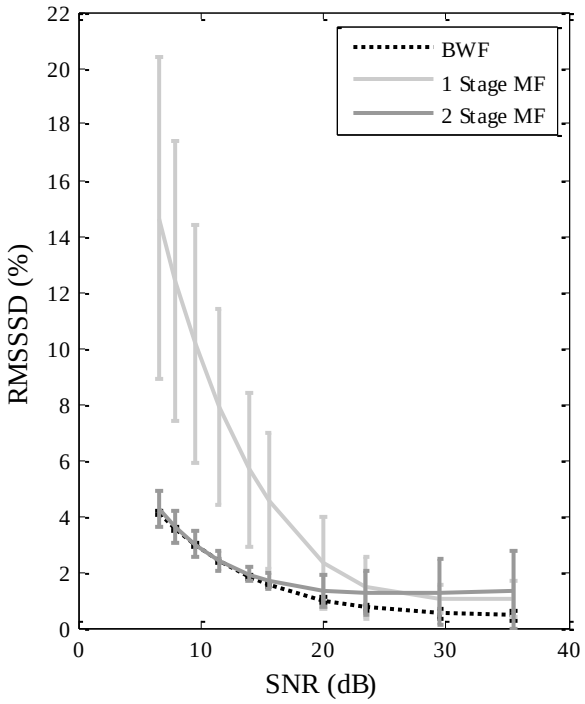

Fig 6 Root mean squared steady state difference for one and two stage MFs and the BWF across a range of signal-to-noise ratios.

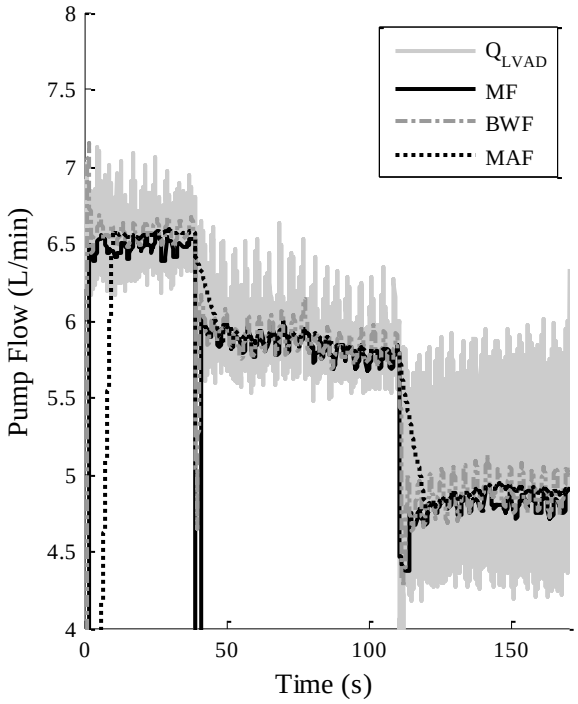

Fig 7 Rotary LVAD flow data obtained in-vivo, and filtered using three different filtering techniques.

Tables

Table 1 Attenuation across the range of heart beat frequencies for the two linear filters used for comparison.

Filter	Order	Cut-off Frequency (Hz)	Attenuation (dB)			
			0.1 Hz	0.5 Hz	1 Hz	2 Hz
BWF	3	0.5	0.0	-3.0	-18.3	-36.1
MAF	1000	0.04	-13.3	-24.0	-29.9	-36.0

Table 2 Response times for all filters and RMSSSD between MF and MAF, and BWF and MAF, using in-vivo source data

Speed Change	Response Time (sec)			RMSSSD (%)	
	MF	BWF	MAF	MF	BWF
1	0.04	0.23	9.14	1.24	1.33
2	0.11	0.43	7.09	2.08	1.77